

General Disclaimer

One or more of the Following Statements may affect this Document

- This document has been reproduced from the best copy furnished by the organizational source. It is being released in the interest of making available as much information as possible.
- This document may contain data, which exceeds the sheet parameters. It was furnished in this condition by the organizational source and is the best copy available.
- This document may contain tone-on-tone or color graphs, charts and/or pictures, which have been reproduced in black and white.
- This document is paginated as submitted by the original source.
- Portions of this document are not fully legible due to the historical nature of some of the material. However, it is the best reproduction available from the original submission.



Technical Memorandum 86064



Documentation of the GLAS Fourth Order General Circulation Model

Volume I: Model Documentation

E. Kalnay, R. Balgovind, W. Chao, D. Edlmann,
J. Pfaendtnier, L. Takacs, and K. Takano

December 1983

(NASA-TM-86064-Vol-1) DOCUMENTATION OF THE
GLAS FOURTH ORDER GENERAL CIRCULATION MODEL.
VOLUME 1: MODEL DOCUMENTATION (NASA) 381 p
HC A17/MF A01 CSCL 04B

N84-24048

Unclas
G3/47 19206

Laboratory for Atmospheric Sciences
Global Modeling and Simulation Branch

National Aeronautics and
Space Administration

Goddard Space Flight Center
Greenbelt, Maryland 20771

DOCUMENTATION OF THE GLAS FOURTH ORDER GENERAL CIRCULATION MODEL

VOLUME I: MODEL DOCUMENTATION

E. Kalnay¹, R. Balgovind², W. Chao³, D. Edelman²,

J. Pfaendtner², L. Takacs², and K. Takano⁴

Laboratory for Atmospheric Sciences
NASA/Goddard Space Flight Center
Greenbelt, Md 20771

December 1983

AFFILIATIONS

- ¹ Laboratory for Atmospheric Sciences
- ² M/A-COM Sigma Data Services Corporation
- ³ Laboratory for Planetary Atmospheres
- ⁴ Applied Research Corporation

PRECEDING PAGE BLANK NOT FILMED

ACKNOWLEDGMENTS

We are very grateful to Drs. Mark Helfand and Yogesh Sud for their advice in the analysis of the parameterizations of the model's physical processes, and to Mr. Mark Iredell for his efforts in the early stages of the documentation. The expert assistance of Ms. Mary Ann Wells in the technical typing, and of Ms. Laura Rumburg and Mr. Brian Sherbs in the drafting of the figures and the preparation of the manuscript is gratefully acknowledged. The computer plots in the appendix were carefully designed and prepared by Mr. Robert Rosenberg and Mr. Farhad Tahmasebi. The collaboration of many other members of the Global Modeling and Simulation Branch and of Sigma Data Services Corporation has also been essential to the completion of this work. Finally, we would like to express our deep gratitude to Dr. Milton Halem, former head of the branch, and to NASA management for their support and encouragement.

TABLE OF CONTENTS

Affiliations	iii
Acknowledgments	iv
List of Illustrations	x
List of Tables	xii
I. Introduction	I-1
II. Model Grid	II-1
II.1 Horizontal Grid	II-1
II.2 Vertical Grid	II-2
III. Model Equations	III-1
III.1 Introduction	III-1
III.2 Governing Equations	III-4
i. Zonal (u) Momentum Equation	III-4
ii. Meridional (v) Momentum Equation	III-4
iii. Thermodynamic Energy Equation	III-4
iv. Moisture Balance Equation	III-5
v. Continuity (Pressure Tendency) Equation	III-5
vi. Equation of State	III-6
vii. Hydrostatic Equation	III-6
viii. Equation for the Geopotential	III-6
ix. Vertical Velocity (Ω and \dot{S}) Equation	III-6
III.3 Derivation of the Polar Equations	III-9
i. Stereographic and Spherical Velocities	III-9
ii. Continuity (Pressure Tendency) Equation	III-12
iii. Vertical Velocity (Ω and \dot{S}) Equation	III-13
iv. Zonal (U_p) Momentum Equation	III-14
m	
v. Meridional (V_p) Momentum Equation	III-19
m	
vi. Thermodynamic Energy Equation	III-21
vii. Moisture Equation	III-24
viii. Equation for the Geopotential	III-25
IV. Hydrodynamics	IV-1
IV.1 Introduction	IV-1

IV.2	Hydrodynamic Terms (Finite Difference)	IV-3
i.	Horizontal Fluxes (Subroutine COMP1)	IV-3
ii.	Vertical Fluxes (Subroutine COMP1)	IV-3
iii.	Pressure Gradient Force (Subroutine COMP2)	IV-4
iv.	Coriolis Term (Subroutine COMP2)	IV-4
v.	Energy Conversion Terms (Subroutine COMP2)	IV-5
vi.	Mass Convergence (Subroutine COMP1)	IV-5
vii.	Vertical Velocity (Ω and \dot{S}) Equation	IV-6
viii.	Equation for the Geopotential	IV-6
IV.3	Polar Finite Difference Formulation	IV-11
i.	Zonal (U_p) Momentum Equation	IV-12
ii.	Meridional (V_p) Momentum Equation	IV-14
iii.	Thermodynamic Energy Equation	IV-15
iv.	Moisture Equation	IV-18
v.	Continuity (Pressure Tendency) Equation	IV-18
vi.	Vertical Velocity (Ω and \dot{S}) Equation	IV-19
vii.	Equation for the Geopotential	IV-19
IV.4	Time Scheme	IV-20
i.	Matsuno Time Scheme	IV-20
ii.	Smoothed Leapfrog Scheme	IV-20
IV.5	Filtering	IV-22
i.	Periodic (Shapiro) Filtering of Short Waves	IV-22
ii.	High Latitude (Fourier) Filter	IV-23
V.	Parameterization of Physical Processes	V-1
V.1	Introduction	V-1
V.2	Initialization	V-2
i.	Surface Specification	V-2
ii.	Pressure Calculations	V-5
iii.	Surface Winds	V-5
iv.	Surface Drag Coefficient	V-6
V.3	Frictional Dissipation	V-7
i.	Surface Skin Friction	V-7
ii.	Internal Friction (IF) due to Vertical Shear of Horizontal Wind	V-8

V.4	Diabatic Heating (Excluding Release of Latent Heating)	V-11
i.	Vertical Diffusion of Heat	V-11
ii.	Dry Adiabatic Adjustment	V-13
iii.	Determination of Surface Layer Temperature	V-14
iv.	Surface Sensible Heat Flux	V-21
v.	Radiation	V-22
vi.	Heating due to Absorbed Radiation	V-29
vii.	Determination of Ground Temperature	V-30
V.5	Evaporation and Vertical Flux of Moisture	V-37
i.	Vertical Diffusion of Moisture	V-37
ii.	Surface Moisture Flux	V-38
iii.	Determination of Surface Specific Humidity	V-39
iv.	Elimination of Negative Specific Humidity	V-43
v.	Determination of Saturation Specific Humidity	V-44
V.6	Precipitation Processes	V-46
i.	Large-Scale Precipitation	V-46
ii.	Small-Scale Cumulus Parameterization	V-49
iii.	Moist Adiabatic Adjustment	V-71
V.7	Diagnostics	V-77
i.	Diagnostic Quantities Retained in the History File.	V-77
VI.	Extensions for a Troposphere-Stratosphere Model	VI-1
VI.1	Introduction	VI-1
VI.2	Hybrid ($\sigma - p$) Vertical Coordinate	VI-4
VI.3	Governing Equations	VI-8
VI.4	Vertical Difference Scheme	VI-10
VI.5	Radiation	VI-14
i.	Solar Radiation	VI-14
ii.	Infrared (IR) Radiation	VI-15
VI.6	Changes in the Model Code	VI-16
VI.7	Results from Numerical Forecast Experiments	VI-18
VII.	Code Organization	VII-1
VII.1	Introduction	VII-1

VII.2	Model Grid	VII-3
i.	Horizontal Grid Control Variables	VII-3
ii.	Vertical Grid Control Variables	VII-4
iii.	Control Variables for Filters	VII-5
VII.3	Model Calendar and Time Scheme Variables	VII-7
VII.4	Physical Constants	VII-9
VII.5	Computational Flow	VII-11
i.	Program Control	VII-15
ii.	Input/Output	VII-21
iii.	Hydrodynamics	VII-25
iv.	Physics	VII-33
VIII.	Input/Output	VIII-1
VIII.1	Namelists	VIII-1
i.	Control (INPUTZ)	VIII-1
ii.	Physics (INPHYS)	VIII-2
VIII.2	Boundary Conditions	VIII-3
i.	Topography, Ground Wetness, Albedo, Sea Surface Temperature	VIII-3
ii.	Format of the Surface Boundary Conditions (V8SURF)	VIII-4
iii.	Transmission Functions of Carbon Dioxide and Ozone	VIII-6
VIII.3	Model History Data Sets	VIII-9
i.	Sigma Coordinate Model History (V8SIGM)	VIII-10
ii.	Pressure Coordinate Model History (V8MAND)	VIII-17
iii.	Sigma Coordinate Model Restart (V8RSTR)	VIII-21
IX.	User's Guide	IX-1
IX.1	Introduction	IX-1
IX.2	Running a Forecast Experiment	IX-2
IX.3	Model Production Code	IX-4
IX.4	How to Produce Modified Code	IX-6
IX.5	Files and Tapes Used by the Model	IX-11
IX.6	Production Run Procedures	IX-15
IX.7	Altering the Production Procedures	IX-21

IX.8	Namelist and Initial Condition Data Sets	IX-23
IX.9	Running the Experiment	IX-26
IX.10	Error Messages	IX-30
IX.11	Looking at the Results	IX-33
X.	Code Management Procedures	X-1
X.1	Introduction	X-1
X.2	The Model Group Library Machine F400M	X-2
X.3	Management of the Production Code	X-3
X.4	Utility Programs for the Production Run Procedures	X-5
X.5	The Libraries CYPROCLB, CYGWSLIB and CYBINLIB	X-7
X.6	Benchmark Procedures and Documentation of Changes	X-10
Appendix A	Namelist Variables	A-1
Appendix B	Contents of the Header Record (Standard for V8SIGM, V8RSTR & V8MAND)	B-1
Appendix C	Bit Configuration for Cloud Data	C-1
Appendix D	Global Maps of the Boundary Fields	D-1
i.	Continental Outline	D-2
ii.	Orography	D-3
iii.	Sea Surface Temperature	D-4
iv.	Ground Wetness	D-16
v.	Surface Albedo	D-28
Appendix E	Tables of the Longwave Radiation Data Sets	E-1
i.	Carbon Dioxide	E-2
ii.	Ozone	E-4
Appendix F	Test Initial Conditions for the Model's Dynamics	F-1
Appendix G	Comparison of Simulated and Observed January and July Climatologies	G-1
Bibliography	H-1

LIST OF ILLUSTRATIONS

Fig. II.1a	Horizontal Grid for the Model	II-1
Fig. II.2a	Vertical Grid for the 9 Level Model	II-3
Fig. III.3a	The $x'-y'$ Coordinates Relative to the $x-y$ Coordinates After a Rotation by λ Degrees	III-10
Fig. III.3b	North Pole View of the Horizontal Fields (U_λ, V_λ) on the Stereographic Plane	III-10
Fig. III.3c	South Pole View of the Horizontal Fields (U_λ, V_λ) on the Stereographic Plane	III-11
Fig. V.2a	Determination of Surface Condition	IV-4
Fig. V.4a	Surface Layer Temperature	V-14
Fig. V.4b	Temperature Correction Due to Change of Phase of Moisture ..	V-35
Fig. V.6a	GLAS/UCLA Strapping Parameterization	V-49
Fig. V.6b	UCLA Cumulus Parameterization Variables	V-52
Fig. V.6c	Cumulus Convection Types	V-53
Fig. V.6d	Middle-Level Convection	V-55
Fig. V.6e	Penetrating Convection	V-59
Fig. V.6f	Low-Level Convection	V-64
Fig. V.6g	Moist Adiabatic Adjustment	V-71
Fig. VI.2a	Vertical Structure for the Troposphere/Stratosphere Model ..	VI-6
Fig. VI.4a	Vertical Indices for the Troposphere/Stratosphere Model	VI-12
Fig. VI.7a	Minor Warming 500 mb Geopotential Height	VI-19
Fig. VI.7b	Minor Warming 10 mb Geopotential Height	VI-20
Fig. VI.7c	Minor Warming 5 mb Geopotential Height	VI-21
Fig. VI.7d	Minor Warming 1 mb Geopotential Height	VI-22
Fig. VI.7e	Major Warming 500 mb Geopotential Height	VI-23
Fig. VI.7f	Major Warming 10 mb Geopotential Height	VI-24
Fig. VI.7g	Major Warming 5 mb Geopotential Height	VI-25

Fig. VI.7h Major Warming 1 mb Geopotential Height	VI-26
Fig. VII.3a Schematic Description of Time Marching	VII-8
Flow Diagram - Program Control	VII-16
Flow Diagram - Input/Output	VII-22
Flow Diagram - Hydrodynamics	VII-26
Flow Diagram - Physics	VII-34
Fig. VIII.3a Typical Organization of the Logical Records in the V8SIGM Data Set	VIII-16
Fig. IX.4a Schematic View of the Update Process	IX-7

LIST OF TABLES

Table IV.5a	Empirically Derived Damping Coefficients as Used in the 4° X 5° Model	IV-27
Table V.2a	Latitudes for Northern Snow Line	V-3
Table V.4a	Optical Thickness	V-28
Table IX.8a	Possible Actions of the CMS Exec GCMICSET	IX-25

CHAPTER I

INTRODUCTION

EUGENIA KALNAY

I. INTRODUCTION

In these three Technical Memoranda, we have compiled a detailed documentation of the GLAS Fourth Order General Circulation Model. This model has been extensively used in many assimilation and forecast experiments using FGGE data (Halem et al., 1982, Baker et al., 1983, Kalnay et al., 1983, and others), as well as in several general circulation and forecast experiments (Paegle and Baker, 1983, and several papers in preparation). It has proven to be a reasonably accurate forecast model even at the coarse resolution of four degrees latitude by five degrees longitude and nine vertical levels, and its reproduction of the circulation of the atmosphere is comparable to some of the best currently used general circulation models (see Appendix G for results of summer and winter climate simulations). The previously available documentation (Kalnay-Rivas and Hoitsma, 1979a) was not complete, had several errors, and did not include a description of the parameterization of the subgrid scale physical processes, and of improvements in the numerical scheme. These drawbacks and the wide present use of the model made it necessary to prepare the present documentation.

The GLAS Fourth Order GCM was first discussed in Kalnay-Rivas et al. (1977). The numerical computation of the hydrodynamics was developed based on the following ideas, discussed in detail by Kalnay-Rivas and Hoitsma (1979b): We used an unstaggered horizontal grid, in order to allow an efficient implementation of fourth order accuracy in all the terms containing horizontal differences. We implemented quadratically (energy) conserving differences, rather than either advective or enstrophy conserving differences, again because of their simple and efficient implementation. The quadratically conservative, fourth order scheme is accurate for waves with wavelength longer than four grid increments, but still very inaccurate for the shortest, unresolved waves. Therefore, we combined it with the application of a sixteenth order Shapiro (1970) filter every

two hours. This has the effect of eliminating waves shorter than four gridlengths (which we consider subgrid scale) before they acquire finite amplitude and interact spuriously with longer waves. As a result, the scheme has virtually no horizontal diffusion in the adequately resolved waves, and, in practice, it approximately conserves potential enstrophy even though this is not formally guaranteed by the finite differences.

The parameterization of subgrid scale physical processes in the model version described in this documentation is still basically similar to that in Somerville et al. (1974), although a number of changes and improvements have been implemented. Among them we should mention the use of the longwave radiation scheme of Wu (1976), some modifications in the frictional surface layer, the definition of the orography, the use of the ground wetness fields of Mintz and Serafini (1981), and the modification of the dry convective adjustment to allow mixing of moisture and momentum in addition to heat, as well as many minor modifications and corrections of the previous formulation. There have also been several changes in the numerics from Kalnay-Rivas et al., (1977), especially in the Shapiro and high latitude fourier filtering.

This version of the GLAS Fourth Order GCM is intended to be a baseline, i.e., a model which can be used either for experimental forecasts or simulations, as well as a benchmark with which to test further advanced numerical schemes or physical parameterizations. For this reason, every effort has been made to make the documentation as complete and self-contained as possible. Volume I contains not only detailed descriptions of the hydrodynamics and physics formulations, but, equally important, sections devoted to user's guide and code management procedures. A "user friendly" system guides a new user into the procedures for running the model and modifying its code for experimental runs. The documentation also includes a thorough description of input climatological

fields and the default output fields, both prognostic and diagnostic, and an indication on how to modify the choice of output diagnostic fields. A special chapter (Chapter 6) describes the modifications to the GLAS Fourth Order GCM implemented in the development of the Tropospheric/Stratospheric Model of the Laboratory for Planetary Atmospheres under the direction of Dr. M. Geller. The tropospheric/stratospheric version of the model, available at the present on the Amdahl computer in scalar form, will also be vectorized for use on the Cyber 205 in the near future.

The documentation is completed by Volumes II and III which contain the Cyber 205 scalar and vector codes of the model, list of variables, cross references, etc.

We hope that the documentation will be found helpful by users of the model both within NASA and in the academic community. If so, the large effort devoted to its preparation will have been worthwhile.

CHAPTER II

MODEL GRID

JAMES W. PFAENDTNER

II. MODEL GRID

II.1 Horizontal Grid

The model equations presented in Chapter III are defined and integrated on a finite difference grid. Geographic spherical coordinates are used to define the uniform horizontal grid. All quantities used by the model (u , v , T , q , ϕ , ω , etc.) are defined at the same (nonstaggered) horizontal grid points.

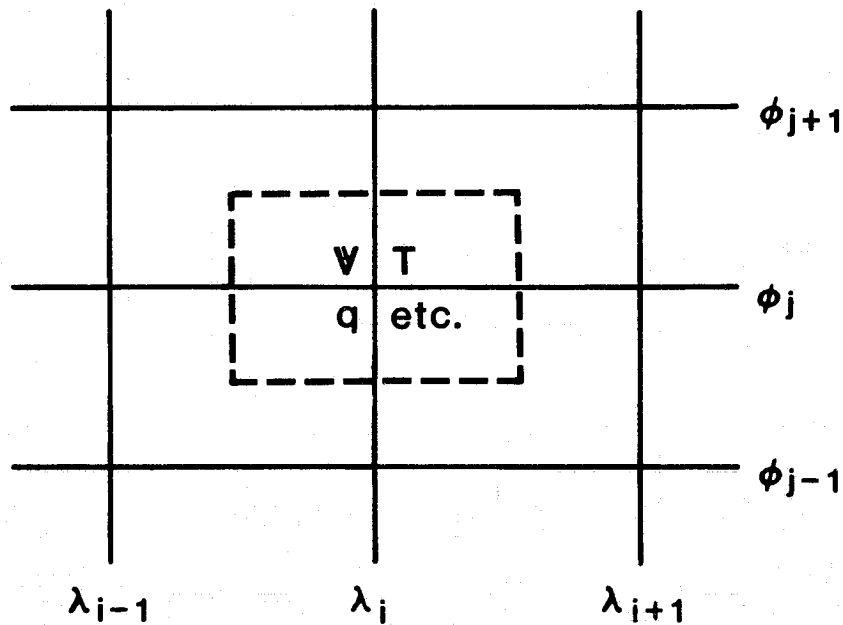


Fig. II.1a Horizontal Grid for the Model

The horizontal grid resolution is determined by two integers, IM and JM, through the equations

$$\Delta\lambda = 2\pi/IM$$

$$\Delta\phi = \pi/JM$$

The grid points (λ_i , ϕ_j) are located at longitudes

$$\lambda_i = (i - 1)\Delta\lambda - \pi \quad i = 1, 2, \dots, IM$$

ORIGINAL PAGE IS
OF POOR QUALITY

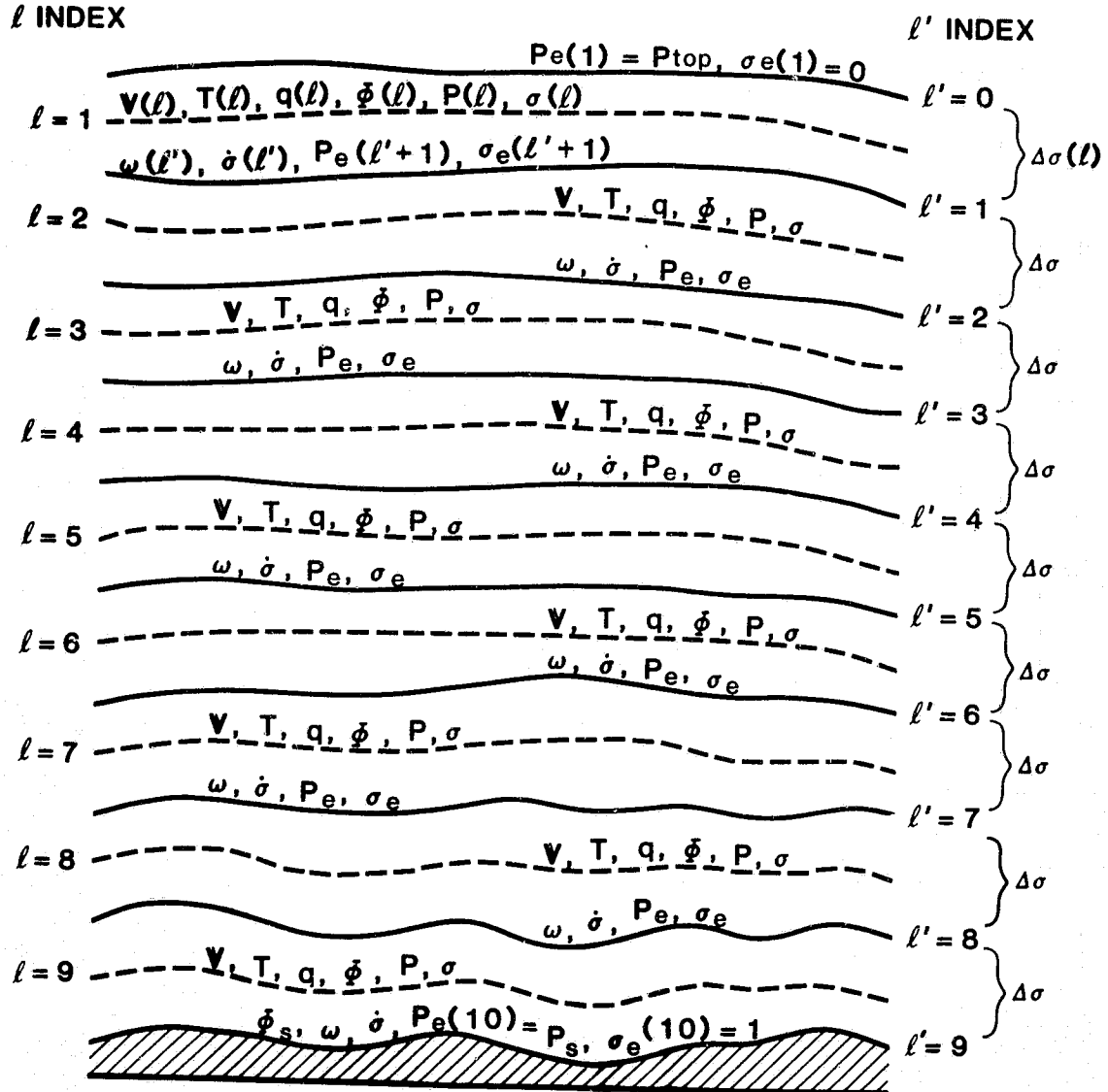


Fig. II.2a Vertical Grid for the 9 Level Model

CHAPTER III

MODEL EQUATIONS

RAMESH C. BALGOVIND

III. MODEL EQUATIONS

III.1 Introduction

This chapter contains a presentation of the governing equations of the atmosphere in analytic form. The equations are expressed in spherical coordinates with a sigma (σ) coordinate system in the vertical. Where necessary a derivation of the equations from basic principles is also given.

The independent variables

λ = longitude

ϕ = latitude

$\sigma = (p - p_{top})/\Pi$

t = time

are used to write the tendency equations for the five primary dependent variables of the model

Π = difference of surface pressure and pressure
at the top of the model in mb

u = zonal wind component (west to east) in $m \text{ sec}^{-1}$

v = meridional wind component (south to north)
in $m \text{ sec}^{-1}$

T = temperature in $^{\circ}K$

q = water vapor mixing ratio (dimensionless)

The differential equations described in Section 2 contain the following physical constants

a = radius of the earth

f = Coriolis parameter

C_p = dry air specific heat at constant pressure

R = dry air specific gas constant

The differential equations also contain the following secondary dependent quantities

ϕ = geopotential in $m^2 \text{ sec}^{-2}$

$\dot{\sigma} = \frac{d\sigma}{dt}$, sigma vertical velocity in sec^{-1}

$p = p_{\text{top}} + p_{\text{top}}$, pressure in mb where p_{top} is the (constant) pressure at the top of the model

x = dimensionless eastward coordinate

y = dimensionless northward coordinate

Lastly, the differential equations contain forcing terms resulting from physical processes

F = horizontal frictional force per unit mass
(see Chapter V, Section 3)

Q = diabatic heating rate per unit mass
(see Chapter V, Section 4)

E = source term

C = sink term

The model also separates thermodynamic variables into mean adiabatic values and their departures from the mean

$\phi' = \phi - \bar{\phi}$ (geopotential height)

$T' = T - \bar{\theta} p^{\kappa}$ (temperature)

$\theta' = \theta - \bar{\theta}$ (scaled potential temperature)

where

$\bar{\theta} = 280^\circ\text{K}/1000^\kappa$

$\kappa = R/C_p = .2861328125$

$\bar{\phi} = C_p \bar{\theta} (1000^\kappa - p^\kappa)$

Since the hydrostatic equation is satisfied for both components

$$\frac{\partial \bar{\Phi}}{\partial p^k} = -C_p \bar{\theta}$$

and

$$\frac{\partial \Phi'}{\partial p^k} = -C_p \theta'$$

the pressure gradient term

$$\Pi \left(\nabla_{\sigma} \bar{\Phi} + \frac{\sigma R T}{p} \nabla \Pi \right)$$

in the momentum equations can be transformed into

$$\begin{aligned} & \Pi \left(\nabla_{\sigma} \Phi' + \nabla_{\sigma} \bar{\Phi} + \frac{\sigma R (T' + \bar{\theta}_p^k)}{p} \nabla \Pi \right) \\ &= \Pi \left(\nabla_{\sigma} \Phi' + \frac{\sigma R T'}{p} \nabla \Pi \right) + \Pi \left(\nabla_{\sigma} \bar{\Phi} + \frac{\sigma R \bar{\theta}_p^k}{p} \nabla \Pi \right) \\ &= \Pi \left(\nabla_{\sigma} \Phi' + \frac{\sigma R T'}{p} \nabla \Pi \right) \end{aligned}$$

Since the second parenthesis is zero

$$\nabla_{\sigma} \bar{\Phi} + \sigma R \bar{\theta} \frac{p^k}{p} \nabla \Pi = -C_p \bar{\theta} \nabla_{\sigma} p^k + R \bar{\theta} \frac{p^k}{p} \nabla p = 0.$$

In regions of steep orography, the individual terms in the second parenthesis are much larger than those in the first. When the horizontal pressure gradient terms are computed in their original form, the near cancellation of the two terms introduces large truncation errors. The procedure of using departures from the mean thermodynamic variables, as suggested by Phillips (1974), greatly reduces this truncation error.

III.2 Governing Equations

III.2i Zonal (u) Momentum Equation

The u-momentum equation in flux form is given by

Tendency	Horizontal Advection	Vertical Advection	Pressure Gradient Force
$\frac{\partial(\Pi u)}{\partial t} = - \frac{1}{a \cos \phi} \left[\frac{\partial(\Pi u u)}{\partial \lambda} + \frac{\partial(\Pi v \cos \phi u)}{\partial \phi} \right] - \frac{\partial(\Pi \dot{\sigma} u)}{\partial \sigma} - \frac{\Pi}{a \cos \phi} \left[\frac{\partial \Phi'}{\partial \lambda} + \frac{\sigma R T'}{p} \frac{\partial \Pi}{\partial \lambda} \right]$			
		Coriolis Term	Dissipation
		$+ \left(f + \frac{u \tan \phi}{a} \right) \Pi v + \Pi F_x \quad (2.1)$	

III.2ii Meridional (v) Momentum Equation

The v-momentum equation in flux form is given by

Tendency	Horizontal Advection	Vertical Advection	Pressure Gradient Force
$\frac{\partial(\Pi v)}{\partial t} = - \frac{1}{a \cos \phi} \left[\frac{\partial(\Pi u v)}{\partial \lambda} + \frac{\partial(\Pi v \cos \phi v)}{\partial \phi} \right] - \frac{\partial(\Pi \dot{\sigma} v)}{\partial \sigma} - \frac{\Pi}{a} \left[\frac{\partial \Phi'}{\partial \phi} + \frac{\sigma R T'}{p} \frac{\partial \Pi}{\partial \phi} \right]$			
		Coriolis Term	Dissipation
		$- \left(f + \frac{u \tan \phi}{a} \right) \Pi u + \Pi F_y \quad (2.2)$	

III.2iii Thermodynamic Energy Equation

The thermodynamic equation in flux form is given by

$$\frac{\partial \Pi T}{\partial t} = - \nabla \cdot (\Pi v T) - \frac{\partial}{\partial \sigma} (\Pi \dot{\sigma} T) + \frac{\Pi \omega \alpha}{C_p} + \frac{\Pi Q}{C_p} \quad (2.3)$$

In order to remove the diagnostic variable $\omega = \frac{dp}{dt} = \dot{\sigma} \Pi + \Pi \dot{\sigma}$ from the above equation we see that

$$- \frac{\partial(\Pi \dot{\sigma} T)}{\partial \sigma} = - p^{\kappa} \frac{\partial(\Pi \dot{\sigma} \theta)}{\partial \sigma} - \Pi \dot{\sigma} \frac{\kappa T}{p} \Pi \quad (2.4)$$

and

$$\frac{\Pi \omega \alpha}{C_p} = \Pi \dot{\alpha} \Pi \frac{\kappa T}{p} + \Pi \dot{\Pi} \sigma \frac{\kappa T}{p} \quad (2.5)$$

Adding equations (2.4) and (2.5) and inserting the result in equation (2.3), we obtain the thermodynamic equation as used in the model

Tendency Horizontal Advection

$$\frac{\partial \Pi T}{\partial t} = - \frac{1}{a \cos \phi} \left[\frac{\partial(\Pi u T)}{\partial \lambda} + \frac{\partial(\Pi v \cos \phi T)}{\partial \phi} \right]$$

Energy Conversion Terms

Diabatic
Heating Terms

$$- p^{\kappa} \frac{\partial \Pi \dot{\sigma} T / p^{\kappa}}{\partial \sigma} + \frac{\Pi \sigma \kappa T}{p} \left(\frac{\partial \Pi}{\partial t} + \frac{u}{a \cos \phi} \frac{\partial \Pi}{\partial \lambda} + \frac{v}{a} \frac{\partial \Pi}{\partial \phi} \right) + \frac{\Pi Q}{C_p} \quad (2.6)$$

III.2iv Moisture Balance Equation

The moisture equation in flux form is given by

Tendency Horizontal Advection

Vertical
Advection

Moisture Source and
Sink Terms

$$\frac{\partial \Pi q}{\partial t} = - \frac{1}{a \cos \phi} \left[\frac{\partial(\Pi u q)}{\partial \lambda} + \frac{\partial(\Pi v \cos \phi q)}{\partial \phi} \right] - \frac{\partial(\Pi \dot{\sigma} q)}{\partial \sigma} + \Pi (E - C) \quad (2.7)$$

III.2v Continuity (Pressure Tendency) Equation

The surface pressure tendency equation is obtained by vertically integrating the continuity equation

$$\frac{\partial \Pi}{\partial t} = - \frac{1}{a \cos \phi} \left[\frac{\partial \Pi u}{\partial \lambda} + \frac{\partial(\Pi v \cos \phi)}{\partial \phi} \right] - \frac{\partial(\Pi \dot{\sigma})}{\partial \sigma} \quad (2.8)$$

$$- \frac{\partial(\Pi \dot{\sigma} T)}{\partial \sigma} = - p^{\kappa} \frac{\partial(\Pi \dot{\sigma} \theta)}{\partial \sigma} - \Pi \dot{\sigma} \frac{\kappa T}{p} \Pi \quad (2.4)$$

and

$$\frac{\Pi \omega \alpha}{C_p} = \Pi \dot{\alpha} \Pi \frac{\kappa T}{p} + \Pi \dot{\Pi} \sigma \frac{\kappa T}{p} \quad (2.5)$$

Adding equations (2.4) and (2.5) and inserting the result in equation (2.3), we obtain the thermodynamic equation as used in the model

Tendency Horizontal Advection

$$\frac{\partial \Pi T}{\partial t} = - \frac{1}{a \cos \phi} \left[\frac{\partial(\Pi u T)}{\partial \lambda} + \frac{\partial(\Pi v \cos \phi T)}{\partial \phi} \right]$$

Energy Conversion Terms

Diabatic
Heating Terms

$$- p^{\kappa} \frac{\partial \Pi \dot{\sigma} T / p^{\kappa}}{\partial \sigma} + \frac{\Pi \sigma \kappa T}{p} \left(\frac{\partial \Pi}{\partial t} + \frac{u}{a \cos \phi} \frac{\partial \Pi}{\partial \lambda} + \frac{v}{a} \frac{\partial \Pi}{\partial \phi} \right) + \frac{\Pi Q}{C_p} \quad (2.6)$$

III.2iv Moisture Balance Equation

The moisture equation in flux form is given by

Tendency Horizontal Advection

Vertical
Advection Moisture Source and
Sink Terms

$$\frac{\partial \Pi q}{\partial t} = - \frac{1}{a \cos \phi} \left[\frac{\partial(\Pi u q)}{\partial \lambda} + \frac{\partial(\Pi v \cos \phi q)}{\partial \phi} \right] - \frac{\partial(\Pi \dot{\sigma} q)}{\partial \sigma} + \Pi (E - C) \quad (2.7)$$

III.2v Continuity (Pressure Tendency) Equation

The surface pressure tendency equation is obtained by vertically integrating the continuity equation

$$\frac{\partial \Pi}{\partial t} = - \frac{1}{a \cos \phi} \left[\frac{\partial \Pi u}{\partial \lambda} + \frac{\partial(\Pi v \cos \phi)}{\partial \phi} \right] - \frac{\partial(\Pi \dot{\sigma})}{\partial \sigma} \quad (2.8)$$

from the surface to the top of the atmosphere, resulting in

$$\begin{array}{cc} \text{Tendency} & \text{Mass Convergence} \\ \frac{\partial \Pi}{\partial \tau} = - \int_0^1 \frac{1}{a \cos \phi} \left[\frac{\partial \Pi u}{\partial \lambda} + \frac{\partial (\Pi v \cos \phi)}{\partial \phi} \right] d\sigma & \end{array} \quad (2.9)$$

In equation (2.9) we have made use of the boundary condition $\dot{\sigma}(0) = \dot{\sigma}(1) = 0$.

III.2vi Equation of State

$$\alpha = RT/p$$

III.2vii Hydrostatic Equation

The following are equivalent forms of the hydrostatic equation and are used interchangeably in the derivations

$$\begin{array}{l} \frac{\partial p}{\partial \phi} = - \rho = \frac{1}{\alpha} \\ \text{or} \\ \frac{\partial \phi}{\partial p^\kappa} = - C_p \theta \\ \text{or} \\ \frac{\partial p}{\partial \sigma} = \Pi \\ \text{or} \\ \frac{\partial \phi}{\partial \sigma} = - \Pi \alpha \end{array}$$

III.2viii Equation for the Geopotential

By integrating the hydrostatic equation $\frac{\partial \phi'}{\partial p^\kappa} = - C_p \theta'$ from level $(\ell + 1)$ to level (ℓ) we obtain

$$\begin{aligned} \phi'_\ell - \phi'_{\ell+1} &= -C_p \int_{p_{\ell+1}^\kappa}^{p_\ell^\kappa} \theta' dp^\kappa \\ &= -C_p \int_{p_{\ell+1}^\kappa}^{p_\ell^\kappa} (-\bar{\theta} + \theta) dp^\kappa \\ &= C_p \bar{\theta} (p_\ell^\kappa - p_{\ell+1}^\kappa) + C_p \int_{p_\ell^\kappa}^{p_{\ell+1}^\kappa} \theta dp^\kappa \\ &= C_p \bar{\theta} (p_\ell^\kappa - p_{\ell+1}^\kappa) + C_p \int_{p_\ell^\kappa}^{p_{\ell+1}^\kappa} \frac{T}{p^\kappa} dp^\kappa \end{aligned}$$

or
$$\phi'_\ell = \phi'_{\ell+1} + C_p \bar{\theta} (p_\ell^\kappa - p_{\ell+1}^\kappa) + C_p \int_{p_\ell}^{p_{\ell+1}} \frac{T}{p^\kappa} dp^\kappa \quad (2.10)$$

The equation for ϕ'_{NLAY} is derived in finite difference form in Section 2 of Chapter IV using the following forms of the hydrostatic equation

$$\frac{\partial(\phi\sigma)}{\partial\sigma} = \phi - \sigma\Pi\alpha$$

and

$$\frac{\partial\phi}{\partial p^\kappa} = -C_p \theta$$

III.2ix Vertical Velocity (Ω and \dot{S}) Equation

From the continuity equation in Section 2v of this chapter we have

$$\frac{\partial\Pi}{\partial t} = - \frac{1}{a\cos\phi} \left[\frac{\partial\Pi u}{\partial\lambda} + \frac{\partial(\Pi v\cos\phi)}{\partial\phi} \right] - \frac{\partial(\Pi\dot{\sigma})}{\partial\sigma} \quad (2.8)$$

and

$$\frac{\partial\Pi}{\partial t} = - \int_0^1 \frac{1}{a\cos\phi} \left[\frac{\partial\Pi u}{\partial\lambda} + \frac{\partial(\Pi v\cos\phi)}{\partial\phi} \right] d\sigma \quad (2.9)$$

Vertical integration of equation (2.8) from 0 to σ results in

$$\sigma \frac{\partial\Pi}{\partial t} = - \int_0^\sigma \frac{1}{a\cos\phi} \left[\frac{\partial\Pi u}{\partial\lambda} + \frac{\partial(\Pi v\cos\phi)}{\partial\phi} \right] d\sigma - \Pi\dot{\sigma} \Big|_0^\sigma$$

and by substituting equation (2.9) in the LHS of the above equation, we obtain

$$\begin{aligned} \Pi\dot{\sigma} &= \sigma \int_0^1 \frac{1}{a\cos\phi} \left[\frac{\partial\Pi u}{\partial\lambda} + \frac{\partial(\Pi v\cos\phi)}{\partial\phi} \right] d\sigma \\ &\quad - \int_0^\sigma \frac{1}{a\cos\phi} \left[\frac{\partial\Pi u}{\partial\lambda} + \frac{\partial(\Pi v\cos\phi)}{\partial\phi} \right] d\sigma \end{aligned} \quad (2.11)$$

The equation for Omega is defined as

$$\begin{aligned}
 \omega &= \dot{\sigma}\Pi + \sigma\dot{\Pi} \\
 &= \Pi\dot{\sigma} + \sigma \left(\frac{\partial \Pi}{\partial t} + \underline{V} \cdot \nabla \Pi \right) \\
 &= \Pi\dot{\sigma} + \sigma \frac{\partial \Pi}{\partial t} + \sigma \underline{V} \cdot \nabla \Pi .
 \end{aligned}$$

Substituting the terms from equations (2.9) and (2.11), we obtain the analytic form

$$\omega = - \int_0^{\sigma} \frac{1}{a \cos \phi} \left[\frac{\partial \Pi_u}{\partial \lambda} + \frac{\partial (\Pi v \cos \phi)}{\partial \phi} \right] d\sigma + \frac{\sigma u}{a \cos \phi} \frac{\partial \Pi}{\partial \lambda} + \frac{\sigma v}{a} \frac{\partial \Pi}{\partial \phi} \quad (2.12)$$

At this point we also define $\dot{S} = \Pi\dot{\sigma}$, sometimes referred to in the model as vertical velocity, as

$$\dot{S} = - \int_0^{\sigma} \left\{ \frac{1}{a \cos \phi} \left[\frac{\partial \Pi_u}{\partial \lambda} + \frac{\partial (\Pi v \cos \phi)}{\partial \phi} \right] + \frac{\partial \Pi}{\partial t} \right\} d\sigma \quad (2.13)$$

III.3 Derivation of the Polar Equations

This section contains a presentation of the model equations at the poles in analytic form. The method of stereographic mapping of the velocities at the poles is presented first and this is followed by the derivations of the equations. The polar singularities are removed by integrating the spherical coordinate equations over a polar cap

$$\int_{\phi_1}^{\phi_2} a \cos \phi \, d\lambda \, d\phi$$

where $[\phi_1, \phi_2] = [(-1)^m \frac{\pi}{2}, (-1)^m (\frac{\pi}{2} - k\Delta\phi)]$

and $m = \begin{cases} 1 & \text{for the south pole} \\ 2 & \text{for the north pole} \end{cases}$

to the respective hydrodynamic equation.

III.3i Stereographic and Spherical Velocities

A stereographic projection is used to produce a well defined velocity vector (U_p, V_p) at the poles. To accomplish this we first look at the rotation of the axes on a plane as illustrated in Fig. III.3a. From that figure, we see that

$$u' = \frac{u}{\cos \lambda} + v' \frac{(\sin \lambda)}{\cos \lambda}$$

and $v' = \frac{v}{\cos \lambda} - u' \frac{(\sin \lambda)}{\cos \lambda}$.

Then, in matrix form
$$\begin{pmatrix} u \\ v \end{pmatrix} = \begin{pmatrix} \cos \lambda & -\sin \lambda \\ \sin \lambda & \cos \lambda \end{pmatrix} \begin{pmatrix} u' \\ v' \end{pmatrix} \quad (3.1)$$

and
$$\begin{pmatrix} u' \\ v' \end{pmatrix} = \begin{pmatrix} \cos \lambda & \sin \lambda \\ -\sin \lambda & \cos \lambda \end{pmatrix} \begin{pmatrix} u \\ v \end{pmatrix} \quad (3.2)$$

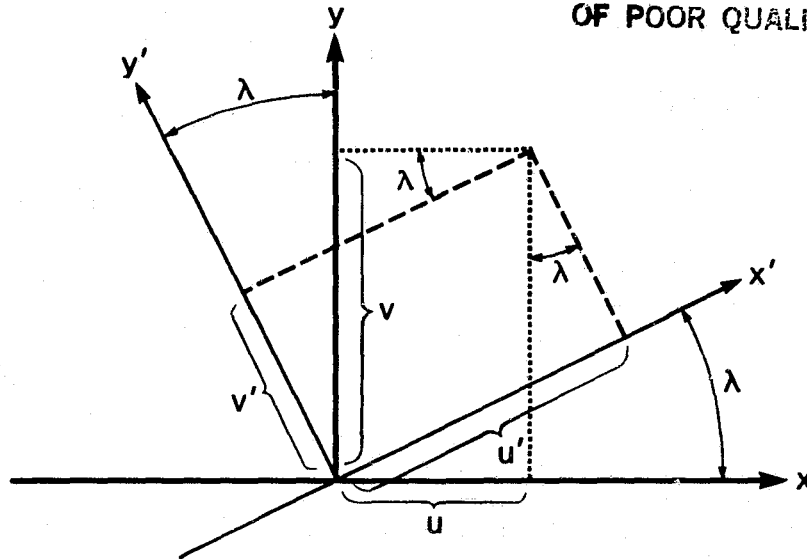


Fig. III.3a The $x'-y'$ Coordinates Relative to the $x-y$ Coordinates After a Rotation by λ Degrees

Taking a bird's eye view of the north pole (cap), we see that the stereographic velocities (U_p, V_p) can be expressed in terms of polar spherical coordinate velocities (U_λ, V_λ). From Fig. III.3b we see that the coordinate plane of (U_p, V_p) must be rotated by $(\frac{\pi}{2} + \lambda)$ in order to achieve alignment with the coordinate plane of (U_λ, V_λ).

From equation (3.1) it follows that

$$U_p = U_\lambda \cos(\frac{\pi}{2} + \lambda) - V_\lambda \sin(\frac{\pi}{2} + \lambda)$$

$$V_p = U_\lambda \sin(\frac{\pi}{2} + \lambda) + V_\lambda \cos(\frac{\pi}{2} + \lambda)$$

or

$$U_p = -U_\lambda \sin \lambda - V_\lambda \cos \lambda$$

$$V_p = U_\lambda \cos \lambda - V_\lambda \sin \lambda$$

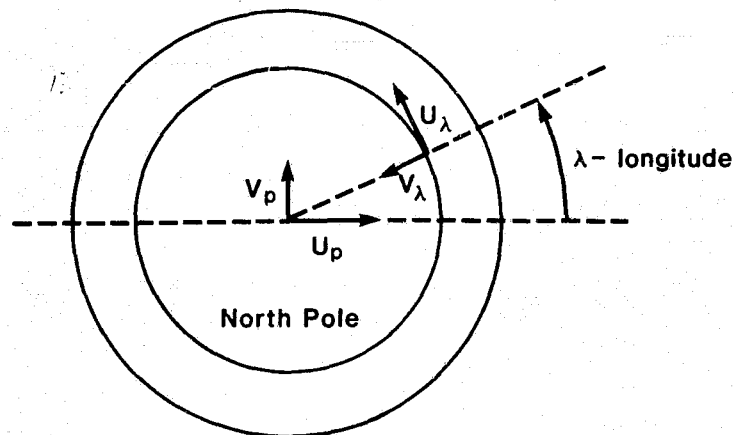


Fig. III.3b North Pole View of the Horizontal Fields (U_λ, V_λ) on the Stereographic Plane

For the south pole we see from Fig. III.3c that a rotation of $(\frac{3\pi}{2} - \lambda)$ is required to achieve the alignment of the two planes. Hence, from equation (3.1) it follows that

$$\begin{aligned} U_p &= -U_\lambda \sin \lambda + V_\lambda \sin \lambda \\ V_p &= -U_\lambda \cos \lambda - V_\lambda \sin \lambda \end{aligned}$$

In general, we have

$$\begin{aligned} U_{p_m} &= -U_\lambda \sin \lambda - (-1)^m V_\lambda \cos \lambda \\ V_{p_m} &= (-1)^m U_\lambda \cos \lambda - V_\lambda \sin \lambda \end{aligned} \quad (3.3)$$

and

$$\begin{aligned} U_\lambda &= -U_{p_m} \sin \lambda + (-1)^m V_{p_m} \cos \lambda \\ V_\lambda &= -(-1)^m U_{p_m} \cos \lambda - V_{p_m} \sin \lambda \end{aligned} \quad (3.4)$$

where

$$m = \begin{cases} 1 & \text{for the north pole} \\ 2 & \text{for the south pole} \end{cases}$$

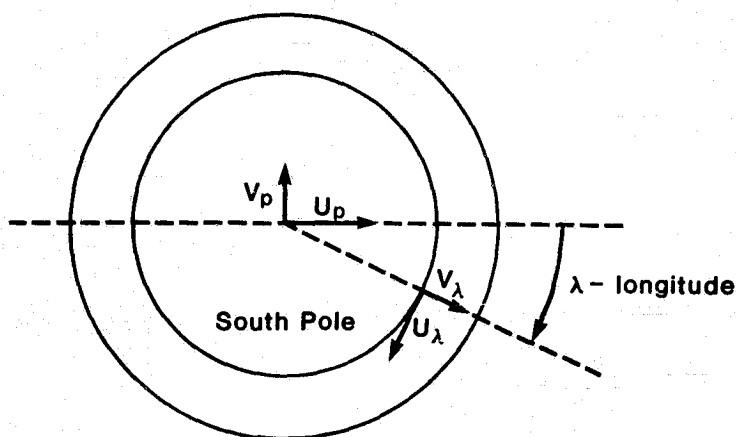


Fig. III.3c South Pole View of the Horizontal Fields (U_λ, V_λ) on the Stereographic Plane

III.3ii Continuity (Pressure Tendency) Equation

Applying to the pressure tendency equation (2.9) of Section 2 of this chapter

$$\frac{\partial \Pi}{\partial t} = - \int_0^1 \frac{1}{a \cos \phi} \left[\frac{\partial \Pi_1}{\partial \lambda} + \frac{\partial (\Pi v \cos \phi)}{\partial \phi} \right] d\sigma \quad (3.5)$$

the operator $\int_{\phi_1}^{\phi_2} \int_0^{2\pi} a \cos \phi d\lambda d\phi$

where

$$[\phi_1, \phi_2] = [(-1)^m \frac{\pi}{2}, (-1)^m (\frac{\pi}{2} - k\Delta\phi)]$$

we obtain

$$\int_0^{2\pi} \int_{\phi_1}^{\phi_2} a \cos \phi \frac{\partial \Pi}{\partial t} d\phi d\lambda = - \int_0^{2\pi} \int_{\phi_1}^{\phi_2} \int_0^1 \left[\frac{\partial \Pi_1}{\partial \lambda} + \frac{\partial (\Pi v \cos \phi)}{\partial \phi} \right] d\sigma d\phi d\lambda$$

or

$$\begin{aligned} \frac{\partial \Pi}{\partial t} \Big|_{P_m} \int_0^{2\pi} \int_{\phi_1}^{\phi_2} a \cos \phi d\phi d\lambda = & - \int_0^{2\pi} \left\{ \int_{\phi_1}^{\phi_2} \int_0^1 \frac{\partial \Pi_1}{\partial \lambda} d\lambda d\phi \right. \\ & \left. + \int_0^{2\pi} \int_{\phi_1}^{\phi_2} \frac{\partial (\Pi v \cos \phi)}{\partial \phi} d\phi d\lambda \right\} d\sigma \end{aligned}$$

(Note that in estimating the area averages of $\frac{\partial \Pi}{\partial t}$ over the polar cap by its value at the pole, we are introducing second order truncation errors (proportional to the area of the cap). Hence equation (3.6) as well as all the polar cap tendency equations of this section are accurate to within $O(\Delta\phi)^2$. In the remainder of this section, the notation $|_{P_m}$ indicates that the function is evaluated at the pole, and $|_{k_m}$ indicates that the function is evaluated at $k\Delta\phi$ degrees away from the pole.)

$$\text{or } 2\pi a (-1)^m [\cos(k\Delta\phi) - 1] \frac{\partial \Pi}{\partial t} \Big|_{P_m} = - \int_0^1 \int_0^{2\pi} [\Pi v \cos \phi] \Big|_{\phi_1}^{\phi_2} d\lambda d\sigma$$

$$\text{or } 2\pi a(-1)^m [\cos(k\Delta\phi) - 1] \left. \frac{\partial \Pi}{\partial t} \right|_{p_m} = - \int_0^1 \int_0^{2\pi} [\Pi v] \Big|_{k_m} \sin(k\Delta\phi) d\lambda d\sigma$$

$$\text{or } \left. \frac{\partial \Pi}{\partial t} \right|_{p_m} = (-1)^m \frac{\sin(k\Delta\phi)}{2\pi a[1 - \cos(k\Delta\phi)]} \int_0^1 \int_0^{2\pi} [\Pi v] \Big|_{k_m} d\lambda d\sigma \quad (3.6)$$

III.3iii Vertical Velocity (\dot{S}) Equation

$$\text{Applying the operator } \int_{\phi_1}^{\phi_2} \int_0^{2\pi} a \cos \phi d\lambda d\phi$$

$$\text{where } [\phi_1, \phi_2] = [(-1)^m \frac{\pi}{2}, (-1)^m (\frac{\pi}{2} - k\Delta\phi)]$$

to the \dot{S} equation (2.13) of Section 2 of this chapter

$$\dot{S} = - \int_0^\sigma \left\{ \frac{1}{a \cos \phi} \left[\frac{\partial \Pi_1}{\partial \lambda} + \frac{\partial (\Pi v \cos \phi)}{\partial \phi} \right] + \frac{\partial \Pi}{\partial t} \right\} d\sigma \quad (3.7)$$

we obtain

$$\int_{\phi_1}^{\phi_2} \int_0^{2\pi} a \cos \phi \dot{S} d\lambda d\phi = - \int_{\phi_1}^{\phi_2} \int_0^{2\pi} \int_0^\sigma \left\{ \frac{\partial \Pi_1}{\partial \lambda} + \frac{\partial (\Pi v \cos \phi)}{\partial \phi} \right. \\ \left. + a \cos \phi \frac{\partial \Pi}{\partial t} \right\} d\sigma d\lambda d\phi$$

or

$$\dot{S} \Big|_{p_m} \int_{\phi_1}^{\phi_2} \int_0^{2\pi} a \cos \phi d\lambda d\phi = - \int_0^1 \left\{ \int_{\phi_1}^{\phi_2} \int_0^{2\pi} \frac{\partial \Pi_1}{\partial \lambda} d\lambda d\phi + \int_{\phi_1}^{\phi_2} \frac{\partial}{\partial \phi} \left[\left(\int_0^{2\pi} \Pi v d\lambda \right) \cos \phi \right] \right. \\ \left. + \left(\frac{\partial \Pi}{\partial t} \right) \Big|_{p_m} \int_{\phi_1}^{\phi_2} \int_0^{2\pi} a \cos \phi d\lambda d\phi \right\} d\sigma$$

or

$$\dot{S} \Big|_{p_m} 2\pi a (-1)^m [\cos(k\Delta\phi) - 1] = - \int_0^\sigma \left\{ \left[\int_0^{2\pi} \Pi v d\lambda \cos \phi \right] \Big|_{\phi_1}^{\phi_2} \right. \\ \left. + \left(\frac{\partial \Pi}{\partial t} \right) \Big|_{p_m} 2\pi a (-1)^m [\cos(k\Delta\phi) - 1] \right\} d\sigma$$

or

$$\dot{S} \Big|_{P_m} = - \int_0^\sigma \left\{ \frac{(-1)^m}{2\pi a [\cos(k\Delta\phi) - 1]} \int_0^{2\pi} [\Pi v] \Big|_{k_m} d\lambda \sin(k\Delta\phi) + \left(\frac{\partial \Pi}{\partial t} \right) \Big|_{P_m} \right\} d\sigma$$

or

$$\dot{S} \Big|_{P_m} = - \int_0^\sigma \left\{ \frac{(-1)^m \sin(k\Delta\phi)}{2\pi a [\cos(k\Delta\phi) - 1]} \int_0^{2\pi} [\Pi v] \Big|_{k_m} d\lambda + \left(\frac{\partial \Pi}{\partial t} \right) \Big|_{P_m} \right\} d\sigma \quad (3.8)$$

Although Omega is not computed at the poles, the "operator" could be applied to equation (2.12) of Section 2 of this chapter in order obtain an equation for Omega.

III.3iv Zonal (U_p) Momentum Equation

At the poles, we want the equations for the tendencies of the stereographic wind components (U_p , V_p). They are obtained by multiplying the u-momentum equation (2.1) and the v-momentum equation (2.2) of Section 2 of this chapter by two functions, $s(\lambda)$ and $c(\lambda)$ respectively, and by adding the terms. This results in the following equation

$$\begin{aligned} \frac{\partial}{\partial t} [\Pi(us(\lambda) + vc(\lambda))] = & - \frac{1}{a \cos \phi} \left\{ \frac{\partial}{\partial \lambda} [\Pi u(us(\lambda) + vc(\lambda))] \right. \\ & + \frac{\partial}{\partial \phi} [\Pi v \cos \phi (us(\lambda) + vc(\lambda))] \} \\ & - \frac{\partial}{\partial \sigma} [\Pi \dot{\sigma} (us(\lambda) + vc(\lambda))] \\ & - \frac{\Pi s(\lambda)}{a \cos \phi} \left[\frac{\partial \phi}{\partial \lambda} + \frac{\sigma R T}{p} \frac{\partial \Pi}{\partial \lambda} \right] - \frac{\Pi c(\lambda)}{a} \left[\frac{\partial \phi}{\partial \phi} + \frac{\sigma R T}{p} \frac{\partial \Pi}{\partial \phi} \right] \\ & + f \Pi (vs(\lambda) - uc(\lambda)) + \Pi [F_x s(\lambda) + F_y c(\lambda)] \\ & + \frac{\Pi u}{a \cos \phi} \left[u \frac{\partial s(\lambda)}{\partial \lambda} + v \frac{\partial c(\lambda)}{\partial \lambda} \right] \\ & - \frac{u \Pi \tan \phi}{a} [uc(\lambda) - vs(\lambda)] \end{aligned} \quad (3.9)$$

This is the general equation that will be used to express the u and v momentum equations at the poles.

From equation (3.3)

$$U_{p_m} = (-\sin\lambda) u + (-(-1)^m \cos\lambda) v.$$

Comparing this expression with the left hand side of equation (3.9) we see that an equation for U_{p_m} at the pole can be obtained by taking $s(\lambda) = -\sin\lambda$ and $c(\lambda) = -(-1)^m \cos(\lambda)$.

Substituting these terms in equation (3.9) we obtain

$$\begin{aligned} \frac{\partial}{\partial t} (\Pi U_{p_m}) = & - \frac{1}{a \cos \phi} \frac{\partial}{\partial \lambda} (\Pi u U_{p_m}) \\ & - \frac{1}{a \cos \phi} \frac{\partial}{\partial \phi} (\Pi v \cos \phi U_{p_m}) \\ & - \frac{\partial}{\partial \sigma} (\Pi \sigma U_{p_m}) \\ & + \frac{\Pi}{a} \frac{\sin \lambda}{\cos \phi} \left[\frac{\partial \phi'}{\partial \lambda} + \frac{\sigma R T'}{p} \frac{\partial \Pi}{\partial \phi} \right] \\ & + \frac{(-1)^m \Pi \cos \lambda}{a} \left[\frac{\partial \phi'}{\partial \phi} + \frac{\sigma R T'}{p} \frac{\partial \Pi}{\partial \phi} \right] \\ & + f \Pi V_{p_m} \\ & + \Pi \left[-F_x \sin \lambda - (-1)^m F_y \cos \lambda \right] \\ & - \frac{\Pi u V_{p_m}}{a \cos \phi} \left[(-1)^m - \sin \phi \right] \end{aligned} \quad (3.10)$$

The last term is neglected since it is $O(\Delta\phi)^2$ smaller than the other terms near the poles.

Next we apply the operator $\int_{\phi_1}^{\phi_2} \int_0^{2\pi} () a \cos \phi d\lambda d\phi$

where $[\phi_1, \phi_2] = [(-1)^m \frac{\pi}{2}, (-1)^m (\frac{\pi}{2} - k\Delta\phi)]$

and $m = \begin{cases} 1 & \text{for the south pole} \\ 2 & \text{for the north pole} \end{cases}$

to equation (3.10) and obtain the following for each of the terms

$$\begin{aligned} \text{LHS} &= \int_{\phi_1}^{\phi_2} \int_0^{2\pi} a \cos \phi \frac{\partial}{\partial t} (\Pi U_{P_m}) d\lambda d\phi \\ &= \frac{\partial}{\partial t} (\Pi U_{P_m}) \Big|_{P_m} \int_{\phi_1}^{\phi_2} \int_0^{2\pi} a \cos \phi d\lambda d\phi \\ &= \frac{\partial}{\partial t} (\Pi U_{P_m}) \Big|_{P_m} 2\pi a [\sin \phi_2 - \sin \phi_1] \\ &= \frac{\partial}{\partial t} (\Pi U_{P_m}) 2\pi a (-1)^m [\cos(k\Delta\phi) - 1] \end{aligned}$$

RHS

$$\begin{aligned} \text{First Term} &= - \int_{\phi_1}^{\phi_2} \int_0^{2\pi} \frac{\partial}{\partial \lambda} (\Pi u U_{P_m}) d\lambda d\phi \\ &= 0 \end{aligned}$$

$$\begin{aligned} \text{Second Term} &= - \int_{\phi_1}^{\phi_2} \int_0^{2\pi} \frac{\partial}{\partial \phi} (\Pi v \cos \phi U_{P_m}) d\lambda d\phi \\ &= - \int_{\phi_1}^{\phi_2} \frac{\partial}{\partial \phi} \left[\left(\int_0^{2\pi} \Pi v U_{P_m} d\lambda \right) \cos \phi \right] d\phi \\ &= - \left[\int_0^{2\pi} \Pi v U_{P_m} d\lambda \cos \phi \right]_{\phi_1}^{\phi_2} \\ &= - \left[\int_0^{2\pi} \Pi v U_{P_m} d\lambda \right] \Big|_{k_m} \sin(k\Delta\phi) \end{aligned}$$

$$\begin{aligned} \text{Third term} &= - \int_{\phi_1}^{\phi_2} \int_0^{2\pi} a \cos \phi \frac{\partial}{\partial \sigma} (\Pi \dot{\sigma} U_{P_m}) d\lambda d\phi \\ &= - \frac{\partial}{\partial \sigma} (\Pi \dot{\sigma} U_{P_m}) \Big|_{P_m} \int_{\phi_1}^{\phi_2} \int_0^{2\pi} a \cos \phi d\lambda d\phi \end{aligned}$$

$$= - \frac{\partial}{\partial \sigma} (\Pi \sigma U_{p_m}) \Big|_{p_m} 2\pi a (-1)^m [\cos(k\Delta\phi) - 1]$$

$$\begin{aligned} \text{Fourth Term} &= \int_{\phi_1}^{\phi_2} \int_0^{2\pi} \Pi \sin \lambda \left[\frac{\partial \Phi'}{\partial \lambda} + \frac{\sigma RT'}{p} \frac{\partial \Pi}{\partial \lambda} \right] d\lambda d\phi \\ &\approx \Pi_{p_m} \int_{\phi_1}^{\phi_2} \left\{ \int_0^{2\pi} \sin \lambda \frac{\partial \Phi'}{\partial \lambda} + \left(\frac{\sigma RT'}{p} \right) \Big|_{p_m} \int_0^{2\pi} \sin \lambda \frac{\partial \Pi}{\partial \lambda} d\lambda \right\} d\phi \\ &= \Pi_{p_m} \int_{\phi_1}^{\phi_2} \left\{ \left[\sin \lambda \Phi' \right]_0^{2\pi} - \int_0^{2\pi} \Phi' \cos \lambda d\lambda \right. \\ &\quad \left. + \left(\frac{\sigma RT'}{p} \right)_{p_m} \left[\sin \lambda \Pi \right]_0^{2\pi} - \left(\frac{\sigma RT'}{p} \right)_{p_m} \int_0^{2\pi} \cos \lambda \Pi d\lambda \right\} d\phi \\ &= \Pi_{p_m} \int_{\phi_1}^{\phi_2} \left\{ 0 - \Phi'_{p_m} \int_0^{2\pi} \cos \lambda d\lambda \right. \\ &\quad \left. + \left(\frac{\sigma RT'}{p} \right)_{p_m} (0) - \left(\frac{\sigma RT'}{p} \right)_{p_m} \Pi_{p_m} \int_0^{2\pi} \cos \lambda d\lambda \right\} d\phi \\ &= 0 \end{aligned}$$

$$\begin{aligned} \text{Fifth Term} &= (-1)^m \int_{\phi_1}^{\phi_2} \int_0^{2\pi} \Pi \cos \lambda \cos \phi \left[\frac{\partial \Phi'}{\partial \phi} + \frac{\sigma RT'}{p} \frac{\partial \Pi}{\partial \phi} \right] d\lambda d\phi \\ &= (-1)^m \Pi_{p_m} \int_0^{2\pi} \cos \lambda \left\{ \int_{\phi_1}^{\phi_2} \cos \phi \frac{\partial \Phi'}{\partial \phi} d\phi + \left(\frac{\sigma RT'}{p} \right)_{p_m} \int_{\phi_1}^{\phi_2} \cos \phi \frac{\partial \Pi}{\partial \phi} d\phi \right\} d\lambda \\ &= (-1)^m \Pi_{p_m} \int_0^{2\pi} \cos \lambda \left\{ \left[\Phi' \cos \phi \right]_{\phi_1}^{\phi_2} + \int_{\phi_1}^{\phi_2} \Phi' \sin \phi d\phi \right. \\ &\quad \left. + \left(\frac{\sigma RT'}{p} \right)_{\text{pole}} \left(\left[\Pi \cos \phi \right]_{\phi_1}^{\phi_2} + \int_{\phi_1}^{\phi_2} \Pi \sin \phi d\phi \right) \right\} d\lambda \end{aligned}$$

ORIGINAL PAGE 14
OF POOR QUALITY.

$$\begin{aligned}
 &= (-1)^m \Pi_{p_m} \int_0^{2\pi} \cos \lambda \left\{ \Phi' \Big|_{k_m} \sin(k\Delta\phi) + \Phi'_{p_m} \int_{\phi_1}^{\phi_2} \sin \phi \, d\phi \right. \\
 &\quad \left. + \left(\frac{\sigma RT'}{p} \right)_{p_m} \left[\Pi \Big|_{k_m} \sin(k\Delta\phi) + \Pi_{p_m} \int_{\phi_1}^{\phi_2} \sin \phi \, d\phi \right] \right\} d\lambda \\
 &= (-1)^m \Pi_{p_m} \int_0^{2\pi} \cos \lambda \left\{ \Phi' \Big|_{k_m} \sin(k\Delta\phi) + \left(\frac{\sigma RT'}{p} \right)_{p_m} \Pi \Big|_{k_m} \sin(k\Delta\phi) \right\} d\lambda \\
 &= (-1)^m \sin(k\Delta\phi) \Pi_{p_m} \int_0^{2\pi} \cos \lambda \left[\Phi' \Big|_{k_m} + \left(\frac{\sigma RT'}{p} \right)_{p_m} \Pi \Big|_{k_m} \right] d\lambda
 \end{aligned}$$

$$\begin{aligned}
 \text{Sixth Term} &= \int_0^{2\pi} \int_{\phi_1}^{\phi_2} f \Pi v_{p_m} a \cos \phi \, d\phi \, d\lambda \\
 &= (f \Pi v_{p_m})_{p_m} 2\pi a (-1)^m [\cos(k\Delta\phi) - 1]
 \end{aligned}$$

$$\begin{aligned}
 \text{Seventh Term} &= \int_0^{2\pi} \int_{\phi_1}^{\phi_2} \Pi F_{x_{p_m}} a \cos \phi \, d\phi \, d\lambda \\
 &= \Pi_{p_m} F_{x_{p_m}} 2\pi a (-1)^m [\cos(k\Delta\phi) - 1]
 \end{aligned}$$

Therefore, the fully integrated equation (3.10) is

$$\begin{aligned}
 &2\pi a (-1)^m [\cos(k\Delta\phi) - 1] \frac{\partial}{\partial t} (\Pi_{p_m}) \\
 &= -\sin(k\Delta\phi) \left[\int_0^{2\pi} \Pi v_{p_m} \, d\lambda \right] \Big|_{k_m}
 \end{aligned}$$

$$\begin{aligned}
 & - 2\pi a (-1)^m [\cos(k\Delta\phi) - 1] \frac{\partial}{\partial \sigma} (\Pi \sigma U_{P_m}) \Big|_{P_m} \\
 & + (-1)^m \sin(k\Delta\phi) \Pi_{P_m} \int_0^{2\pi} \cos \lambda \left[\phi' \Big|_{k_m} + \left(\frac{\sigma R T'}{P} \right)_{P_m} \Pi' \Big|_{k_m} \right] d\lambda \\
 & + (f \Pi V_{P_m})_{P_m} 2\pi a (-1)^m [\cos(k\Delta\phi) - 1] \\
 & + \Pi_{P_m} F_{x_{P_m}} 2\pi a (-1)^m [\cos(k\Delta\phi) - 1] \tag{3.11}
 \end{aligned}$$

or

$$\begin{aligned}
 \frac{\partial}{\partial t} (\Pi U_{P_m}) & = \frac{(-1)^m \sin(k\Delta\phi)}{2\pi a [1 - \cos(k\Delta\phi)]} \int_0^{2\pi} \Pi v U_{P_m} d\lambda \Big|_{k_m} \\
 & - \frac{\partial}{\partial \sigma} (\Pi \sigma U_{P_m}) \Big|_{P_m} \\
 & - \frac{\sin(k\Delta\phi)}{2\pi a [1 - \cos(k\Delta\phi)]} \Pi_{P_m} \int_0^{2\pi} \cos \lambda \left[\phi' \Big|_{k_m} + \left(\frac{\sigma R T'}{P} \right)_{P_m} \Pi \Big|_{k_m} \right] d\lambda \\
 & + (f \Pi V_{P_m}) \Big|_{P_m} \\
 & + \Pi_{P_m} F_{x_{P_m}} \tag{3.12}
 \end{aligned}$$

III.3v Meridional (V_{P_m}) Momentum Equation

As with the zonal momentum equation, from equation (3.3) we see that in order to obtain the equation for V_{P_m} at the pole we need to take $s(\lambda) = (-1)^m \cos \lambda$ and $c(\lambda) = -\sin \lambda$.

This results in the equation

ORIGINAL PAGE IS
OF POOR QUALITY

$$\begin{aligned}
 \frac{\partial}{\partial t} (\Pi V_{p_m}) = & - \frac{1}{a \cos \phi} \frac{\partial}{\partial \lambda} (\Pi u V_{p_m}) \\
 & - \frac{1}{a \cos \phi} \frac{\partial}{\partial \phi} (\Pi v \cos \phi V_{p_m}) \\
 & - \frac{\partial}{\partial \sigma} (\Pi \dot{\sigma} V_{p_m}) \\
 & - (-1)^m \frac{\Pi \cos \lambda}{a \cos \phi} \left[\frac{\partial \Phi'}{\partial \lambda} + \frac{\sigma RT'}{p} \frac{\partial \Pi}{\partial \lambda} \right] \\
 & + \frac{\Pi \sin \lambda}{a} \left[\frac{\partial \Phi'}{\partial \phi} + \frac{\sigma RT'}{p} \frac{\partial \Pi}{\partial \phi} \right] \\
 & - f \Pi U_{p_m} \\
 & + \Pi [(-1)^m F_x \cos \lambda - F_y \sin \lambda] \\
 & + \frac{\Pi u U}{a \cos \phi} [(-1)^m - \sin \phi]
 \end{aligned} \tag{3.13}$$

The derivation of the ΠV_{p_m} equation for the polar cap is similar to that of ΠU_{p_m} and results in

$$\begin{aligned}
 \frac{\partial}{\partial t} (\Pi V_{p_m}) = & \frac{(-1)^m \sin(k\Delta\phi)}{2\pi a [1 - \cos(k\Delta\phi)]} \left[\int_0^{2\pi} \Pi v V_{p_m} d\lambda \right] \Big|_{k_m} \\
 & - \left[\frac{\partial}{\partial \sigma} (\Pi \dot{\sigma} V_{p_m}) \right] \Big|_{p_m} \\
 & - \frac{(-1)^m \sin(k\Delta\phi)}{2\pi a [1 - \cos(k\Delta\phi)]} \Pi_{p_m} \int_0^{2\pi} \sin \lambda \left[\Phi' \Big|_{k_m} + \left(\frac{\sigma RT'}{p} \right)_{p_m} \Pi \Big|_{k_m} \right] d\lambda \\
 & - (f \Pi U_{p_m})_{p_m} \\
 & + \Pi_{p_m} F_{y_p}
 \end{aligned} \tag{3.14}$$

III.3vi Thermodynamic Energy Equation

From the thermodynamic equation (2.6) of Section 2 of this chapter we have

$$\begin{aligned}
 \frac{\partial}{\partial t} (\Pi T) &= - \frac{1}{a \cos \phi} \frac{\partial}{\partial \lambda} (\Pi u T) \\
 &\quad - \frac{1}{a \cos \phi} \frac{\partial}{\partial \phi} (\Pi v \cos \phi T) \\
 &\quad - p^{\kappa} \frac{\partial}{\partial \sigma} \left(\frac{\Pi \sigma T}{p^{\kappa}} \right) \\
 &\quad + \frac{\Pi \sigma \kappa T}{p} \left\{ \frac{\partial \Pi}{\partial t} + \frac{u}{a \cos \phi} \frac{\partial \Pi}{\partial \lambda} + \frac{v}{a} \frac{\partial \Pi}{\partial \phi} \right\} + \frac{\Pi Q}{C_p}
 \end{aligned} \tag{3.15}$$

By applying the same operator $\int_{\phi_1}^{\phi_2} \int_0^{2\pi} a \cos \phi \, d\lambda \, d\phi$

where $[\phi_1, \phi_2] = [(-1)^m \frac{\pi}{2}, (-1)^m (\frac{\pi}{2} - k\Delta\phi)]$

to each of the terms of equation (3.15) we obtain the following (refer to similar terms for U_p when possible)

$$\begin{aligned}
 \underline{\text{LHS}} &= \int_{\phi_1}^{\phi_2} \int_0^{2\pi} a \cos \phi \frac{\partial}{\partial t} (\Pi T) \, d\lambda \, d\phi \\
 &= \frac{\partial}{\partial t} (\Pi T) \Big|_{p_m} \int_{\phi_1}^{\phi_2} \int_0^{2\pi} a \cos \phi \, d\lambda \, d\phi \\
 &= \frac{\partial}{\partial t} (\Pi T) \Big|_{p_m} 2\pi a [\sin \phi_2 - \sin \phi_1] \\
 &= \frac{\partial}{\partial t} (\Pi T) \Big|_{p_m} 2\pi a (-1)^m [\cos(k\Delta\phi) - 1]
 \end{aligned}$$

RHS

$$\begin{aligned}\text{First Term} &= - \int_0^{\phi_2} \int_{\phi_1}^{2\pi} \frac{\partial}{\partial \lambda} (\Pi T) d\phi d\lambda \\ &= 0\end{aligned}$$

$$\begin{aligned}\text{Second Term} &= - \int_{\phi_1}^{\phi_2} \int_0^{2\pi} \frac{\partial}{\partial \phi} [\Pi v \cos \phi T] d\lambda d\phi \\ &= - \int_{\phi_1}^{\phi_2} \frac{\partial}{\partial \phi} \left[\left(\int_0^{2\pi} \Pi v T d\lambda \right) \cos \phi \right] d\phi \\ &= - \left[\int_0^{2\pi} \Pi v T d\lambda \cos \phi \right] \Big|_{\phi_1}^{\phi_2} \\ &= - \left[\int_0^{2\pi} \Pi v T d\lambda \right] \Big|_{k_m} \sin(k\Delta\phi)\end{aligned}$$

$$\begin{aligned}\text{Third Term} &= - \int_{\phi_1}^{\phi_2} \int_0^{2\pi} a \cos \phi p^\kappa \frac{\partial}{\partial \sigma} \left(\frac{\Pi \dot{\sigma} T}{p^\kappa} \right) d\lambda d\phi \\ &= - \left[p^\kappa \frac{\partial}{\partial \sigma} \left(\frac{\Pi \dot{\sigma} T}{p^\kappa} \right) \right] \Big|_{p_m} \int_{\phi_1}^{\phi_2} \int_0^{2\pi} a \cos \phi d\lambda d\phi \\ &= - \left[p^\kappa \frac{\partial}{\partial \sigma} \left(\frac{\Pi \dot{\sigma} T}{p^\kappa} \right) \right] \Big|_{p_m} 2\pi a (-1)^m [\cos(k\Delta\phi) - 1]\end{aligned}$$

$$\begin{aligned}\text{Fourth Term} &= \int_{\phi_1}^{\phi_2} \int_0^{2\pi} a \cos \phi \frac{\Pi \sigma \kappa T}{p} \left\{ \frac{\partial \Pi}{\partial t} + \frac{u}{a \cos \phi} + \frac{v}{a} \frac{\partial \Pi}{\partial \phi} \right\} d\lambda d\phi \\ &= \left[\frac{\Pi \sigma \kappa T}{p} \right] \Big|_{p_m} \int_{\phi_1}^{\phi_2} \int_0^{2\pi} \left\{ a \cos \phi \frac{\partial \Pi}{\partial t} + u \frac{\partial \Pi}{\partial \lambda} + \cos \phi v \frac{\partial \Pi}{\partial \phi} \right\} d\lambda d\phi \\ &= \left[\frac{\Pi \sigma \kappa T}{p} \right] \Big|_{p_m} \left\{ \frac{\partial \Pi}{\partial t} \right|_{p_m} \int_{\phi_1}^{\phi_2} \int_0^{2\pi} a \cos \phi d\lambda d\phi\end{aligned}$$

ORIGINAL PAGE 18
OF POOR QUALITY

$$\begin{aligned}
 & + u \Big|_{P_m} \int_{\phi_1}^{\phi_2} \int_0^{2\pi} \frac{\partial \Pi}{\partial \lambda} d\lambda d\phi + \int_0^{2\pi} \left(v \frac{\partial \Pi}{\partial \phi} \right) \Big|_{P_m} \int_{\phi_1}^{\phi_2} \cos \phi d\phi d\lambda \Big\} \\
 & = \left[\frac{\Pi \sigma \kappa T}{p} \right] \Big|_{P_m} \left\{ 2\pi a (-1)^m [\cos(k\Delta\phi) - 1] \frac{\partial \Pi}{\partial E} + 0 \right. \\
 & \quad \left. + (-1)^m [\cos(k\Delta\phi) - 1] \int_0^{2\pi} v \Big|_{P_m} \frac{\partial \Pi}{\partial \phi} \Big|_{P_m} d\lambda \right\}
 \end{aligned}$$

(Note that $v \Big|_{P_m} = -(-1)^m U_{P_m} \cos \lambda - V_{P_m} \sin \lambda$.)

$$\begin{aligned}
 \text{Fifth term} & = \int_{\phi_1}^{\phi_2} \int_0^{2\pi} a \cos \phi \frac{\Pi Q}{C_p} d\lambda d\phi \\
 & = \left(\frac{\Pi Q}{C_p} \right) \Big|_{P_m} \int_{\phi_1}^{\phi_2} \int_0^{2\pi} a \cos \phi d\lambda d\phi \\
 & = \left(\frac{\Pi Q}{C_p} \right) \Big|_{P_m} 2\pi a (-1)^m [\cos(k\Delta\phi) - 1]
 \end{aligned}$$

As a result, the fully integrated equation (3.15) is

$$\begin{aligned}
 & 2\pi a (-1)^m [\cos(k\Delta\phi) - 1] \left(\frac{\partial \Pi T}{\partial t} \right) \Big|_{P_m} \\
 & = - \sin(k\Delta\phi) \left[\int_0^{2\pi} \Pi v T d\lambda \right] \Big|_{k_m} \\
 & \quad - 2\pi a (-1)^m [\cos(k\Delta\phi) - 1] \left[p^\kappa \frac{\partial}{\partial \sigma} \left(\frac{\Pi \sigma T}{p^\kappa} \right) \right] \Big|_{P_m} \\
 & \quad + \left[\frac{\Pi \sigma \kappa T}{p} \right]_{P_m} \left\{ 2\pi a (-1)^m [\cos(k\Delta\phi) - 1] \frac{\partial \Pi}{\partial E} \Big|_{P_m} \right. \\
 & \quad \left. + (-1)^m [\cos(k\Delta\phi) - 1] \int_0^{2\pi} v \Big|_{P_m} \frac{\partial \Pi}{\partial \phi} \Big|_{P_m} d\lambda \right\} \\
 & \quad + 2\pi a (-1)^m [\cos(k\Delta\phi) - 1] \left(\frac{\Pi Q}{C_p} \right) \Big|_{P_m} \tag{3.16}
 \end{aligned}$$

or

$$\begin{aligned}
 \left(\frac{\partial \Pi}{\partial t} \right) \Big|_{p_m} &= \frac{(-1)^m \sin(k\Delta\phi)}{2\pi a [1 - \cos(k\Delta\phi)]} \left[\int_0^{2\pi} \Pi v T d\lambda \right] \Big|_{k_m} \\
 &\quad - \left[p^\kappa \frac{\partial}{\partial \sigma} \left(\frac{\Pi \dot{\sigma} T}{p^\kappa} \right) \right] \Big|_{p_m} \\
 &\quad + \left[\frac{\Pi \sigma \kappa T}{p} \right]_{p_m} \left\{ \frac{\partial \Pi}{\partial t} \Big|_{p_m} + \frac{1}{2\pi a} \int_0^{2\pi} v \Big|_{p_m} \frac{\partial \Pi}{\partial \phi} \Big|_{p_m} d\lambda \right\} \\
 &\quad + \left(\frac{\Pi Q}{C_p} \right) \Big|_{p_m}
 \end{aligned} \tag{3.17}$$

III.3vii Moisture Equation

Similarly, we apply to the moisture equation (2.7) of Section 2 of this chapter

$$\begin{aligned}
 \frac{\partial}{\partial t} (\Pi q) &= - \frac{1}{a \cos \phi} \frac{\partial}{\partial \lambda} (\Pi u q) \\
 &\quad - \frac{1}{a \cos \phi} \frac{\partial}{\partial \lambda} (\Pi v \cos \phi q) \\
 &\quad - \frac{\partial}{\partial \sigma} (\Pi \dot{\sigma} q) \\
 &\quad + \Pi (E - C)
 \end{aligned} \tag{3.18}$$

the operator $\int_{\phi_1}^{\phi_2} \int_0^{2\pi} a \cos \phi d\lambda d\phi$

where $[\phi_1, \phi_2] = [(-1)^m \frac{\pi}{2}, (-1)^m (\frac{\pi}{2} - k\Delta\phi)]$

and obtain

$$\begin{aligned}
 \frac{\partial}{\partial t} (\Pi q) \Big|_{p_m} &= \frac{(-1)^m \sin(k\Delta\sigma)}{2\pi a [1 - \cos(k\Delta\phi)]} \left[\int_0^{2\pi} \Pi v q d\lambda \right] \Big|_{k_m} \\
 &\quad - \left[\frac{\partial}{\partial \sigma} (\Pi \dot{\sigma} q) \right] \Big|_{p_m} \\
 &\quad + \left[\Pi (E - C) \right] \Big|_{p_m}
 \end{aligned} \tag{3.19}$$

III.3viii Equation for the Geopotential

The equation for the geopotential at the pole has the same form as the equation for non-polar grid points.

CHAPTER IV

HYDRODYNAMICS

RAMESH C. BALGOVIND

IV. HYDRODYNAMICS

IV.1 Introduction

In this chapter we present the hydrodynamic terms of the governing equations in finite difference form.

The following operators will be used throughout this chapter:

$$\bar{q}_{i,j}^{\lambda} = \frac{1}{2} (q_{i+1/2,j} + q_{i-1/2,j}) \quad (\text{averaging})$$

$$\bar{q}_{i,j}^{2\lambda} = \frac{1}{2} (q_{i+1,j} + q_{i-1,j})$$

$$\delta_{\lambda} q_{i,j} = \frac{1}{\Delta\lambda} (q_{i+1/2,j} - q_{i-1/2,j}) \quad (\text{2nd order } \frac{\partial q}{\partial \lambda})$$

$$\delta_{\lambda} \bar{q}_{i,j}^{\lambda} = \delta_{2\lambda} q_{i,j} = \frac{1}{2\Delta\lambda} (q_{i+1,j} - q_{i-1,j})$$

Using these definitions, fourth order differences for $\frac{\partial q}{\partial \lambda}$ may be expressed as

$$\left(\frac{\partial q}{\partial \lambda} \right)_{i,j} = \frac{4}{3} \delta_{\lambda} (\bar{q}_{i,j}^{\lambda}) - \frac{1}{3} \delta_{2\lambda} (\bar{q}_{i,j}^{2\lambda})$$

Similar finite difference operators are defined for $\delta_{\phi} q$, \bar{q}^{ϕ} , etc.

When meridional finite differences are evaluated at latitudes one or two grid points away from the poles, it becomes necessary to make use of quantities q_{ij} defined at the poles or "beyond" the poles. In that case the following definitions are used:

$$q_{i,JP} = q_{JP} \quad (\text{evaluation at the pole})$$

where q_{JP} is the value of q at the polar latitude JP . If $q_{i,JP}$ is a spherical velocity component, then q_{JP} is the corresponding spherical velocity component evaluated as in III.3i, equation (3.4) with $\lambda = \lambda_1$.

And

$$q_{i,JP+1} = s \, q_{i \pm IM/2,JP-1} \quad (\text{evaluation "beyond" the pole})$$

This corresponds to the value of $q_{i,JP1}$ obtained by going "over the pole" along the continuation of the meridian of longitude λ_1 , which has a longitude $\lambda_1 \pm \pi$. The model variable INDEX(I) identifies the index $i \pm IM/2$. The sign s is +1 for scalars and -1 for vector components.

IV.2 Hydrodynamic Terms (Finite Difference)

IV.2i Horizontal Fluxes (Subroutine COMPl)

Let Q be any arbitrary quantity undergoing horizontal advection. Then the horizontal divergence of mass flux of Q, expressed by

$$\frac{1}{a \cos \phi} \left[\frac{\partial (\Pi u Q)}{\partial \lambda} + \frac{\partial (\Pi v \cos \phi Q)}{\partial \phi} \right]$$

is approximated in finite difference form at grid point (i, j, k) as

$$\begin{aligned} & \frac{1}{a \cos \phi_j} \left\{ \frac{4}{3} \delta_\lambda \left[(\overline{\Pi u})_{i,j}^\lambda \overline{Q}_{i,j}^\lambda \right] - \frac{1}{3} \delta_{2\lambda} \left[(\overline{\Pi u})_{i,j}^{2\lambda} \overline{Q}_{i,j}^{2\lambda} \right] \right. \\ & \left. + \frac{4}{3} \delta_\phi \left[(\overline{\Pi v \cos \phi})_{i,j}^\phi \overline{Q}_{i,j}^\phi \right] - \frac{1}{3} \delta_{2\phi} \left[(\overline{\Pi v \cos \phi})_{i,j}^{2\phi} \overline{Q}_{i,j}^{2\phi} \right] \right\} \end{aligned} \quad (2.1)$$

IV.2ii Vertical Fluxes (Subroutine COMPl)

Let Q be any arbitrary quantity undergoing vertical advection. The vertical gradient of mass flux of Q, defined by

$$\frac{\partial (\Pi \dot{\sigma} Q)}{\partial \sigma} \quad \text{or} \quad \frac{\partial (\dot{S} Q)}{\partial \sigma} \quad \text{where } \dot{S} = \Pi \dot{\sigma} ,$$

is approximated in finite difference form at grid point (i, j, k) as

$$\frac{\dot{S}_{k-1} (q_k + q_{k-1}) - \dot{S}_k (q_k + q_{k+1})}{2 \Delta \sigma_k} \quad (2.2)$$

For clarity, the use of the subscripts i and j has been discontinued.

For the computation of moisture flux, the code is modified to ensure that no flux of moisture leaves a grid cell which is already dry. Thus, if $(\Pi q)_{ijl}^n \leq 0$ then the moisture fluxes out of grid point ijl are required to be zero.

IV.2iii Pressure Gradient Force (Subroutine COMP2)

The longitudinal component of the pressure gradient is given by

$$\frac{\Pi}{a \cos \phi} \left[\frac{\partial \phi'}{\partial \lambda} + \frac{\sigma RT'}{p} \frac{\partial \Pi}{\partial \lambda} \right]$$

This is approximated in finite difference form at grid point (i, j, k) by

$$\begin{aligned} & \frac{\Pi_{i,j}}{a \cos \phi_j} \left\{ \left[\frac{4}{3} \delta_\lambda (\bar{\phi}_{i,j,k}^\lambda) - \frac{1}{3} \delta_{2\lambda} (\bar{\phi}_{i,j,k}^{2\lambda}) \right] \right. \\ & \left. + \frac{\sigma_k RT'_{i,j,k}}{p_{i,j,k}} \left[\frac{4}{3} \delta_\lambda (\bar{\Pi}_{i,j}^\lambda) - \frac{1}{3} \delta_{2\lambda} (\bar{\Pi}_{i,j}^{2\lambda}) \right] \right\} \end{aligned} \quad (2.3)$$

Similarly, the meridional component of the pressure gradient, given by

$$\frac{\Pi}{a} \left[\frac{\partial \phi'}{\partial \phi} + \frac{\sigma RT'}{p} \frac{\partial \Pi}{\partial \phi} \right],$$

is approximated by

$$\begin{aligned} & \frac{\Pi_{i,j}}{a} \left\{ \left[\frac{4}{3} \delta_\phi (\bar{\phi}_{i,j,k}^\phi) - \frac{1}{3} \delta_{2\phi} (\bar{\phi}_{i,j,k}^{2\phi}) \right] \right. \\ & \left. + \frac{\sigma_k RT'_{i,j,k}}{p_{i,j,k}} \left[\frac{4}{3} \delta_\phi (\bar{\Pi}_{i,j}^\phi) - \frac{1}{3} \delta_{2\phi} (\bar{\Pi}_{i,j}^{2\phi}) \right] \right\} \end{aligned} \quad (2.4)$$

IV.2iv Coriolis Term (Subroutine COMP2)

The Coriolis term for the u-momentum equation is

$$\left(f_j + \frac{u_{i,j,k} \tan \phi}{a} \right) (\Pi v)_{i,j,k}$$

and for the v-momentum equation the Coriolis term is

$$\left(f_j + \frac{u_{i,j,k} \tan \phi}{a} \right) (\Pi u)_{i,j,k} \quad (2.5)$$

IV.2v Energy Conversion Terms (Subroutine COMP2)

The term

$$\frac{\pi \sigma k T}{p} \left(\frac{\partial \pi}{\partial t} + \frac{u}{a \cos \phi} \frac{\partial \pi}{\partial \lambda} + \frac{v}{a} \frac{\partial \pi}{\partial \phi} \right)$$

for the thermodynamic equation is expressed in finite difference form at grid point (i, j, k) as

$$\begin{aligned} & \frac{\sigma_{i,j,k} k T_{i,j,k}}{p_{i,j,k}} \left\{ \pi_{i,j} \frac{\partial \pi_{i,j,k}}{\partial t} \right. \\ & + \frac{(\pi u)_{i,j,k}}{a \cos \phi_j} \left[\frac{4}{3} \delta_\lambda (\bar{\pi}_{i,j}^\lambda) - \frac{1}{3} \delta_{2\lambda} (\bar{\pi}_{i,j}^{2\lambda}) \right] \\ & \left. + \frac{(\pi v)_{i,j,k}}{a} \left[\frac{4}{3} \delta_\phi (\bar{\pi}_{i,j}^\phi) - \frac{1}{3} \delta_{2\phi} (\bar{\pi}_{i,j}^{2\phi}) \right] \right\} \quad (2.6) \end{aligned}$$

IV.2vi Mass Convergence (Subroutine COMPl)

The term

$$\int_0^1 \frac{1}{a \cos \phi} \left[\frac{\partial(\pi u)}{\partial \lambda} + \frac{\partial(\pi v \cos \phi)}{\partial \phi} \right] d\sigma$$

for the continuity equation is expressed as

$$\begin{aligned} & \frac{1}{a \cos \phi_j} \sum_{k=1}^{NLAY} \Delta \sigma_k \left\{ \left[\frac{4}{3} \delta_\lambda (\bar{\pi} u_{i,j,k}^\lambda) - \frac{1}{3} \delta_{2\lambda} (\bar{\pi} u_{i,j,k}^{2\lambda}) \right] \right. \\ & \left. + \left[\frac{4}{3} \delta_\phi (\bar{\pi} v_{i,j,k}^\phi) - \frac{1}{3} \delta_{2\phi} (\bar{\pi} v_{i,j,k}^{2\phi}) \right] \right\} \quad (2.7) \end{aligned}$$

IV.2vii Vertical Velocity (Omega and \dot{S}) Equation

Writing the \dot{S} equation (2.13) of Section 2, Chapter III in finite difference form we obtain

$$\begin{aligned} \dot{S}_n = - \sum_{\ell=1}^n \left\{ \frac{1}{\text{acos } \phi_j} \left[\frac{4}{3} \delta_\lambda (\overline{\Pi u})_{i,j}^\lambda - \frac{1}{3} \delta_{2\lambda} (\overline{\Pi v})_{i,j}^{2\lambda} \right. \right. \\ \left. \left. + \frac{4}{3} \delta_\phi (\overline{\Pi v \cos \phi})_{i,j}^\phi - \frac{1}{3} \delta_{2\phi} (\overline{\Pi v})_{i,j}^{2\phi} \right]_\ell \right. \\ \left. + \left(\frac{\partial \Pi}{\partial t} \right)_\ell \right\} \Delta \sigma_\ell \end{aligned} \quad (2.8)$$

And discretizing the ω equation (2.12) of Section 2, Chapter III we obtain

$$\begin{aligned} \omega_n = - \sum_{\ell=1}^n (\nabla \cdot \Pi \mathbf{V})_\ell \Delta \sigma_\ell + \sigma_n \mathbf{V} \cdot \nabla \Pi \\ = - \sum_{\ell=1}^n \frac{1}{\text{acos } \phi_j} \left[\frac{4}{3} \delta_\lambda (\overline{\Pi u})_{i,j}^\lambda - \frac{1}{3} \delta_{2\lambda} (\overline{\Pi u})_{i,j}^{2\lambda} \right. \\ \left. + \frac{4}{3} \delta_\phi (\overline{\Pi v \cos \phi})_{i,j}^\phi - \frac{1}{3} \delta_{2\phi} (\overline{\Pi v})_{i,j}^{2\phi} \right]_\ell \\ + \frac{\sigma_n}{2} \left\{ \left[u_{i,j,n+1} + u_{i,j,n} \right] \left[\frac{4}{3} \delta_\lambda \overline{\Pi}^\lambda - \frac{1}{3} \delta_{2\lambda} \overline{\Pi}^{2\lambda} \right] \right. \\ \left. + \left[v_{i,j,n+1} + v_{i,j,n} \right] \left[\frac{4}{3} \delta_\phi \overline{\Pi}^\phi - \frac{1}{3} \delta_{2\phi} \overline{\Pi}^{2\phi} \right] \right\} \quad (2.9) \end{aligned}$$

IV.2viii Equation for the Geopotential

Discretizing equation (2.10) of Section 2, Chapter III

$$\phi'_\ell = \phi'_{\ell+1} + c_p \bar{\theta} (p_\ell^\kappa - p_{\ell+1}^\kappa) + c_p \int_{p_\ell}^{p_{\ell+1}} \frac{T}{p^\kappa} dp^\kappa$$

we obtain

$$\begin{aligned} \phi'_\ell &= \phi'_{\ell+1} + C_p \bar{\theta} (p^\kappa_\ell - p^\kappa_{\ell+1}) \\ &\quad + \frac{1}{2} C_p \left[\frac{T_\ell}{p^\kappa_\ell} + \frac{T_{\ell+1}}{p^\kappa_{\ell+1}} \right] [p^\kappa_{\ell+1} - p^\kappa_\ell] \end{aligned}$$

or

$$\phi'_\ell = \phi'_{\ell+1} + \frac{1}{2} C_p (p^\kappa_{\ell+1} - p^\kappa_\ell) \left[\left(\frac{T_{\ell+1}}{p^\kappa_{\ell+1}} + \frac{T_\ell}{p^\kappa_\ell} \right) - 2\bar{\theta} \right] \quad (2.10)$$

where for clarity the subscripts i and j have been omitted.

The expression for ϕ'_{NLAY} is derived as follows:

First, the hydrostatic equation

$$\frac{\partial \phi}{\partial p^\kappa} = -C_p \theta$$

is expressed as

$$\phi_{\ell+1} - \phi_\ell = -C_p (p^\kappa_{\ell+1} - p^\kappa_\ell) (\theta_{\ell+1} + \theta_\ell). \quad (2.11)$$

Next, we integrate a different form of the hydrostatic equation, i.e.,

$$\frac{\partial(\phi\sigma)}{\partial\sigma} = \phi - \sigma\Pi\alpha$$

from $\sigma = 0$ to $\sigma = \ell$. This results in

$$\phi\sigma \Big|_{\sigma=0}^{\sigma=\ell} = \sum_{\ell=1}^{NLAY} (\phi_\ell - \sigma_\ell \Pi \alpha_\ell) \Delta\sigma_\ell$$

or

$$\begin{aligned} \phi_s &= \sum_{\ell=1}^{NLAY} \phi_\ell \Delta\sigma_\ell - \sum_{\ell=1}^{NLAY} \sigma_\ell \Pi \alpha_\ell \Delta\sigma_\ell \\ &= \sum_{\ell=1}^{NLAY} \phi_\ell (\sigma_{e\ell+1} - \sigma_{e\ell}) - \sum_{\ell=1}^{NLAY} \sigma_\ell \Pi \alpha_\ell \Delta\sigma_\ell \end{aligned}$$

$$= \phi_{NLAY} + \sum_{\ell=1}^{NLAY-1} \sigma_{e_{\ell+1}} (\phi_{\ell} - \phi_{\ell+1}) - \sum_{\ell=1}^{NLAY} \sigma_{\ell} \Pi_{\alpha_{\ell}} \Delta \sigma_{\ell} \quad (2.12)$$

By substituting equation (2.11) in equation (2.12) we obtain

$$\begin{aligned} \phi_s = \phi_{NLAY} + \sum_{\ell=1}^{NLAY-1} \sigma_{e_{\ell+1}} C_p (p_{\ell+1}^{\kappa} - p_{\ell}^{\kappa}) \left(\frac{\theta_{\ell+1} + \theta_{\ell}}{2} \right) \\ - \sum_{\ell=1}^{NLAY} \sigma_{\ell} \Pi_{\alpha_{\ell}} \Delta \sigma_{\ell} \end{aligned}$$

or

$$\begin{aligned} \phi_{NLAY} = \phi_s - \frac{C_p}{2} \sum_{\ell=1}^{NLAY-1} \sigma_{e_{\ell+1}} (p_{\ell+1}^{\kappa} - p_{\ell}^{\kappa}) (\theta_{\ell+1} + \theta_{\ell}) + \sum_{\ell=1}^{NLAY} \sigma_{\ell} \Pi_{\alpha_{\ell}} \Delta \sigma_{\ell} \\ = \phi_s - \frac{C_p}{2} \sum_{\ell=2}^{NLAY} \sigma_{e_{\ell}} (p_{\ell}^{\kappa} - p_{\ell-1}^{\kappa}) (\theta_{\ell} + \theta_{\ell-1}) + \sum_{\ell=1}^{NLAY} \sigma_{\ell} \Pi_{\alpha_{\ell}} \Delta \sigma_{\ell} \quad (2.13) \end{aligned}$$

Finally, by using $\alpha = \frac{RT}{p}$, $T = \theta p^{\kappa}$, $\bar{\phi} = C_p \bar{\theta} (1000^{\kappa} - p^{\kappa})$, $\phi = \phi' + \bar{\phi}$, and $\sigma_e(\ell=1) = 0$ in equation (2.13), we obtain

$$\begin{aligned} \phi'_{NLAY} + \bar{\phi}_{NLAY} = \phi_s - \frac{C_p}{2} \sum_{\ell=2}^{NLAY} \sigma_{e_{\ell}} (p_{\ell}^{\kappa} - p_{\ell-1}^{\kappa}) \frac{T_{\ell}}{p_{\ell}^{\kappa}} \\ - \frac{C_p}{2} \sum_{\ell=2}^{NLAY} \sigma_{e_{\ell}} (p_{\ell}^{\kappa} - p_{\ell-1}^{\kappa}) \frac{T_{\ell-1}}{p_{\ell-1}^{\kappa}} \\ + \sum_{\ell=1}^{NLAY} \sigma_{\ell} \Pi \frac{R}{p} T_{\ell} \Delta \sigma_{\ell} \quad (2.14) \end{aligned}$$

or

$$\begin{aligned}\Phi'_{NLAY} &= \Phi_s - C_p \theta (1000^\kappa - p_{NLAY}^\kappa) \\ &\quad - \frac{C_p}{2} \sum_{\ell=3}^{NLAY+1} \sigma_{e_{\ell-1}} (p_{\ell-1}^\kappa - p_{\ell-2}^\kappa) \frac{T_{\ell-1}}{p_{\ell-1}^\kappa} \\ &\quad - \frac{C_p}{2} \sum_{\ell=2}^{NLAY} \sigma_{e_\ell} (p_\ell^\kappa - p_{\ell-1}^\kappa) \frac{T_{\ell-1}}{p_{\ell-1}^\kappa} \\ &\quad + \sum_{\ell=1}^{NLAY} \sigma_\ell \Pi \frac{R}{p_\ell} T_\ell \Delta \sigma_\ell\end{aligned}$$

or

$$\begin{aligned}\Phi'_{NLAY} &= \Phi_s - C_p \bar{\theta} (1000^\kappa - p_{NLAY}^\kappa) \\ &\quad - \frac{C_p}{2} \sigma_{e_{NLAY}} (p_{NLAY}^\kappa - p_{NLAY-1}^\kappa) \frac{T_{NLAY}}{p_{NLAY}^\kappa} \\ &\quad - \frac{C_p}{2} \sum_{\ell=3}^{NLAY} \{ [\sigma_{e_{\ell-1}} (p_{\ell-1}^\kappa - p_{\ell-2}^\kappa)] \\ &\quad \quad + [\sigma_{e_\ell} (p_\ell^\kappa - p_{\ell-1}^\kappa)] \} \frac{T_{\ell-1}}{p_{\ell-1}^\kappa} \\ &\quad - \frac{C_p}{2} [\sigma_{e_2} (p_2^\kappa - p_1^\kappa)] \frac{T_1}{p_1^\kappa} \\ &\quad + \sum_{\ell=1}^{NLAY} \sigma_\ell \Pi \frac{R}{p_\ell} T_\ell \Delta \sigma_\ell\end{aligned} \tag{2.15}$$

In computing the previous expression we take (following Phillips, 1974)

$$p^\kappa = \frac{1}{\kappa+1} \frac{\partial p^{\kappa+1}}{\partial p}$$

or

$$p_\ell^\kappa = \frac{1}{\kappa+1} \frac{p_{e_{\ell+1}}^{\kappa+1} - p_{e_\ell}^{\kappa+1}}{p_{e_{\ell+1}} - p_{e_\ell}}$$

(Note that on the left hand side the pressures are defined at the center of the layers and on the right hand side at the edges of the layers.)

or

$$p_{\ell}^{\kappa} = \frac{p_{e\ell+1}^{\kappa+1} - p_{e\ell}^{\kappa+1}}{(\kappa+1) \Delta\sigma_{\ell}\Pi} \quad (2.16)$$

IV.3 Polar Finite Difference Formulation

In this section we present the polar equations in finite difference form. In developing the analytic equations in Section 3 of Chapter III, we have made the second order approximation

$$\iint_{\substack{\text{pole} \\ \text{cap}}} \alpha \, dS = \alpha_{\text{pole}} \text{Area} + O(\text{Area})$$

for any arbitrary quantity α (see Note d below) and area.

As in the rest of the globe, fourth-order differences are therefore obtained by averaging second-order differences obtained by using values $\Delta\phi$ and $2\Delta\phi$ degrees away from the poles.

That is

$$\boxed{\text{Fourth Order Scheme}} = \frac{4}{3} \boxed{\text{Second Order Scheme, } k=1} - \frac{1}{3} \boxed{\text{Second Order Scheme, } k=2}$$

where $k\Delta\phi$ is the distance away from the pole.

NOTES

- a) Note that $\frac{\sin(2x)}{[1 - \cos(2x)]} = \cotan(x)$.
- b) We use $k_m=r$ to mean "at the first grid point away from the pole" and $k_m=s$ to mean "at the second grid point away from the pole".
- c) IM is the number of grid points in the longitudinal direction along a circle of latitude.
- d) Consider the polar cap as a disk of radius r .

Let

$$\begin{aligned} x &= r \cos\lambda \\ y &= r \sin\lambda \\ r &= a \sin\Delta\phi. \end{aligned}$$

Then, within the polar circle

$$\begin{aligned}
 \int \int_{\text{polar cap}} \alpha \, dS &= \int_{-r}^r \int_{-\sqrt{r^2-x^2}}^{\sqrt{r^2-x^2}} \alpha \, dy \, dx \\
 &= \int_{-r}^r \int_{-\sqrt{r^2-x^2}}^{\sqrt{r^2-x^2}} \left[\alpha_0 + \left(\frac{\partial \alpha}{\partial x} \right)_0 x + \left(\frac{\partial \alpha}{\partial y} \right)_0 y \right. \\
 &\quad \left. + \left(\frac{\partial^2 \alpha}{\partial x^2} \right)_0 \frac{x^2}{2} + \left(\frac{\partial^2 \alpha}{\partial x \partial y} \right)_0 xy + \left(\frac{\partial^2 \alpha}{\partial y^2} \right)_0 \frac{y^2}{2} \right. \\
 &\quad \left. + \dots \right] dx \, dy \\
 &= \alpha_0 \pi r^2 + 0 + \left(\frac{\partial^2 \alpha}{\partial x^2} \right)_0 \frac{r^4 \pi}{8} + 0 + 0(r^6)
 \end{aligned}$$

where $()_0$ indicates evaluation at the pole.

This implies that

$$\frac{\int \int \alpha d\text{Area}}{\text{Area}} = \alpha_0 + \left(\frac{\partial^2 \alpha}{\partial x^2} \right)_0 \frac{r^2}{8} + 0(r^4)$$

IV.3i Zonal (U_p) Momentum Equation

From equation (3.12) of Section 3, Chapter III we obtain

$$\begin{aligned}
 \frac{\partial}{\partial t} (M_{p_m}) \Big|_{p_m} &= \frac{4}{3} \frac{\partial}{\partial t} (M_{p_m}) \Big|_{k_m=r} - \frac{1}{3} \frac{\partial}{\partial t} (M_{p_m}) \Big|_{k_m=s} \\
 &= \frac{4}{3} \left[\frac{(-1)^m}{2\pi a} \right] \cot\left(\frac{\Delta\phi}{2}\right) \int_0^{2\pi} \Pi v U_{p_m} \, d\lambda \Big|_r \\
 &\quad - \frac{1}{3} \left[\frac{(-1)^m}{2\pi a} \right] \cot(\Delta\phi) \int_0^{2\pi} \Pi v U_{p_m} \, d\lambda \Big|_s
 \end{aligned}$$

$$- \frac{\partial}{\partial \sigma} (\Pi \dot{\sigma} U_{p_m}) \Big|_{p_m}$$

$$- \frac{4}{3} \left(\frac{1}{2\pi a} \right) \cot\left(\frac{\Delta\phi}{2}\right) \Pi_{p_m} \int_0^{2\pi} \cos(\lambda) \left[\Phi' \Big|_r + \left(\frac{\sigma RT}{p} \right)_{p_m} \Pi \Big|_r \right] d\lambda$$

$$+ \frac{1}{3} \left(\frac{1}{2\pi a} \right) \cot(\Delta\phi) \Pi_{p_m} \int_0^{2\pi} \cos(\lambda) \left[\Phi' \Big|_s + \left(\frac{\sigma RT}{p} \right)_{p_m} \Pi \Big|_s \right] d\lambda$$

$$+ (f \Pi V_{p_m}) \Big|_{p_m}$$

$$+ \Pi_{p_m} F_{x_{p_m}}$$

and in finite differences we obtain

$$\begin{aligned} \frac{\partial}{\partial t} (\Pi U)_{p_m} &= (-1)^m \left\{ \frac{4 \cot\left(\frac{\Delta\phi}{2}\right)}{3aIM} (-1) \sum_{i=1}^{IM} \Pi_{i,r} v_{i,r,\ell} [u_{i,r,\ell} \sin \lambda_i \right. \\ &\quad \left. + (-1)^m v_{i,r,\ell} \cos \lambda_i] \right. \\ &\quad \left. - \frac{\cot(\Delta\phi)}{3aIM} (-1) \sum_{i=1}^{IM} \Pi_{i,s} v_{i,s,\ell} [u_{i,s,\ell} \sin \lambda_i \right. \\ &\quad \left. + (-1)^m v_{i,s,\ell} \cos \lambda_i] \right\} \end{aligned}$$

$$\begin{aligned} &- \left(\frac{1}{2\Delta\sigma_\ell} \right) \{ [(\Pi \dot{\sigma})_\ell (U_{\ell+1} + U_\ell)]_{p_m} \\ &\quad - [(\Pi \dot{\sigma})_{\ell-1} (U_\ell + U_{\ell-1})]_{p_m} \} \end{aligned}$$

$$+ \Pi_{p_m} \left\{ - \frac{4 \cot\left(\frac{\Delta\phi}{2}\right)}{3aIM} \sum_{i=1}^{IM} \cos(\lambda_i) [\Phi'_{i,s,\ell} \right.$$

$$\left. + \left(\frac{\sigma_{\ell} RT'}{p_\ell} \right)_{p_m} \Pi_{i,s,\ell} \right]$$

$$\begin{aligned}
& + \frac{\cot(\Delta\phi)}{3aIM} \sum_{i=1}^{IM} \cos(\lambda_i) \left[\Phi'_{i,r,\ell} + \left(\frac{\sigma_{\ell} RT'_{\ell}}{p_{\ell}} \right)_{p_m} \Pi_{i,r,\ell} \right] \} \\
& + f_{p_m} \Pi_{p_m} V_{p_m,\ell} \\
& + \Pi_{p_m} F_{x_{p_m,\ell}}
\end{aligned} \tag{3.1}$$

IV.3ii Meridional (V_p) Momentum Equation

From equation (3.14) of Section 3, Chapter III, we derive the finite difference equation

$$\begin{aligned}
\frac{\partial}{\partial t} (IV)_{p_m} &= (-1)^m \left\{ \frac{4\cot(\frac{\Delta\phi}{2})}{3aIM} \sum_{i=1}^{IM} \Pi_{i,r} v_{i,r,\ell} [(-1)^m u_{i,r,\ell} \cos \lambda_i \right. \\
&\quad \left. - v_{i,r,\ell} \sin \lambda_i] \right. \\
&\quad - \frac{\cot(\Delta\phi)}{3aIM} \sum_{i=1}^{IM} \Pi_{i,s} v_{i,r,\ell} [(-1)^m u_{i,s,\ell} \cos \lambda_i \\
&\quad \left. - v_{i,s,\ell} \sin \lambda_i] \right. \\
&\quad - \left(\frac{1}{2\Delta\sigma_{\ell}} \right) \left\{ [(\Pi\sigma)_{\ell} (V_{\ell+1} + V_{\ell})]_{p_m} \right. \\
&\quad \left. - [(\Pi\sigma)_{\ell-1} (V_{\ell} + V_{\ell-1})]_{p_m} \right\} \\
&\quad + (-1)^m \Pi_{p_m} \left\{ - \frac{4\cot(\frac{\Delta\phi}{2})}{3aIM} \sum_{i=1}^{IM} \sin(\lambda_i) [\Phi'_{i,s,\ell} \right. \\
&\quad \left. + \left(\frac{\sigma_{\ell} RT'_{\ell}}{p_{\ell}} \right)_{p_m} \Pi_{i,s,\ell}] \right. \\
&\quad + \frac{\cot(\Delta\phi)}{3aIM} \sum_{i=1}^{IM} \sin(\lambda_i) [\Phi'_{i,r,\ell} \\
&\quad \left. + \left(\frac{\sigma_{\ell} RT'_{\ell}}{p_{\ell}} \right)_{p_m} \Pi_{i,r,\ell}] \right\} \\
&\quad - f_{p_m} \Pi_{p_m} U_{p_m,\ell} + \Pi_{p_m} F_{y_{p_m,\ell}}
\end{aligned} \tag{3.2}$$

IV.3iii Thermodynamic Energy Equation

From equation (3.17) of Section 3, Chapter III we obtain

$$\begin{aligned} \frac{\partial}{\partial t} (\Pi T) \Big|_{P_m} &= \frac{4}{3} \frac{\partial}{\partial t} (\Pi T) \Big|_{k_m=r} - \frac{1}{3} \frac{\partial}{\partial t} (\Pi T) \Big|_{k_m=s} \\ &= \frac{4}{3} \left[\frac{(-1)^m}{2\pi a} \right] \cot\left(\frac{\Delta\phi}{2}\right) \int_0^{2\pi} \Pi v T \, d\lambda \Big|_r \\ &\quad - \frac{1}{3} \left[\frac{(-1)^m}{2\pi a} \right] \cot(\Delta\phi) \int_0^{2\pi} \Pi v T \, d\lambda \Big|_s \\ &\quad - p^\kappa \frac{\partial}{\partial t} \left(\frac{\Pi \dot{\sigma} T}{p^\kappa} \right) \Big|_{P_m} \\ &\quad + \left[\frac{\Pi \sigma \kappa T}{p} \right]_{P_m} \left\{ \frac{\partial \Pi}{\partial t} \Big|_{P_m} + \frac{1}{2\pi a} \int_0^{2\pi} v \Big|_{P_m} \frac{\partial \Pi}{\partial \phi} \Big|_{P_m} d\lambda \right\} \\ &\quad + \left(\frac{\Pi Q}{C_p} \right) \Big|_{P_m} \end{aligned}$$

and in finite differences

$$\begin{aligned} \frac{\partial}{\partial t} (\Pi T)_{P_m} &= (-1)^m \left\{ \frac{4 \cot\left(\frac{\Delta\phi}{2}\right)}{3aIM} \sum_{i=1}^{IM} \Pi_{i,r} v_{i,r,\ell} T_{i,r,\ell} \right. \\ &\quad \left. - \frac{\cot(\Delta\phi)}{3aIM} \sum_{i=1}^{IM} \Pi_{i,s} v_{i,s,\ell} T_{i,s,\ell} \right\} \\ &\quad - \frac{1}{2\Delta\sigma_\ell} p_{P_m,\ell} \left\{ (\Pi \dot{\sigma})_\ell \left[\left(\frac{T_{\ell-1}}{p_{\ell+1}^\kappa} \right) + \left(\frac{T_\ell}{p_\ell^\kappa} \right) \right] \right. \\ &\quad \left. - (\Pi \dot{\sigma})_{\ell-1} \left[\left(\frac{T_\ell}{p_\ell^\kappa} \right) + \left(\frac{T_{\ell-1}}{p_{\ell-1}^\kappa} \right) \right] \right\}_{P_m} \end{aligned}$$

$$+ \left[\frac{\Pi_{p_m} \sigma_{\ell} \kappa T_{p_m, \ell}}{p_{p_m, \ell}} \right] \left\{ \frac{\partial \Pi_{p_m}}{\partial t} \right.$$

$$+ \frac{\Delta \lambda}{2\pi a} \sum_{i=1}^{IM} v|_{p_{m, \ell}} \left[\frac{4}{3} \left(\frac{\Pi_{i, p_m+1} - \Pi_{i, p_m-1}}{\Delta \phi} \right) - \frac{1}{3} \left(\frac{\Pi_{i, p_m+2} - \Pi_{i, p_m-2}}{2\Delta \sigma} \right) \right] \left. \right\}$$

$$+ \frac{\Pi_{p_m} Q_{p_m, \ell}}{C_p}$$

where $v|_p = -(-1)^m U_{p_m} \cos \lambda - V_{p_m} \sin \lambda$, and p_m+1 means going "over the pole".

Since $v|_{p_m} (\text{at } \lambda + \pi) = -v|_{p_m}$, we have that

$$\sum_{i=1}^{IM} v|_{p_{m, \ell}} (\Pi_{i, p_m+1} - \Pi_{i, p_m-1})$$

$$= \sum_{i=1}^{IM} v|_{p_{m, \ell}} (\text{at } \lambda_i) [\Pi_{i, p_m+1} - \Pi_{i, p_m-1}]$$

$$= \sum_{i=1}^{IM} -v|_{p_{m, \ell}} (\text{at } \lambda_i + \frac{\pi}{2}) \Pi_{i, p_m+1} - \sum_{i=1}^{IM} v|_{p_{m, i}} (\text{at } \lambda_i) \Pi_{i, p_m-1}$$

$$= \sum_{i=1}^{IM} -v|_{p_{m, \ell}} (\text{at } \lambda_i) \Pi_{i, p_m-1} - \sum_{i=1}^{IM} v|_{p_{m, \ell}} (\text{at } \lambda_i) \Pi_{i, p_m-1}$$

$$= \sum_{i=1}^{IM} [-v|_{p_{m, \ell}}] [2\Pi_{i, p_m-1}]$$

$$= 2 \sum_{i=1}^{IM} [-v|_{p_{m, \ell}} \Pi_{i, r}]$$

Similarly, we have that

$$\sum_{i=1}^{IM} v|_{p_{m,l}} (\Pi_{i,p_m+2} - \Pi_{i,p_m+2}) = 2 \sum_{i=1}^{IM} [-v|_{p_{m,l}} \Pi_{i,s}]$$

Hence we write the thermodynamic equation as

$$\begin{aligned} \frac{\partial}{\partial t} (\Pi T)_{p_m} = & (-1)^m \left\{ \frac{4 \cot(\frac{\Delta \phi}{2})}{3aIM} \sum_{i=1}^{IM} \Pi_{i,r} v_{i,r,l} T_{i,r,l} \right. \\ & - \frac{\cot(\Delta \phi)}{3aIM} \sum_{i=1}^{IM} \Pi_{i,s} v_{i,s,l} T_{i,s,l} \left. \right\} \\ & + \frac{1}{2\Delta \sigma_\ell} p_{p_m,l} \left\{ (\Pi \dot{\sigma})_\ell \left[\left(\frac{T_{\ell+1}}{p_{\ell-1}^\kappa} \right) + \left(\frac{T_\ell}{p_\ell^\kappa} \right) \right] \right. \\ & - (\Pi \dot{\sigma})_{\ell-1} \left[\left(\frac{T_\ell}{p_\ell^\kappa} \right) + \left(\frac{T_{\ell-1}}{p_{\ell-1}^\kappa} \right) \right] \left. \right\} p_m \\ & + \left[\frac{\Pi_{p_m} \sigma_\ell^\kappa T_{p_m,l}}{p_{p_m,l}} \right] \left\{ \frac{\partial \Pi_{p_m}}{\partial t} + \right. \\ & \left. \left(-\frac{1}{3aIM} \right) \left(-\frac{1}{\Delta \phi} \right) \sum_{i=1}^{IM} (-v|_{p_{m,l}}) [8 \Pi_{i,r} - \Pi_{i,s}] \right\} \\ & + \frac{\Pi_{p_m} Q_{p_m,l}}{C_p} \end{aligned} \quad (3.3)$$

IV.3iv Moisture Equation

From equation (3.19) of Section 3, Chapter III we obtain

$$\begin{aligned}
 \frac{\partial}{\partial t} (\Pi q) \Big|_{p_m} &= \frac{4}{3} \frac{\partial}{\partial t} (\Pi q) \Big|_{k_m=r} - \frac{1}{3} \frac{\partial}{\partial t} (\Pi q) \Big|_{k_m=s} \\
 &= \frac{4}{3} \left[\frac{(-1)^m}{2\pi a} \right] \cot\left(\frac{\Delta\phi}{2}\right) \int_0^{2\pi} \Pi v q \, d\lambda \Big|_r \\
 &\quad - \frac{1}{3} \left[\frac{(-1)^m}{2\pi a} \right] \cot(\Delta\phi) \int_0^{2\pi} \Pi v q \, d\lambda \Big|_s \\
 &\quad - \frac{\partial}{\partial \sigma} (\Pi \dot{\sigma} q) \Big|_{p_m} + \Pi_{p_m} (E_{p_m} - C_{p_m})
 \end{aligned}$$

and in finite differences

$$\begin{aligned}
 \frac{\partial}{\partial t} (\Pi q)_{p_m} &= (-1)^m \left\{ \frac{4 \cot\left(\frac{\Delta\phi}{2}\right)}{3aIM} \sum_{i=1}^{IM} \Pi_{i,r} v_{i,r,\ell} q_{i,r,\ell} \right. \\
 &\quad \left. - \frac{\cot(\Delta\phi)}{3aIM} \sum_{i=1}^{IM} \Pi_{i,s} v_{i,s,\ell} q_{i,s,\ell} \right. \\
 &\quad \left. - \left(\frac{1}{2\Delta\sigma_\ell} \right) \{ (\Pi \dot{\sigma})_\ell [q_{\ell+1} + q_\ell]_{p_m} \right. \\
 &\quad \left. - (\Pi \dot{\sigma})_{\ell-1} [q_\ell - q_{\ell-1}]_{p_m} \right\} \\
 &\quad + \Pi_{p_m} (E_{p_m} - C_{p_m})
 \end{aligned} \tag{3.4}$$

IV.3v Continuity (Pressure Tendency) Equation

From equation (3.6) of Section 3, Chapter III we obtain

$$\begin{aligned}
 \left(\frac{\partial \Pi}{\partial t} \right) \Big|_{p_m} &= \frac{4}{3} \left(\frac{\partial \Pi}{\partial t} \right) \Big|_{k_m=r} - \frac{1}{3} \left(\frac{\partial \Pi}{\partial t} \right) \Big|_{k_m=s} \\
 &= \frac{4}{3} \left[\frac{(-1)^m}{2\pi a} \right] \cot\left(\frac{\Delta\phi}{2}\right) \int_0^1 \int_0^{2\pi} [\Pi v] \, d\lambda \, d\sigma \Big|_{k_m=r} \\
 &\quad - \frac{1}{3} \left[\frac{(-1)^m}{2\pi a} \right] \cot(\Delta\phi) \int_0^1 \int_0^{2\pi} [\Pi v] \, d\lambda \, d\sigma \Big|_{k_m=s}
 \end{aligned}$$

and in finite differences

$$\left(\frac{\partial \Pi}{\partial t} \right) \Big|_{P_m} = \sum_{\ell=1}^{NLAY} (-1)^m \left\{ \frac{4 \cot(\frac{\Delta \phi}{2})}{3aIM} \sum_{i=1}^{IM} \Pi_{i,r} v_{i,r,\ell} - \frac{\cot(\Delta \phi)}{3aIM} \sum_{i=1}^{IM} \Pi_{i,s} v_{i,s,\ell} \right\} \Delta \sigma_\ell \quad (3.5)$$

IV.3vi Vertical Velocity (Omega and \dot{S}) Equation

From equation (3.8) of Section 3, Chapter III we obtain

$$\begin{aligned} \dot{S} \Big|_{P_m} &= \frac{4}{3} \dot{S} \Big|_{k_m=r} - \frac{1}{3} \dot{S} \Big|_{k_m=s} \\ &= - \int_0^\sigma \left\{ \frac{4}{3} \left[\frac{(-1)^m}{2\pi a} \right] \cot(\frac{\Delta \phi}{2}) \int_0^{2\pi} \Pi_v d\lambda \Big|_{k=r} - \frac{1}{3} \left[\frac{(-1)^m}{2\pi a} \right] \cot(\Delta \phi) \int_0^{2\pi} \Pi_v d\lambda \Big|_{k=s} + \left(\frac{\partial \Pi}{\partial t} \right) \Big|_{P_m} \right\} d\sigma \end{aligned}$$

and in finite differences

$$\begin{aligned} \dot{S} \Big|_{P_{m,n}} &= - \sum_{\ell=1}^n \left\{ (-1)^m \left[\frac{4 \cot(\frac{\Delta \phi}{2})}{3aIM} \sum_{i=1}^{IM} \Pi_{i,r} v_{i,r,\ell} - \frac{\cot(\Delta \phi)}{3aIM} \sum_{i=1}^{IM} \Pi_{i,s} v_{i,s,\ell} \right] + \left(\frac{\partial \Pi}{\partial t} \right) \Big|_{P_m} \right\} \Delta \sigma_\ell \quad (3.6) \end{aligned}$$

IV.3vii Equation for the Geopotential

The equation for the geopotential at the pole has the same form as the equation for the non-polar grid points.

IV.4 Time Scheme

The model has the option of using either the Matsuno (Euler-backward) or the smoothed leapfrog time schemes or a combination of both. See Section 3 of Chapter VII for a description of the FORTRAN control variables used to define the time scheme.

IV.4i Matsuno Time Scheme

Let Q^n represent a typical variable which is to be updated to time $n+1$, and let $D(Q^n)$ represent the non-linear space differences evaluated using Q^n . The Matsuno (Euler-backward) scheme consists of two steps:

$$\tilde{Q} = Q^n + \Delta t D(Q^n) \quad (\text{Predictor step})$$

and

$$Q^{n+1} = Q^n + \Delta t D(\tilde{Q}) \quad (\text{Corrector step})$$

IV.4ii Smoothed Leapfrog Scheme

The smoothed leapfrog scheme also consists of two steps:

$$Q^{n+1} = \bar{Q}^{n-1} + 2\Delta t D(Q^n) \quad (\text{Predictor step})$$

and

$$\bar{Q}^n = (1 - \nu) Q^n + 0.5\nu (\bar{Q}^{n-1} + Q^{n+1}) \quad (\text{Smoothing step})$$

A modification to the above scheme is made to include the source terms. If source terms are to be included (and computed) at time step n , the time averaged values at time step $n-1$ are also altered by the addition of the same source terms.

The following steps are taken:

$$Q_{*}^n = \bar{Q}^{n-2} + 2\Delta t D(Q^{n-1})$$

$$\bar{Q}_{*}^{n-1} = (1 - \nu) Q^{n-1} + 0.5\nu (\bar{Q}^{n-2} + Q^n)$$

$$Q^n = Q_{*}^n + (k\Delta t)S(Q_{*}^n)$$

$$\overline{Q}^{n-1} = \overline{Q}_{*}^{n-1} + (k\Delta t)S(Q_{*}^n)$$

where k is the number of time steps between evaluation of the source terms and $S(Q_{*}^n)$ is the tendency due to the source terms evaluated using the fields Q_{*}^n .

IV.5 Filtering

IV.5i Periodic (Shapiro) Filtering of Short Waves

Global filtering of unresolved shortwaves is performed using a sixteenth order Shapiro (1979) filter. The filter is presently applied to sea level pressure, sea level temperature over land, potential temperature and winds. The sea level pressure, sea level temperature and potential temperature are filtered both in the latitudinal and longitudinal directions. As a result of studies (in shallow water experiments) which indicate that meridional filtering of winds causes spurious energy and momentum transfers to occur, the winds (u, v) are filtered only in the longitudinal direction (Takacs and Balgovind, 1983).

This filter is applied periodically, i.e. every two hours. The timing of the filter can be controlled by namelist variable NDSHF which has a default value of two and one half hours. See Section 2 of Chapter VII for a description of the FORTRAN control variables used to define the filters.

The global filter has the effect of reducing the amplitude of waves shorter than $4\Delta x$, which are poorly resolved in the model. Waves longer than $4\Delta x$, which are accurately computed by the difference scheme, are not affected by the filter (Kalnay-Rivas and Hoitsma, 1979b). The phase of all waves remains unchanged.

The form of the two-dimensional Shapiro filter consists simply of two passes of the one-dimensional filter applied in succession. To obtain the $(2n)$ th order of the filter, n passes of the 3-point second order operator are used, i.e.,

$$\bar{q}_{i,j} = [1 - (-F_\phi)^n][1 - (-F_\lambda)^n]q_{i,j}$$

where

$$F_\lambda(q_{i,j}) = \frac{1}{4}(q_{i+1,j} - 2q_{i,j} + q_{i-1,j})$$

and

$$F_\phi(q_{i,j}) = \frac{1}{4}(q_{i,j+1} - 2q_{i,j} + q_{i,j-1})$$

The response of the one-dimensional filter when applied to a wave of the form $q_j = \text{Re}\{e^{i2\pi \Delta x j/M}\}$ is $\bar{q}_j = (1 - \sin^{2n}(\frac{\pi \Delta x}{M}))q_j$ where M is the wavelength.

During the filtering process, the equation

$$p_{sl} = p_s \exp \left[\frac{\phi_s}{R(T_s + \frac{\beta \phi_s}{2g})} \right]$$

is used to relate the sea level pressure (p_{sl}) to the surface pressure (p_s).

The equation is derived as follows:

$$\frac{\partial p}{p} = - \frac{\partial \phi}{RT} .$$

Integrating this equation from sea level (sl) to surface (s) we obtain

$$\begin{aligned} p_{sl} &= p_s \exp \left(\frac{1}{R} \int_{sl}^s \frac{\partial \phi}{T} \right) \\ &\approx p_s \exp \left(\frac{1}{RT} \int_{sl}^s \partial \phi \right) \\ &= p_s \exp \left(\frac{1}{RT} \phi_s \right) . \end{aligned}$$

In the above equation we take $\bar{T} = \frac{1}{2} (T_s + T_{sl})$ and define $T_{sl} = T_s + \beta \phi_s/g$ where $\beta = - \frac{\partial T}{\partial z} = 0.0065^\circ\text{K/m}$ is the adiabatic lapse rate and T_s is the surface temperature.

Hence
$$\bar{T} = \frac{1}{2} (2 T_s + \beta \frac{\phi_s}{g}) = T_s + \beta \frac{\phi_s}{2g} .$$

IV.5ii High Latitude (Fourier) Filter

The CFL computational stability condition for latitude-longitude grid point models with explicit time schemes, requires filtering of unstable short waves at high latitudes to avoid the use of prohibitively short time steps (Takacs and Balgovid, 1983). The specific filtering response needed to ensure

stability is defined by the space and time difference schemes used, and by the type of grid structure - in this case the A grid - in the model (Arakawa and Lamb, 1977).

For this purpose, the fourth order model makes use of the fourier filter applied to u, v, modified temperature and specific humidity, and indirectly to Π through the filtering of sea level pressure.

The modified temperature (T^*) and the model temperature are related by the expression

$$T^* = T + \delta T \quad ,$$

where

$$\delta T = - \left(\frac{\partial T}{\partial p} \right) \Delta p$$

is the temperature change required to remove the influence due to topography.

Now

$$\begin{aligned} \Delta p &= \Delta(\Pi\sigma + p_{top}) \\ &= \sigma \Delta\Pi \\ &= \sigma \Delta(p_s - p_{top}) \\ &= \sigma \Delta p_s \quad . \end{aligned}$$

Also, integrating the hydrostatic equation from sea level (p_{s1}) to surface p_s we obtain

$$\int_{p_{s1}}^{p_s} \frac{\partial p}{\partial z} dz = - \int_0^z \rho g dz \quad .$$

Or

$$\Delta p_s \approx - \rho_s \Phi_s \quad .$$

Therefore

$$\Delta p \approx - \sigma \rho_s \Phi_s \quad .$$

Hence

$$\begin{aligned} \delta T &= \sigma \rho_s \Phi_s \left(\frac{\partial T}{\partial p} \right) \\ &= \sigma \frac{p_s \Phi_s}{R T_s} \left(\frac{\partial T}{\partial p} \right) \quad . \end{aligned}$$

In the filtering procedure we follow the following steps:

- (1) Obtain the modified temperature, $T^* = T + \overline{\delta T}$
- (2) Filter T^*
- (3) Obtain smooth temperatures, $T = T^* - \overline{\delta T}$.

In the above, $\overline{\delta T}$ is an approximation of δT . At level ℓ with edges ℓ' and $\ell'+1$ we take

$$(\overline{\delta T})_{\ell} = \frac{\sigma_{\ell}}{R} \phi_s \left[\frac{p_s}{T_s} \frac{\partial T}{\partial p} \right]_{\ell},$$

$$\begin{aligned} \left(\frac{\partial T}{\partial p} \right)_{\ell} &= \frac{T_{\ell'} - T_{\ell'+1}}{p_{\ell'} - p_{\ell'+1}} \\ &= \frac{T_{\ell'} - T_{\ell'+1}}{\Pi (\sigma_{\ell'} - \sigma_{\ell'+1})} \end{aligned}$$

and

$$T_{\ell'+1} = \frac{\Delta \sigma_{\ell+1} T_{\ell} + \Delta \sigma_{\ell} T_{\ell+1}}{\Delta \sigma_{\ell+1} + \Delta \sigma_{\ell}}.$$

Here $[\quad]$ is the zonal mean of $[\quad]$.

Filtering is performed polewards of 60° latitude. The desired smoothing is performed by multiplying the amplitudes of the fourier components of zonal wave number n of the field to be filtered by a transfer (or damping) function.

The model defaults to the analytic form of the damping function

$$d(n, \phi) = \min \left(1, 1.37 \frac{\Delta \lambda}{\Delta \phi} \frac{\cos \phi}{\left[\frac{4}{3} \sin(n \Delta \lambda) - \frac{1}{6} \sin(2n \Delta \lambda) \right]} \right)$$

where n is the zonal wave number. See Takacs and Balgovind (1983) for the derivation.

However, this damping has been found to be unnecessarily strong because it has been derived under the assumption that the filtered quantities are the time tendencies rather than the variables themselves, as in the present

model. Therefore, the model presently uses weaker damping with empirically derived coefficients. Table IV.5a contains these damping coefficients as a function of latitude and zonal wave number, as they are used in the present 5 degree longitude by 4 degree latitude model versions.

Table IV.5a: Empirically Derived Damping Coefficients
as Used in the 4° X 5° Model

GRID POINTS AWAY FROM THE POLE							
WAVE NO.	1	2	3	4	5	6	7
1	1.00	1.00	1.00	1.00	1.00	1.00	1.00
2	0.83	1.00	1.00	1.00	1.00	1.00	1.00
3	0.67	1.00	1.00	1.00	1.00	1.00	1.00
4	0.50	1.00	1.00	1.00	1.00	1.00	1.00
5	0.33	0.83	1.00	1.00	1.00	1.00	1.00
6	0.17	0.67	1.00	1.00	1.00	1.00	1.00
7	0.0	0.50	0.99	0.99	1.00	1.00	1.00
8	0.0	0.33	0.90	0.98	1.00	1.00	1.00
9	0.0	0.17	0.75	0.95	0.99	1.00	1.00
10	0.0	0.0	0.67	0.90	0.95	1.00	1.00
11	0.0	0.0	0.50	0.85	0.92	0.99	1.00
12	0.0	0.0	0.33	0.80	0.87	0.98	1.00
13	0.0	0.0	0.17	0.75	0.85	0.97	1.00
14	0.0	0.0	0.0	0.67	0.80	0.95	1.00
15	0.0	0.0	0.0	0.50	0.80	0.90	0.99
16	0.0	0.0	0.0	0.33	0.75	0.85	0.98
17	0.0	0.0	0.0	0.17	0.70	0.80	0.97
18	0.0	0.0	0.0	0.0	0.60	0.75	0.96
19	0.0	0.0	0.0	0.0	0.50	0.70	0.95
20	0.0	0.0	0.0	0.0	0.33	0.60	0.90
21	0.0	0.0	0.0	0.0	0.17	0.60	0.90
22	0.0	0.0	0.0	0.0	0.0	0.60	0.90
23	0.0	0.0	0.0	0.0	0.0	0.50	0.90
24	0.0	0.0	0.0	0.0	0.0	0.33	0.90
25	0.0	0.0	0.0	0.0	0.0	0.17	0.83
26	0.0	0.0	0.0	0.0	0.0	0.0	0.67
27	0.0	0.0	0.0	0.0	0.0	0.0	0.50
28	0.0	0.0	0.0	0.0	0.0	0.0	0.33
29	0.0	0.0	0.0	0.0	0.0	0.0	0.17
30	0.0	0.0	0.0	0.0	0.0	0.0	0.0
31	0.0	0.0	0.0	0.0	0.0	0.0	0.0
32	0.0	0.0	0.0	0.0	0.0	0.0	0.0
33	0.0	0.0	0.0	0.0	0.0	0.0	0.0
34	0.0	0.0	0.0	0.0	0.0	0.0	0.0
35	0.0	0.0	0.0	0.0	0.0	0.0	0.0
36	0.0	0.0	0.0	0.0	0.0	0.0	0.0

CHAPTER V

PARAMETERIZATION OF PHYSICAL PROCESSES

LAWRENCE L. TAKACS

V. PARAMETERIZATION OF PHYSICAL PROCESSES

V.1 Introduction

This chapter examines the subgrid scale physical processes, or "physics", which are parameterized in the Fourth Order General Circulation Model.

The physics of the GCM concentrates on three general areas:

- 1) Frictional dissipation in the momentum equations,
- 2) Diabatic heating in the thermodynamic equation,
- 3) Moisture sources and sinks in the moisture equation.

In Section 2 of this text, a description is given of the initial setup and the definition of variables needed for the three general areas stated above. In Section 3, frictional dissipation is addressed in terms of surface skin friction and internal friction due to vertical shear of the horizontal wind. Section 4 examines the diabatic heating terms for the thermodynamic equation, while Section 5 examines the sources and sinks of moisture. Both Sections 4 and 5 omit the heating and moisture adjustment due to moist convective processes which are treated separately in Section 6. Finally, Section 7 reviews the diagnostic terms which are calculated in the physics portion of the model.

V.2 Initialization

Each call to the physics routine COMP3 starts with an initialization of variables used by many of the physical processes parameterized by the model physics. First, specification of the ground condition is given for later use in surface heat capacities, surface drag coefficients, ground temperatures, etc. Next, calculations are made for determining pressure at the middle and edges of the layers throughout the atmosphere. Finally, surface winds and surface drag coefficients are derived.

V.2i Surface Specification

The current version of the model allows for five possible ground conditions given by the logical variables LAND, OCEAN, ICE, SNOW, and FROST. These variables, in turn, are determined by the ground wetness GW, ground temperature GT, geopotential height of the surface ϕ_s , and the latitudes of the snow lines SNOWN and SNOWS. The snow lines are assumed to vary sinusoidally in time according to the formulas

$$\phi_{\text{snow}} = \frac{\pi}{12} \cos \left[.9863(\text{NDAY} - 24.668) \frac{\pi}{180} \right], \quad (2.1)$$

$$\text{SNOWN} = \frac{\pi}{3} - \phi_{\text{snow}}, \quad (2.2)$$

and

$$\text{SNOWS} = -\frac{\pi}{3} - \phi_{\text{snow}}, \quad (2.3)$$

where NDAY is the current day of the year obtained by setting January 1 equal to zero. The latitudes of the northern snow line are tabulated in Table V.2a.

Table V.2a: Latitudes for Northern Snow Line

Date (00Z)	SNOWN
01 Jan 73	46.2278
31 Jan 73	45.0890
01 Feb 73	45.1193
28 Feb 73	47.5442
01 Mar 73	47.6899
31 Mar 73	53.5274
01 Apr 73	53.7613
30 Apr 73	61.0531
01 May 73	61.3105
31 May 73	68.5179
01 Jun 73	68.7291
30 Jun 73	73.5036
01 Jul 73	73.6140
31 Jul 73	74.9482
01 Aug 73	74.9245
31 Aug 73	72.2359
01 Sep 73	72.0848
30 Sep 73	66.3560
01 Oct 73	66.1212
31 Oct 73	58.5611
01 Nov 73	58.3043
30 Nov 73	51.3764
01 Dec 73	51.1664
31 Dec 73	46.3323

The determination of the specific surface condition used is shown schematically in Fig. V.2a.

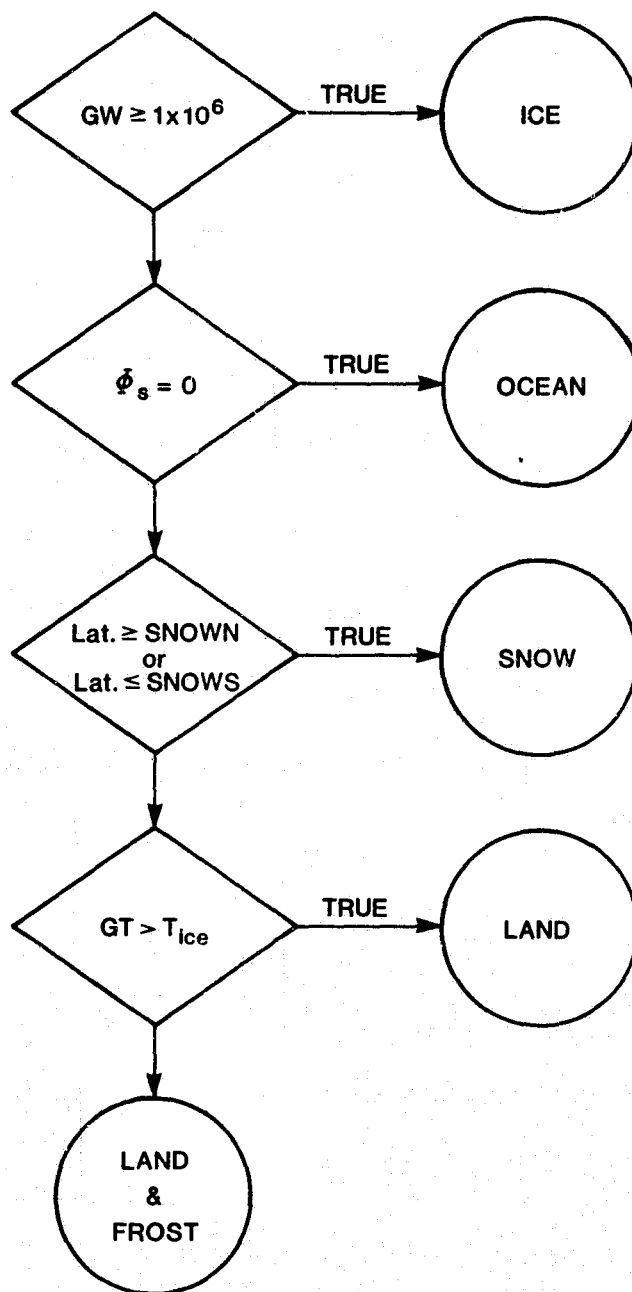


Fig. V.2a Determination of Surface Condition

V.2ii Pressure Calculations

For convenience within the physics portion of the model, pressures are computed at each level in the atmosphere as well as at the edges of each layer. The pressures are given by

$$p(\ell) = \Pi \sigma(\ell) + p_{top} , \quad (2.4)$$

and

$$p_e(\ell) = \Pi \sigma_e(\ell) + p_{top} . \quad (2.5)$$

Notice that $p_e(NLAY + 1)$ is equal to the surface pressure. Finally, p^k is also calculated at each level by

$$p^k(\ell) = EXPBYK (p(\ell)), \quad (2.6)$$

where EXPBYK is a function subprogram which approximates exponentiation of pressure by the power R/C_p .

V.2iii Surface Winds

The surface wind components u_s and v_s are obtained by linear extrapolation from the wind vectors at the two lowest levels. Assuming that the vertical wind shear is constant, we have:

$$\frac{\partial \vec{V}}{\partial \sigma} = \text{CONSTANT} \equiv C . \quad (2.7)$$

Integrating (2.7) between two levels ℓ and $\ell-1$ gives

$$\vec{V}_\ell = \vec{V}_{\ell-1} + C (\sigma_\ell - \sigma_{\ell-1}) . \quad (2.8)$$

Using levels NLAY and NLAYM1, the constant C may be obtained as:

$$C = \frac{\vec{V}_{NLAY} - \vec{V}_{NLAYM1}}{\sigma_{NLAY} - \sigma_{NLAYM1}} . \quad (2.9)$$

Using (2.9) in (2.8), we obtain the expression for the winds at the surface, given by:

$$V_s = V_{NLAY} * STERP1 + V_{NLAYM1} * STERP2 \quad (2.10)$$

where: $STERP1 = (\sigma_s - \sigma_{NLAYM1}) / (\sigma_{NLAY} - \sigma_{NLAYM1})$

$STERP2 = (\sigma_{NLAY} - \sigma_s) / (\sigma_{NLAY} - \sigma_{NLAYM1})$

and $\sigma_s = \sigma_{e_{NLAYP1}} = 1$.

V.2iv Surface Drag Coefficient

The surface drag coefficients for a neutral PBL (i.e. one in which the ground temperature is equal to the surface air temperature) are given by the parametric formulae:

Over Oceans: $C_D = CDX0 * \min (.001 [1 + .07W], .0025), \quad (2.11)$

Not Over Oceans: $C_D = CDXL * (.002 + .006 [Z_s/5000]), \quad (2.12)$

where W is the magnitude of the surface winds given by

$$W = \max ((u_s^2 + v_s^2)^{1/2}, .001), \quad (2.13)$$

and Z_s is the elevation of the ground surface defined by

$$Z_s = \phi_s / g. \quad (2.14)$$

Here ϕ_s is the geopotential height of the surface. The constants CDX0 and CDXL may be used to enhance or reduce the magnitude of the drag coefficients. In the current version of the model, these constants default to 0.5.

V.3 Frictional Dissipation

Two forms of frictional dissipation are parameterized in the model.

Surface skin friction is a parameterization of momentum losses due to surface drag, and internal friction due to vertical shear is a parameterization of momentum changes due to wind shear between the model's layers. Both these terms are computed in subroutine COMP3.

V.3i Surface Skin Friction

The effect of surface skin friction (SF) at the lowest level in the atmosphere is given by

$$\left(\frac{\partial \underline{V}}{\partial t}\right)_{SF} = \frac{1}{\rho} \frac{\partial \underline{\tau}}{\partial z} , \quad (3.1)$$

where $\underline{\tau}$ is the eddy stress vector. Using the hydrostatic equation and the definition of the sigma coordinate system, (3.1) may be rewritten as

$$\left(\frac{\partial \underline{V}}{\partial t}\right)_{SF} = - \frac{g}{\Pi} \frac{\partial \underline{\tau}}{\partial \sigma} . \quad (3.2)$$

Using a forward time integration, (3.2) is approximated for the lowest level as

$$\underline{V}^{n+1}(NLAY) = \underline{V}^n(NLAY) - \Delta t \frac{g}{\Pi} \frac{\Delta \underline{\tau}}{\Delta \sigma(NLAY)} . \quad (3.3)$$

Neglecting $\underline{\tau}$ above the surface, (3.3) becomes

$$\underline{V}^{n+1}(NLAY) = \underline{V}^n(NLAY) - \Delta t \frac{g}{\Pi} \frac{\underline{\tau}_s}{\Delta \sigma(NLAY)} . \quad (3.4)$$

Using bulk formulations, the surface eddy stress $\underline{\tau}_s$ may be related to the surface drag coefficient C_D and the surface winds \underline{V}_s by

$$\underline{\tau}_s = \rho_s D_r \underline{V}_s , \quad (3.5)$$

where ρ_s is the surface air density, V_s are the surface winds extrapolated from above, and D_r is the air/surface interaction coefficient given by

$$D_r = \frac{C_D W^3}{W^2 - 7\Delta T} \quad \text{for a stable PBL, } (\Delta T < 0) \quad (3.6)$$

$$D_r = C_D(W + \Delta T^{1/2}) \quad \text{for an unstable PBL, } (\Delta T \geq 0) . \quad (3.7)$$

The correction for C_D based on PBL stability is related to the temperature drop across the surface layer given by

$$\Delta T = T_g - T_s . \quad (3.8)$$

For a complete description of the determination of PBL stability, the reader is referred to Section V.4iii "Determination of Surface Layer Temperature".

In the current version of the model, the final form of the surface friction calculation is given by

$$\tilde{V}^{n+1}(\text{NLAY}) = \tilde{V}^n(\text{NLAY}) - \text{CDFR} * \Delta t \frac{g}{H} \frac{\rho_s D_r V_s}{\Delta \sigma(\text{NLAY})} , \quad (3.9)$$

where Δt is the time increment between calls to the physics portion of the model, and CDFR is a constant which may enhance or eliminate the effect of surface drag. The default value for CDFR is equal to 1.

V.3ii Internal Friction (IF) due to Vertical Shear of Horizontal Wind

The internal downward transfer of momentum between two levels can be expressed as

$$\left(\frac{\partial V}{\partial t} \right)_{\text{IF}} = \frac{1}{\rho} \frac{\partial}{\partial z} \left(\mu \frac{\partial V}{\partial z} \right) \quad (3.10)$$

where μ is the dynamic coefficient of viscosity. Using the hydrostatic equation and the definition of the sigma coordinate system,

$$\frac{1}{\rho} \frac{\partial}{\partial z} = - \frac{g}{H} \frac{\partial}{\partial \sigma} . \quad (3.11)$$

Therefore, equation (3.10) may be rewritten as

$$\left(\frac{\partial \tilde{v}}{\partial t}\right)_{IF} = - \frac{g}{\Pi} \frac{\partial}{\partial \sigma} \left[-\mu \frac{\rho g}{\Pi} \left(\frac{\partial \tilde{v}}{\partial \sigma}\right) \right] . \quad (3.12)$$

Using the equation of state, equation (3.12) becomes

$$\left(\frac{\partial \tilde{v}}{\partial t}\right)_{IF} = \frac{g^2}{\Pi^2 R} \frac{\partial}{\partial \sigma} \left[\mu \frac{p}{T} \frac{\partial \tilde{v}}{\partial \sigma} \right] . \quad (3.13)$$

The dynamic coefficient of viscosity is proportional to density. An empirical relationship simulating this variation is given by

$$\mu \equiv .00067 \frac{T_{ref}}{T} \frac{p}{p_{ref}} , \quad (3.14)$$

where $T_{ref} = 258^\circ K$ and $p_{ref} = 500$ mb. Equation (3.14) implies that the kinematic coefficient of viscosity, $\nu = \mu/\rho$, is a constant equal to 10^3 cm²/sec (Somerville et al., 1974). Using (3.14) in (3.13) we obtain

$$\frac{\partial \tilde{v}}{\partial t} = \frac{\hat{\mu} g^2}{\Pi^2 R} \frac{\partial}{\partial \sigma} \left[(p/T)^2 \frac{\partial \tilde{v}}{\partial \sigma} \right] , \quad (3.15)$$

where

$$\hat{\mu} \equiv \frac{.00067 T_{ref}}{p_{ref}} . \quad (3.16)$$

For a given level ℓ , equation (3.15) is approximated by

$$\begin{aligned} \tilde{v}_{\ell}^{n+1} &= \tilde{v}_{\ell}^n \\ &+ \frac{\hat{\mu} g^2}{\Pi^2 R} \Delta t \left[\frac{(p/T)_{\ell+1/2}^2 \left(\frac{\partial \tilde{v}}{\partial \sigma}\right)_{\ell+1/2} - (p/T)_{\ell-1/2}^2 \left(\frac{\partial \tilde{v}}{\partial \sigma}\right)_{\ell-1/2}}{\Delta \sigma(\ell)} \right] \end{aligned} \quad (3.17)$$

where

$$(p/T)_{\ell-1/2} = \frac{\Delta\sigma(\ell)(p/T)_{\ell-1} + \Delta\sigma(\ell-1)(p/T)_{\ell}}{\Delta\sigma(\ell-1) + \Delta\sigma(\ell)}, \quad (3.18)$$

$$\left(\frac{\partial \tilde{V}}{\partial \sigma}\right)_{\ell-1/2} = \frac{\tilde{V}_{\ell} - \tilde{V}_{\ell-1}}{\sigma(\ell) - \sigma(\ell-1)}, \quad (3.19)$$

and Δt is the time between calls to the physics portion of the model.

In the current version of the model, the constant 0.00067 in equation (3.16) is represented by the namelist variable FMU. If FMU is set equal to zero, the effect of internal friction on the winds is bypassed.

V.4 Diabatic Heating (Excluding Release of Latent Heating)

The diabatic heating term, Q/C_p in the thermodynamic energy equation, contains contributions from a number of parameterizations. All of these parameterizations, except the calculations for radiative transfer, are found in subroutine COMP3. The calls to the longwave and shortwave radiation packages are found in subroutine RADIO.

V.4i Vertical Diffusion of Heat

The contribution of the time change in temperature due to vertical diffusion of heat is given by

$$\frac{Q_{\text{diff}}}{C_p} = \left(\frac{\partial T}{\partial t} \right)_{\text{diff}} = \frac{K}{\rho} \frac{\partial}{\partial z} \left(\rho p^{\kappa} \frac{\partial \theta}{\partial z} \right), \quad (4.1)$$

where K is the coefficient of vertical diffusion. In the current version of the model $K = 0.2 \text{ ED}$, where ED is a namelist parameter which defaults to $0.5 \text{ m}^2/\text{sec}$.

Using the hydrostatic equation, the equation of state, and the definition of the sigma coordinate system, it can be shown that

$$\frac{1}{\rho} \frac{\partial}{\partial z} = - \frac{g}{\Pi} \frac{\partial}{\partial \sigma}, \quad (4.2)$$

and

$$\rho \frac{\partial}{\partial z} = - \frac{g}{\Pi R^2} (p/T)^2 \frac{\partial}{\partial \sigma}. \quad (4.3)$$

Using (4.2) and (4.3), equation (4.1) may be rewritten as

$$\frac{\partial T}{\partial t} = K \left(\frac{g}{\Pi R} \right)^2 \frac{\partial}{\partial \sigma} \left(p^{\kappa} (p/T)^2 \frac{\partial \theta}{\partial \sigma} \right). \quad (4.4)$$

Since the exchange and transport of heat takes place across the interface of the model's levels, (4.4) may be approximated as

$$T_{\ell}^{n+1} = T_{\ell}^n + \Delta t K \left(\frac{g}{\Pi R} \right)^2 * \left[\frac{p_{\ell+1/2}^{\kappa} (p/T)_{\ell+1/2}^2 \left(\frac{\partial \theta}{\partial \sigma} \right)_{\ell+1/2} - p_{\ell-1/2}^{\kappa} (p/T)_{\ell-1/2}^2 \left(\frac{\partial \theta}{\partial \sigma} \right)_{\ell-1/2}}{\Delta \sigma_{\ell}} \right], \quad (4.5)$$

where Δt is the time between calls to the physics portion of the model.

The values of p^{κ} at the interface between two levels is approximated by

$$\begin{aligned} p_{\ell+1/2}^{\kappa} &= p_{\ell}^{\kappa} + \left(\frac{\partial p^{\kappa}}{\partial \sigma} \right) \frac{1}{2} \Delta \sigma_{\ell} \\ &= p_{\ell}^{\kappa} + \frac{p_{\ell+1}^{\kappa} - p_{\ell}^{\kappa}}{\frac{1}{2}(\Delta \sigma_{\ell+1} + \Delta \sigma_{\ell})} \frac{1}{2} \Delta \sigma_{\ell} \\ &= \frac{\Delta \sigma_{\ell+1} p_{\ell}^{\kappa} + \Delta \sigma_{\ell} p_{\ell+1}^{\kappa}}{\Delta \sigma_{\ell} + \Delta \sigma_{\ell+1}}. \end{aligned} \quad (4.6)$$

Similarly,

$$(p/T)_{\ell+1/2} = \frac{\Delta \sigma_{\ell+1} (p/T)_{\ell} + \Delta \sigma_{\ell} (p/T)_{\ell+1}}{\Delta \sigma_{\ell} + \Delta \sigma_{\ell+1}}. \quad (4.7)$$

The change in potential temperature between the two levels is given by

$$\left(\frac{\partial \theta}{\partial \sigma} \right)_{\ell+1/2} = \left(\frac{\theta_{\ell+1} - \theta_{\ell}}{\sigma_{\ell+1} - \sigma_{\ell}} \right). \quad (4.8)$$

Once new temperatures are found, potential temperatures are updated using

$$\theta_{\ell}^{n+1} = T_{\ell}^{n+1} / p_{\ell}^{\kappa}. \quad (4.9)$$

V.4ii Dry Adiabatic Adjustment

A conventional dry convective adjustment is employed to stabilize super-dry-adiabatic lapse rates. This is done by examining potential temperatures at two adjacent levels for unstable stratification. Potential temperatures, θ_ℓ , are first defined by setting

$$\theta_\ell = T_\ell / p_\ell^\kappa \quad . \quad (4.10)$$

Then, beginning at the top of the atmosphere, potential temperatures are adjusted to a mean potential temperature whenever a condition of instability exists, i.e., $\theta_\ell > \theta_{\ell-1}$. The adjustment redefines θ such that

$$\theta_\ell = \theta_{\ell-1} = \bar{\theta} \equiv \left(\frac{\bar{T}}{\bar{p}^\kappa} \right) \quad (4.11)$$

where \bar{T} and \bar{p}^κ are mean values of T_ℓ and p_ℓ^κ between the two levels, weighted by the thickness of each layer, i.e.,

$$\bar{T} \equiv (T_\ell \Delta\sigma_\ell + T_{\ell-1} \Delta\sigma_{\ell-1}) / (\Delta\sigma_\ell + \Delta\sigma_{\ell-1}) \quad (4.12a)$$

$$\bar{p}^\kappa \equiv (p_\ell^\kappa \Delta\sigma_\ell + p_{\ell-1}^\kappa \Delta\sigma_{\ell-1}) / (\Delta\sigma_\ell + \Delta\sigma_{\ell-1}) \quad . \quad (4.12b)$$

New temperatures are then computed using the mean potential temperature

$$T_\ell = \bar{\theta} p_\ell^\kappa \quad (4.13a)$$

and

$$T_{\ell-1} = \bar{\theta} p_{\ell-1}^\kappa \quad . \quad (4.13b)$$

This process is also applied to the mixing of momentum and moisture. By writing the total vertically integrated momentum for the two levels as

$$\frac{\Pi}{g} (\Delta\sigma_\ell \tilde{V}_\ell + \Delta\sigma_{\ell-1} \tilde{V}_{\ell-1}),$$

and assuming that the resulting winds are constant, then the winds at each level are simply the total momentum divided by the total mass, i.e.,

$$\tilde{v}_{l-1} = \tilde{v}_l = \frac{\Delta\sigma_l \tilde{v}_l + \Delta\sigma_{l-1} \tilde{v}_{l-1}}{\Delta\sigma_l + \Delta\sigma_{l-1}} . \quad (4.14)$$

Moisture is similarly mixed and given by

$$q_{l-1} = q_l = \frac{\Delta\sigma_l q_l + \Delta\sigma_{l-1} q_{l-1}}{\Delta\sigma_l + \Delta\sigma_{l-1}} . \quad (4.15)$$

This process is continued down to the lowest level, and then repeated two more times to ensure that new adjustments also remain stable.

V.4iii Determination of Surface Layer Temperature

The interaction of the planetary boundary layer (PBL) in the model is parameterized by constructing the PBL as a two layer fluid consisting of a thin surface layer near the ground and a relatively thick mixed layer above.

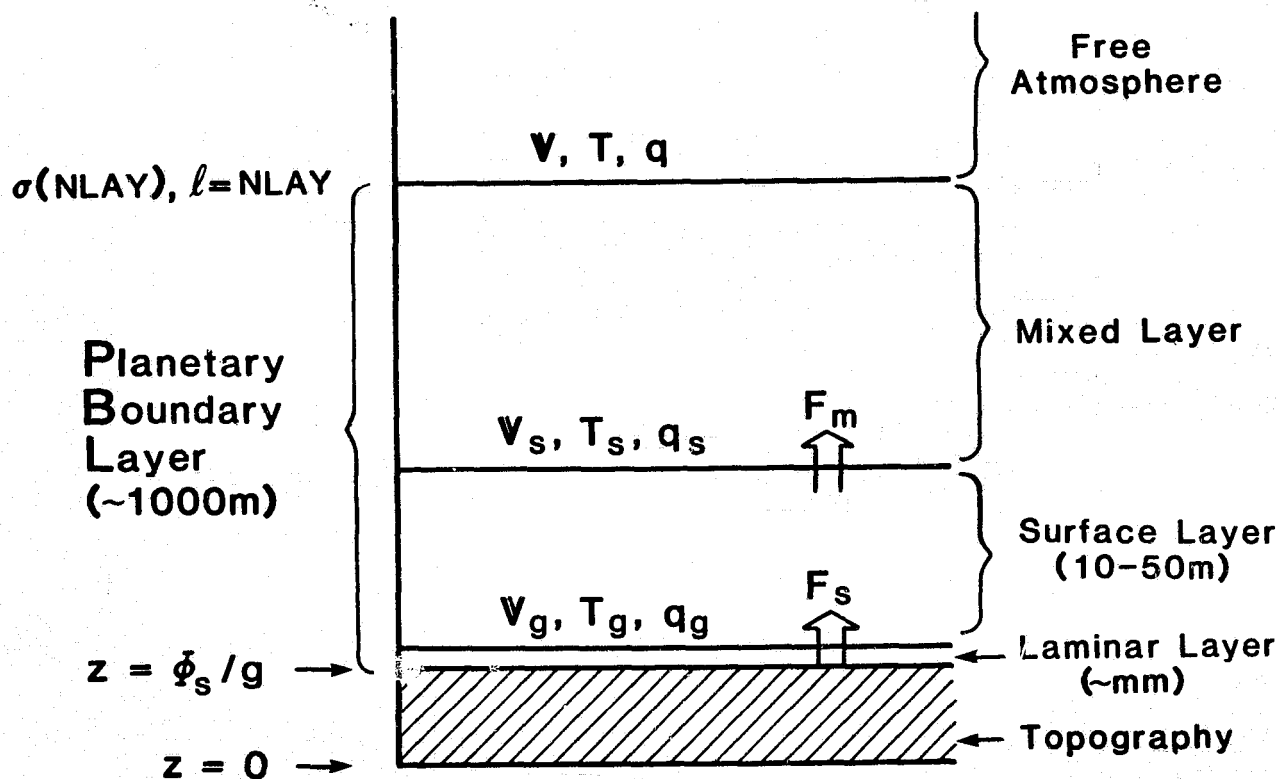


Fig. V.4a Surface Layer Temperature

The thickness of the two layers combined is assumed to be equal to the height of level NLAY (~1000 m). Level NLAY is the only level directly affected by air/surface interactions. The variables at the interface of the mixed layer and surface layer are denoted by subscript s, while those at the interface of the surface layer and ground are denoted by the subscript g.

To calculate the surface layer temperature, T_s , the assumption is made that the flux of moist static energy, $h = C_p T + \phi + Lq$, from the ground into the bottom of the surface layer is equal to the flux from the top of the surface layer into the mixed layer. This assumption implies that the heat and moisture capacities within the surface layer are small and that the net horizontal convergence within the layer may be neglected. In the equation for moist static energy, ϕ is the geopotential, L is the latent heat of condensation parameter, and q is the moisture mixing ratio.

From Fig. V.4a, F_s and F_m are the sensible heat fluxes for the surface layer and mixed layer respectively. Using bulk formulations, F_s may be calculated by

$$F_s = -\rho C_p D_r (T_s - T_g) \quad (4.16)$$

where D_r is an air/surface interaction coefficient dependent on surface winds, surface drag, and convective stability.

F_m is calculated using standard flux parameterizations assuming that it is proportional to $\frac{\partial T}{\partial z} - \left(\frac{\partial T}{\partial z}\right)_{\text{neutral}}$,

$$F_m = -\rho C_p \frac{K}{\Delta z_{\text{PBL}}} (T(\text{NLAY}) - T_s - \Delta T) \quad (4.17)$$

where ΔT is the change in temperature due to the neutral lapse rate. K is the vertical eddy diffusivity of the boundary layer.

Equating the two fluxes gives

$$D_r (T_s - T_g) = \frac{K}{\Delta z_{\text{PBL}}} (T(\text{NLAY}) - T_s - \Delta T) \quad (4.18)$$

$$= \frac{K}{\Delta z_{PBL}} (T(NLAY) - T_s + \Gamma_r \Delta z_{PBL}) , \quad (4.19)$$

where Γ_r is the neutral lapse rate associated with the mixed layer relative humidity r . The neutral lapse rate for the mixed layer is obtained by a linear interpolation of the dry and moist adiabatic lapse rates, weighted by the relative humidity, i.e.,

$$\Gamma_r = r\Gamma_s + (1 - r)\Gamma_d \quad (4.20)$$

where Γ_d and Γ_s are the lapse rates for dry and saturated air respectively, given by

$$\Gamma_d = g/C_p \quad (4.21)$$

$$\Gamma_s = g/C_p \left[\frac{1 + \frac{L}{R} \frac{q^*}{T}}{1 + \frac{L}{C_p} \left(\frac{\epsilon L}{R} \right) \frac{q^*}{T^2}} \right] . \quad (4.22)$$

Here, R is the gas constant for dry air, $\epsilon \equiv M_v/M_d$ where M_v and M_d are the mean molecular weights of water vapor and dry air, C_p is the specific heat at constant pressure, and q^* is the saturation mixing ratio.

Using (4.21) and (4.22) in (4.20) gives

$$\Gamma_r = \Gamma_d - \frac{rg}{C_p} \left[1 - \frac{1 + \frac{L}{R} \frac{q^*}{T}}{1 + \frac{L}{C_p} \left(\frac{\epsilon L}{R} \right) \frac{q^*}{T^2}} \right] . \quad (4.23)$$

Using (4.23) in (4.19) gives

$$D_r (T_s - T_g) = \frac{K}{\Delta z_{PBL}} (T(NLAY) - T_s + (\Gamma_d - \gamma_c) \Delta z_{PBL}) , \quad (4.24)$$

where

$$\gamma_c = \frac{rg}{C_p} \left[1 - \frac{1 + \frac{L}{R} \frac{q_s^*}{T_s}}{1 + \frac{L}{C_p} \left(\frac{\epsilon L}{R} \right) \frac{q_s^*}{T_s^2}} \right] \quad (4.25)$$

In the current version of the model, $\epsilon = .622$, $L = 597.2$ cal/gm,

$C_p = 0.24$ cal/(gm°K), and $R = 287$ m²/(°K sec²).

The depth of the PBL is given by

$$\Delta z_{PBL} = \frac{\Delta \sigma(NLAY)}{2} \left(\frac{R}{g} \right) \frac{T_s \Pi}{p_s} \quad (4.26)$$

and the relative humidity in the PBL is the harmonic mean of the relative humidity at level NLAY and the scaled ground wetness g_w , i.e.,

$$\frac{1}{r} = \frac{1}{2} \left(\frac{1}{r(NLAY)} + \frac{1}{g_w} \right) \quad (4.27)$$

Now, $T(NLAY) + (\Gamma_d - \gamma_c) \Delta z_{PBL}$ is the temperature that a parcel at level NLAY would acquire if brought adiabatically to the ground, i.e.,

$$\theta(NLAY) = T(NLAY) + (\Gamma_d - \gamma_c) \Delta z_{PBL}, \quad (4.28)$$

where the potential temperature defined here uses surface pressure as the reference pressure and includes the effect of moisture. Therefore, equation (4.24) can be rewritten as

$$D_r (T_g - T_s) = \frac{K}{\Delta z_{PBL}} (T_s - \theta(NLAY)) \quad (4.29)$$

or

$$D_r (\Delta \theta - \delta \theta) = \frac{K}{\Delta z_{PBL}} \delta \theta, \quad (4.30)$$

where

$$\begin{aligned}\Delta\theta &= T_g - \theta(NLAY) , \\ \delta\theta &= T_s - \theta(NLAY) .\end{aligned}\tag{4.31}$$

For a given air/surface coefficient D_r and vertical eddy diffusivity coefficient K , (4.30) may be solved for $\delta\theta$ which may then be used to calculate T_s .

Stability of the PBL and Determination of the Interaction Coefficient D_r

The convective stability in the PBL is defined by examining the difference in potential temperature between the ground and the top of the PBL:

$$\Delta\theta = T_g - \theta(NLAY) ,\tag{4.32}$$

where $\theta(NLAY)$ uses a reference pressure equal to the surface pressure and includes the effect of moisture. If $\Delta\theta < 0$, a stable PBL is said to exist.

If $\Delta\theta > 0$, an unstable regime prevails.

Case 1: Stable PBL

For the case of a stable PBL, the air/surface interaction coefficient D_r is given by the empirical expression

$$D_r = \frac{C_D W^3}{W^2 - 7(\Delta\theta - \delta\theta)}\tag{4.33}$$

where $W = (u_s^2 + v_s^2)^{1/2}$ and C_D is the surface drag coefficient. The vertical eddy diffusivity coefficient K is given by

$$K = \frac{60}{1 + 8R_1} ,\tag{4.34}$$

where R_1 is the bulk Richardson number defined as

$$R_1 = \frac{-\delta\theta g \Delta z_{PBL}}{\theta_g (\Delta u^2 + \Delta v^2)} ,\tag{4.35}$$

and

$$\Delta u = u(NLAY) - u_s ,$$

$$\Delta v = v(NLAY) - v_s .$$

Here, θ_g in (4.35) is equal to the ground temperature T_g .

Using (4.33) and (4.34) in (4.30) a quadratic expression in $\delta\theta$ may be obtained, given by

$$A \delta\theta^2 + B \delta\theta + C = 0 \quad (4.36)$$

where

$$A = \frac{7 \times 60}{C_D W^3 \Delta z_{PBL}} - \frac{8 g \Delta z_{PBL}}{(\Delta u^2 + \Delta v^2) \theta_g} ,$$

$$B = 1 + \frac{60}{C_D W \Delta z_{PBL}} - \frac{7 \times 60 \Delta\theta}{C_D W^3 \Delta z_{PBL}} + \frac{8 g \Delta\theta \Delta z_{PBL}}{(\Delta u^2 + \Delta v^2) \theta_g} ,$$

$$C = -\Delta\theta$$

The temperature drop across the mixed layer, $\delta\theta$, may now be obtained by use of the quadratic formula

$$\delta\theta = \frac{-B + \sqrt{B^2 - 4AC}}{2A} . \quad (4.37)$$

If the constant A in (4.37) is small, i.e.: $|A| \leq .01$, a limiting expression for $\delta\theta$ is used, given by

$$\begin{aligned} \delta\theta &= \frac{-B + B(1 - 4AC/B^2)^{1/2}}{2A} \\ &\approx \frac{-B + B(1 - 2AC/B^2 - 2A^2C^2/B^4)}{2A} \\ &= \frac{-C}{B} \left(1 + \frac{AC}{B^2}\right) . \end{aligned} \quad (4.38)$$

Before a final value for $\delta\theta$ is used, a check is made against a minimum value allowed for $\delta\theta$ derived from using a minimum allowable eddy diffusivity

coefficient. In the current version of the model $K_{\min} = 2$. Using this in (4.30) we have

$$\delta\theta_{\min} = \frac{\Delta\theta}{1 + \frac{K_{\min}}{D_{r_{\min}} \frac{\Delta z}{PBL}}} , \quad (4.39)$$

where $D_{r_{\min}}$ is defined as

$$D_{r_{\min}} = \frac{C_D W^3}{W^2 - 7\Delta\theta} . \quad (4.40)$$

Here we see that in minimizing D_r , $\delta\theta$ has been set equal to zero in equation (4.33).

Once a final version of $\delta\theta$ is found, the surface layer temperature T_s is calculated using

$$T_s = \theta(NLAY) + \delta\theta . \quad (4.41)$$

New values of the air/surface interaction coefficient D_r and eddy diffusivity coefficient K are then computed for use in the calculation of surface fluxes of heat and moisture using the new temperature drop across the surface layer defined by

$$\Delta T = T_g - T_s . \quad (4.42)$$

Case 2: Unstable PBL

For the case of an unstable PBL, the air/surface interaction coefficient is given by

$$D_r = C_D (W + (\Delta\theta - \delta\theta)^{1/2}) , \quad (4.43)$$

and the eddy diffusivity coefficient is given by

$$K = 60 + 100 [1 - \exp(-1200 \frac{\partial\theta}{\partial z})] . \quad (4.44)$$

By using (4.43) and (4.44) in (4.30) a transcendental equation results thereby making an exact solution for $\delta\theta$ not possible. Using possible values for C_D and W , Sud and Abeles (1981) obtained an approximate solution for $\delta\theta$

given by

$$\delta\theta = (0.1382 W C_D^{1/2} + 13.67 C_D) \Delta\theta \quad . \quad (4.45)$$

From (4.45), the surface layer temperature is calculated using

$$T_s = \theta(NLAY) + \delta\theta \quad , \quad (4.46)$$

followed by a recalculation of ΔT , D_r and K .

V.4iv Surface Sensible Heat Flux

The time change of the mass weighted sensible heat in the lowest layer of the atmosphere is equal to the flux of surface sensible heat from the ground into that layer. This can be expressed analytically by

$$\frac{\partial}{\partial t} (\rho \Delta z C_p T) = F_s, \quad (4.47)$$

where F_s is the surface sensible heat flux given by

$$F_s = \rho C_p D_r \Delta T \quad . \quad (4.48)$$

The thickness of the lowest layer is defined by Δz , and the air/surface interaction coefficient D_r is given by

$$D_r = \frac{C_D W^3}{W^2 - 7 \Delta T} \quad \text{for a stable PBL}, \quad (4.49)$$

or

$$D_r = C_D (W + \Delta T^{1/2}) \quad \text{for an unstable PBL}. \quad (4.50)$$

Here C_D is the surface drag coefficient and $W \equiv (u_s^2 + v_s^2)^{1/2}$. The temperature drop across the surface layer, ΔT , is defined by

$$\Delta T = T_g - T_s \quad , \quad (4.51)$$

where the updated surface temperature from Section V.4iii is used. Using the hydrostatic equation and the definition of the sigma coordinate system, equation (4.47) may be written as

$$\frac{\partial T}{\partial t} = \rho g \frac{D_r \Delta T}{\Pi \Delta \sigma} \quad . \quad (4.52)$$

Thus, the temperature at the lowest level in the model is updated due to the flux of surface sensible heat using the equation

$$T^{n+1}(\text{NLAY}) = T^n(\text{NLAY}) + \Delta t \frac{\rho_s g D_r}{\Pi} \frac{\Delta T}{\Delta \sigma(\text{NLAY})} \quad (4.53)$$

where ρ_s is the surface air density and Δt is the time between calls to the physics subroutines.

V.4v Radiation

The calculation of shortwave and longwave radiation fluxes in the model is a very complex problem, both physically and computationally. The following is a brief summary of the techniques presently used, and the appropriate references for more detailed explanations.

Shortwave Radiation

In the current version of the model, the amount of solar energy absorbed at the earth's surface is computed using a parametric method with the formulas and the coefficients based on accurate multiple-scattering computations (Somerville et al., 1974). In this treatment the absorption depends on the amount and type of clouds, the humidity, the zenith angle of the sun, and the albedo of the earth's surface. Within the stratosphere the absorption also depends on the ozone distribution.

The following sub-sections briefly review the methods used in the calculation of absorption of solar radiation. For a complete description of the parameterizations used by the model, it is suggested that the reader refer to Somerville, et al. (1974). For a description of the accurate multiple-scattering computations on which these parameterizations are based, the reader should refer to Lacis and Hansen (1974).

A) Absorption due to Ozone

The total amount of solar radiation absorbed by ozone in the ℓ^{th} layer of the atmosphere can be written as the sum of the amount absorbed from the direct beam above plus the amount absorbed from the reflected beam below, i.e.,

$$A_{\ell \text{ oz}} = A^{\downarrow} + A^{\uparrow} \quad , \quad (4.54)$$

where

$$A^{\downarrow} = S_o \cos \theta_o [F_{\text{oz}}(X_{\ell+1}^{\downarrow}) - F_{\text{oz}}(X_{\ell}^{\downarrow})] \quad , \quad (4.55)$$

$$A^{\uparrow} = S_o \cos \theta_o R [F_{\text{oz}}(X_{\ell}^{\uparrow}) - F_{\text{oz}}(X_{\ell+1}^{\uparrow})] \quad . \quad (4.56)$$

Here, S_o is the solar constant, θ_o is the local zenith angle, X^{\downarrow} is the amount of ozone traversed by the direct beam, X^{\uparrow} is the amount of ozone traversed by the reflected beam, and R is a measure of the ground and lower atmosphere albedo. If no clouds are present, the albedo of the atmosphere is taken to be the effective albedo due to Rayleigh scattering averaged over the ozone bands;

$$R_a = \frac{.02186}{1 + .816 \cos \theta_o} \quad . \quad (4.57)$$

If clouds are present, R_a is taken to be the cloud albedo as computed from subroutine CLOUDS. In either case, the effective albedo of the ground and atmosphere is given by

$$R = R_a + (1 - R_a)(1 - \bar{R}_a)R_g / (1 - \bar{R}_a R_g) \quad (4.58)$$

where \bar{R}_a is the average of R_a over all solar angles and R_g is the albedo of the ground.

The fractional amount of absorbed solar radiation, F_{oz} , by passing through an ozone amount $X(\text{cm})$, is given by

$$F_{\text{oz}}(X) = \frac{1.082 X}{(1 + 138.6X)^{.805}} + \frac{.0658 X}{1 + (103.6X)^3} + \frac{.02118 X}{1 + .042X + .000323X^2} \quad , \quad (4.59)$$

with an error $< 0.5\%$ for $10^{-4} \leq X \leq 1$ (Somerville et al., 1974). The first two terms in (4.59) represent absorption in the ultraviolet, while the third term represents absorption in the visible.

The amount of ozone traversed in reaching the ℓ^{th} layer by the direct and reflected beams is given, respectively, by

$$X_{\ell}^{\downarrow} = \mu_{\ell} M, \quad (4.60)$$

and

$$X_{\ell}^{\uparrow} = \mu_t M + 1.9 (\mu_t - \mu_{\ell}), \quad (4.61)$$

where μ_{ℓ} is the ozone amount in a vertical path above the ℓ^{th} layer, and μ_t is the ozone amount in a vertical path above the reflecting layer (i.e., the ground for clear skies, or the cloud top for cloudy skies). M is a magnification factor which accounts for the slant path and refraction of the solar beam, and is given by

$$M = \frac{35}{(1 + 1224 \cos^2 \theta_0)^{1/2}} \quad (4.62)$$

The factor 1.9 is an average magnification factor for the diffusive upward radiation.

In order to calculate the ozone amounts μ_{ℓ} and μ_t , a separate subroutine, OZONE2, is used. Within this routine, a discrete tabulated data set is given which describes the total, vertical path, amounts of ozone at 5° latitude intervals from 0° latitude to 90° latitude for each of 4 seasons centered about the 15th of January, April, July and October. Linear interpolation is then used to calculate the total ozone amount between the tabulated data for a given model date and location. Ozone for southern latitudes is obtained by recognizing that there is a $1/2$ year phase difference between the seasons of the two hemispheres. Thus, the model date is adjusted for southern latitudes.

Once the total ozone amount for a given model day is determined at each

model grid latitude, an interpolation is made to determine the ozone vertical profile. Within subroutine OZONE2, 4 vertical profiles are tabulated corresponding to total ozone amounts of .22, .30, .38 and .46 cm. Each profile contains 23 vertical levels corresponding to 23 pressure surfaces from 1 mb to 1013.25 mb. An interpolation is made between the known vertical profiles to obtain the characteristic vertical profile for any particular total ozone amount.

Finally, one more interpolation procedure is made to calculate the vertical distribution of ozone associated with the pressures at the sigma edge levels of the model. In the current 9-layer version of the model, this is only done for the first 6 sigma edges. The amount of ozone in any one of the top 5 model levels is thus the difference between the ozone amounts at the sigma edges bordering that level.

B) Absorption due to Water Vapor in Clear Skies

Following Somerville et al., 1974, the amount of solar radiation absorbed, F_w , by passing through an amount of water vapor $Y(\text{cm})$ is given by

$$F_w(Y) = \frac{2.9Y}{(1 + 141.5Y)^{0.635} + 5.925Y} \quad (4.63)$$

with an error $< 1\%$ for $10^{-2} \leq Y \leq 10$. Equation (4.63) applies for a reference pressure p_0 equal to 1013.25 mb and a reference temperature T_0 equal to 273.16°K. To account for general temperatures and pressures, the effective water vapor amount for a given specific humidity q at level l is given by

$$Y_{\text{eff}} = \frac{1}{2 g p_0} \left(\frac{T_0}{T(l)} \right)^{1/2} (p_e^2(l+1) - p_e^2(l)) q(l) \quad (4.64)$$

The calculation used for the absorption of solar radiation due to the presence of water vapor is similar to that of ozone. In the spectral region

of significant water vapor absorption, Rayleigh scattering is negligible. Thus, for clear skies, the absorption of solar radiation due to water vapor is given by

$$A_{\ell w} = A^{\downarrow} + A^{\uparrow} \quad (4.65)$$

where

$$A^{\downarrow} = S_0 \cos \theta_0 [F_w(Y_{\ell+1}^{\downarrow}) - F_w(Y_{\ell}^{\downarrow})] , \quad (4.66)$$

and

$$A^{\uparrow} = S_0 \cos \theta_0 R [F_w(Y_{\ell}^{\uparrow}) - F_w(Y_{\ell+1}^{\uparrow})] , \quad (4.67)$$

where the terms are defined in an analogous manner as that for absorption due to ozone. For the water vapor amounts traversed by the direct and reflected solar beams, we have

$$Y_{\ell}^{\downarrow} = \mu_{\ell} M , \quad (4.68)$$

and

$$Y_{\ell}^{\uparrow} = \mu_t M + 1.66 (\mu_t - \mu_{\ell}) . \quad (4.69)$$

The amounts of water vapor in a vertical path above a given level ℓ (or reflecting surface t) is simply the sum of the effective water vapor amounts from the top of the atmosphere down to the desired level. The effective albedo R is equal to the ground albedo multiplied by the fractional amount of solar radiation reaching the surface, i.e.,

$$R = R_g (1 - F_w(Y_{NLAY+1}^{\downarrow})) . \quad (4.70)$$

The amount of solar radiation absorbed at the ground is calculated as the sum of two terms, one for the wavelength region where the absorption coefficient of water is significant

$$S_{g_1} = S_0 \cos \theta_0 [(1 - F_w(Y_{NLAY+1}^{\downarrow})) - .647] (1 - R_g) , \quad (4.71)$$

and the other for the remaining wavelengths

$$S_{g_2} = .647 S_0 \cos \theta_0 \left[1 - (R_a + (1 - R_a)(1 - \bar{R}_a)R_g / (1 - \bar{R}_a R_g)) \right] \quad (4.72)$$

where R_a is the albedo for the Rayleigh atmosphere for the total solar spectrum.

To within 1%, R_a may be expressed as

$$R_a = \frac{.433}{1 + 6.43 \cos \theta_0} \quad (4.73)$$

\bar{R}_a is the spherical albedo of the Rayleigh atmosphere for illumination from below, given by

$$\bar{R}_a = .093 \quad (4.74)$$

C) Calculation of Cloudiness Parameters

In calculating the effects of clouds on the absorption of solar radiation, it is necessary to know the fractional area covered by clouds for each horizontal grid point as well as the associated optical thickness of the cloud at each level. This information is passed to subroutine SOLAR1 through the array CLOUD which is computed in subroutine CUMULO for small-scale convective type clouds, and in subroutine COMP3 for large-scale supersaturation clouds.

In the current version of the model, if any cloud type exists at a particular longitudinal grid point I and vertical index L, the cloud is assumed to occupy the entire grid element. Thus, the array CLOUD (I, L) is set equal to 1, thereby producing a fractional area covered by clouds, FLOUD, equal to 1 and a fractional area covered by clear skies, FCLEAR, equal to 0. The present code however, is written to handle fractional cloudiness (i.e., CLOUD(I, L) < 1) provided CLOUD(I, L) is suitably defined.

The optical thickness associated with the clouds depends on the cloud type. Using the first nine levels of the CLOUD array, if any cloud type exists, the value corresponding to the lowest optical thickness, i.e. those of super-

saturation clouds, is assigned. Next, a check is made for the presence of small-scale convective clouds. From the CLOUD array we have

CLOUD(I, NLAY + 1) = 1, 2 for LOW-LEVEL (levels 7,8)
 CLOUD(I, NLAY + 2) = 1, 2 for MID-LEVEL (levels 5,6)
 CLOUD(I, NLAY + 3) = 1, 2, 3 for PENETRATING (levels 4, 5, 6)

If convective clouds are found, then the sigma levels containing convective clouds are assigned optical thickness for that cloud.

Table V.4a shows the optical thickness used as a function of cloud type and level

Table V.4a: Optical Thickness

Cloud-Type \ Level	1	2	3	4	5	6	7	8	9
Super-Saturation	0	1	2	4	6	6	8	8	8
Low-Level							16	16	
Mid-Level					8	8			
Penetrating	0	0	8	8	8	8	8	8	8

D) Absorption due to Water Vapor in Cloudy Skies

The absorption of solar radiation due to water vapor in the presence of clouds is calculated in subroutine CLOUDS. From the driving routine SOLAR1, information is passed concerning the cloud-top levels at each horizontal grid point and the cloud optical thicknesses.

The first step of the routine simply calculates the absorption of incident radiation above the cloud-top level in a similar manner as described for clear skies. Next, for each layer of the atmosphere and each frequency range considered, the reflection, absorption, and transmission of solar radiation are approximated as functions of the single scattering albedo, cloud optical thickness, and

specific humidity. The layers are then combined to obtain the flux distribution of solar radiation throughout the atmosphere. The total absorption in each layer is obtained by summing over all significant frequency ranges.

Longwave Radiation

In the longwave radiation routine developed by Wu and Kaplan (Wu, 1976), the absorption depends on the amounts of water vapor, ozone, and carbon dioxide. Only the water vapor absorption calculation is carried out in detail, and transmission functions for ozone and carbon dioxide are precalculated. Clouds predicted by the model are presently assumed to be black bodies, and grid volumes are either fully clear or cloudy. (This aspect of cloud-radiation interaction is presently being modified). The reader is referred to the documentation of the Wu-Kaplan radiation by Krishnamurthy (1982) for complete details.

Final Note

During execution of the model, longwave and shortwave radiation may be bypassed entirely by setting the namelist parameter NFLW equal to zero. Otherwise, a non-zero NFLW will instruct the solar radiation package to be executed every time the physics of the model is called. The frequency of execution of the longwave radiation also depends on a namelist parameter called NDHOG. If NDHOG is equal to zero, longwave radiation will be skipped. Otherwise, longwave radiation will be executed at NDHOG time intervals, where NDHOG is of the form hour-minute-second (hhmmss). If the physics is invoked between calls to the longwave radiation package, the physics uses the same values of the longwave radiative fluxes as in the preceeding call to the physics.

V.4vi Heating due to Absorbed Radiation

The heating effect due to absorbed solar and terrestrial radiation at a

given level ℓ can be described as

$$\frac{\partial}{\partial t} (\rho \Delta z C_p T)_{\text{RAD}} = A_\ell + R_{\ell+1} - R_\ell, \quad (4.75)$$

where $A_\ell = S_\ell - S_{\ell+1}$ is the net flux of solar radiation absorbed in the layer and $(R_{\ell+1} - R_\ell)$ is the net flux of terrestrial radiation absorbed in the layer. Using the hydrostatic equation and the definition of the sigma coordinate system, (4.75) may be written as

$$\left(\frac{\partial T}{\partial t} \right)_{\text{RAD}} = (A_\ell + R_{\ell+1} - R_\ell) \frac{g}{\Pi \Delta \sigma_\ell C_p}. \quad (4.76)$$

Thus, the updated temperature at level ℓ is given by

$$T_\ell^{n+1} = T_\ell^n + (A_\ell + R_{\ell+1} - R_\ell) g \Delta t / (\Pi \Delta \sigma_\ell C_p), \quad (4.77)$$

where the fluxes of long and shortwave radiation are obtained from the radiation routines. In the current version of the model, a scaling factor of 10 is needed to obtain the correct units of the right hand side of equation (4.76).

V.4vii Determination of Ground Temperature

The prediction equation for the ground temperature T_g is given by

$$C \frac{\partial T_g}{\partial t} = S_s - R_s - F_s - LE_s + Q, \quad (4.78)$$

where

- C is the total heat capacity of the ground
- S_s is the net downward flux of solar radiation absorbed at the ground
- R_s is the net upward flux of longwave radiation
- F_s is the net upward flux of sensible heat
- LE_s is the net upward flux of latent heat
- Q is the net heating or cooling due to conduction through sea ice from the ocean below.

The subscript s denotes the ground surface. Since R_s , F_s , LE_s and Q all depend on T_g , a backward implicit method is used to solve for T_g .

For any function f , we may approximate $f(T_g^{n+1})$ by

$$f(T_g^{n+1}) = f(T_g^n) + \left(\frac{\partial f}{\partial T_g} \right)^n \Delta T_g . \quad (4.79)$$

Using (4.79) and (4.78) we have

$$\begin{aligned} C \left(\frac{T_g^{n+1} - T_g^n}{\Delta t} \right) = & S_s(T_g^n) - \\ & R_s(T_g^n) - \frac{\partial R}{\partial T_g} \Delta T_g \\ & - F_s(T_g^n) - \frac{\partial F}{\partial T_g} \Delta T_g \\ & - LE_s(T_g^n) - L \frac{\partial E}{\partial T_g} \Delta T_g \\ & + Q(T_g^n) + \frac{\partial Q}{\partial T_g} \Delta T_g . \end{aligned} \quad (4.80)$$

Defining $\Delta T_g = T_g^{n+1} - T_g^n$, we have

$$\Delta T_g = \frac{[S_s - R_s - F_s - LE_s + Q]}{C/\Delta t + \left(\frac{\partial R}{\partial T_g} + \frac{\partial F}{\partial T_g} + L \frac{\partial E}{\partial T_g} - \frac{\partial Q}{\partial T_g} \right)} , \quad (4.81)$$

and the updated ground temperature becomes

$$T_g^{n+1} = T_g^n + \Delta T_g . \quad (4.82)$$

The individual terms in equation (4.81) are given as follows:

S_s and R_s , in ly/day, are known from the radiation routines (see subroutine RADIO) and are given by

$$S_s - R_s = SG - RE(NLAYP1) \equiv RADTRM . \quad (4.83)$$

To calculate the change of R_s with respect to T_g , it is assumed that

$$R_s = \sigma T^4 , \quad (4.84)$$

where σ is the Stefan-Boltzman constant equal to $1.171 \times 10^{-7} \frac{\text{ly}}{\text{day } ^\circ\text{K}^4}$.

From (4.84) we see that

$$\frac{\partial R_s}{\partial T_g} = 4 \sigma T_g^3 . \quad (4.85)$$

F_s and LE_s , as defined in Section V.4iv "Surface Sensible Heat Flux" and Section V.5ii "Surface Moisture Flux", are given by

$$F_s = \rho_s C_p D_r (T_g - T_s), \quad (4.86)$$

and

$$LE_s = \rho_s \beta D_r L (q_g^* - q_s) , \quad (4.87)$$

where D_r is the air/surface interaction coefficient, β is the evapotranspiration coefficient, and q_g^* is the saturation specific humidity at the ground. It should be noted that since the surface densities used in equations (4.86) and (4.87) were determined using pressures in units of millibars, the resulting fluxes of sensible and latent heat are in units of deca-langley/unit time. Therefore, a scaling factor of 10 is needed to match the units of langley/unit time of the remaining variables in equation (4.81).

To calculate the change of sensible heat flux with respect to ground temperature, we have

$$\frac{\partial F_s}{\partial T_g} = \rho_s C_p D_r \left(1 - \frac{\partial T_s}{\partial T_g} \right) , \quad (4.88)$$

where ρ_s and D_r are assumed to be independent of T_g . From Section V.4iii, "Determination of Surface Layer Temperature", we know that

$$D_r (T_g - T_s) = \frac{K}{\Delta z_{PBL}} (T_s - \theta(NLAY)) \quad (4.89)$$

where K is the eddy diffusivity coefficient and Δz_{PBL} is the thickness of the PBL. Equation (4.89) comes from the assumption that the flux of sensible heat from the ground into the surface layer is equal to the flux of sensible heat from

the surface layer into the mixed layer. Solving (4.89) for T_s we have

$$T_s = \frac{D_r T_g + K/\Delta z_{PBL} \theta(NLAY)}{D_r + K/\Delta z_{PBL}} \quad (4.90)$$

Thus,

$$\frac{\partial T_s}{\partial T_g} = \frac{D_r}{D_r + K/\Delta z_{PBL}} \quad (4.91)$$

where again we have assumed D_r and K to be independent of T_g .

Using (4.91) in (4.88) we have

$$\frac{\partial F_s}{\partial T_g} = \rho_s C_p D_r \left(\frac{K/\Delta z_{PBL}}{D_r + K/\Delta z_{PBL}} \right) \quad (4.92)$$

To calculate the change of latent heat flux with respect to ground temperature, we first substitute into equation (4.87) the expression for surface specific humidity found in Section V.5iii "Determination of Surface Specific Humidity", given by

$$q_s = \frac{\beta D_r q_g^* + K/\Delta z_{PBL} q(NLAY)}{\beta D_r + K/\Delta z_{PBL}} \quad (4.93)$$

Thus, equation (4.87) becomes

$$LE_s = \rho_s \beta D_r L \frac{K/\Delta z_{PBL} (q_g^* - q(NLAY))}{\beta D_r + K/\Delta z_{PBL}} \quad (4.94)$$

Differentiating, we find

$$L \frac{\partial E_s}{\partial T_g} = \rho_s \beta D_r L \left(\frac{K/\Delta z_{PBL}}{\beta D_r + K/\Delta z_{PBL}} \right) \frac{\partial q_g^*}{\partial T_g} \quad (4.95)$$

The change of ground saturation specific humidity with respect to ground temperature may also be found under "Determination of Surface Specific Humidity",

and is given by

$$\frac{\partial q_g^*}{\partial T_g} = \left(\frac{\epsilon L}{R} \right) \frac{q_g^*}{T_g^2}, \quad (4.96)$$

where ϵ is the ratio of molecular weights of water vapor and dry air. Using (4.96) in (4.95) we have

$$L \frac{\partial E_s}{\partial T_g} = \rho_s \beta D_r L \left(\frac{K / \Delta z_{PBL}}{\beta D_r + K / \Delta z_{PB}} \right) \left(\frac{\epsilon L}{R} \right) \frac{q_g^*}{T_g^2}. \quad (4.97)$$

Finally, the heating or cooling due to conduction through sea ice is given by

$$Q = 0, \quad \text{if the grid point does not have ice or the ice is over land} \quad (4.98)$$

$$Q = \frac{C_{ice}}{H_{ice}} (T_{ice} - T_g), \quad \text{if the grid point has ice and } z < .1 \text{ (i.e., ocean ice)}$$

Here, C_{ice} is the thermal conductivity of ice equal to $0.0052 \frac{\text{ly cm}}{\text{sec } ^\circ\text{K}}$, H_{ice} is the effective ice thickness equal to 300 cm, and T_{ice} is the melting point of ice equal to 273.16°K . From (4.77) we see that for non-zero Q ,

$$\frac{\partial Q}{\partial T_g} = - \frac{C_{ice}}{H_{ice}}. \quad (4.99)$$

The total heat capacity C and coefficient of latent heat L used in equation (4.81) are summarized below:

	OCEAN	ICE	SNOW	FROST	LAND
$L(\text{cal/gm})$	597.2	680	680	680	597.2
$C(\text{cal } ^\circ\text{K}^{-1} \text{ cm}^{-2})$	∞	5.1	2.3	C_{frost}	C_{land}

where

$$C_{\text{frost}} = ((.331 + .075\text{GW})(2 + 2.5\text{GW}) .001 \frac{\text{SDAY}}{2\pi})^{1/2}, \quad (4.100)$$

and

$$C_{\text{land}} = \left((.386 + .15GW)(1 + GW) .002 \frac{\text{SDAY}}{2\pi} \right)^{1/2} . \quad (4.101)$$

In equations (4.100) and (4.101), GW is the scaled ground wetness and SDAY is the number of seconds per day.

Before a final value for the ground temperature is prescribed, a check is made to determine whether a change in phase of moisture has occurred between the previous and current time-steps. If so, a correction is made to compensate for the differing heat capacities between frost and frost-free land.

From Fig. V.4b we see that for a given total heating ΔQ , the change in temperature can be schematically shown as:

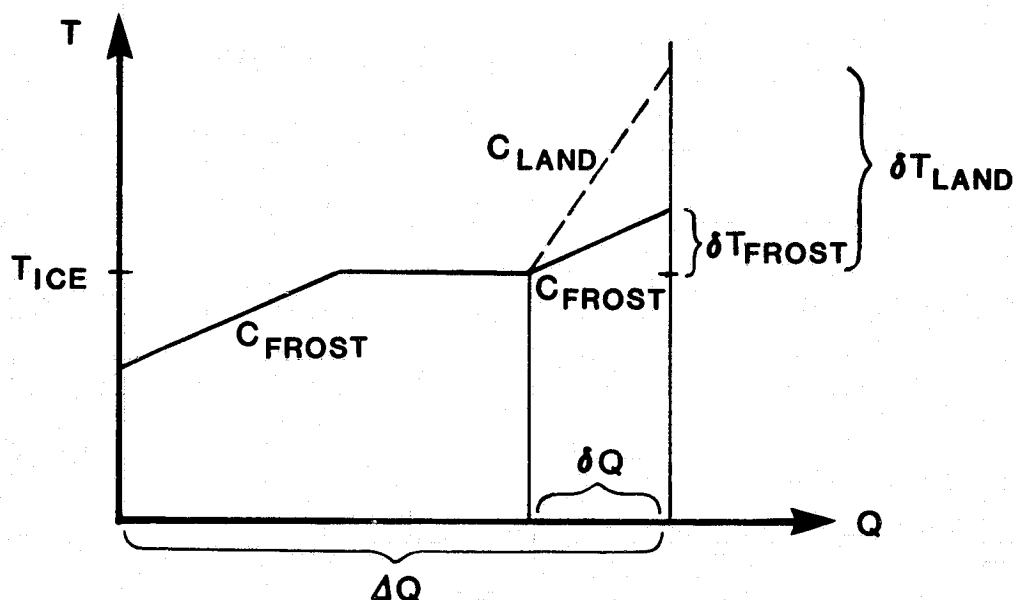


Fig. V.4b Temperature Correction Due to Change of Phase of Moisture

The increase in temperature above T_{ice} due to the heating δQ using identical heat capacities before and after the phase change is given by

$$\delta T_{\text{frost}} = \delta Q / C_{\text{frost}} , \quad (4.102)$$

or

$$\delta Q = C_{\text{frost}} \delta T_{\text{frost}} \quad . \quad (4.103)$$

The increase in temperature using the correct heat capacity, however, is given by

$$\delta T_{\text{land}} = \delta Q / C_{\text{land}} \quad . \quad (4.104)$$

Thus, using (4.103) in (4.104) we see that

$$\delta T_{\text{land}} = \frac{C_{\text{frost}}}{C_{\text{land}}} \delta T_{\text{frost}} \quad . \quad (4.105)$$

This correction is then added to T_{ice} to give a better approximation to the true ground temperature. For a phase change in the opposite direction, the reverse of the above procedure is performed.

Finally, it should be noted that the ICE and SNOW grid locations are pre-determined seasonal values and are thus non-prognostic. Should one of these locations have a ground temperature greater than T_{ice} , a correction is immediately made to set it back to the freezing temperature.

Both of these last corrections are performed in subroutine COMP35 after the ground temperature has been updated using equation (4.82).

V.5 Evaporation and Vertical Flux of Moisture

Examined in this section are the moisture sources obtained from both vertical diffusion and surface flux. Also examined is the determination of surface specific humidity. A brief discussion is given concerning the elimination of negative specific humidities, as well as the procedure used to compute the saturation specific humidity.

The parameterizations discussed here may be found in subroutine COMP3. The elimination of negative specific humidity is also computed in subroutine SHCORN which is used by the hydrodynamics portion of the model. The external function QSAT is used to calculate saturation specific humidities.

V.5i Vertical Diffusion of Moisture

The contribution to the time change of specific humidity due to vertical diffusion of moisture is given by

$$\left(\frac{\partial q}{\partial t}\right)_{\text{diff}} = \frac{K}{\rho} \frac{\partial}{\partial z} \left(\rho \frac{\partial q}{\partial z} \right), \quad (5.1)$$

where K is the coefficient of vertical diffusion. In the current version of the model $K = 0.2 \text{ ED}$, where ED is a namelist parameter which defaults to $0.5 \text{ m}^2/\text{sec}$.

Using the hydrostatic equation, equation of state, and the definition of the sigma coordinate system, equation (5.1) may be written as

$$\left(\frac{\partial q}{\partial t}\right)_{\text{diff}} = K \left(\frac{g}{\Pi R}\right)^2 \frac{\partial}{\partial \sigma} \left((p/T)^2 \frac{\partial q}{\partial \sigma} \right). \quad (5.2)$$

For a given level ℓ , this is approximated by

$$q_{\ell}^{n+1} = q_{\ell}^n + \Delta t K \left(\frac{g}{\Pi R}\right)^2 *$$

$$\frac{\left((p/T)^2 \frac{\partial q}{\partial \sigma}\right)_{\ell+1/2} - \left((p/T)^2 \frac{\partial q}{\partial \sigma}\right)_{\ell-1/2}}{\Delta \sigma_{\ell}} \quad (5.3)$$

where

$$(p/T)_{\ell-1/2} = \frac{\Delta\sigma_{\ell-1}(p/T)_{\ell} + \Delta\sigma_{\ell}(p/T)_{\ell-1}}{\Delta\sigma_{\ell} + \Delta\sigma_{\ell-1}}, \quad (5.4)$$

and

$$\left(\frac{\partial q}{\partial \sigma}\right)_{\ell-1/2} = \frac{q_{\ell} - q_{\ell-1}}{\sigma_{\ell} - \sigma_{\ell-1}}. \quad (5.5)$$

The time increment Δt is equal to the time between calls to the physics subroutines.

V.5i1 Surface Moisture Flux

The time change of the mass weighted specific humidity in the lowest layer of the atmosphere, due to the flux of surface moisture from the ground into that layer, is given by

$$\left(\frac{\partial}{\partial t} \rho \Delta z q\right)_{\text{evap}} = F_s, \quad -1 \quad (5.6)$$

where F_s is the surface moisture flux given by

$$F_s = \rho \beta D_r (q_s^* - q_s), \quad (5.7)$$

and Δz is the thickness of the lowest layer. The air/surface interaction coefficient D_r is given by

$$D_r = \frac{C_D W^3}{W^2 - 7\Delta T} \quad \text{for a stable PBL,} \quad (5.8)$$

or

$$D_r = C_D (W + \Delta T^{1/2}) \quad \text{for an unstable PBL.} \quad (5.9)$$

C_D is the surface drag coefficient and $W = (u_s^2 + v_s^2)^{1/2}$. The temperature drop across the surface layer, ΔT , is defined by

$$\Delta T = T_g - T_s, \quad (5.10)$$

whose sign is used to determine PBL stability. β in equation (5.7) is the soil evapotranspiration coefficient given by

$$\beta = \min (1, \text{WET}/\text{FWET}) , \quad (5.11)$$

where WET is the ground wetness and FWET is the limiting ground wetness at which land surface evapotranspiration occurs at its potential rate. FWET is a namelist parameter which defaults to 0.5. Finally, q_g^* is the saturation specific humidity at the ground while q_s is the surface specific humidity.

Using the hydrostatic equation and the definition of the sigma coordinate system, equation (5.6) may be written as

$$\left(\frac{\partial q}{\partial t} \right)_{\text{evap}} = \frac{\rho_s g}{\Pi} \beta D_r \left(\frac{q_g^* - q_s}{\Delta \sigma} \right) . \quad (5.12)$$

This is approximated for the specific humidity at the lowest level by

$$q_{\text{NLAY}}^{n+1} = q_{\text{NLAY}}^n + \Delta t \frac{\rho_s g}{\Pi} \beta D_r \left(\frac{q_g^* - q_s}{\Delta \sigma_{\text{NLAY}}} \right) , \quad (5.13)$$

where ρ_s is the surface air density and Δt is the time increment between physics calls.

V.5iii Determination of Surface Specific Humidity

The formulation used to calculate the specific humidity at the top of the surface layer is similar to that used in the determination of the surface temperature. The assumption is made that the flux of moist static energy from the ground into the bottom of the surface layer is equal to the flux from the top of the surface layer into the mixed layer, where the moist static energy is defined by

$$h = C_p T + \phi + Lq . \quad (5.14)$$

For these calculations, however, the individual fluxes of heat and moisture are treated separately, since the heat and moisture capacities within the surface layer are assumed to be negligible. For a complete description of this process the reader should refer to Section V.4iii, "Determination of Surface Layer Temperature".

The flux of moisture from the ground into the bottom of the surface layer is given by

$$F_s = \rho \beta D_r (q_g^* - q_s), \quad (5.15)$$

where β is the soil evapotranspiration coefficient and D_r is the air/surface interaction coefficient (see Section V.5ii, "Surface Moisture Flux" for details). The saturation specific humidity at the ground is given by q_g^* , while q_s is the surface specific humidity.

The flux of moisture from the top of the surface layer into the mixed layer is given by

$$F_m = \rho \frac{K}{\Delta z_{PBL}} (q_s - q(NLAY)), \quad (5.16)$$

where Δz_{PBL} is the thickness of the PBL and K is the updated vertical eddy diffusivity coefficient (see Section V.4iii, "Determination of Surface Layer Temperature" for its functional form).

Equating (5.15) and (5.16), the surface specific humidity may be derived, given by

$$q_s = \frac{\beta D_r q_g^* + K/\Delta z_{PBL} q(NLAY)}{\beta D_r + K/\Delta z_{PBL}}. \quad (5.17)$$

Since the surface temperature and surface specific humidity are determined independently, the possibility exists that the new surface specific humidity is super-saturated. Thus, a check is made by comparing the new surface specific humidity with a saturation surface specific humidity computed from the surface pressure and the updated surface temperature. If the new surface specific humidity is larger than the saturation surface specific humidity, a correction is made to the new surface specific humidity and new surface temperature to account for the release of moisture through condensation and its latent heating effect.

Under adiabatic processes, moist static energy is conserved for a saturated air parcel moving vertically, i.e.,

$$\frac{dh^*}{dz} = c_p \frac{dT}{dz} + g + L \frac{dq^*}{dz} = 0. \quad (5.18)$$

Expanding $\frac{dq^*}{dz}$ gives

$$\frac{dq^*}{dz} = \left(\frac{\partial q^*}{\partial T} \right)_p \frac{dT}{dz} + \left(\frac{\partial q^*}{\partial p} \right)_T \frac{dp}{dz}. \quad (5.19)$$

Replacing (5.19) in (5.18) we find

$$-\frac{dT}{dz} = \frac{\frac{g}{c_p} - \frac{L}{c_p} \rho g \left(\frac{\partial q^*}{\partial p} \right)_T}{1 + \frac{L}{c_p} \left(\frac{\partial q^*}{\partial T} \right)_p}. \quad (5.20)$$

Now, the definition of q^* is given by

$$q^* = \frac{\epsilon e^*}{p - e^*}, \quad (5.21)$$

where e^* is the saturation vapor pressure and $\epsilon = 0.622$ is the ratio of molecular weights of water and dry air.

Thus,

$$\left(\frac{\partial q}{\partial T}\right)_p = \frac{p}{e^*} \left(\frac{\partial e^*}{\partial T}\right)_p \frac{q^*}{(p - e^*)} . \quad (5.22)$$

From the Clausius-Clapeyron equation, an expression for $\left(\frac{\partial e^*}{\partial T}\right)_p$ is obtained, given by

$$\left(\frac{\partial e^*}{\partial T}\right)_p = \frac{M_v L e^*}{R^* T^2} \quad (5.23)$$

where L is the latent heat of condensation, M_v is the molecular weight of water vapor and R^* is the universal gas constant. Using (5.23) in (5.22) and assuming $p - e^* \approx p$, we have

$$\left(\frac{\partial q}{\partial T}\right)_p = \left(\frac{M_v L}{R^*}\right) \frac{q^*}{T^2} . \quad (5.24)$$

We may replace the universal gas constant R^* with the gas constant for dry air, R , using the relations

$$R = \frac{R^* \epsilon}{M_v} , \quad (5.25)$$

and

$$\epsilon = \frac{M_v}{M_{dry}} . \quad (5.26)$$

Thus, equation (5.24) becomes

$$\left(\frac{\partial q}{\partial T}\right)_p = \left(\frac{\epsilon L}{R}\right) \frac{q^*}{T^2} . \quad (5.27)$$

Using (5.27) in equation (5.20), the temperature change due to the effect of latent heating of condensation is given by

$$-\frac{dT}{dz} = \frac{\frac{-L}{C_p} \rho g \left(\frac{\partial q}{\partial p}\right)_T}{1 + \frac{L}{C_p} \left(\frac{\epsilon L}{R}\right) \frac{q^*}{T^2}} . \quad (5.28)$$

This may be approximated as

$$\Delta T = \frac{-\frac{L}{C_p} \Delta q^*}{1 + \frac{L}{C_p} \left(\frac{\epsilon L}{R} \right) \frac{q^*}{T^2}}, \quad (5.29)$$

where the relation $\Delta p = -\rho g \Delta z$ has been used.

Therefore, letting Δq^* be the difference between the new surface specific humidity and the saturation surface specific humidity, the increase in surface temperature is given by

$$T_s = T_s^o + \frac{L}{C_p} \frac{(q_s^o - q^*)}{\left(1 + \frac{L}{C_p} \left(\frac{\epsilon L}{R} \right) \frac{q^*}{T_s^{o2}} \right)}, \quad (5.30)$$

where q^* is determined from T_s^o and the surface pressure. Here superscript o represents the initial quantities. Once the change in temperature is found, the change in surface specific humidity is given by

$$q_s = q_s^o - \frac{C_p}{L} \Delta T, \quad ,$$

or

$$q_s = q_s^o - \frac{(q_s^o - q^*)}{\left(1 + \frac{L}{C_p} \left(\frac{\epsilon L}{R} \right) \frac{q^*}{T_s^{o2}} \right)}. \quad (5.31)$$

This updated surface specific humidity is, of course, saturated.

V.5iv Elimination of Negative Specific Humidity

Before and after large and small-scale moist convective processes are computed, a check is made to ensure that specific humidities are not negative. Starting from the top of the atmosphere, if negative specific humidity does exist in a grid volume, moisture is "borrowed" from the grid volume below so

that the vertically integrated moisture is conserved, i.e.,

$$\left(\int_{\ell-1}^{\ell} q \, d\sigma \right)_{\text{final}} = \left(\int_{\ell-1}^{\ell} q \, d\sigma \right)_{\text{initial}} . \quad (5.32)$$

Approximating (5.32) by

$$\frac{1}{2} (q_{\ell} \Delta\sigma_{\ell} + q_{\ell-1} \Delta\sigma_{\ell-1})_{\text{final}} = \frac{1}{2} (q_{\ell} \Delta\sigma_{\ell} + q_{\ell-1} \Delta\sigma_{\ell-1})_{\text{initial}} , \quad (5.33)$$

an expression for the updated moisture at level ℓ is given by

$$q_{\ell \text{ final}} = (q_{\ell} + q_{\ell-1} \frac{\Delta\sigma_{\ell-1}}{\Delta\sigma_{\ell}})_{\text{initial}} - q_{\ell-1 \text{ final}} \frac{\Delta\sigma_{\ell-1}}{\Delta\sigma_{\ell}} . \quad (5.34)$$

Assuming that $q_{\ell-1}$ is initially negative, we require that its final value is set to zero. Thus we have

$$q_{\ell-1 \text{ final}} = 0 , \quad (5.35)$$

$$q_{\ell \text{ final}} = (q_{\ell} + q_{\ell-1} \frac{\Delta\sigma_{\ell-1}}{\Delta\sigma_{\ell}})_{\text{initial}} . \quad (5.36)$$

This process is repeated until the lowest level is reached. If the resulting $q(\text{NLAY})$ is negative, it is simply set to zero. It should be noted that this process is also performed after advection in the hydrodynamics.

V.5v Determination of Saturation Specific Humidity

Saturation specific humidity, q^* , is given by the formula

$$q^* = \frac{\epsilon e^*}{p - e^*} , \quad (5.37)$$

where e^* is the saturation water vapor pressure which is a function of temperature only.

In the current version of the model, a look-up table is used to determine e^* for a given temperature value. The table has 139 vapor pressures associated with integer temperatures between 200°K and 338°K. Assuming a linear fit

between known values, for a given temperature T we have

$$e^*(T) = e_1^* + \Delta T(e_2^* - e_1^*), \quad (5.38)$$

where

$$e_1^* = e^*(\text{INT}(T)), \quad (5.39)$$

$$e_2^* = e^*(\text{INT}(T) + 1), \quad (5.40)$$

and

$$\Delta T = T - \text{INT}(T) . \quad (5.41)$$

Once $e^*(T)$ is determined, equation (5.37) is used to calculate q^* for a given temperature and pressure. This is performed by the external function QSAT.

V.6 Precipitation Processes

In this section we examine the effect of moisture and latent heat release on the large-scale environment due to large-scale supersaturation and sub-grid scale cumulus convection. The calculations for large-scale supersaturation are found in subroutine COMP3. The preparations for the cumulus parameterization are located in subroutine COMP3 while the parameterization scheme is located in subroutine CUMULO.

V.6i Large-Scale Precipitation

In the current version of the model, large-scale condensation and release of latent heat is said to occur when the air becomes saturated on the scale of the entire grid element. The excess water, removed from an atmosphere layer in this way, precipitates into the layer immediately below. The falling precipitation either evaporates completely in that layer or it brings the layer to saturation and then passes the excess moisture to the next layer below, where the process is repeated.

Large scale or supersaturation precipitation occurs at a particular level when the specific humidity at that level exceeds the saturation value, i.e.,

$$q_\ell > q_\ell^* , \quad (6.1)$$

where q_ℓ^* is the saturation specific humidity. The derivation for the amount of water vapor released through condensation is identical to that shown in Section V.5iii for the determination of surface specific humidity and is given by

$$\Delta q_\ell = \frac{(q_\ell - q_\ell^*)}{1 + \frac{L}{C_p} \left(\frac{\epsilon L}{R} \right) \frac{q_\ell^*}{T_\ell^2}} . \quad (6.2)$$

The heating effect due to the release of latent heat through condensation will increase the temperature for that level by an amount

$$\Delta T_{\ell} = \frac{L}{C_p} \Delta q_{\ell} \quad . \quad (6.3)$$

Therefore, the updated values for T_{ℓ} and q_{ℓ} are given by

$$T_{\ell} = T_{\ell}^o + \Delta T_{\ell} \quad , \quad (6.4)$$

$$q_{\ell} = q_{\ell}^o - \Delta q_{\ell} \quad , \quad (6.5)$$

where superscript o represents the initial quantities.

Equations (6.4) and (6.5) show the changes in temperature and specific humidity per unit mass for the level ℓ . Before we can determine the effect of the precipitating moisture on the next level below, we must first compute the amount of moisture per unit area released from this level. This is given by

$$\rho \Delta z_{\ell} \Delta q_{\ell} = \frac{\Pi \Delta \sigma_{\ell}}{g} \Delta q_{\ell} \quad , \quad (6.6)$$

where $\rho \Delta z_{\ell}$ is the mass/unit area for level ℓ . We now assume that this moisture is evaporated into the next layer below, i.e., $\ell+1$. Doing so causes the temperature in this level to decrease due to the heat needed for evaporation.

To calculate the change in specific humidity in layer $\ell+1$, we must first scale equation (6.6) by the mass/unit area within this new layer, i.e.,

$$\Delta q_{\ell+1} = \left(\frac{\Pi \Delta \sigma_{\ell}}{g} \Delta q_{\ell} \right) / \left(\frac{\Pi \Delta \sigma_{\ell+1}}{g} \right) \quad , \quad (6.7)$$

or

$$\Delta q_{\ell+1} = \frac{\Delta \sigma_{\ell}}{\Delta \sigma_{\ell+1}} \Delta q_{\ell} \quad . \quad (6.8)$$

The decrease in temperature in layer $\ell+1$ is related again by

$$\Delta T_{\ell+1} = \frac{L}{C_p} \Delta q_{\ell+1} \quad . \quad (6.9)$$

Now, the updated values for $T_{\ell+1}$ and $q_{\ell+1}$ are given as

$$T_{\ell+1} = T_{\ell+1}^0 - \Delta T_{\ell+1} , \quad (6.10)$$

and

$$q_{\ell+1} = q_{\ell+1}^0 + \Delta q_{\ell+1} . \quad (6.11)$$

Using the updated temperature $T_{\ell+1}$, a new saturation specific humidity $q_{\ell+1}^*$ is calculated to check for supersaturation. The entire process is repeated until the lowest level, NLAY, is reached.

For the lowest level in the model, it is found that an iterative procedure is needed for better accuracy. The analytical expression simulated by these adjustments is given by

$$-L \delta q = C_p \delta T , \quad (6.12)$$

and

$$q + \delta q = q^*(T + \delta T, p). \quad (6.13)$$

Since this system is implicit in q and T , three iterations of the condensation process are used to calculate the temperature and specific humidity changes in the lowest layer. Once the final moisture adjustment is known, it is assumed to precipitate to the ground, given by

$$\begin{aligned} \text{Large Scale Precipitation from level NLAY} &= \rho \Delta z_{\text{NLAY}} \Delta q_{\text{NLAY}} \\ &= \frac{\Pi \Delta \sigma (\text{NLAY})}{g} \Delta q_{\text{NLAY}} . \end{aligned} \quad (6.14)$$

It should be noted that as stated in (6.14), the units of the precipitated moisture are in decimeters per Δt , where Δt is the time elapsed between calls to the physics routine. For diagnostic purposes, a conversion is made to 0.1 mm/day.

V.611 Small-Scale Cumulus Parameterization

Small-scale moist convection, as indicated by Somerville et al, (1974), is crucial to the atmospheric budgets of heat, water and energy. It typically occurs on the space scale of cumulus clouds, 2-3 orders of magnitude smaller than the horizontal finite difference grid size. Thus, it cannot be resolved explicitly and must be treated parametrically.

The moist convection parameterization scheme in the current version of the model is an adaptation of Arakawa's scheme for the UCLA 3-level model (Arakawa, 1972). Using 9 levels in the vertical, cumulus convection is limited to the lowest 6 levels which are then strapped in pairs to simulate the 3 levels of the UCLA model (see Fig. V.6a). The strong restriction implied by this vertical strapping has been lifted in a more recent version of the model (see Final Note in this section).

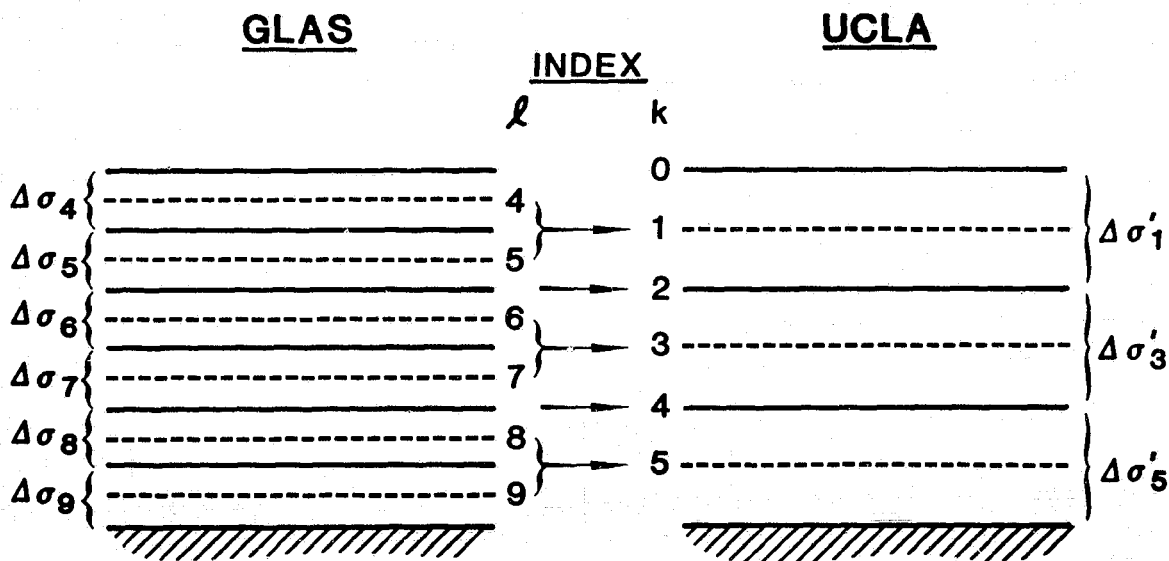


Fig. V.6a GLAS/UCLA Strapping Parameterization

From Fig. V.6a we see that the k -index refers to the level in the UCLA model while the l -index refers to the level in the GLAS model. For any variable ζ defined in the GLAS vertical structure, a similar variable ζ'

may be defined on the UCLA vertical grid as

UCLA variable <-- GLAS variable

$$\zeta'(k) = \zeta_e(k+4) \quad \text{for } k = 2, 4 \quad (6.15)$$

$$\zeta'(k) = \frac{1}{2} (\zeta(k+3) + \zeta(k+4)) \quad \text{for } k = 1, 3, 5 \quad (6.16)$$

where $\zeta'_e(l)$ is the "edge" value between layers $l-1$ and l .

The stability parameters used in determining the onset of cumulus convection are the dry and moist static energies given by

$$s = C_p T + \phi, \quad (6.17)$$

and

$$h = C_p T + \phi + Lq, \quad (6.18)$$

respectively. Also, saturation moist static energy is given by

$$h^* = C_p T + \phi + Lq^*, \quad (6.19)$$

where q^* is the saturation specific humidity. During dry and saturated adiabatic processes, h^* is conserved and is thus a convenient measure for convective stability.

The first step, then, in the parameterization of cumulus convection is to calculate the dry and moist static energies at the mid and edge levels in the model. Using the hydrostatic relation, we may express the vertical change of dry static energy as

$$\frac{\partial s}{\partial \sigma} = C_p p^\kappa \frac{\partial \theta}{\partial \sigma}, \quad (6.20)$$

where $\theta = T/p^\kappa$. For convenience, a new parameter, capital S, is defined by

$$\frac{\partial S}{\partial \sigma} = \frac{\partial}{\partial \sigma} (s/C_p) = p^\kappa \frac{\partial \theta}{\partial \sigma}. \quad (6.21)$$

Integrating (6.21) from level ℓ to edge ℓe , we have

$$\int_{\ell}^{\ell e} \frac{\partial S}{\partial \sigma} d\sigma = \int_{\ell}^{\ell e} p^{\kappa} \frac{\partial \theta}{\partial \sigma} d\sigma .$$

Treating p^{κ} constant in the layer, this becomes

$$S_{\ell e} = S_{\ell} + p_{\ell}^{\kappa} (\theta_{\ell e} - \theta_{\ell}) . \quad (6.22)$$

Since $\theta_{\ell e}$ is the potential temperature at the interface of the two levels ℓ and $\ell-1$, it may be approximated by

$$\theta_{\ell e} = \frac{\Delta \sigma_{\ell-1} \theta_{\ell} + \Delta \sigma_{\ell} \theta_{\ell-1}}{\Delta \sigma_{\ell} + \Delta \sigma_{\ell-1}} .$$

Using this in (6.22), we have

$$S_{\ell e} = S_{\ell} + \frac{\Delta \sigma_{\ell}}{\Delta \sigma_{\ell} + \Delta \sigma_{\ell-1}} p_{\ell}^{\kappa} (\theta_{\ell-1} - \theta_{\ell}) ,$$

or

$$S_{\ell e} = S_{\ell} + \frac{\Delta \sigma_{\ell}}{\Delta \sigma_{\ell} + \Delta \sigma_{\ell-1}} \left[T_{\ell-1} \frac{p_{\ell}^{\kappa}}{p_{\ell-1}^{\kappa}} - T_{\ell} \right] . \quad (6.23)$$

Similarly, integrating (6.21) from edge ℓe to level $\ell-1$, we have

$$S_{\ell-1} = S_{\ell e} + \frac{\Delta \sigma_{\ell-1}}{\Delta \sigma_{\ell} + \Delta \sigma_{\ell-1}} \left[T_{\ell-1} - T_{\ell} \frac{p_{\ell-1}^{\kappa}}{p_{\ell}^{\kappa}} \right] . \quad (6.24)$$

As our boundary condition, we set S_{NLAY} equal to zero.

Moist static energies, defined at mid and edge levels, are then given by

$$H_{\ell} \equiv h_{\ell}/C_p = S_{\ell} + \frac{L}{C_p} q_{\ell} , \quad (6.25)$$

$$H_{\ell e} \equiv h_{\ell e}/C_p = S_{\ell e} + \frac{L}{C_p} q_{\ell e} , \quad (6.26)$$

and

$$H_{\ell}^* \equiv h_{\ell}^*/C_p = S_{\ell} + \frac{L}{C_p} q_{\ell}^* . \quad (6.27)$$

Here, q_{le} is given by

$$q_{le} = \min \left\{ \bar{q}_{le}, q_{le-1}^* + \frac{C_p}{L} \Delta S \right\}, \quad (6.28)$$

where

$$\bar{q}_{le} = \begin{cases} 0 & \text{for } \Delta\sigma_{\ell} q_{\ell-1} + \Delta\sigma_{\ell-1} q_{\ell} = 0 \\ \frac{q_{\ell} q_{\ell-1} (\Delta\sigma_{\ell} + \Delta\sigma_{\ell-1})}{\Delta\sigma_{\ell} q_{\ell-1} + \Delta\sigma_{\ell-1} q_{\ell}} & \text{for } \Delta\sigma_{\ell} q_{\ell-1} + \Delta\sigma_{\ell-1} q_{\ell} \neq 0 \end{cases} \quad (6.29)$$

and

$$\Delta S = S_{\ell-1} - S_{le}. \quad (6.30)$$

Equation (6.28) ensures that q_{le} will be no larger than the saturation value determined from the conservation of moist static energy with height under adiabatic processes, i.e.,

$$\Delta H^* = \Delta S + \frac{L}{C_p} \Delta q^* = 0. \quad (6.31)$$

Once these quantities are found, they are then strapped in pairs such that the following is defined on the UCLA vertical coordinate system:

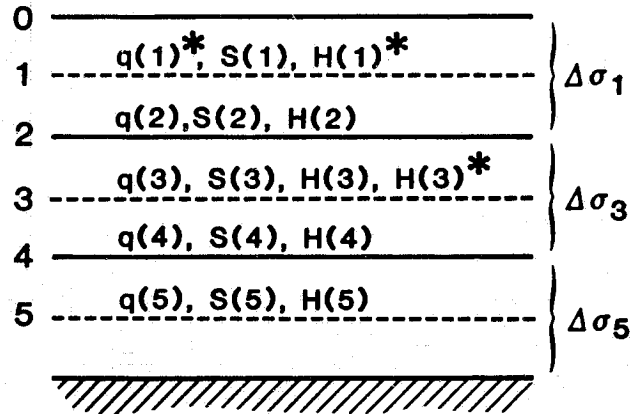


Fig. V.6b UCLA Cumulus Parameterization Variables

Here, the strapping conventions of (6.15) and (6.16) are used. Note that in Fig. V.6b the primed notation has been dropped.

There are three types of convection simulated by this parameterization. They are 1) middle-level convection, 2) penetrating convection, and 3) low-level convection, shown schematically in Fig. V.6c. Each type of cumulus convection is taken to be an ensemble of uniformly spaced convective elements whose statistical effect is the same as a single, steady-state plume.

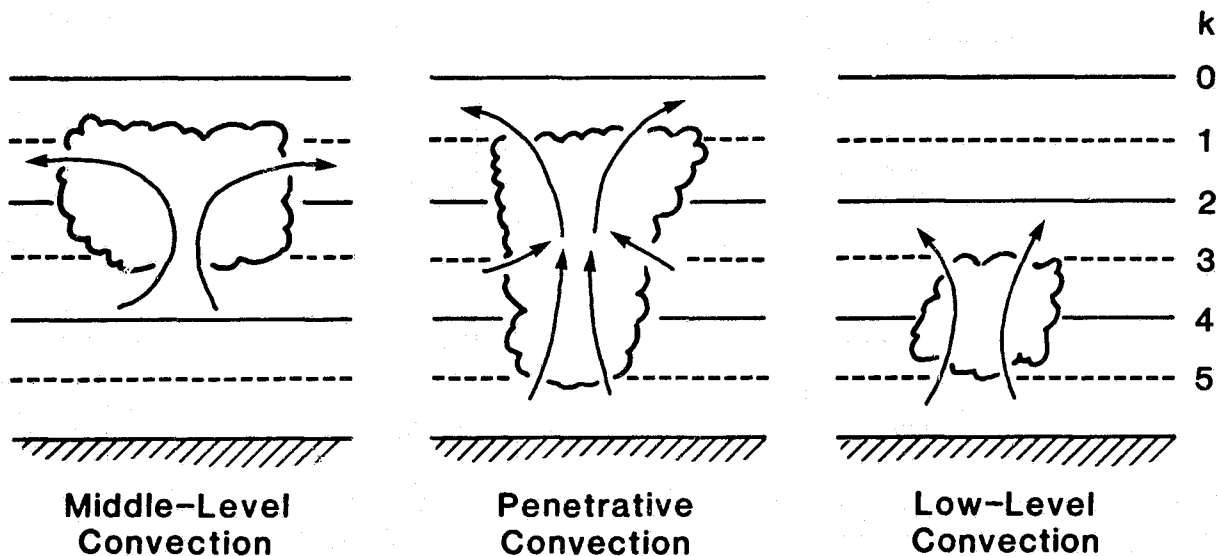


Fig. V.6c Cumulus Convection Types

In order for any of these convective types to occur, the air at the base of the cumulus cloud must become buoyant if it rises moist adiabatically to the cloud-top layer. Energetically speaking, the moist static energy at the base of the cloud must have enough thermal and potential energy such that it exceeds the saturation moist static energy of the ambient air at the cloud-top layer. Thus, we have the following criteria for convective instability:

$$\text{Middle-Level Convection:} \quad H_3 > H_1^* \quad (6.32)$$

$$\text{Penetrating Convection:} \quad H_5 > H_3^* > H_1^* \quad \text{Type A} \quad (6.33)$$

$$H_5 > H_1^* > H_3^* \quad \text{Type B} \quad (6.34)$$

$$\text{Low-Level Convection:} \quad H_1^* > H_5 > H_3^* \quad . \quad (6.35)$$

The underlying principle in each of the 3 types of cumulus convection in Fig. V.6c is the following:

Assuming large-scale processes are sufficiently slow, the time tendency of the instability mechanism for the convective adjustment is such that an equilibrium state between the cloud and its environment is achieved. From this equilibrium state, a diagnostic equation for the mass flux into the cloud may be obtained which can then be used to update the values of q and S , or correspondingly q and T .

Before proceeding to the specific cumulus convection types, it will be helpful to develop certain equations relating quantities within the cloud to quantities within the environment at a particular level. Specifically, the moist static energy within the cloud and within the environment may be expressed respectively as

$$H_c = T_{c_k} + \frac{\phi_k}{C_p} + \frac{L}{C_p} q_{c_k}^* \quad (6.36)$$

and

$$H_k^* = T_k + \frac{\phi_k}{C_p} + \frac{L}{C_p} q_k^* \quad . \quad (6.37)$$

Subtracting (6.37) from (6.36) we have

$$T_{c_k} - T_k = (H_c - H_k^*) - \frac{L}{C_p} (q_{c_k}^* - q_k^*) \quad , \quad (6.38)$$

or

$$T_{c_k} - T_k = \frac{H_c - H_k^*}{1 + \gamma_k} \quad (6.39)$$

where

$$\gamma_k = \frac{L}{C_p} \left(\frac{q_{c_k}^* - q_k^*}{T_{c_k} - T_c} \right) \approx \frac{L}{C_p} \left(\frac{\partial q_k^*}{\partial T_k} \right)_p = \frac{L}{C_p} \left(\frac{\epsilon L}{R} \right) \frac{q_k^*}{T_k^2}, \quad (6.40)$$

(see Section V.5iii for details leading to the final result in equation (6.40)).

Since $T_{c_k} - T_k = S_{c_k} - S_k$, then from (6.39) we see that

$$S_{c_k} = S_k + \frac{H_c - H_k^*}{1 + \gamma_k}. \quad (6.41)$$

From (6.41) we also see that

$$\frac{\partial H_k^*}{\partial t} = (1 + \gamma_k) \frac{\partial S_k}{\partial t}. \quad (6.42)$$

Finally, using (6.39) and (6.40), we have

$$q_{c_k}^* = q_k^* + \gamma_k \frac{C_p}{L} \left(\frac{H_c - H_k^*}{1 + \gamma_k} \right). \quad (6.43)$$

We will now look at each type of cumulus convection in detail.

Middle-Level Convection

The cloud structure assumed for middle-level convection is shown schematically in Fig. V.6d

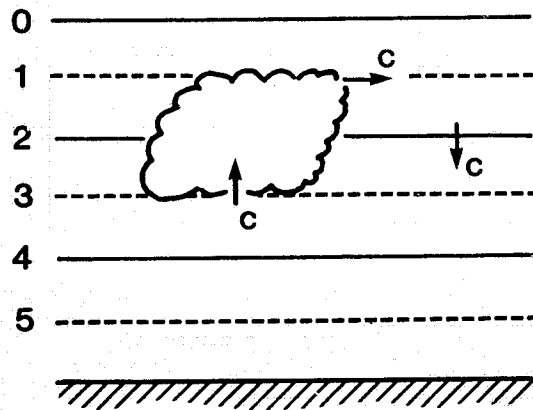


Fig. V.6d Middle-Level Convection

Here, C is the total mass flux into the cloud from level 3. From the continuity of mass, the budgets of q and S , as suggested by Fig. V.6d, are given by

$$\frac{\Pi \Delta \sigma_1}{g} \left(\frac{\partial q_1}{\partial t} \right)_{\text{cum}} = C[q_{c_1} - q_2] , \quad (6.44)$$

$$\frac{\Pi \Delta \sigma_3}{g} \left(\frac{\partial q_3}{\partial t} \right)_{\text{cum}} = C[q_2 - q_3] , \quad (6.45)$$

$$\frac{\Pi \Delta \sigma_1}{g} \left(\frac{\partial S_1}{\partial t} \right)_{\text{cum}} = C[S_{c_1} - S_2] , \quad (6.46)$$

and

$$\frac{\Pi \Delta \sigma_3}{g} \left(\frac{\partial S_3}{\partial t} \right)_{\text{cum}} = C[S_2 - S_3] , \quad (6.47)$$

where $\Pi \Delta \sigma_k / g$ is the mass/unit area of level k , and q_{c_1} and S_{c_1} are the specific humidity and dry static energy respectively within the cloud. The effects of large-scale mass convergence on q and S in this and the remaining convection types have been neglected since their response time is assumed to be sufficiently slow.

The prognostic equation for moist static energy at level 3 derived from (6.45) and (6.47), is given by

$$\frac{\Pi \Delta \sigma_3}{g} \frac{\partial H_3}{\partial t} = C[H_2 - H_3] , \quad (6.48)$$

while that for saturation moist static energy at level 1 is, using (6.42), given by

$$\frac{\Pi \Delta \sigma_1}{g} \frac{\partial H_1^*}{\partial t} = C(1 + \gamma_1) [S_{c_1} - S_2] . \quad (6.49)$$

Subtracting (6.49) from (6.48) gives the time tendency of the instability mechanism for middle-level convection:

$$\frac{\partial}{\partial t} (H_3 - H_1^*) = \frac{gC}{\Pi} \left[\left(\frac{H_2 - H_3}{\Delta \sigma_3} \right) - \left(\frac{1 + \gamma_1}{\Delta \sigma_1} \right) (S_{c_1} - S_2) \right] . \quad (6.50)$$

Using equation (6.41), (6.50) may be rewritten as

$$\frac{\partial}{\partial t} (H_3 - H_1^*) = \frac{gC}{\Pi} \left[\frac{H_2 - H_3}{\Delta\sigma_3} - \frac{1}{\Delta\sigma_1} ((1 + \gamma_1)(S_1 - S_2) + H_3 - H_1^*) \right] \quad (6.51)$$

where we have used $H_c = H_3$.

If $H_3 > H_1^*$, middle-level convection is said to occur. Integrating (6.51) in time, and assuming the right-hand side is constant during the time increment, we have

$$\begin{aligned} (H_3 - H_1^*)_{\text{final}} - (H_3 - H_1^*)_{\text{initial}} \\ = \frac{g}{\Pi} C \Delta t \left[\frac{H_2 - H_3}{\Delta\sigma_3} - \frac{1}{\Delta\sigma_1} ((1 + \gamma_1)(S_1 - S_2) + H_3 - H_1^*) \right] . \end{aligned} \quad (6.52)$$

Assuming that the final state created by the convective adjustment is a balance between the moist static energies of the cloud and its surrounding environment, then

$$(H_3 - H_1^*)_{\text{final}} = 0 . \quad (6.53)$$

Thus, the net mass flux into the cloud may then be given as

$$\frac{g}{\Pi} C \Delta t = \frac{H_3 - H_1^*}{\left[\frac{H_3 - H_2}{\Delta\sigma_3} + \frac{1}{\Delta\sigma_1} ((1 + \gamma_1)(S_1 - S_2) + H_3 - H_1^*) \right]} . \quad (6.54)$$

Before using $\frac{g}{\Pi} C \Delta t$ in the budget equations, a check is made to guarantee that the mass flux is no larger than the physically maximum value, i.e.,

$$C \Delta t \leq \frac{\Pi \Delta\sigma_3}{g} , \quad (6.55)$$

or

$$\left(\frac{g}{\Pi} C \Delta t \right)_{\text{max}} = \Delta\sigma_3 . \quad (6.56)$$

Once $\frac{g}{\Pi} C \Delta t$ is determined, the budget equations (6.44-6.47) are used to calculate the changes in specific humidity and temperature, given by

$$\Delta q_1 = \left(\frac{g}{\Pi} C \Delta t \right) \left[q_1^* + \gamma_1 \frac{C_p}{L} \left(\frac{H_3 - H_1^*}{1 + \gamma_1} \right) - q_2 \right] / \Delta \sigma_1 , \quad (6.57)$$

$$\Delta q_3 = \left(\frac{g}{\Pi} C \Delta t \right) [q_2 - q_3] / \Delta \sigma_3 , \quad (6.58)$$

$$\Delta T_1 = \left(\frac{g}{\Pi} C \Delta t \right) \left[S_1 + \frac{H_3 - H_1^*}{1 + \gamma_1} - S_2 \right] / \Delta \sigma_1 , \quad (6.59)$$

and
$$\Delta T_3 = \left(\frac{g}{\Pi} C \Delta t \right) [S_2 - S_3] / \Delta \sigma_3 , \quad (6.60)$$

where we have used equations (6.41) and (6.43) together with the approximation that

$$\frac{\partial S_k}{\partial t} \approx \frac{\partial T_k}{\partial t} . \quad (6.61)$$

These changes are then used to update the original quantities, denoted by superscript 0, given by

$$q_1 = q_1^0 + \Delta q_1 , \quad (6.62)$$

$$q_3 = q_3^0 + \Delta q_3 , \quad (6.63)$$

$$S_1 = S_1^0 + \Delta T_1 , \quad (6.64)$$

$$S_3 = S_3^0 + \Delta T_3 , \quad (6.65)$$

as well as the moist and saturated moist static energies

$$H_3 = H_3^0 + \Delta T_3 + \frac{L}{C_p} \Delta q_3 , \quad (6.66)$$

$$H_1^* = H_1^{*0} + (1 + \gamma_1) \Delta T_1 , \quad (6.67)$$

$$H_3^* = H_3^{*0} + (1 + \gamma_3) \Delta T_3 , \quad (6.68)$$

and the saturation specific humidity

$$q_1^* = q_1^{*0} + \frac{C_p}{L} \gamma_1 \Delta T_1 . \quad (6.69)$$

Finally, it is assumed that all condensation precipitates, given by

$$P_{\text{mid}} = -(\Delta q_1 \Delta \sigma_1 + \Delta q_3 \Delta \sigma_3) \frac{\Pi}{g} \quad (6.70)$$

As stated in (6.70), the units of the precipitated moisture are in decimeters (per Δt). For diagnostic purposes, a conversion is later made to change the units to 0.1 mm/day.

Middle-level convection is assumed to produce clouds in layers 5 or 6, but not both. The appropriate layer is chosen to be the one with the highest relative humidity.

Penetrating Convection

The cloud structure for penetrating convection is shown in Fig. V.6e

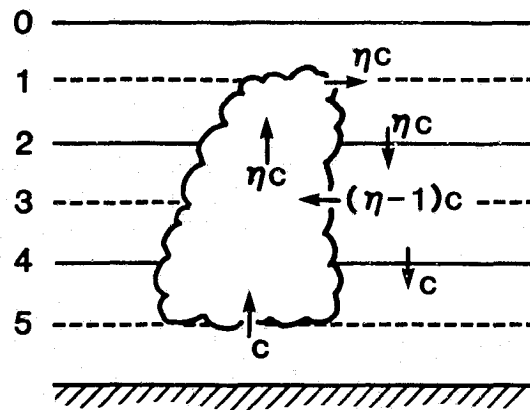


Fig. V.6e Penetrating Convection

Here, C is the total mass flux into the cloud from the boundary layer and $(\eta - 1)C$ is the horizontal entrainment into the cloud from the surrounding air. The net mass flux into the cloud after entrainment is given by ηC .

The budget equation for q and S as suggested by Fig. V.6e are given by

$$\frac{\Pi \Delta \sigma_1}{g} \frac{\partial q_1}{\partial t} = \eta C [q_{c1} - q_2] \quad (6.71)$$

$$\frac{\pi \Delta \sigma_3}{g} \frac{\partial q_3}{\partial t} = \eta C \left[(q_2 - q_3) + \frac{1}{\eta} (q_3 - q_4) \right] , \quad (6.72)$$

$$\frac{\pi \Delta \sigma_5}{g} \frac{\partial q_5}{\partial t} = \eta C \left[\frac{1}{\eta} (q_4 - q_5) \right] , \quad (6.73)$$

and

$$\frac{\pi \Delta \sigma_1}{g} \frac{\partial S_1}{\partial t} = \eta C [S_{c1} - S_2] , \quad (6.74)$$

$$\frac{\pi \Delta \sigma_3}{g} \frac{\partial S_3}{\partial t} = \eta C \left[(S_2 - S_3) + \frac{1}{\eta} (S_3 - S_4) \right] , \quad (6.75)$$

$$\frac{\pi \Delta \sigma_5}{g} \frac{\partial S_5}{\partial t} = \eta C \left[\frac{1}{\eta} (S_4 - S_5) \right] . \quad (6.76)$$

As stated by equations (6.33) and (6.34), two possible penetrating convection types exist. These are given by

$$\text{Type A: } H_5 > H_3^* > H_1^* , \quad (6.77)$$

and

$$\text{Type B: } H_5 > H_1^* > H_3^* . \quad (6.78)$$

Prognostic equations for H_5 , H_1^* , and H_3^* are obtained by combining the appropriate budget equations, giving

$$\frac{\pi \Delta \sigma_5}{g} \frac{\partial H_5}{\partial t} = \eta C \left[\frac{1}{\eta} (H_4 - H_5) \right] , \quad (6.79)$$

$$\frac{\pi \Delta \sigma_1}{g} \frac{\partial H_1^*}{\partial t} = \eta C \left[(1 + \gamma_1)(S_1 - S_2) + H_c - H_1^* \right] , \quad (6.80)$$

and

$$\frac{\pi \Delta \sigma_3}{g} \frac{\partial H_3^*}{\partial t} = \eta C \left[(1 + \gamma_3) \left((S_2 - S_3) + \frac{1}{\eta} (S_3 - S_4) \right) \right] . \quad (6.81)$$

To calculate the entrainment factor $\frac{1}{\eta}$, we assume that the cloud entrains as much environmental air as it can until neutral buoyancy is achieved with respect to one of the upper levels but is still positively buoyant with respect to the remaining level. In this calculation, we first define the total moist static energy of the cloud as

$$H_c = \frac{CH_5 + (\eta - 1)C H_3}{C + (\eta - 1)C} \quad (6.82)$$

or

$$H_c = H_3 + \frac{1}{\eta} (H_5 - H_3) . \quad (6.83)$$

Solving for $\frac{1}{\eta}$ we have

$$\frac{1}{\eta} = \frac{H_c - H_3}{H_5 - H_3} . \quad (6.84)$$

Thus, for Type A penetrating convection we have

$$\frac{1}{\eta_A} = \frac{H_3^* - H_3}{H_5 - H_3} , \quad (6.85)$$

while for Type B penetrating convection we have

$$\frac{1}{\eta_B} = \frac{H_1^* - H_3}{H_5 - H_3} . \quad (6.86)$$

For Type A penetrating convection, the governing equation for $(H_5 - H_3^*)$, obtained from (6.79) and (6.81), is given by

$$\begin{aligned} \frac{\partial}{\partial t} (H_5 - H_3^*) &= \frac{g}{\Pi} \eta C \left[\frac{1}{\Delta \sigma_5} \frac{1}{\eta_A} (H_4 - H_5) \right. \\ &\quad \left. - \frac{(1 + \gamma_3)}{\Delta \sigma_3} ((S_2 - S_3) + \frac{1}{\eta_A} (S_3 - S_4)) \right] . \end{aligned} \quad (6.87)$$

Integrating (6.87) in time and assuming the final state is in balance, we obtain

$$(\frac{g}{\Pi} \eta C \Delta t)_A = \frac{H_5 - H_3^*}{\left[\frac{1 + \gamma_3}{\Delta \sigma_3} ((s_2 - s_3) + \frac{1}{\eta_A} (s_3 - s_4)) + \frac{1}{\Delta \sigma_5} \frac{1}{\eta_A} (H_5 - H_4) \right]} \quad (6.88)$$

For Type B penetrating convection, the governing equation for $(H_5 - H_1^*)$, obtained from (6.79) and (6.80), is given by

$$\frac{\partial}{\partial t} (H_5 - H_1^*) = \frac{g}{\Pi} \eta C \left[\frac{1}{\Delta \sigma_5} \frac{1}{\eta_B} (H_4 - H_5) - \frac{(1 + \gamma_1)}{\Delta \sigma_1} (s_1 - s_2) \right], \quad (6.89)$$

since $H_c = H_1^*$. Again, integrating in time and assuming a balanced final state, the expression for ηC is given by

$$(\frac{g}{\Pi} \eta C \Delta t)_B = \frac{H_5 - H_1^*}{\left[\frac{1 + \gamma_1}{\Delta \sigma_1} (s_1 - s_2) + \frac{1}{\Delta \sigma_5} \frac{1}{\eta_B} (H_5 - H_4) \right]} \quad (6.90)$$

Before proceeding to the budget equations, a check is made to guarantee that the computed net mass flux from either Type A or Type B penetrating convection is not larger than the physically maximum allowable value. For example, at the entrainment level we have

$$(\eta - 1) C \Delta t \leq \frac{\Pi \Delta \sigma_3}{g}, \quad (6.91)$$

thus

$$(\frac{g}{\Pi} \eta C \Delta t)_{\max} = \Delta \sigma_3 / (1 - 1/\eta). \quad (6.92)$$

In the boundary layer, we have

$$C \Delta t \leq \frac{\Pi}{g} \Delta \sigma_5, \quad (6.93)$$

thus

$$(\frac{g}{\Pi} \eta C \Delta t)_{\max} = \Delta \sigma_5 / (1/\eta). \quad (6.94)$$

From this point, Type A and Type B penetrating convections are identical. Using the budget equations (6.71-6.76) together with the approximation (6.61), the changes in temperature and specific humidity are given by

$$\Delta q_1 = \left(\frac{g}{\Pi} \eta C \Delta t \right) \left[q_1^* - q_2 + \frac{\gamma_1 C_p}{L} \left(\frac{H_c - H_1^*}{1 + \gamma_1} \right) \right] / \Delta \sigma_1 , \quad (6.95)$$

$$\Delta q_3 = \left(\frac{g}{\Pi} \eta C \Delta t \right) \left[q_2 - q_3 + \frac{1}{\eta} (q_3 - q_4) \right] / \Delta \sigma_3 , \quad (6.96)$$

$$\Delta q_5 = \left(\frac{g}{\Pi} \eta C \Delta t \right) \left[\frac{1}{\eta} (q_4 - q_5) \right] / \Delta \sigma_5 , \quad (6.97)$$

$$\Delta T_1 = \left(\frac{g}{\Pi} \eta C \Delta t \right) \left[S_1 - S_2 + \frac{H_c - H_1^*}{1 + \gamma_1} \right] / \Delta \sigma_1 , \quad (6.98)$$

$$\Delta T_3 = \left(\frac{g}{\Pi} \eta C \Delta t \right) \left[S_2 - S_3 + \frac{1}{\eta} (S_3 - S_4) \right] / \Delta \sigma_3 , \quad (6.99)$$

and

$$\Delta T_5 = \left(\frac{g}{\Pi} \eta C \Delta t \right) \left[\frac{1}{\eta} (S_4 - S_5) \right] / \Delta \sigma_5 , \quad (6.100)$$

where

$$H_c = \begin{cases} H_3^* & \text{for Type A} \\ H_1^* & \text{for Type B} \end{cases} . \quad (6.101)$$

These changes are then added to those from middle-level convection. The moisture and energy fields that are used in the next type of cumulus convection, i.e., low-level, are then updated by

$$S_3 = S_3^0 + \Delta T_3 , \quad (6.102)$$

$$S_5 = S_5^0 + \Delta T_5 , \quad (6.103)$$

$$q_3 = q_3^0 + \Delta q_3 , \quad (6.104)$$

$$q_5 = q_5^0 + \Delta q_5 , \quad (6.105)$$

$$H_1^* = H_1^{*0} + (1 + \gamma_1) \Delta T_1 , \quad (6.106)$$

$$H_3^* = H_3^{*0} + (1 + \gamma_3) \Delta T_3 , \quad (6.107)$$

$$H_3 = H_3^0 + \Delta T_3 + \frac{L}{C_p} \Delta q_3 , \quad (6.108)$$

and

$$H_5 = H_5^0 + \Delta T_5 + \frac{L}{C_p} \Delta q_5 . \quad (6.109)$$

Finally, penetrating convection is assumed to produce clouds in 4 levels of the GLAS GCM. Three patterns are used for the cloud level placement. These are given by

- a) levels 4, 5, 6, 7
- b) levels 5, 6, 7, 8
- c) levels 6, 7, 8, 9

Patterns (a), (b) and (c) are assumed to have the occurrence probability of 25%, 50% and 25% respectively. This is implemented by introducing the variable NCL which assumes a cyclically varying value from 1 to 4. NCL values 1 and 3 correspond to pattern (b). NCL values 2 and 4 correspond to patterns (c) and (a) respectively. The total precipitation obtained from penetrating convection is given by

$$P = -(\Delta q_1 \Delta \sigma_1 + \Delta q_3 \Delta \sigma_3 + \Delta q_5 \Delta \sigma_5) \frac{g}{\Pi} . \quad (6.110)$$

Low-Level Convection

The cloud structure for low-level convection is shown in Fig. V.6f.

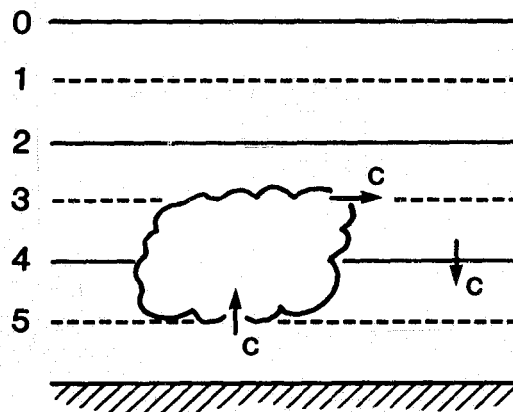


Fig. V.6f Low-Level Convection

The budget equations for q and S as suggested by Fig. V.6f are given by

$$\frac{\pi \Delta \sigma_3}{g} \frac{\partial q_3}{\partial t} = C [q_{c_3} - q_4] , \quad (6.111)$$

$$\frac{\pi \Delta \sigma_5}{g} \frac{\partial q_5}{\partial t} = C [q_4 - q_5] , \quad (6.112)$$

$$\frac{\pi \Delta \sigma_3}{g} \frac{\partial S_3}{\partial t} = C [s_{c_3} - s_4] , \quad (6.113)$$

and

$$\frac{\pi \Delta \sigma_5}{g} \frac{\partial S_5}{\partial t} = C [s_4 - s_5] . \quad (6.114)$$

Due to the shallowness of the lower layers, it is assumed that the horizontal cloud size is small. Because of this, the assumption is made that the cloud does not precipitate but rather re-evaporates its moisture into the model layer. By adding equations (6.113) and (6.114), we see that the total net heating in the two layers is expressed as

$$\frac{\pi}{g} \left(\Delta \sigma_3 \frac{\partial S_3}{\partial t} + \Delta \sigma_5 \frac{\partial S_5}{\partial t} \right) = C [s_{c_3} - s_5] . \quad (6.115)$$

Letting ΔT represent the total heating, we have

$$\Delta T \equiv s_{c_3} - s_5 = s_3 - s_5 + \frac{H_5 - H_3^*}{1 + \gamma_3} \quad (6.116)$$

where we have used $H_c = H_5$. The moisture adjustment evaporated by this heating is given by

$$\Delta q_E = \frac{C_p}{L} \Delta T = \frac{C_p}{L} \left(s_3 - s_5 + \frac{H_5 - H_3^*}{1 + \gamma_3} \right) . \quad (6.117)$$

This moisture is now added back into the budget equations as an extra source

term, i.e.,

$$\frac{\pi \Delta \sigma_3}{g} \frac{\partial q_3}{\partial t} = C [q_{e3} - q_4 + \Delta q_{E3}] , \quad (6.118)$$

and

$$\frac{\pi \Delta \sigma_5}{g} \frac{\partial q_5}{\partial t} = C [q_4 - q_5 + \Delta q_{E5}] , \quad (6.119)$$

where Δq_{E3} and Δq_{E5} are mass-weighted adjustments to Δq_E , i.e.,

$$\Delta q_{E3} = \left(\frac{\Delta \sigma_3}{\Delta \sigma_3 + \Delta \sigma_5} \right) \Delta q_E , \quad (6.120)$$

and

$$\Delta q_{E5} = \left(\frac{\Delta \sigma_5}{\Delta \sigma_3 + \Delta \sigma_5} \right) \Delta q_E . \quad (6.121)$$

Correspondingly, the heating required for this evaporation is removed from the budgets of S_3 and S_5 , i.e.,

$$\frac{\pi \Delta \sigma_3}{g} \frac{\partial S_3}{\partial t} = C [s_{e3} - s_4 - \frac{L}{C_p} \Delta q_{E3}] , \quad (6.122)$$

and

$$\frac{\pi \Delta \sigma_5}{g} \frac{\partial S_5}{\partial t} = C [s_4 - s_5 - \frac{L}{C_p} \Delta q_{E5}] . \quad (6.123)$$

The mechanism for instability for low-level convection is given by

$$H_5 > H_3^* . \quad (6.124)$$

Using equation (6.118), (6.119), (6.122), and (6.123), we see that

$$\frac{\partial H_5}{\partial t} = \frac{g}{\pi} C \left[\frac{H_4 - H_5}{\Delta \sigma_5} \right] , \quad (6.125)$$

and

$$\frac{\partial H_3^*}{\partial t} = \frac{g}{\pi} C \left[\frac{1 + \gamma_3}{\Delta \sigma_3} (s_3 - s_4 - \frac{L}{C_p} \Delta q_{E3}) + \frac{H_5 - H_3^*}{\Delta \sigma_3} \right] . \quad (6.126)$$

Subtracting (6.126) from (6.125) we have

$$\frac{\partial}{\partial t} (H_5 - H_3^*) = \frac{g}{\Pi} C \left[\frac{H_4 - H_5}{\Delta\sigma_5} - \frac{(1 + \gamma_3)(S_3 - S_4 - \frac{L}{C_p} \Delta q_{E_3}) + H_5 - H_3^*}{\Delta\sigma_3} \right] \quad (6.127)$$

Integrating in time and assuming a balanced final state, the expression for the mass flux becomes

$$\left(\frac{g}{\Pi} C \Delta t \right) = \frac{H_5 - H_3^*}{\left[\frac{H_5 - H_4}{\Delta\sigma_5} + \frac{(1 + \gamma_3)(S_3 - S_4 - \frac{L}{C_p} \Delta q_{E_3}) + H_5 - H_3^*}{\Delta\sigma_3} \right]} \quad (6.128)$$

A check is then made to ensure that

$$C \Delta t \leq \frac{\Pi \Delta\sigma_5}{g} \quad , \quad (6.129)$$

or

$$\left(\frac{g}{\Pi} C \Delta t \right)_{\max} = \Delta\sigma_5 \quad . \quad (6.130)$$

Once $\frac{g}{\Pi} C \Delta t$ is determined, the changes in q and T are given using the modified budget equations (6.118), (6.119), (6.122) and (6.123), i.e.,

$$\Delta T_3 = \left(\frac{g}{\Pi} C \Delta t \right) \left[S_3 + \frac{H_5 - H_3^*}{1 + \gamma_3} - S_4 - \frac{L}{C_p} \Delta q_{E_3} \right] / \Delta\sigma_3 \quad , \quad (6.131)$$

$$\Delta T_5 = \left(\frac{g}{\Pi} C \Delta t \right) \left[S_4 - S_5 - \frac{L}{C_p} \Delta q_{E_5} \right] / \Delta\sigma_5 \quad , \quad (6.132)$$

and

$$\Delta q_5 = \left(\frac{g}{\Pi} C \Delta t \right) [q_4 - q_5 + \Delta q_{E_5}] / \Delta\sigma_5 \quad . \quad (6.133)$$

To ensure that no moisture precipitates, Δq_3 is set to

$$\Delta q_3 = -\Delta q_5 \frac{\Delta\sigma_5}{\Delta\sigma_3} \quad . \quad (6.134)$$

Clouds due to low-level convection are assumed to form in level 7 or level 8 in the GLAS GCM depending on which has the higher relative humidity.

Conversion to the GLAS Vertical Grid

Once all three types of convective processes are completed, the heating and moisture adjustments due to the convection must now be converted to adjustments in the GLAS vertical grid.

As a first step in converting temperature changes, we see from Fig. V.6a that we may write

$$\Delta T_5 = \frac{1}{2} (\Delta T'_1 + \Delta T'_2) , \quad (6.135)$$

and

$$\Delta T_8 = \frac{1}{2} (\Delta T'_4 + \Delta T'_5) , \quad (6.136)$$

where the primed variable is on the UCLA grid and the unprimed variable is on the GLAS grid. Letting

$$\Delta T'_2 = \frac{1}{2} (\Delta T'_1 + \Delta T'_3) , \quad (6.137)$$

and

$$\Delta T'_4 = \frac{1}{2} (\Delta T'_3 + \Delta T'_5) \quad (6.138)$$

equations (6.135) and (6.136) become

$$\Delta T_5 = \frac{3}{4} \Delta T'_1 + \frac{1}{4} \Delta T'_3 , \quad (6.139)$$

and

$$\Delta T_8 = \frac{3}{4} \Delta T'_5 + \frac{1}{4} \Delta T'_3 . \quad (6.140)$$

Using the fact that

$$\Delta T'_1 = \frac{1}{2} (\Delta T_4 + \Delta T_5) , \quad (6.141)$$

and

$$\Delta T_5' = \frac{1}{2} (\Delta T_8 + \Delta T_9) , \quad (6.142)$$

then, incorporating (6.139) and (6.140), we see that

$$\Delta T_4 = \frac{5}{4} \Delta T_1' - \frac{1}{4} \Delta T_3' , \quad (6.143)$$

and

$$\Delta T_9 = \frac{5}{4} \Delta T_5' - \frac{1}{4} \Delta T_3' . \quad (6.144)$$

Finally, letting

$$\Delta T_6 = \frac{1}{2} (\Delta T_2' + \Delta T_3') , \quad (6.145)$$

and

$$\Delta T_7 = \frac{1}{2} (\Delta T_3' + \Delta T_4') , \quad (6.146)$$

and using the fact that

$$\Delta T_3' = \frac{1}{2} (\Delta T_6 + \Delta T_7) , \quad (6.147)$$

it can be shown that

$$\Delta T_6 = \Delta T_3' + \frac{1}{8} (\Delta T_1' - \Delta T_5') , \quad (6.148)$$

and

$$\Delta T_7 = \Delta T_3' - \frac{1}{8} (\Delta T_1' - \Delta T_5') . \quad (6.149)$$

The redistribution of moisture back onto the GLAS vertical grid is accomplished as follows:

$$\text{Define } f_1 = \begin{cases} q(k+3)/\bar{q} & \text{if } \Delta q'(k) < 0 \\ q^*(k+3)/\bar{q}^* & \text{if } \Delta q'(k) > 0 \end{cases} \quad k=1, 3, 5 \quad (6.150)$$

and

$$f_2 = 2 - f_1 , \quad (6.151)$$

where

$$\bar{q} = \frac{1}{2} (q(k+3) + q(k+4)) , \quad (6.152)$$

$$\text{and} \quad \bar{q}^* = \frac{1}{2} (q^*(k+3) + q^*(k+4)) . \quad (6.153)$$

Then,

$$\Delta q(k+3) = f_1 \Delta q'(k), \quad (6.154)$$

and

$$\Delta q(k+4) = f_2 \Delta q'(k) . \quad (6.155)$$

These temperature and specific humidity adjustments are then used to give updated values for temperature, specific humidity, saturation specific humidity, and the latent heating parameter.

Final Note

It should be noted that the parameterization schemes used by the model are subject to change due to continuing research and development. Presently, the current 9-level assumption implicit in the cumulus parameterization scheme is being rewritten to allow for a more general vertical structure. Therefore, the particular strapping and conversion equations between the GLAS model and the UCLA model will be modified in the forthcoming version of the model with variable vertical resolution.

V.6i1i1 Moist Adiabatic Adjustment

The current method of cumulus parameterization requires a transformation from the GLAS vertical grid to that used in the UCLA 3-layer model (Arakawa, 1972). Once the moisture and temperature field adjustments are calculated in the 3-layer model, another transformation is made back to the GLAS vertical grid. This process cannot relieve moist convective instability which occurs within the lowest two levels of the GLAS model and thus it has been observed that excess moisture accumulates in the lowest model layer. As a result, the frequency of large-scale supersaturation clouds in the lowest layer tends to be significantly higher than observed. For this reason, a moist adiabatic adjustment routine is used immediately after the execution of the cumulus parameterization. Whenever moist convective instability occurs, the scheme mixes moisture and temperature moist adiabatically in the vertical while conserving the vertically integrated moisture and temperature fields.

The cloud structure generated from the moist adiabatic adjustment process is shown in Fig. V.6g.

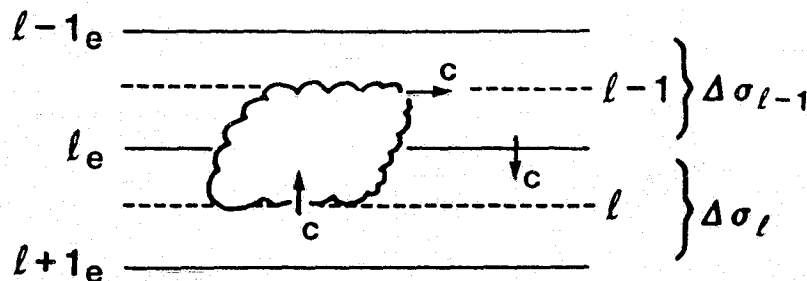


Fig. V.6g Moist Adiabatic Adjustment

The criteria for moist adiabatic adjustment to occur between any two adjacent layers ℓ and $\ell-1$ is similar to that required for low-level cumulus convection, i.e.,

$$H_{\ell} > H_{\ell-1}^* \quad . \quad (6.156)$$

Here H , H^* , and all subsequent variables are defined as in Section V.611.

Following the notation and assumptions used in Section V.611, we see from Fig. V.6g that the budget equations for q and S are given by

$$\frac{\Pi \Delta \sigma_{\ell-1}}{g} \frac{\partial q_{\ell-1}}{\partial t} = C [q_{c_{\ell-1}} - q_{\ell_e}] \quad , \quad (6.157)$$

$$\frac{\Pi \Delta \sigma_{\ell}}{g} \frac{\partial q_{\ell}}{\partial t} = C [q_{\ell_e} - q_{\ell}] \quad , \quad (6.158)$$

$$\frac{\Pi \Delta \sigma_{\ell-1}}{g} \frac{\partial S_{\ell-1}}{\partial t} = C [S_{c_{\ell-1}} - S_{\ell_e}] \quad , \quad (6.159)$$

$$\frac{\Pi \Delta \sigma_{\ell}}{g} \frac{\partial S_{\ell}}{\partial t} = C [S_{\ell_e} - S_{\ell}] \quad . \quad (6.160)$$

As with low-level convection, we assume that the clouds generated by the moist adiabatic adjustment algorithm are too shallow to precipitate. In order to conserve the total moisture in the two layers, any moisture condensed during the moist adiabatic adjustment is re-evaporated and added back to the budget equations (6.157) and (6.158). The heat required for the re-evaporation is removed from (6.159) and (6.160). In a manner similar to that discussed in Section V.611 on low-level cumulus convection, the new budget equations with this adjustment are given by

$$\frac{\Pi \Delta \sigma_{\ell-1}}{g} \frac{\partial q_{\ell-1}}{\partial t} = C [q_{c_{\ell-1}} - q_{\ell_e} + \Delta q_{E_{\ell-1}}] \quad , \quad (6.161)$$

ORIGINAL PAGE IS
OF POOR QUALITY

$$\frac{\pi \Delta \sigma_{\ell}}{g} \frac{\partial q_{\ell}}{\partial t} = C [q_{\ell_e} - q_{\ell} + \Delta q_{E\ell}] , \quad (6.162)$$

$$\frac{\pi \Delta \sigma_{\ell-1}}{g} \frac{\partial S_{\ell-1}}{\partial t} = C \left[S_{\ell-1} - S_{\ell_e} - \frac{L}{C_p} \Delta q_{E\ell-1} \right] , \quad (6.163)$$

and

$$\frac{\pi \Delta \sigma_{\ell}}{g} \frac{\partial S_{\ell}}{\partial t} = C \left[S_{\ell_e} - S_{\ell} - \frac{L}{C_p} \Delta q_{E\ell} \right] , \quad (6.164)$$

where

$$\Delta q_{E\ell-1} = \frac{\Delta \sigma_{\ell-1}}{\Delta \sigma_{\ell} + \Delta \sigma_{\ell-1}} \Delta q_E , \quad (6.165)$$

$$\Delta q_{E\ell} = \frac{\Delta \sigma_{\ell}}{\Delta \sigma_{\ell} + \Delta \sigma_{\ell-1}} \Delta q_E , \quad (6.166)$$

and

$$\Delta q_E = \frac{C_p}{L} \left[S_{\ell-1} - S_{\ell} + \frac{H_{\ell} - H_{\ell-1}^*}{1 + \gamma_{\ell-1}} \right] . \quad (6.167)$$

To obtain the edge values for S_{ℓ_e} , we note from equations (6.23) and (6.24) that

$$S_{\ell_e} = S_{\ell} + \frac{\Delta \sigma_{\ell}}{\Delta \sigma_{\ell} + \Delta \sigma_{\ell-1}} \left[T_{\ell-1} \frac{p_{\ell}^{\kappa}}{p_{\ell-1}^{\kappa}} - T_{\ell} \right] , \quad (6.168)$$

and

$$S_{\ell-1} = S_{\ell_e} + \frac{\Delta \sigma_{\ell-1}}{\Delta \sigma_{\ell} + \Delta \sigma_{\ell-1}} \left[T_{\ell-1} - T_{\ell} \frac{p_{\ell-1}^{\kappa}}{p_{\ell}^{\kappa}} \right] . \quad (6.169)$$

Combining (6.168) and (6.169) we may write

$$S_{\ell_e} = \frac{\Delta\sigma_{\ell-1} S_{\ell} + \Delta\sigma_{\ell} S_{\ell-1}}{\Delta\sigma_{\ell} + \Delta\sigma_{\ell-1}} + \frac{\Delta\sigma_{\ell} \Delta\sigma_{\ell-1}}{(\Delta\sigma_{\ell} + \Delta\sigma_{\ell-1})^2} \left[T_{\ell-1} \left(\frac{p_{\ell}^{\kappa}}{p_{\ell-1}^{\kappa}} - 1 \right) - T_{\ell} \left(1 - \frac{p_{\ell-1}^{\kappa}}{p_{\ell}^{\kappa}} \right) \right] . \quad (6.170)$$

By writing $\frac{p_{\ell}^{\kappa}}{p_{\ell-1}^{\kappa}} - 1$ as

$$\frac{p_{\ell}^{\kappa}}{p_{\ell-1}^{\kappa}} - 1 = \left(1 + \frac{p_{\ell} - p_{\ell-1}}{p_{\ell-1}} \right)^{\kappa} - 1 \quad (6.171)$$

and using binomial expansion, (6.171) may be approximated by

$$\frac{p_{\ell}^{\kappa}}{p_{\ell-1}^{\kappa}} - 1 \approx \kappa \frac{p_{\ell} - p_{\ell-1}}{p_{\ell-1}} . \quad (6.172)$$

Similarly,

$$1 - \frac{p_{\ell-1}^{\kappa}}{p_{\ell}^{\kappa}} \approx \kappa \frac{p_{\ell} - p_{\ell-1}}{p_{\ell-1}} . \quad (6.173)$$

Using (6.172) and (6.173) in (6.170), we have

$$S_{\ell_e} = \frac{\Delta\sigma_{\ell-1} S_{\ell} + \Delta\sigma_{\ell} S_{\ell-1}}{\Delta\sigma_{\ell} + \Delta\sigma_{\ell-1}} + \kappa \frac{\Delta\sigma_{\ell} \Delta\sigma_{\ell-1}}{(\Delta\sigma_{\ell} + \Delta\sigma_{\ell-1})^2} \left(\frac{p_{\ell} - p_{\ell-1}}{p_{\ell-1}} \right) (T_{\ell-1} - T_{\ell}) . \quad (6.174)$$

Moisture at the edge level is computed the same as that given by (6.28).

For moist adiabatic adjustment to occur, we require that

$$H_{\ell} - H_{\ell-1}^* > 0 . \quad (6.175)$$

Recalling from Section V.6ii that

ORIGINAL PAGE IS
OF POOR QUALITY

$$H_{\ell} = S_{\ell} + \frac{L}{C_p} q_{\ell} \quad , \quad (6.176)$$

and

$$\frac{\partial H_{\ell-1}^*}{\partial t} = (1 + \gamma_{\ell-1}) \frac{\partial S_{\ell-1}}{\partial t} \quad , \quad (6.177)$$

equations (6.161) through (6.164) may be combined to obtain

$$\begin{aligned} \frac{\partial}{\partial t} (H_{\ell} - H_{\ell-1}^*) &= \frac{gC}{\Pi} \left[\frac{H_{\ell_e} - H_{\ell}}{\Delta\sigma_{\ell}} \right. \\ &\quad \left. - \left(\frac{1 + \gamma_{\ell-1}}{\Delta\sigma_{\ell-1}} \right) (S_{\ell-1} - S_{\ell_e} - \frac{L}{C_p} \Delta q_{E\ell-1}) \right] \quad , \end{aligned} \quad (6.178)$$

or

$$\begin{aligned} \frac{\partial}{\partial t} (H_{\ell} - H_{\ell-1}^*) &= \frac{gC}{\Pi} \left[\frac{H_{\ell_e} - H_{\ell}}{\Delta\sigma_{\ell}} - \frac{(1 + \gamma_{\ell-1})}{\Delta\sigma_{\ell-1}} \right. \\ &\quad \left. (S_{\ell-1} - S_{\ell_e} - \frac{L}{C_p} \Delta q_{E\ell-1}) - \frac{H_{\ell} - H_{\ell-1}^*}{\Delta\sigma_{\ell-1}} \right] \quad , \end{aligned} \quad (6.179)$$

where $H_{\ell_e} = S_{\ell_e} + \frac{L}{C_p} q_{\ell_e}$. Assuming that equilibrium is established after a given adjustment time period (currently 30 minutes), then the mass flux into the cloud may be expressed as

$$\begin{aligned} \frac{gC\Delta t}{\Pi} &= (H_{\ell} - H_{\ell-1}^*) / \left[\frac{H_{\ell} - H_{\ell_e}}{\Delta\sigma_{\ell}} \right. \\ &\quad \left. + \frac{(H_{\ell} - H_{\ell-1}^*) + (1 + \gamma_{\ell-1})(S_{\ell-1} - S_{\ell_e} - \frac{L}{C_p} \Delta q_{E\ell-1})}{\Delta\sigma_{\ell-1}} \right] \quad . \end{aligned} \quad (6.180)$$

A check is then made to ensure that this flux is no larger than the minimum of $\frac{\Pi\Delta\sigma_{\ell}}{g}$ and $\frac{\Pi\Delta\sigma_{\ell-1}}{g}$, i.e., the maximum flux physically allowed.

Once the mass flux into the cloud is calculated, the budget equations are used to update the temperature and moisture fields,

$$\Delta q_{l-1} = \frac{gC\Delta t}{\Pi} [q_{l-1}^* - q_{l_e} + \Delta q_{E_{l-1}} + \gamma_{l-1} \frac{C_p}{L} (\frac{H_l - H_{l-1}^*}{1 + \gamma_{l-1}})] / \Delta \sigma_{l-1} \quad (6.181)$$

$$\Delta q_l = \frac{gC\Delta t}{\Pi} [q_{l_e} - q_l + \Delta q_{E_l}] / \Delta \sigma_l, \quad (6.182)$$

$$\Delta T_{l-1} = \frac{gC\Delta t}{\Pi} [S_{l-1} - S_{l_e} - \frac{L}{C_p} \Delta q_{E_{l-1}} + \frac{H_l - H_{l-1}^*}{1 + \gamma_{l-1}}] / \Delta \sigma_{l-1} \quad (6.183)$$

$$\Delta T_l = \frac{gC\Delta t}{\Pi} [S_{l_e} - S_l - \frac{L}{C_p} \Delta q_{E_l}] / \Delta \sigma_l, \quad (6.184)$$

where we have used

$$q_{c_{l-1}} = q_{l-1}^* + \gamma_{l-1} \frac{C_p}{L} (\frac{H_l - H_{l-1}^*}{1 + \gamma_{l-1}}), \quad (6.185)$$

$$S_{c_{l-1}} = S_{l-1} + \frac{H_l - H_{l-1}^*}{1 + \gamma_{l-1}}, \quad (6.186)$$

$$\Delta T_{l-1} \approx \Delta S_{l-1}, \quad (6.187)$$

$$\Delta T_l \approx \Delta S_l. \quad (6.188)$$

It should be noted that

$$\Delta \sigma_{l-1} \Delta q_{l-1} + \Delta \sigma_l \Delta q_l = 0, \quad (6.189)$$

and

$$\Delta \sigma_{l-1} \Delta T_{l-1} + \Delta \sigma_l \Delta T_l = 0, \quad (6.190)$$

thus conserving the vertically integrated moisture field and internal energy.

This process is executed from the top of the atmosphere, $l=1$, to the lowest level, $l=N_{LAY}$, and then repeated two more times.

V.7 Diagnostics

In this section we examine the default diagnostic variables calculated in the physics portion of the model. These diagnostic terms may be found in subroutine COMP3 unless otherwise noted.

V.7i Diagnostic Quantities Retained in the History File

The diagnostic terms calculated in the physics portion of the model are used to keep a cumulative record of various physical processes occurring during the model forecast. In most cases, the diagnostic terms are average values over the period between FORTRAN writes to the history file. In the particular case of the upward flux of longwave radiation, however, the value saved on the history file is the most current value. This is done so that it can be used as an approximate value for the longwave radiative flux during times when the longwave radiation package is not called.

The following is a list and description of the diagnostic terms calculated in the physics portion of the model. It should be noted that most diagnostic terms are expressed as units/day, and are re-initialized after every FORTRAN write to the history file.

HFLUX (ly/day) \equiv Net upward flux of sensible heat

$$= \frac{1}{M} \sum_{i=1}^M \rho_s C_p D_r (T_g - T_s) , \quad (7.1)$$

where $M = \text{DTOUT}/\text{DTC3}$, DTOUT is the number of seconds between writes to the history file, and DTC3 is the number of seconds between calls to the physics.

EFLUX (ly/day) \equiv Upward flux of latent heat

$$= \frac{1}{M} \sum_{i=1}^M \rho_s \beta D_r L (q_g^* - q_s) . \quad (7.2)$$

FUSION (ly/day) \equiv Net heating or cooling due to conduction through sea ice

$$= \frac{1}{M} \sum_{i=1}^M \frac{C_{ice}}{H_{ice}} (T_{ice} - T_g) \quad (7.3)$$

RADSW (ly/day) \equiv Net short wave radiation absorbed at level ℓ

$$= \frac{1}{M} \sum_{i=1}^M A_s(\ell) \quad (7.4)$$

RADSWG (ly/day) \equiv Net shortwave radiation absorbed at the ground

$$= \frac{1}{M} \sum_{i=1}^M SG \quad (7.5)$$

RADLW (ly/day) \equiv Upward flux of longwave radiation at level ℓ

$$= RE(\ell) \quad (7.6)$$

RADLWG (ly/day) \equiv Upward flux of longwave radiation at the ground

$$= RE(NLAYPl) \quad (7.7)$$

DIABAT (.1°K/day) = 10*CUMDAY* ΔT_{total} (7.8)

where $\Delta T_{total} = \sum_{i=1}^M [\Delta T_{L+S} + \Delta T_{rad}]$, (7.9)

ΔT_{L+S} \equiv Temperature change due to Latent and Sensible Heat,

and ΔT_{rad} \equiv Temperature change due to radiation

$$= \frac{g \Delta t}{10 \pi C_p \Delta \sigma(\ell)} [A_s(\ell) + RE(\ell+1) - RE(\ell)] . \quad (7.10)$$

CUMDAY is the number of FORTRAN writes to the history file per day. Since DIABAT is initialized after every history write, then ΔT_{total} is the sum of

the diabatic heating for the time period between history records. Multiplying by CUMDAY thus gives the daily diabatic heating rate.

TMIN (°K) ≡ Minimum surface temperature for the current forecast day.
This diagnostic variable is initialized daily.

TMAX (°K) ≡ Maximum surface temperature for the current forecast day.
This diagnostic variable is initialized daily.

PREACC (.1mm/day) ≡ Total accumulated precipitation from large and small scale processes.

PRECON (.1mm/day) ≡ Total accumulated precipitation from small scale cumulus convection.

ICLOUD is a diagnostic array which provides instantaneous information concerning cloud structure. The following table illustrates the possible values ICLOUD may have for each of the 4 cloud types:

<u>CLOUD TYPE</u>	<u>POSSIBLE ICLOUD VALUES</u>	<u>CORRESPONDING LEVELS</u>
Mid-Level	2 ⁰ , 2 ¹	5, 6
Penetrating	2 ² , 2 ³ , 2 ² + 2 ³	4, 5, 6
Low-Level	2 ⁴ , 2 ⁵	7, 8
Super-Saturation	2 ⁶ , 2 ⁷ , 2 ⁸ , ..., 2 ¹⁴	1, 2, 3, ..., 9

If a given cloud type exists at a particular location, its corresponding value is added to the current value of ICLOUD. The total sum for all cloud types is then written to the history file.

CHAPTER VI

EXTENSIONS FOR A TROPOSPHERE-STRATOSPHERE MODEL

KENJI TAKANO and WINSTON C. CHAO

VI. EXTENSIONS FOR A TROPOSPHERE-STRATOSPHERE MODEL

VI.1 Introduction

In this chapter, the 9-layer GLAS Fourth Order General Circulation Model originally developed for the troposphere as described in the previous chapters, is extended to include a well-resolved stratosphere. The current major changes made for the extension include; (a) use of a hybrid vertical coordinate which incorporates the use of a pressure coordinate in the stratosphere above the original σ coordinate used in the troposphere, (b) use of potential temperature as a prognostic variable instead of temperature, (c) adoption of a new vertical difference scheme, and (d) implementation of a hybrid GLAS/NRL radiation routine for the troposphere/stratosphere.

The purpose behind these changes has been to improve both the radiation parameterization in the stratosphere and the accuracy of the vertical finite difference scheme and to obtain increased vertical resolution in the stratosphere through better computational efficiency, while minimizing the modification to the original model structure. Since the model will be used in a forecast/analysis cycle of the troposphere/stratosphere, the distribution of vertical levels was designed to minimize interpolation between model levels and the mandatory pressure levels used in the analysis.

The main advantage of the sigma (σ) coordinate is that the bottom boundary condition (i.e., $\dot{\sigma} = 0$, at $\sigma \approx 1$) is very simple. However this advantage is accompanied by the disadvantage of an extra term in the pressure gradient force (i.e., the $\sigma \frac{RT}{p} \nabla \sigma$ term in Eqs. III.2.1 and III.2.2) as compared with the pressure coordinate. Another disadvantage of the σ coordinate is the interpolation to and from the p coordinate involved in the input/output preparation. The advantage of the σ coordinate outweighs its disadvantages and the σ coordinate is thus used in most general circulation models including the current model

as described in Chapter II. However, since the advantage of the σ coordinate is related to the bottom boundary condition only, one can use the σ coordinate in the lower part of the model and use the pressure coordinate in the upper part of the model. This hybrid vertical coordinate, which has been used in many other general circulation models, provides computational efficiency for models extending to the stratosphere and the mesosphere.

There are various constraints adhered to in the vertical differencing scheme described in Chapters III and IV. For example, difference analogues of the energy conversion term should have the same form in the kinetic energy and thermodynamic equations and the total θ^2 (θ being potential temperature) should be conserved under adiabatic processes. Because of these constraints the hydrostatic equation, in its finite difference form, is constrained to give the height of the bottom level as a function of temperatures at all levels (Eq. IV.2.15). This non-local dependence is not correct and creates an error in evaluating the pressure gradient force. This problem is particularly severe over steep terrain where the pressure gradient force is a small difference between two large terms, one of which is related to the geopotential height. To overcome this problem Arakawa and Suarez (1983) suggested abandoning the constraint of θ^2 conservation and thus keeping the local dependence of the bottom level hydrostatic equation. Here we adopt Arakawa and Suarez's vertical finite difference scheme. This scheme uses potential temperature as a prognostic variable to simplify the thermodynamic energy equation. This scheme is used in the tropospheric part of the model only. In the stratospheric part of the model the vertical differencing scheme described in Chapters III and IV with modifications to conserve $\ln \theta$ instead of θ^2 (Arakawa and Lamb, 1977) is used.

The other portions of the original model are extensively used. Specifically, the fourth order horizontal difference scheme, and the Shapiro and polar filters

described in Chapter III and IV, are directly applied to the stratospheric part. The parameterizations of physical processes in the troposphere, documented in Chapter V, are also incorporated in the lower part of the model and input/output processes are kept almost the same. These are, of course, accompanied by minor modifications to facilitate the use of the new vertical coordinate system and potential temperature as a prognostic variable.

In Section 2 the hybrid vertical coordinate of the model is described. The governing equations are discussed in Section 3. Section 4 introduces the revised vertical difference scheme. The new radiation routine is briefly documented in Section 5. Comments on the coding for the extensions are made in Section 6. Finally, some results from numerical forecast experiments are shown in Section 7.

As an aside, special test initial conditions useful in detecting errors in the model's dynamics are introduced in Appendix F.

VI.2 Hybrid ($\sigma - p$) Vertical Coordinate

The vertical coordinate introduced in the model is a combination of the σ coordinate for the lower part of the atmosphere, as used in the original model, and the pressure coordinate for the upper part. Fig. VI.2a shows the vertical structure of a 19 level version of the model. The lower boundary, which follows the earth's surface, is a coordinate surface. There the surface pressure, P_S , which varies with the horizontal coordinates and time, is defined. The upper boundary, assumed to be a material surface, is placed at a constant pressure surface, $P_T (= 0.305 \text{ mb})$, which is near the height of the stratopause. The atmosphere between P_S and P_T is divided into 19 layers and the edges of these layers are defined by the following generalized σ coordinate, with $P_{INT} (= 120 \text{ mb})$ chosen as a constant pressure near the tropopause,

$$\sigma = \frac{p - P_{INT}}{\Pi} \quad (2.1)$$

where

$$\Pi = \begin{cases} \Pi_1 = P_{INT} - P_T & \text{for } P_T \leq P \leq P_{INT} \\ \Pi_2 = P_S - P_{INT} & \text{for } P_{INT} \leq P \leq P_S. \end{cases} \quad (2.2)$$

Note that the σ coordinate above P_{INT} is identical to the pressure coordinate since Π_1 is constant, and Π_2 is a function of the horizontal coordinates and time.

From (2.1) and (2.2),

$$\sigma = \begin{cases} -1 & \text{for } p = P_T \\ 0 & \text{for } p = P_{INT} \\ 1 & \text{for } p = P_S \end{cases} \quad (2.3)$$

and the pressure is obtained by

$$p = \begin{cases} \text{specified pressure} & -1 < \sigma < 0 \\ \sigma \Pi_2 + P_{INT} & 0 < \sigma \leq 1 \end{cases} \quad (2.4)$$

When $P_{INT} = P_T$, this vertical coordinate system reduces to the σ coordinate used in the original model. The lower 8 layers and the upper 11 layers have equal $\Delta\sigma$ and $\Delta \ln p$, respectively. The choice of equal $\Delta \ln p$, with the use of (4.7) in Section VI.4, prevents spurious computational reflection of wave energy due to vertical discretization for a resting isothermal atmosphere (Tokiooka, 1978). The prognostic variables are defined at center in σ below P_{INT} and in $\ln p$ above P_{INT} . Note that the choice of levels minimizes the vertical interpolation errors between the levels of model and mandatory pressure levels. The pressure coordinate is computationally efficient, because it avoids the conversion to and from σ coordinate (2.4), when the initialization and post-processing are performed. Also note that the original model involves the restrictive assumptions of 6 layer strapping of cumulus convection and the precomputed transmittances of CO_2 and O_3 at the specified pressure levels in the Wu-Kaplan longwave radiation routine. Thus the lowest 8 levels are also chosen to be approximately the same as those in the original 9 level model.

From (2.1), we obtain the vertical pressure velocity,

$$\omega = \frac{Dp}{Dt} = \Pi \dot{\sigma} + \begin{cases} 0 & -1 \leq \sigma \leq 0 \\ \sigma \left(\frac{\partial \Pi_2}{\partial t} + \mathbf{V} \cdot \nabla \Pi_2 \right) & 0 \leq \sigma \leq 1 \end{cases} \quad (2.5)$$

Since the top and bottom boundaries are assumed to be material surfaces,

$$\Pi \dot{\sigma} = 0 \quad \text{at } \sigma = -1 \quad (\omega_{p=p_T} = 0) \quad (2.7)$$

$$\text{and} \quad \Pi \dot{\sigma} = 0 \quad \text{at } \sigma = 1 \quad (\dot{\sigma} = 0) \quad (2.8)$$

At $\sigma = 0$ the dynamic interface condition (i.e., pressure being the same on either side of the interface) is already incorporated in the definition of σ . The kinematic interface condition (i.e., mass flux being continuous across the boundary) is

$$(\Pi \dot{\sigma})_{\sigma=0_-} = (\Pi \dot{\sigma})_{\sigma=0_+} = \omega_{INT},$$

which is evident from (2.5).

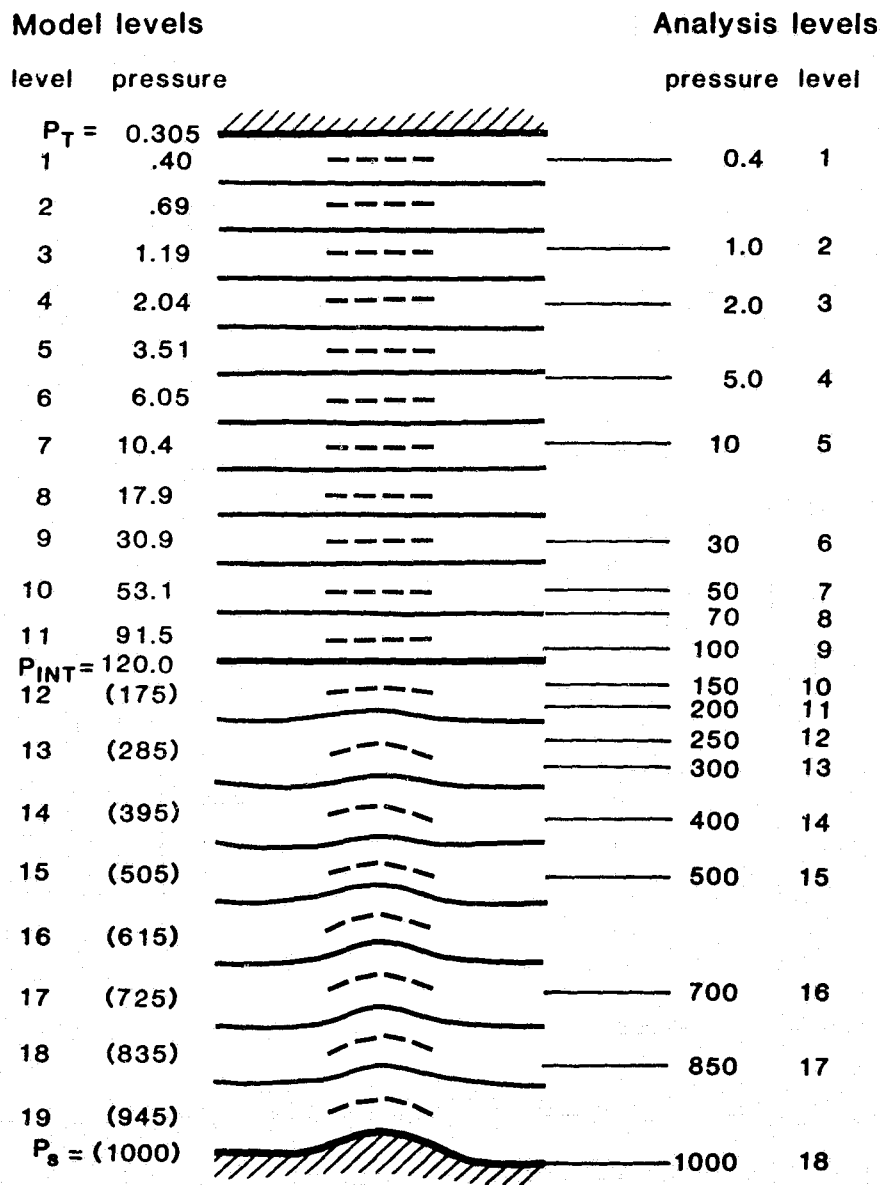


Fig. VI.2a Vertical Structure for the Troposphere/Stratosphere Model

The horizontal gradients in the pressure and σ coordinates are related by

$$\nabla_p = \nabla_\sigma + \nabla_p \sigma \frac{\partial}{\partial \sigma} \quad (2.9)$$

Operating ∇_p on (2.4), we obtain $\nabla_p \sigma = -(\sigma/\Pi) \nabla \Pi$. Then, (2.9) is expressed by

$$\nabla_p = \nabla_\sigma - \begin{cases} 0 & -1 < \sigma < 0 \end{cases} \quad (2.10)$$

$$\frac{\sigma}{\Pi_2} \nabla \Pi_2 \frac{\partial}{\partial \sigma} \quad 0 < \sigma < 1 \quad (2.11)$$

where $\nabla \Pi_1 = 0$ for $-1 \leq \sigma < 0$ has been applied.

VI.3 Governing Equations

Since Π_1 is constant, the governing equations in the pressure coordinate ($-1 \leq \sigma < 0$) are simply derived by neglecting the terms which include $\partial \Pi_1 / \partial t$ and $\nabla \Pi_1$ in the equations in the σ coordinate (discussed in the previous chapters, and previously applied only to the lower part of the model, $0 < \sigma \leq 1$). The only exception are equations written in terms of the temperature.

Here we discuss only the equations which need to be changed to allow for the new coordinate system and the potential temperature as a prognostic variable.

- The continuity equation may be written as

$$\frac{\partial \Pi}{\partial t} = -[\nabla_{\sigma} \cdot (\Pi \mathbf{V}) + \frac{\partial}{\partial \sigma} (\Pi \dot{\sigma})] \quad (3.1)$$

and used to obtain $\Pi \dot{\sigma}$ and $\partial p_s / \partial t$.

Integrating (3.1) with respect to σ from -1 to σ and using (2.7) gives

$$\int_{-1}^{\sigma} \frac{\partial \Pi}{\partial t} d\sigma = - \int_{-1}^{\sigma} \nabla_{\sigma} \cdot (\Pi \mathbf{V}) d\sigma - \Pi \dot{\sigma} \quad (3.2)$$

Since $\partial \Pi / \partial t = \partial \Pi_1 / \partial t = 0$ and $\partial \Pi / \partial t = \partial \Pi_2 / \partial t$ for the upper and lower parts of the model, respectively, then

$$\Pi \dot{\sigma} = - \int_{-1}^{\sigma} \nabla_{\sigma} \cdot (\Pi \mathbf{V}) d\sigma - \begin{cases} 0 & \text{for } -1 < \sigma < 0 \\ \sigma \frac{\partial \Pi_2}{\partial t} & \text{for } 0 < \sigma < 1 \end{cases} \quad (3.3)$$

$$(3.4)$$

From (3.4) applied at the earth's surface ($\sigma = 1$), where $\Pi \dot{\sigma} = 0$ (2.8), we obtain

$$\frac{\partial \Pi_2}{\partial t} = \frac{\partial p_s}{\partial t} = - \int_{-1}^1 \nabla \cdot (\Pi \mathbf{V}) d\sigma \quad (3.5)$$

Equation (3.5) is also used to compute $\Pi \dot{\sigma}$ for $0 < \sigma < 1$.

- The equation of state may be expressed by using the potential temperature, θ , as

$$\frac{1}{\rho} = \alpha = C_p \theta \frac{dP}{dp} \quad (3.6)$$

where $P = \left(\frac{p}{p_0}\right)^\kappa$, $\theta = T/P$ and $\kappa = R/C_p$. Using (2.4) under constant horizontal coordinates and time or under constant σ , (3.6) yields two forms

$$\alpha = C_p \theta \frac{1}{\Pi} \frac{\partial P}{\partial \sigma} \quad (3.7)$$

$$\alpha = C_p \theta \frac{1}{\sigma} \left(\frac{\partial P}{\partial \Pi} \right)_\sigma \quad (3.8)$$

- The hydrostatic equation, $-d\phi = \alpha dp$, is then rewritten as

$$-d\phi = C_p \theta dP \quad (3.9)$$

$$-d\phi = C_p \theta \frac{\Pi}{\sigma} \left(\frac{\partial P}{\partial \Pi} \right)_\sigma d\sigma \quad (3.10)$$

- The pressure gradient force obtained by applying (2.10) and (2.11) to ϕ and using (3.10), is given by

$$-\nabla_p \phi = -\nabla_\sigma \phi - \begin{cases} 0 & -1 < \sigma < 0 \\ C_p \theta \left(\frac{\partial P}{\partial \Pi} \right)_\sigma \nabla \Pi_2 & 0 < \sigma < 1 \end{cases} \quad (3.11)$$

$$-\nabla_p \phi = -\nabla_\sigma \phi - \begin{cases} 0 & -1 < \sigma < 0 \\ C_p \theta \left(\frac{\partial P}{\partial \Pi} \right)_\sigma \nabla \Pi_2 & 0 < \sigma < 1 \end{cases} \quad (3.12)$$

- The thermodynamic equation can be simply written in terms of the potential temperature as

$$\frac{\partial}{\partial t} (\Pi \theta) + \nabla_\sigma \cdot (\Pi \nabla_\sim \theta) + \frac{\partial}{\partial \sigma} (\Pi \sigma \dot{\theta}) = Q \quad (3.13)$$

Note that since the use of the pressure coordinate simplifies the governing equations as discussed above, it also offers computational efficiency when the model contains a large number of layers in the stratosphere. The advantage of the potential temperature compared with the temperature is not only in simplifying the thermodynamic equation, but also in being readily applied to the Shapiro and the polar filters without conversion (which involves the exponential calculation).

VI.4 Vertical Difference Scheme

The vertical index of the model is shown in Fig. VI.4a. The model atmosphere is divided into NLAY layers with LS layers in the pressure coordinate. The quantities defined for the mid-layers and the edges of layers are identified by integer subscripts and half-integer subscripts of ℓ , respectively. A caret is used for the quantities at half-integer levels.

The vertical difference schemes for (3.9), (3.11), (3.12) and (3.13) are then written in the following revised forms:

- The hydrostatic equation

$$\phi_{\text{NLAY}} - \hat{\phi}_{\text{NLAY}+1/2} = C_p \theta_{\text{NLAY}} (\hat{P}_{\text{NLAY}+1/2} - P_{\text{NLAY}}) \quad \text{for NLAY} \quad (4.1)$$

$$\phi_{\ell} - \phi_{\ell+1} = C_p \hat{\theta}_{\ell+1/2} (P_{\ell+1} - P_{\ell}) \quad \text{for layers above NLAY} \quad (4.2)$$

- The pressure gradient force

$$-(\nabla_p \phi)_{\ell} = -(\nabla_{\sigma} \phi)_{\ell} - \begin{cases} 0 & -1 < \sigma < 0 \\ C_p \theta_{\ell} \frac{dP}{d\Pi} \nabla \Pi_2 & 0 < \sigma < 1 \end{cases} \quad (4.3)$$

$$C_p \theta_{\ell} \frac{dP}{d\Pi} \nabla \Pi_2 \quad 0 < \sigma < 1 \quad (4.4)$$

- The thermodynamic equation

$$\begin{aligned} \frac{\partial}{\partial t} (\Pi \theta_{\ell}) + \nabla_{\sigma} \cdot (\Pi \underline{v}_{\ell} \theta_{\ell}) + \frac{1}{\Delta \sigma_{\ell}} [(\Pi \dot{\sigma})_{\ell+1/2} \hat{\theta}_{\ell+1/2} \\ - (\Pi \dot{\sigma})_{\ell-1/2} \hat{\theta}_{\ell-1/2}] = Q_{\ell} \quad \text{for } -1 < \sigma < 1 \end{aligned} \quad (4.5)$$

Here $\Delta \sigma_{\ell} = \sigma_{\ell+1/2} - \sigma_{\ell-1/2}$, and $\Pi \dot{\sigma}$ is obtained from (3.3) and (3.4). The specification of $\hat{\theta}$, P and $dP/d\Pi$ are given as follows: In the pressure coordinate ($-1 < \sigma < 0$), $\hat{\theta}_{\ell+1/2}$ is chosen to conserve an analog of the global mass integral of $\ln \theta$ under adiabatic processes. It is given by

$$\hat{\theta}_{\ell+1/2} = \frac{\ln \theta_{\ell} - \ln \theta_{\ell+1}}{1/\theta_{\ell+1} - 1/\theta_{\ell}} \quad (4.6)$$

with

$$P_\ell = [\sqrt{\hat{P}_{\ell-1/2} \hat{P}_{\ell+1/2}} / p_0]^\kappa \quad (4.7)$$

The motivation for these choices is given by Arakawa and Lamb (1977) and Tokioka (1978) (see also Section VI.2).

In the σ coordinate ($0 < \sigma < 1$), $\hat{\theta}_{\ell+1/2}$ is specified by

$$\hat{\theta}_{\ell+1/2} = \frac{(\hat{P}_{\ell+1/2} - P_\ell) \theta_\ell + (P_{\ell+1} - \hat{P}_{\ell+1/2}) \theta_{\ell+1}}{P_{\ell+1} - P_\ell} \quad (4.8)$$

with

$$P_\ell = \frac{1}{1+\kappa} \frac{[\hat{P}_{\ell+1/2} \hat{P}_{\ell+1/2} - \hat{P}_{\ell-1/2} \hat{P}_{\ell-1/2}]}{\hat{P}_{\ell+1/2} - \hat{P}_{\ell-1/2}} \quad (4.9)$$























where $\hat{P}_{\ell+1/2} = (\hat{P}_{\ell+1/2}/p_0)^\kappa$, $\hat{P}_{\ell+1/2} = \hat{\sigma}_{\ell+1/2} \Pi_2 + P_{INT}$, and $p_0 = 1000$ mb.

From differentiation of (4.9), we obtain

$$\frac{dP_\ell}{d\Pi} = \frac{\hat{\sigma}_{\ell+1/2} (\hat{P}_{\ell+1/2} - P_\ell) + \hat{\sigma}_{\ell-1/2} (P_\ell - \hat{P}_{\ell-1/2})}{\hat{P}_{\ell+1/2} - \hat{P}_{\ell-1/2}} \quad (4.10)$$

The vertical difference scheme, (4.1), (4.2), (4.4) and (4.5), with the choices of (4.8), (4.9), and (4.10), has the following properties:

- (i) The hydrostatic equation for the height of the lowest level has a local form.
- (ii) The hydrostatic equation is exact for a vertically isentropic atmosphere.
- (iii) The pressure gradient force generates no circulation of vertically integrated momentum along a contour of the surface topography.
- (iv) The pressure gradient force is exact for three-dimensionally isentropic atmospheres and, when the model top is at $p = 0$, for atmospheres in which $T = a + b (p/p_0)^\kappa$.
- (v) The finite difference analogues of the energy conversion terms have the same form in the kinetic energy and thermodynamic equations.

ℓ		$\pi \dot{\sigma} = 0$	$\sigma = -1$
$\frac{1}{2}$		\underline{V}, θ	
1		$\pi \dot{\sigma}$	
$1\frac{1}{2}$		\underline{V}, θ	
2			
			
LS		\underline{V}, θ	
LS + $\frac{1}{2}$		$\pi \dot{\sigma}$	$\sigma = 0$
LS + 1		\underline{V}, θ	
			
			
$\ell - 1$		\underline{V}, θ	
$\ell - \frac{1}{2}$		$\pi \dot{\sigma}$	
ℓ		\underline{V}, θ	
$\ell + \frac{1}{2}$		$\pi \dot{\sigma}$	
$\ell + 1$		\underline{V}, θ	
			
			
NLAY - 1		\underline{V}, θ	
NLAY - $\frac{1}{2}$		$\pi \dot{\sigma}$	
NLAY		\underline{V}, θ	
NLAY + $\frac{1}{2}$		$\pi \dot{\sigma} = 0$	$\sigma = 1$

VI-12

(vi) The global mass integral of the potential temperature is conserved under adiabatic processes.

For further details, the reader is referred to Arakawa and Suarez (1983).

VI.5 Radiation

The model presently uses a hybrid GLAS/NRL (Naval Research Laboratory) radiation routine for the troposphere/stratosphere. This section briefly describes the NRL algorithm. The reader is referred to Strobel (1978) and Apruzese et al. (1982) for more details. A description of the GLAS radiation routine is given in Chapter V.

VI.51 Solar Radiation

Since in the middle atmosphere the solar radiative heating due to ozone (O_3) and oxygen (O_2) is the dominant energy source which drives the general circulation, an accurate and computationally efficient parameterization of heating developed by Strobel (1978) is incorporated. This includes heating by absorption of O_3 and O_2 for six spectral regions of solar radiation:

- The Hartley region (2425-2775Å), heating due to O_3 absorption in this region is the dominant heat source between 45km and 85km, and produces the high temperature region centered at the stratopause (~ 50km).
- The Huggins bands (2775-3600Å), O_3 absorption gives the dominant heat source between 28km and 45km.
- The Chappius bands (4500-7500Å), O_3 absorption dominates below 28km.
- The Herzberg continuum (2060-2425Å), both O_3 and O_2 absorptions make a small contribution to the heating rate between 35km and 55km.
- The Schumann-Runge bands (1750-2050Å), O_2 absorption dominates between 88km and 96km.
- The Schumann-Runge continuum (1250-1750Å), O_2 absorption in this region is most important above 96km.

The solar heating routine also incorporates the formulation of Lacis and Hansen (1974), used in the GLAS radiation routine, to account for solar heating

of water vapor in the 0.9-6.3 μ m region and the calculation procedure of Ramanathan and Cess (1974) for carbon dioxide (CO₂) heating in the 2.0-4.7 μ m region.

VI.5i1 Infrared (IR) Radiation

A computationally efficient two-stream parameterization of IR cooling due to CO₂ and O₃ developed by Apruzese et al. (1982) is used in the NRL routine. This has been derived by using a rectangular band approximation, which requires only one spatial integral of the monochromatic transfer equation, based on the fact that CO₂ and O₃ radiate in relatively narrow spectral bands near 15 μ and 9.6 μ , respectively, while accounting for Lorentz line broadening, line wing overlap and interaction of broad-band radiation emitted by the earth and clouds with the IR cooling constituent.

The two-stream parameterization requires the calculation of total band absorptance of CO₂ and O₃ to space. The tables and interpolation technique of Fels and Schwartzkopf (1981) are used for CO₂, and the analytic formulation of Ramanathan (1976) is used for O₃.

The model presently uses a hybrid IR radiation scheme which includes the Wu-Kaplan scheme, as used in the GLAS radiation routines, below 120 mb and the NRL IR radiation scheme above. This option was selected because the NRL scheme was originally developed for the middle atmosphere and does not include the accurate calculation of cooling rate of water vapor and the detailed interaction between radiation and clouds. The Wu-Kaplan scheme on the other hand, provides the necessary calculation and interaction but extends only as high as the lower stratosphere. Moreover, it requires precomputed transmittances of CO₂ and O₃. Therefore, the Wu-Kaplan scheme is suitable for the troposphere but not for the whole stratosphere and mesosphere, for which the NRL scheme was mainly designed. The two schemes are joined by interpolation at the interfacial level.

VI.6 Changes in the Model Code

The coding to incorporate the changes described in the previous sections has been done by keeping as much as possible the structure of the original model. Nevertheless, almost all the major subroutines required some level of modification. The most important of these are summarized below:

- The determination of a new σ coordinate through expressions (2.1) and (2.2) is done in subroutine DEFALT by introducing constant layer pressures, PSL(L), and edge pressures, PSE(L).
- A new array, PA(I,LP(L),J), is introduced to express Π_1 and Π_2 in equation (2.2). It replaces the original array P(I,N,J) in subroutines COMPl and COMP2

$$LP(L) = \begin{cases} 1 & -1 < \sigma < 0 \\ 2 & 0 < \sigma < 1 \end{cases}$$

$$\begin{cases} \Pi_1 = PA(I,1,J) = PIS = PINT - PTOP & -1 < \sigma < 0 \\ \Pi_2 = PA(I,2,J) = P(I,N,J) & 0 < \sigma < 1 \end{cases}$$

The above conversions are done in subroutine GEOHT.

- A new array, FAC(L), distinguishes the governing equations in the pressure coordinate from those in the σ coordinate

$$FAC(L) = \begin{cases} 0. & -1 < \sigma < 0 \\ 1. & 0 < \sigma < 1 \end{cases}$$

FAC(L) is used in subroutines COMPl and COMP2 to eliminate unnecessary terms for the pressure coordinate as described in Section VI.3.

- The calculations of variables for the new vertical difference scheme, equations (4.6)-(4.10), except for equation (4.7) which is constant and calculated in subroutine DEFALT, are done in subroutine GEOHT. Four new arrays, THETM(I,L,5), PKT(I,L,5), PKTE(I,L,5) and TERMW(I,L,5) are

introduced for $\hat{\theta}$, P , \hat{P} and $dP/d\Pi$, respectively. The geopotential height is determined by expressions (4.1) and (4.2) in subroutine GEOHT. The array THETM(I,L,5) is used in subroutine COMPl to obtain the vertical advection in the thermodynamic equation (4.5) and the array TERMW(I,L,5) is passed to subroutine COMP2 to determine the pressure gradient force as defined by equation (4.4).

- The NRL algorithm and the reorganized GLAS radiation are combined in the new subroutine GCMRAD2.
- The code for the conversion from temperature to potential temperature is eliminated from subroutines AVRX and SMSHAP. Additional code is written in subroutine INPUT for conversion of the initial condition temperature and in subroutine COMP3 to pass potential temperature to the radiation routine. The definition of potential temperature in the surface physics portion of subroutine COMP3 is changed for consistency.
- Many vertical indices in subroutine CUMULO were changed to allow the variable NLAY (total number of model levels) to take numbers other than nine.

VI.7 Results from Numerical Forecast Experiments

The model (4° by 5° and 19 levels) is now (December 1983) ready for production and has been used for numerical forecast experiments to simulate the stratospheric sudden warming events observed during the winter of 1979 (FGGE period). This section presents some examples of the results from these experiments. The detailed analysis of the results will be published in the near future.

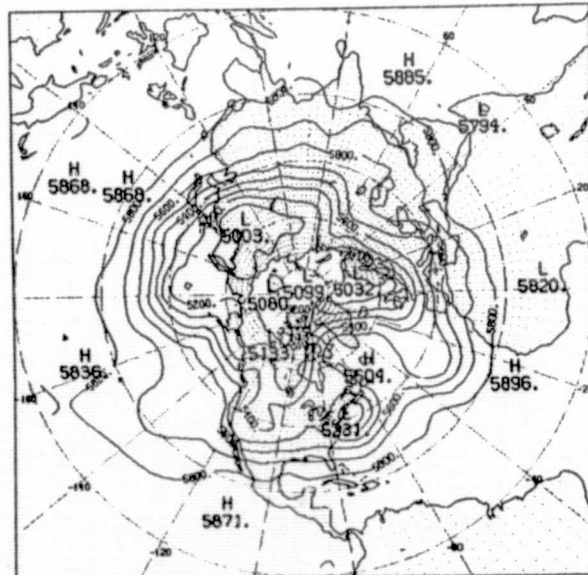
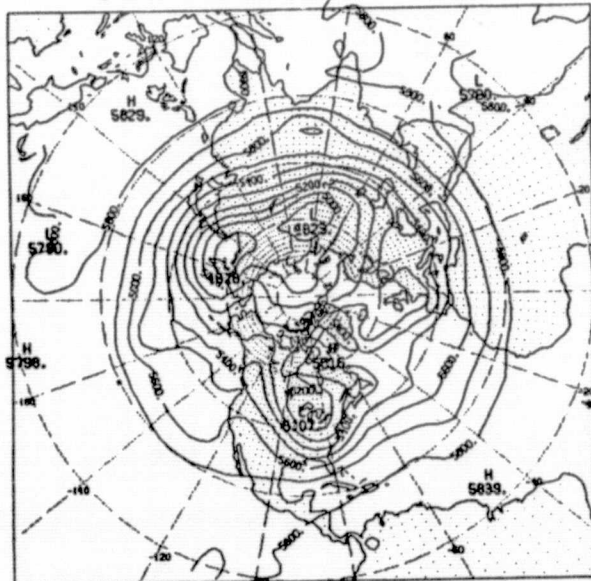
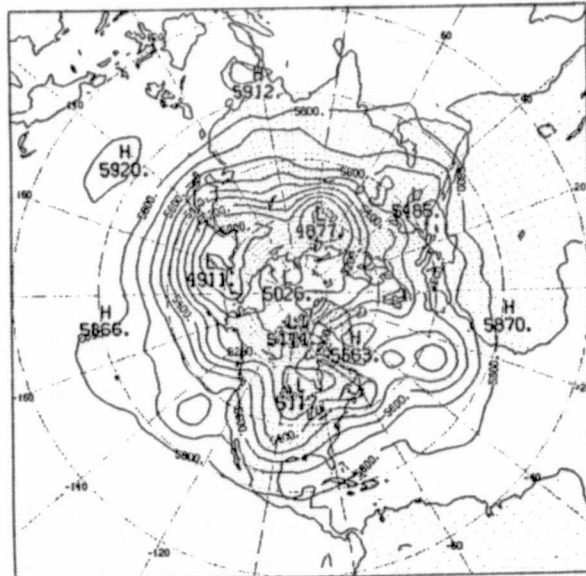
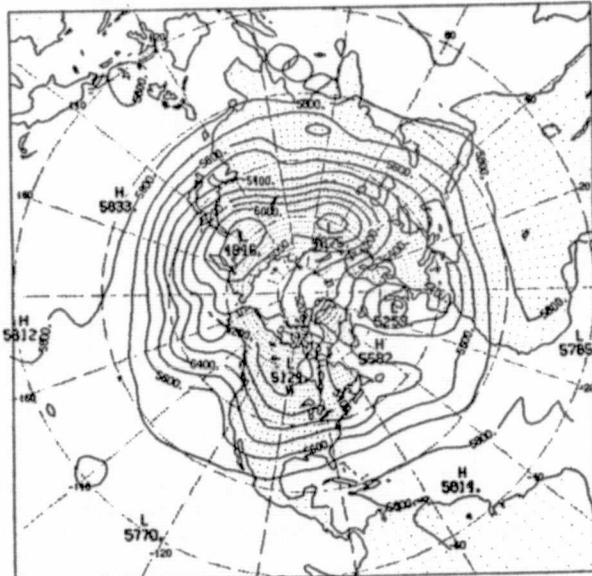
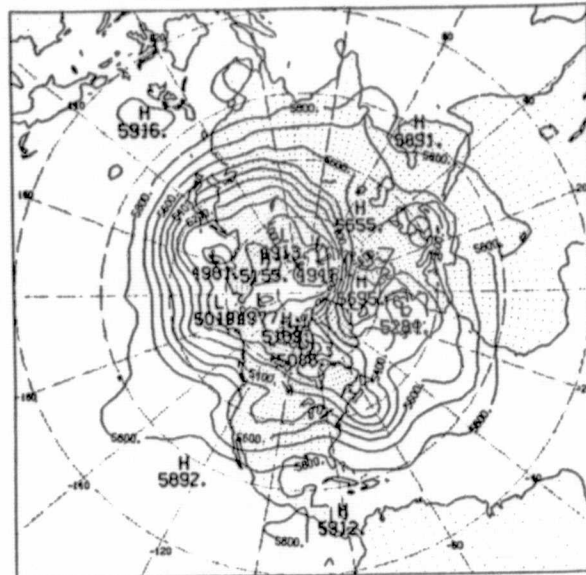
Two 10-day forecast experiments starting from 12Z, January 19 and 12Z, February 17 were performed in order to simulate the wave-one dominated (minor) warming observed in January and the wave-two dominated (major) warming observed in February. Initial data were constructed for the hybrid vertical coordinate by interpolating analysed data produced by the 9-layer GLAS GCM to the model σ levels below 120 mb, and the NMC temperature analysis and geostrophic winds to the constant model pressure levels between 120 mb and 0.305 mb. The model was integrated in time by the Matsuno scheme for the first two days to eliminate initial noise in the stratosphere, and by the leapfrog scheme mixed with the Matsuno scheme every fourth step, thereafter. A time increment of 7.5 minutes was used.

Northern hemisphere maps of the geopotential height of the 500 mb, 10 mb, 5 mb, and 1 mb surfaces for 4 and 7-day forecasts (left), along with the verifications (right) are shown in Fig. VI.7a through Fig. VI.7d for the minor warming. The corresponding maps for the major warming case are depicted in Fig. VI.7e through Fig. VI.7h. The model was quite successful in predicting the evolution of geopotential heights associated with the warmings over the period and demonstrated an important capability for troposphere-stratosphere forecasting.

ORIGINAL PAGE IS
OF POOR QUALITY

Fig. VI.7a Minor Warming

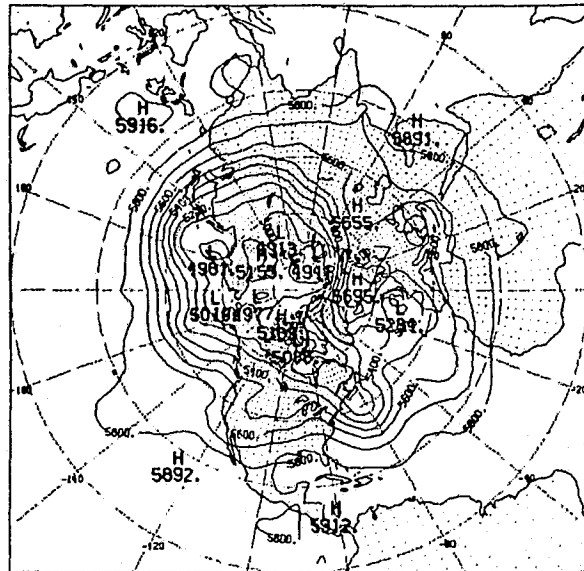
500 mb Geopotential Height



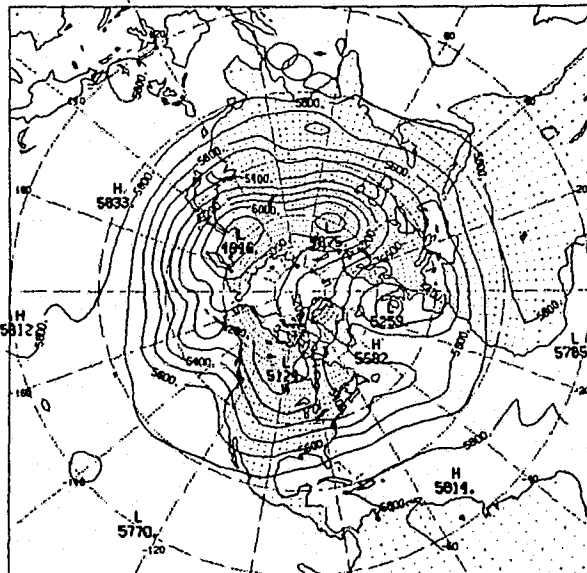
ORIGINAL PAGE IS
OF POOR QUALITY

Fig. VI.7a Minor Warming
500 mb Geopotential Height

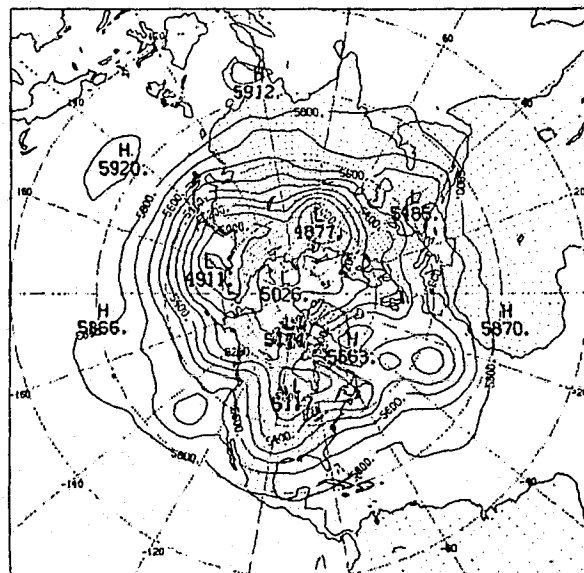
Z (M) AT 500 MB 1/ 19/ 79 12Z



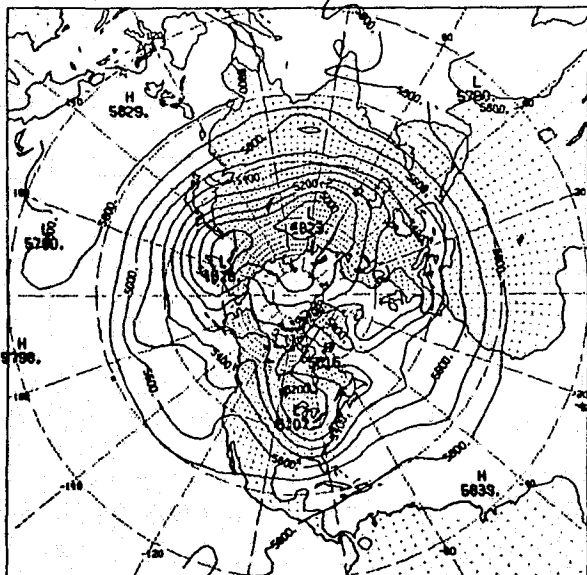
Z (M) AT 500.0 MB 23 JAN 79 12Z



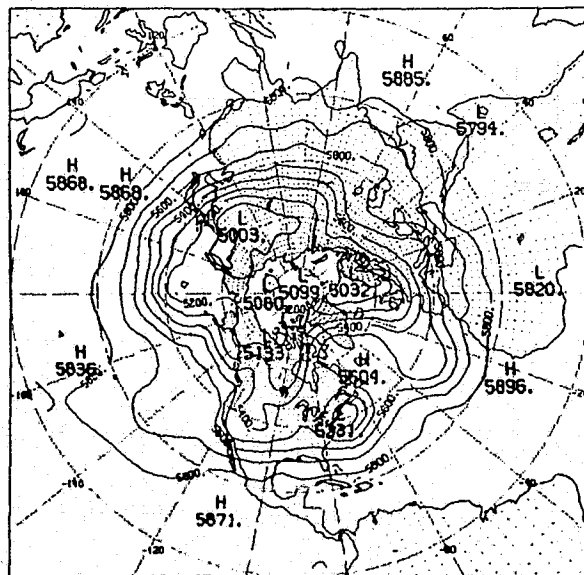
Z (M) AT 500 MB 1/ 23/ 79 12Z



Z (M) AT 500.0 MB 26 JAN 79 12Z

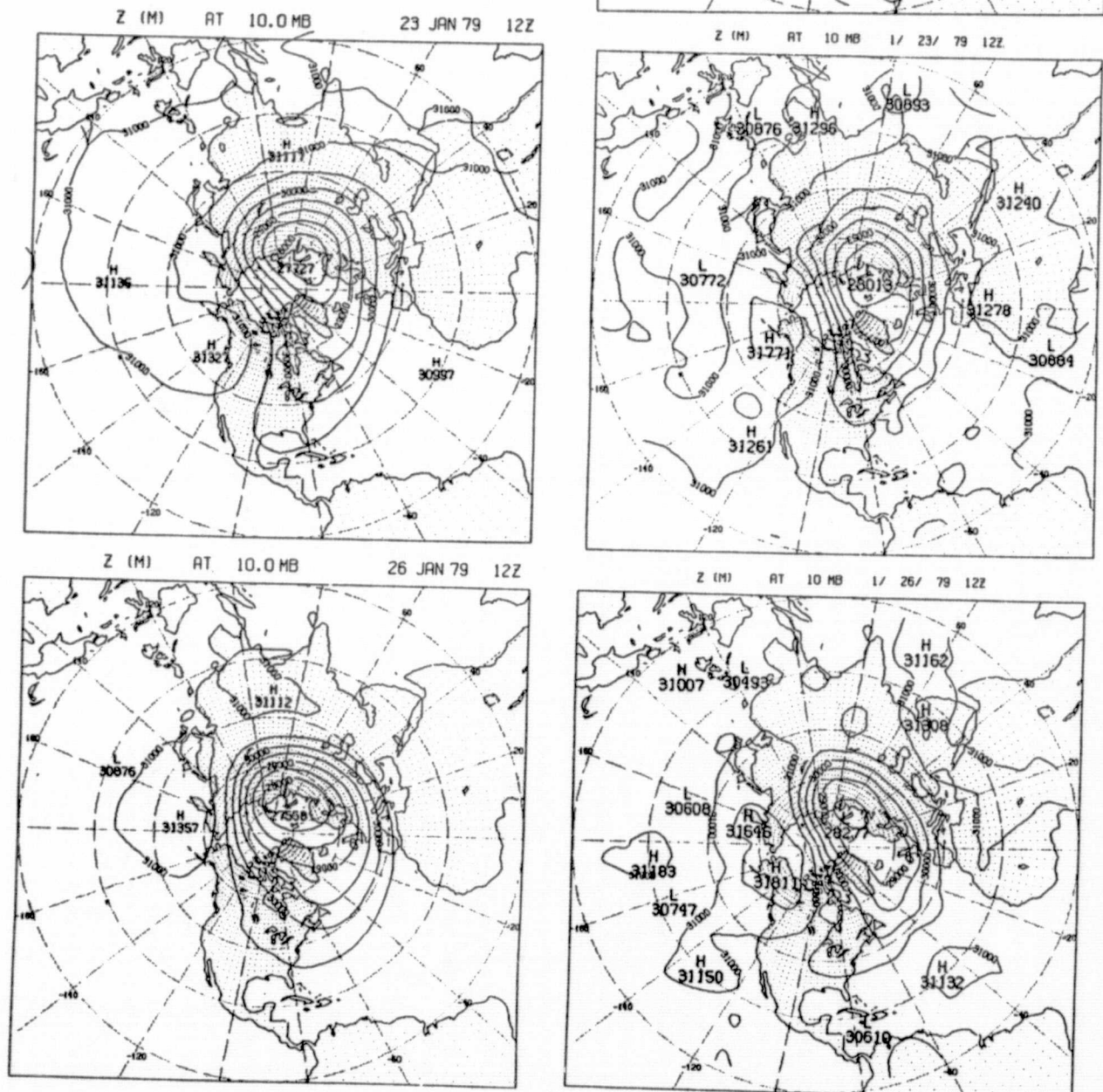


Z (M) AT 500 MB 1/ 26/ 79 12Z



ORIGINAL PAGE 19
OF POOR QUALITY

Fig. VI.7b Minor Warming
10 mb Geopotential Height

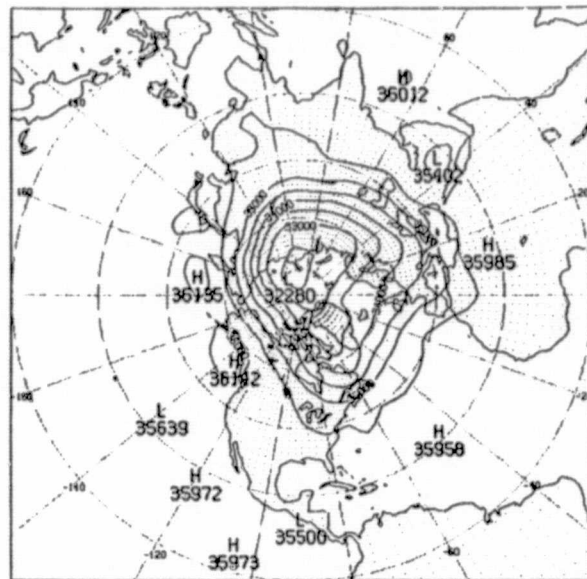


ORIGINAL PAGE IS
OF POOR QUALITY

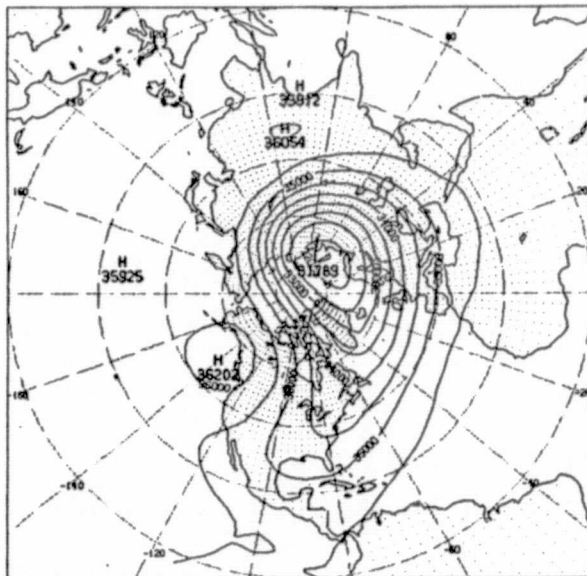
Fig. VI.7c Minor Warming

5 mb Geopotential Height

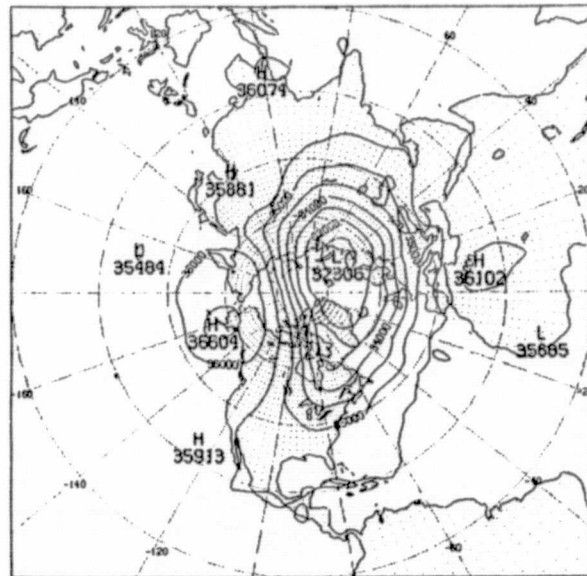
Z (M) AT 5 MB 1/ 19/ 79 12Z



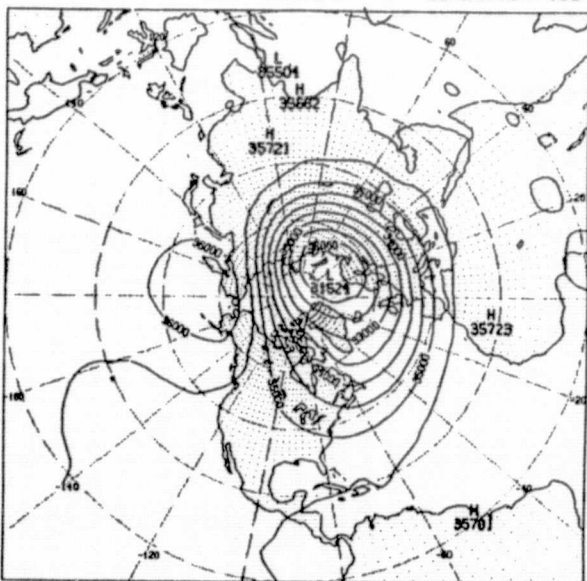
Z (M) AT 5.0 MB 23 JAN 79 12Z



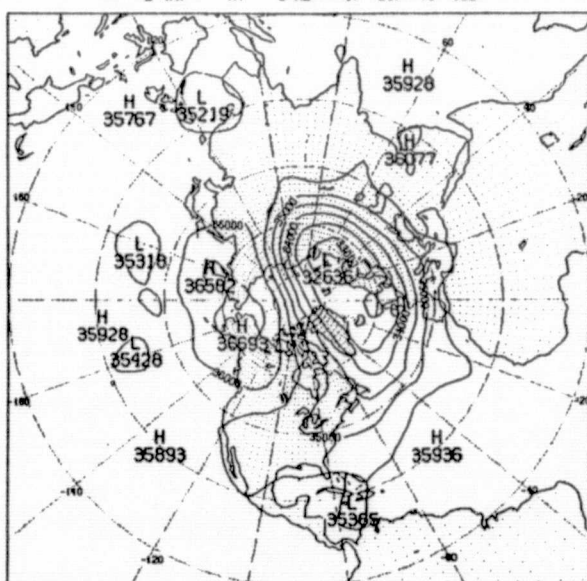
Z (M) AT 5 MB 1/ 23/ 79 12Z



Z (M) AT 5.0 MB 26 JAN 79 12Z

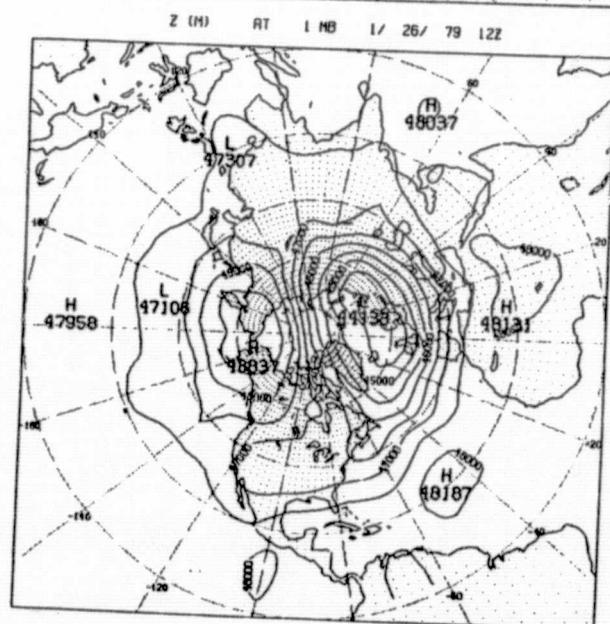
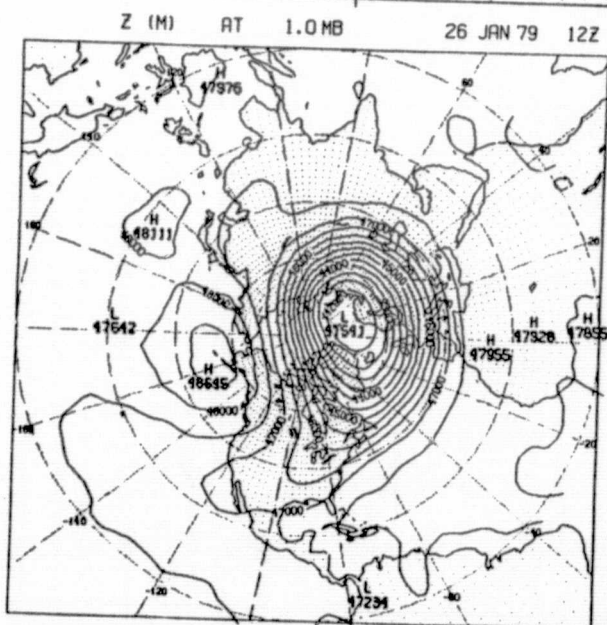
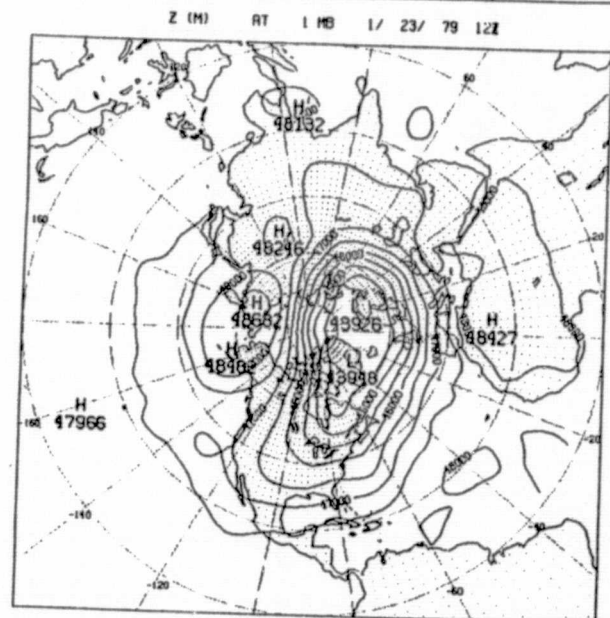
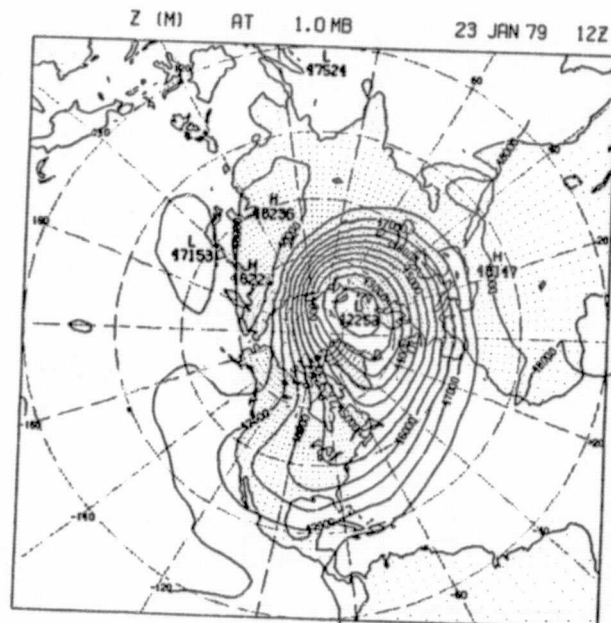
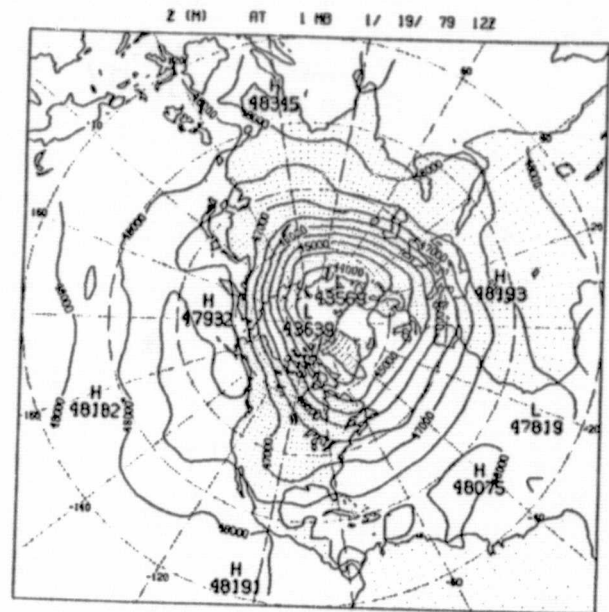


Z (M) AT 5 MB 1/ 26/ 79 12Z



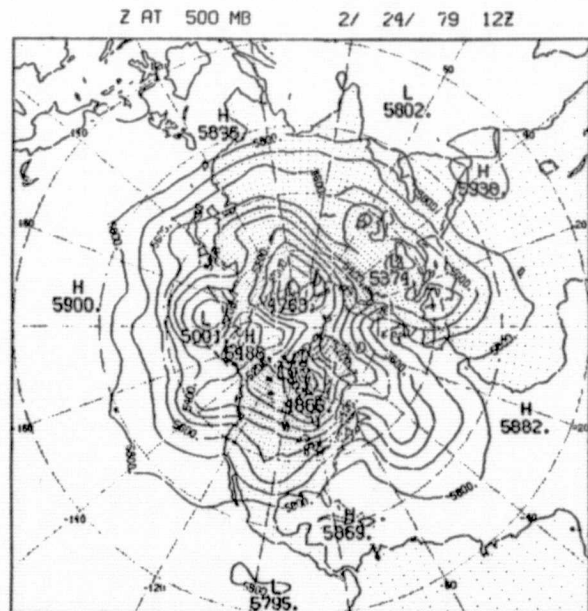
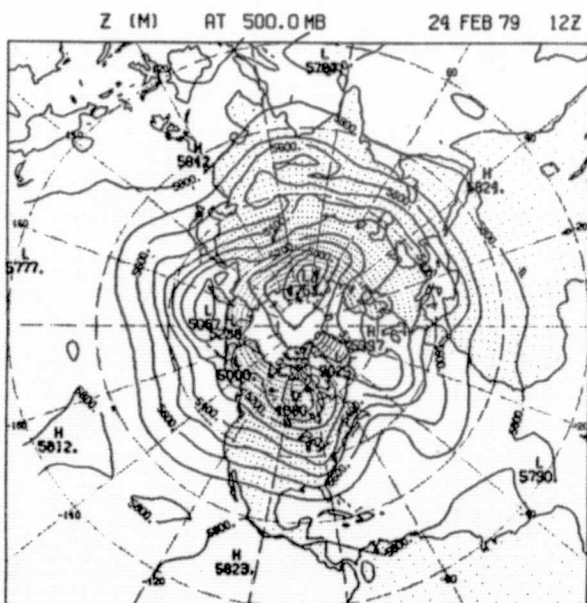
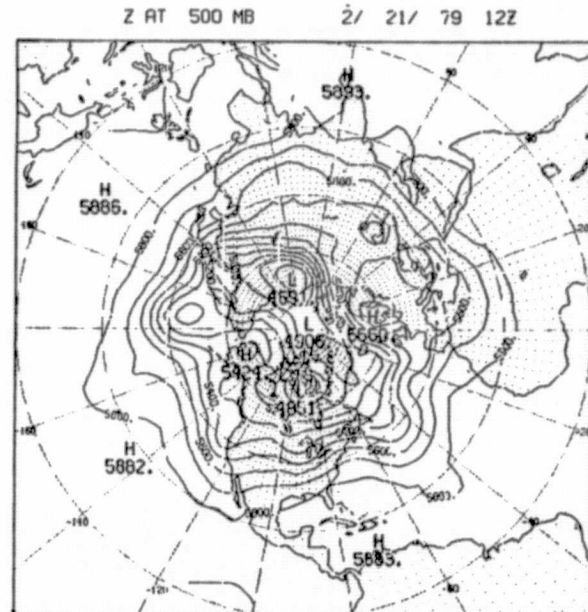
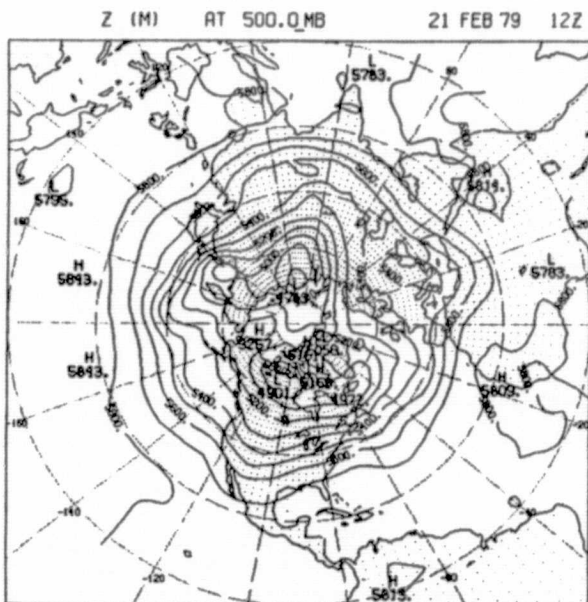
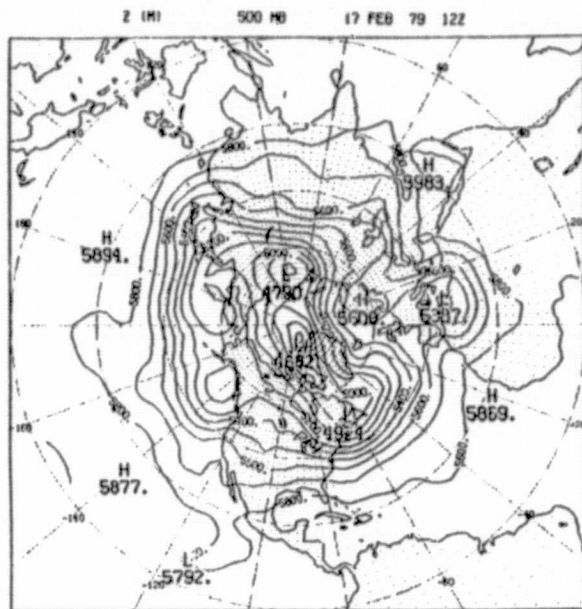
ORIGINAL PAGE IS
OF POOR QUALITY

Fig. VI.7d Minor Warming
1 mb Geopotential Height



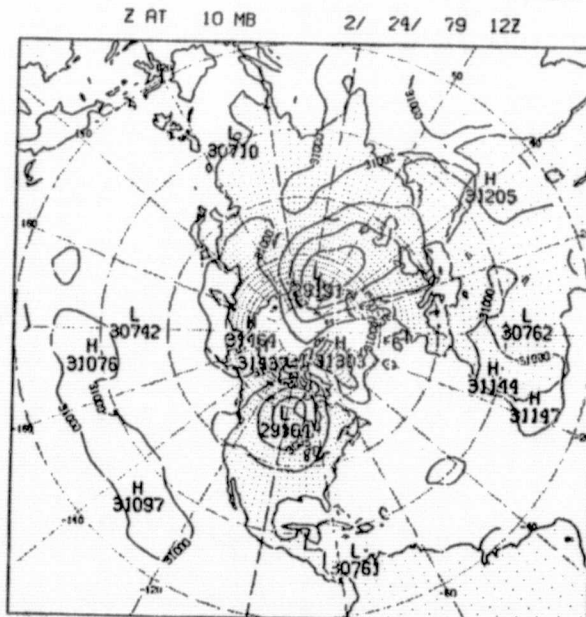
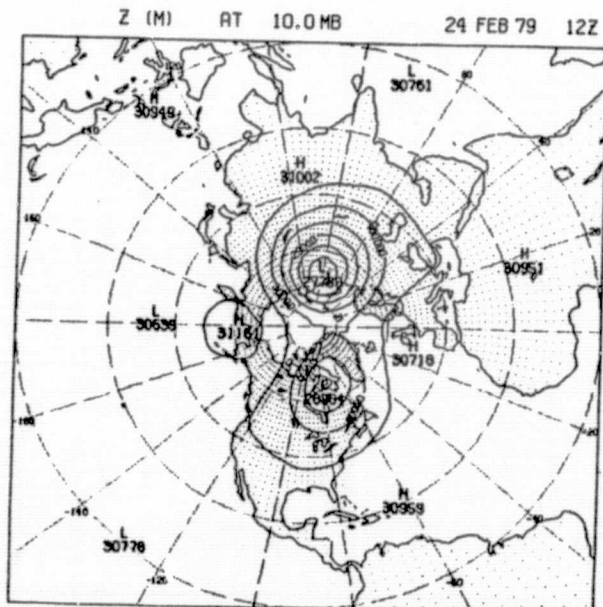
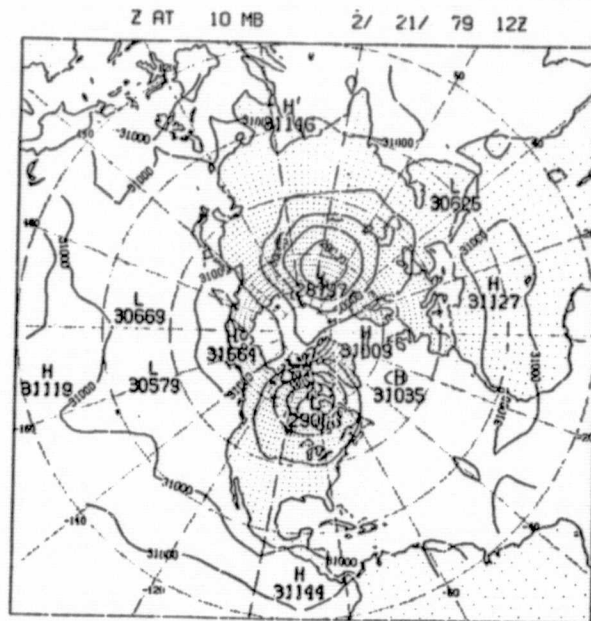
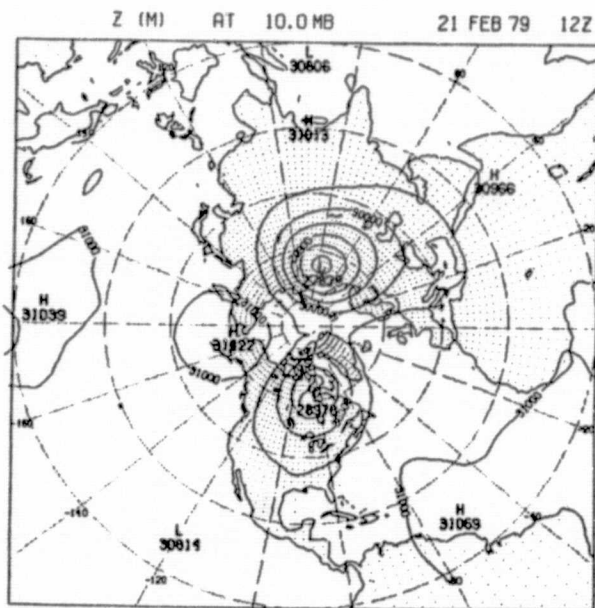
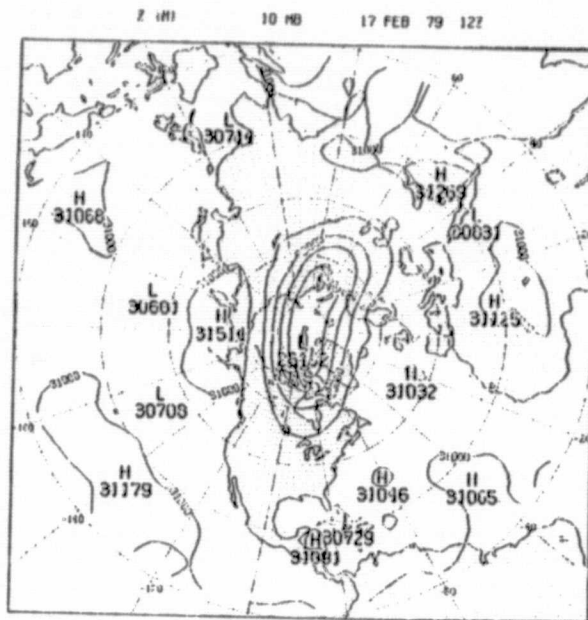
ORIGINAL PAGE 13
OF POOR QUALITY.

Fig. VI.7e Major Warming
500 mb Geopotential Height



ORIGINAL PAGE IS
OF POOR QUALITY

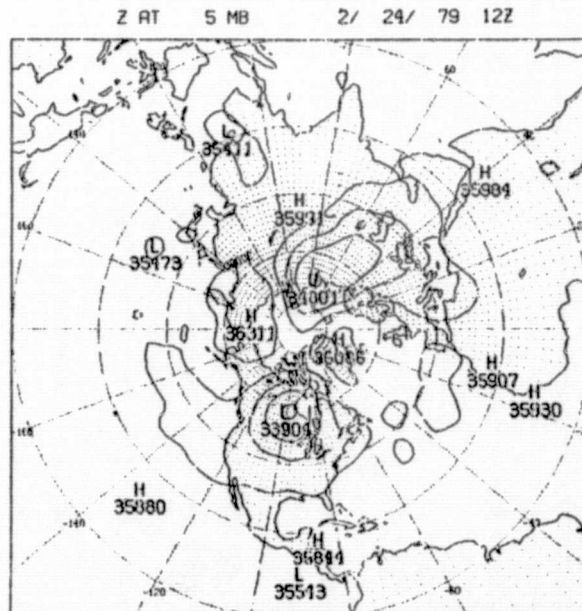
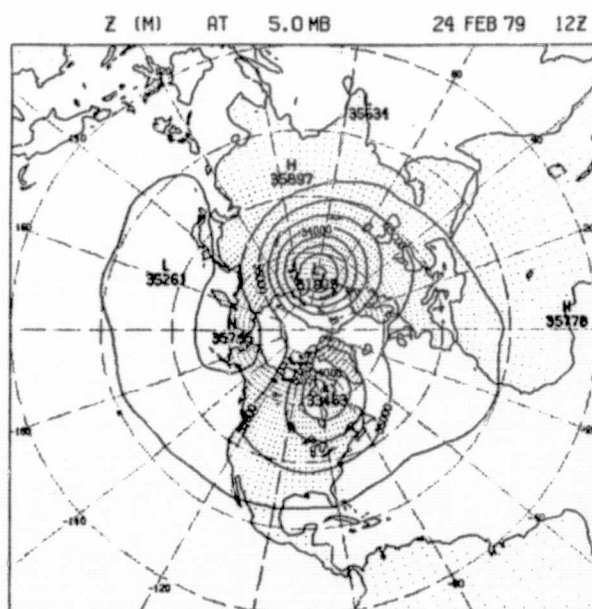
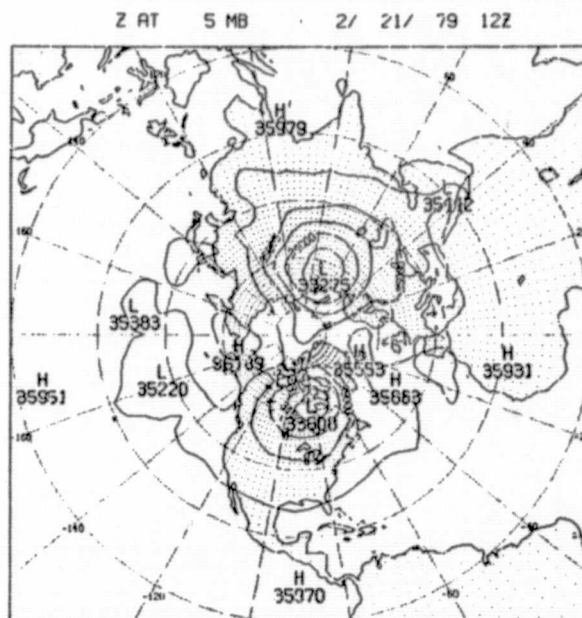
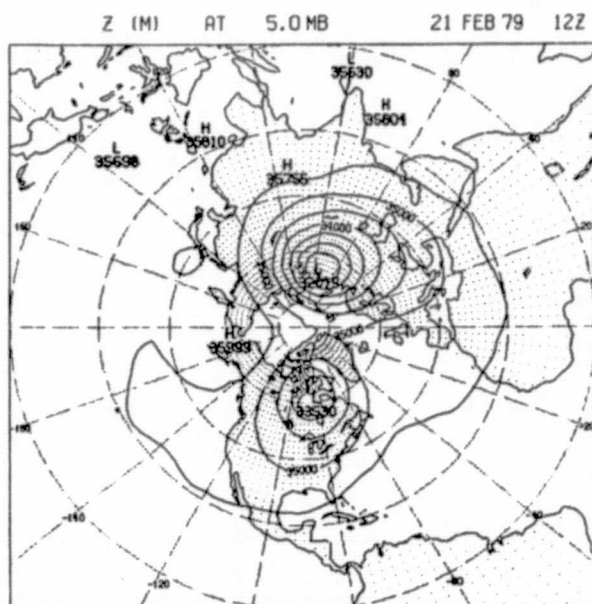
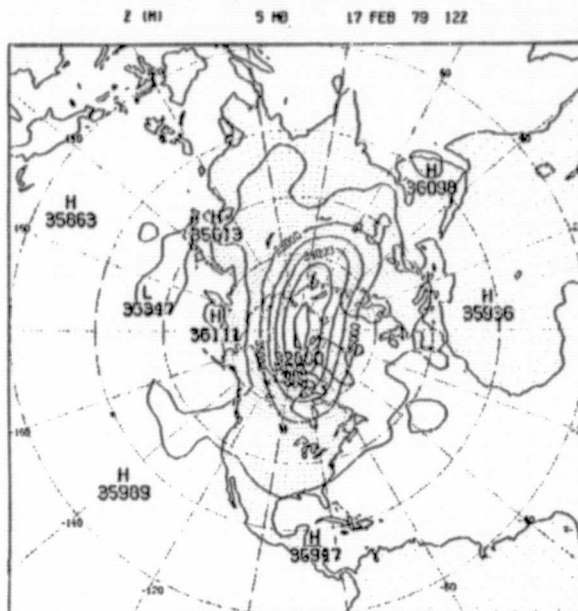
Fig. VI.7f Major Warming
10 mb Geopotential Height



ORIGINAL PAGE 19
OF POOR QUALITY

Fig. VI.7g Major Warming

5 mb Geopotential Height

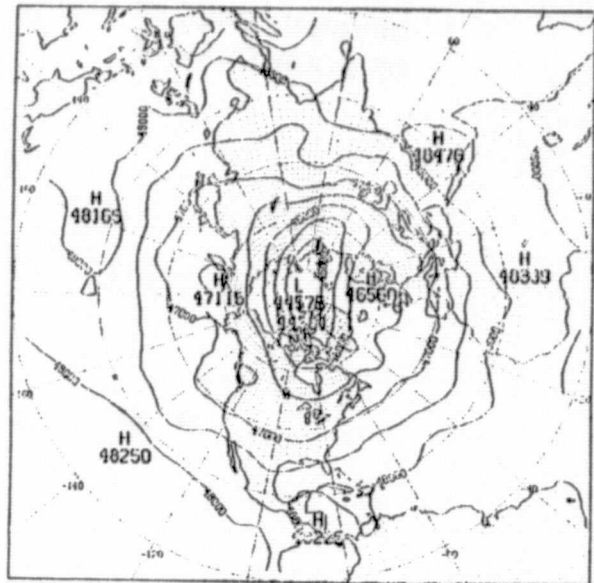


ORIGINAL PAGE IS
OF POOR QUALITY

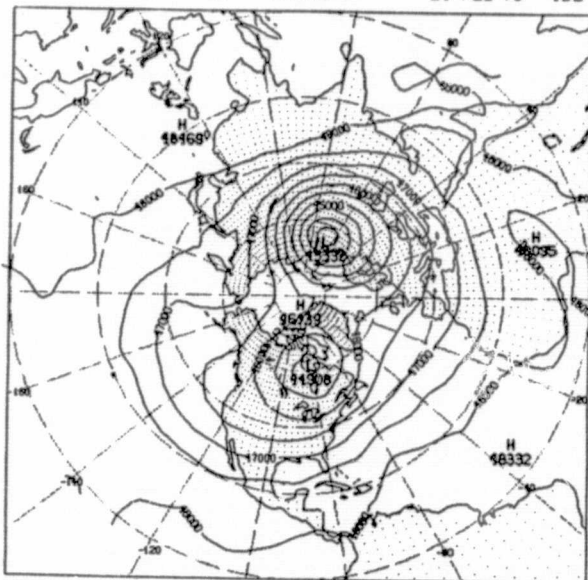
Fig. VI.7h Major Warming

1 mb Geopotential Height

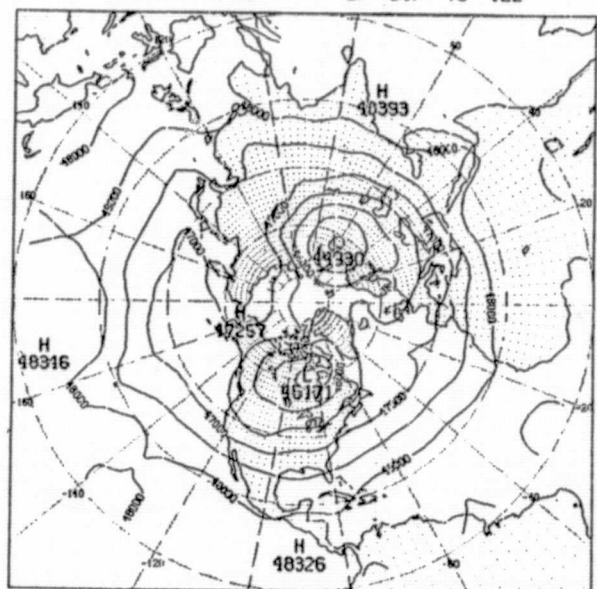
Z (M) 1 MB 17 FEB 79 12Z



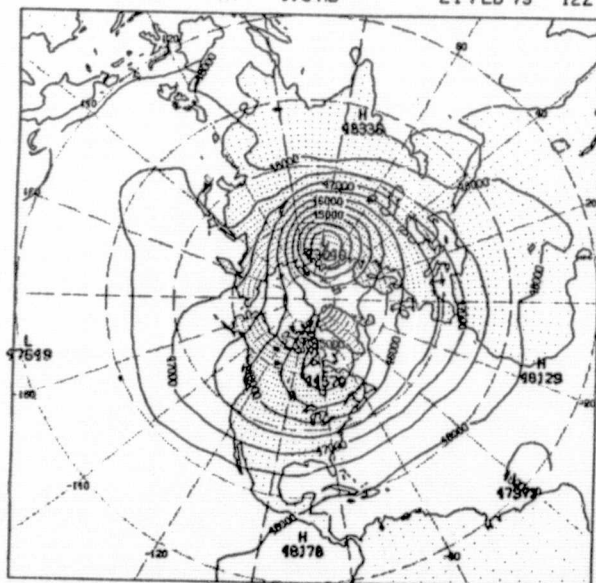
Z (M) AT 1.0 MB 21 FEB 79 12Z



Z AT 1 MB 2/ 21/ 79 12Z



Z (M) AT 1.0 MB 24 FEB 79 12Z



CHAPTER VII

CODE ORGANIZATION

JAMES W. PFAENDTNER

VII. CODE ORGANIZATION

VII.1 Introduction

The model code is designed to run on a computer incorporating a virtual addressing concept which allows for dimensioning larger than the physical size of the computer's central memory. To help minimize the amount of time spent moving data about in a non productive fashion, care has been taken to organize the code so that references to non resident storage locations will be made in an orderly cyclic manner.

The model reads two sets of control variables (namelists), INPUTZ and INPHYS from unit 5. INPUTZ is read first (in subroutine INPUT) and contains parameters which control model resolution, time scheme, history and restart write intervals, filtering constants and the time intervals for evaluation of the forcing terms and filters. INPHYS is read second (in subroutine DEPEND) and contains parameters used in the parameterizations of physical processes. A complete description of these namelists can be found in Section 1 of Chapter VIII.

Initial conditions for the integration (restart conditions if an existing forecast is being extended) are read using subroutine IOQ from unit 12 in subroutine INPUT. The data set is of the V8RSTR variety and is described in Section 3 of Chapter VIII. Common blocks /CCNTRL/, /ICNTRL/, /LCNTRL/ and /RCNTRL/ are initialized using the header record from the initial conditions data set and the parameters in namelist INPUTZ. The initial condition fields are placed in common block /QANDQT/ which is the main storage for model fields. It has space for two time levels of the model prognostic variables as well as a number of diagnostic fields.

As the integration advances in time, the model periodically writes two types of data sets. The output is done utilizing subroutines IOQ and CONHTR which are called from subroutine TWRITE. At an interval determined by the

namelist variable NDRSW, restart data sets (V8RSTR format) are alternately written to units 12 and 14, overwriting any existing information contained in the data set. At the end of the model run (forecast segment) one of these data sets provides the initial conditions for the next forecast segment. The other type of output is the model history (V8SIGM format) data set on unit 8. The interval at which information is appended to the history data set is determined by the namelist parameter NDOUT. Periodically, restart data sets are also imbedded in the history data set to provide forecast reproducibility. These history data sets are the basic archive of the model's results. The V8SIGM format is described in Section 3 of Chapter VIII.

VII.2 Model Grid

VII.2i Horizontal Grid Control Variables

The horizontal grid described in Section 1 of Chapter II is completely determined by specifying the two integers IM and JM. The values of IM and JM used for a particular experiment are read as part of the header record of the V8RSTR format initial conditions data set by subroutine INPUT. The following is a list of derived model variables used to specify the horizontal grid. These values are set by subroutine DEPEND which is called by subroutine INPUT after it has obtained the values of IM and JM.

<u>Variable Name</u>	<u>Location</u>	<u>Description</u>
IM	/ICNTRL/	number of grid points per latitude circle. (read from unit 12 in subroutine INPUT)
JM	/ICNTRL/	number of latitude bands in grid. (read from unit 12 in subroutine INPUT)
IMT2	/ICNTRL/	$IM * 2$
IMD2	/ICNTRL/	$IM/2$
IMD2P1	/ICNTRL/	$(IM/2) + 1$
JMD2	/ICNTRL/	$(JM + 1)/2$
JMT2	/ICNTRL/	$JM * 2$
JNP	/ICNTRL/	$JM + 1$
JSP	/ICNTRL/	1
DLAT	/RCNTRL/	π/JM
DLON	/RCNTRL/	$2\pi/IM$
INDEX(I)	/IDPARM/	$MOD(I + IMD2 - 1, IM) + 1$
COSLON(I)	/RDPARM/	$COS(INDEX(I) * DLON)$
SINLON(I)	/RDPARM/	$SIN(INDEX(I) * DLON)$

IJUMP(J)	/IDPARM/	IM J=JSP or J=JNP { 1 otherwise
JC(J)	/IDPARM/	MOD(J - 1, 5) + 1
MJ(J)	/IDPARM/	1 J=JSP {2 J=JNP 0 otherwise
RLAT(J)	/RDPARM/	DLAT * (J - FJEQ) where FJEQ = 0.5 * (JSP + JNP)
RLATD(J)	/RDPARM/	RLAT(J) * (180/π)
COSL(J)	/RDPARM/	COS(RLAT(J))
SINL(J)	/RDPARM/	SIN(RLAT(J))

VII.2ii Vertical Grid Control Variables

The vertical grid described in Section 2 of Chapter II is determined by specifying the pressure at the top of the model atmosphere, P_{TOP}, the number of sigma layers, N_{LAY}, and the values of sigma at the edges of the layers, S_{IGE}(L). P_{TOP} and N_{LAY} are read as part of the header record of the V8RSTR format initial condition data set by subroutine INPUT. The values of S_{IGE}(L) are set in subroutine DEFALT to specify a uniform sigma resolution. These default values are used unless the user does one of two things:

- (a) leave the namelist parameter SN2FLG set to its default value of .false. and specify S_{IGE}(L) by including it in namelist INPUTZ.
- (b) set the namelist parameter SN2FLG to .true. in namelist INPUTZ.

This has the effect of setting $S_{IGE}(L + 1) = [\sin((\pi/2) * (L/N_{LAY}))]^2$ for $L = 1, 2, \dots, N_{LAY}$, a non-uniform vertical grid which has higher resolution near the ground and at the top of the model.

Two other variables, K_S and K_U, are also obtained from the header record of the initial conditions data set. K_S specifies the number of surface fields (both prognostic and diagnostic) used by the model, and K_U defines the number of upper air fields being used. The following is a list of derived model

variables used to specify grid constants:

<u>Variable Name</u>	<u>Location</u>	<u>Description</u>
PTOP	/RCNTRL/	pressure at top of model atmosphere (mb). (read from unit 12 in subroutine INPUT)
NLAY	/ICNTRL/	number of sigma layers in model atmosphere (read from unit 12 in subroutine INPUT)
SIGE(L)	/RCNTRL/	sigma values at edges of model layers. (see remarks above)
SN2FLG	/LCNTRL/	switch for \sin^2 sigma profile (see remarks above)
KS	/ICNTRL/	number of surface fields read from unit 12 in subroutine INPUT (altered in subroutine DEPEND to reflect choice of diagnostics)
KU	/ICNTRL/	number of upper air fields read from unit 12 in subroutine INPUT (altered in subroutine DEPEND to reflect choice of diagnostics)
NLAYM1	/ICNTRL/	NLAY - 1
NLAYP1	/ICNTRL/	NLAY + 1
DSIG(L)	/RDPARM/	SIGE(L + 1) - SIGE(L)
SIG(L)	/RDPARM/	$0.5 * (SIGE(L + 1) + SIGE(L))$

VII.2111 Control Variables for Filters

The filters described in Section 5 of Chapter IV, and the time filter used in conjunction with the leapfrog time integration scheme, are controlled and adjusted using the following model variables:

<u>Variable Name</u>	<u>Location</u>	<u>Description</u>
NDSHF	/ICNTRL/	controls interval at which Shapiro filtering is done. (read with namelist INPUTZ, default value 023000)

SMTH(N,J)	/QANDQT/	damping coefficients used by the high latitude filter (read with namelist INPUTZ, analytic default values set in subroutine DEFAULT)
FILTER(J)	/LDPARM/	logical set .true. when high latitude filter is to be applied to latitude band J.
GNU2	/RCNTRL/	coefficient to do leapfrog smoothing: GNU2=0, no smoothing; GNU2=.25, maximum smoothing (read with namelist INPUTZ)
GNU1	/RCNTRL/	1.0 - 2.0 * GNU2

VII.3 Model Calendar and Time Scheme Variables

Most times and time intervals used by the model are expressed using the following convention. Dates are designated by an integer set to $10000 * \text{year} + 100 * \text{month} + \text{day}$ where year is the two digit year (1969 = 69), month is the two digit month (May = 05 etc.) and day is the day of the month, i.e. 790612 specifies the 12th of June 1979. Times are designated by an integer set to $10000 * \text{hour} + 100 * \text{minute} + \text{seconds}$ where hour is the hour of the day ($0 \leq \text{hour} < 24$), minutes satisfy ($0 \leq \text{minute} < 60$) and seconds satisfy ($0 \leq \text{second} < 60$), i.e. 221500 specifies 10:15 pm. All times are GMT. The following list contains the variables used for clocks, intervals, interval counters and time scheme control:

<u>Variable Name</u>	<u>Location</u>	<u>Description</u>
NDT	/ICNTRL/	basic model time step in seconds (read with namelist INPUTZ)
DT	/RCNTRL/	set to NDT for Matsuno predictor and corrector steps, 2 x NDT for leapfrog steps.
NYMDO, NHMSO	/ICNTRL/	initial date and time of forecast experiment (set whenever subroutine DEFAULT is called)
NYMD1, NHMS1	/IDPARM/	initial date and time (read with namelist INPUTZ)
NYMDE, NHMSE	/ICNTRL/	ending date and time (read with namelist INPUTZ)
NYMD, NHMS	/ICNTRL/	current date and time for the fields in /QANDQT/
NDPHY	/ICNTRL/	HHMMSS increment for evaluation of "physics" terms other than longwave radiation
NDHOG	/ICNTRL/	HHMMSS increment for evaluation of the longwave radiation
NDSHF	/ICNTRL/	HHMMSS increment for application of the Shapiro filter

NDALT	/ICNTRL/	HHMSS increment for the analysis cycle
NDOUT	/ICNTRL/	HHMSS increment at which V8SIGM history records are written to unit 8
NDRSW	/ICNTRL/	HHMSS increment at which V8RSTR restart records are written to units 12 and 14
NKRSH	/ICNTRL/	control variable for writes of V8RSTR records to unit 8
MATIN	/ICNTRL/	number of Matsuno time steps which are to be done before entering the normal time scheme cycle
NSEQ	/ICNTRL/	number of time steps in one cycle of the normal time scheme
MLF(K)	/ICNTRL/	normal cycle specification; set to 0 for leapfrog, 1 for Matsuno (see Fig. VII.3a for a description of the time scheme)
MATSUN	/ICNTRL/	set to 1 (0) to indicate that the current time step is Matsuno (leapfrog)
MATSNX	/ICNTRL/	set to 1 (0) to indicate that the next time step is Matsuno (leapfrog)

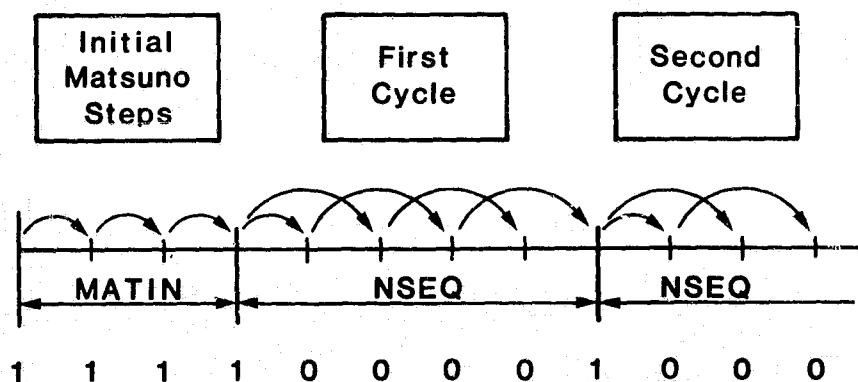


Fig. VII.3a Schematic Description of Time Marching

VII.4 Physical Constants

Several physical and empirical constants are used throughout the code.

Their assigned value, units and description are given below.

APHEL	183. days	Day of the apogee of the earth's orbit
BETA	.0065°K/m	Adiabatic lapse rate
CALTOJ	4186.0 kg J/cal	Conversion factor for calory to joule
CP	1003.5 J/(kg°K)	Specific heat of air at constant pressure
CPP	.24 cal/(gm°K)	Specific heat of air at constant pressure
DAYSPLY	365. days	Number of days in a year
DECMAX	23.5000 * PI180	Maximum declination of the earth's axis
ECCN	.0178	Eccentricity of the planetary orbit
EDNM	2. m ² /s	Minimum allowable diffusivity coefficient used in the determination of surface temperature
EPS	0.6220	Ratio of molecular weight of water vapor to dry air
GRAV	9.81 m/s ²	Gravitational acceleration
HEATW	597.2 cal/gm	Latent heating coefficient over land and water
HEATI	680.0 cal/gm	Latent heating coefficient over ice, snow and frost
HICE	300. cm	Net ocean ice thickness
PTOP	10. mb	Pressure at the top of the model atmosphere
PZERO	1013.25 mb	Reference pressure used in scaling water vapor amounts for solar radiation
RADE	6375000. m	Planetary radius
RGAS	287. m ² /((°Ks ²))	Gas constant for dry air
SDAY	86400. s	Number of seconds per day
SHLTOP	.00002	Specific humidity at the top of the atmosphere used in scaling water vapor amounts for solar radiation
SO	2880.0/RSDIST ly/day	Solar constant modified by the ratio of the actual to mean earth-sun distance (RSDIST)
SOLS	173. days	Day of the year of maximum solar declination

STBO	1.171×10^{-7}	Stefan-Boltzman constant
TICE	273.16°K	Freezing point for ice
TLOWL	16.	Optical thickness associated with low-level cumulus clouds
TLTOP	220.°K	Temperature at the top of the atmosphere used in scaling water vapor amounts for solar radiation
TMIDL	8.	Optical thickness associated with mid-level cumulus clouds

VII.5 Computational Flow

This section describes, by means of flow diagrams, the logical ordering of the computations within the FORTRAN program that constitutes the general circulation model.

The subroutines are separated into generic groups based on their principal computational function, i.e. program control, input and output, hydrodynamics, and physical processes. Only subroutines which act as "drivers" or which contain important computations are included in the diagrams. Subroutines that perform a single operation with little or no logical control outside of their immediate domain (utilities) are not described with the same level of detail.

A brief description of the subroutines and functions which make up the complete scalar and vector models is given below:

ADDQ : Utility subroutine to add fourth order model values

ALTER2 : Driver for the objective analysis program; not a subroutine of the model

AVRX : Fourier filter for base fields near the poles in the x-direction

BLOCK
DATA : Initialization (scalar version only)

BTOLOG : Convert a bit array to a logical array (vector version only)

CLOCKS : Timer

CLOUDS : Calculate the absorption of solar radiation due to clouds

COMP0 : Control differencing scheme (hydrodynamics)

COMP1 : Integrate the horizontal and vertical advection terms of the momentum equations and the continuity equation to advance the prognostic variables one time step

COMP2 : Integrate the coriolis and pressure gradient terms of the momentum equations and the thermodynamics and moisture equations to advance the prognostic variables one time step

COMP3 : Calculate source terms for the momentum, thermodynamic and moisture equations

COMP35 : Correct for phase changes during ground temperature update

CONHTR : Conversion to history format and write to unit 8
 CONSTA : Set time-dependent constants for the physics
 COPYQ : Utility to copy differential fields onto base fields for the Matsuno predictor step
 CUMULO : Cumulus parameterization
 CUTCHK : Check if computation cutoff time has been exceeded; in CYGWSLIB
 DAILY : Update calendar, correct global mean pressure and input climatological surface conditions if at beginning of new day
 DEFAULT : Set default model parameters before reading namelist
 DEPEND : Set model dependent constants
 DIFFQ : Utility subroutine to subtract fourth order model values
 DUMPIJ : Prints the fields u, v, and T at a specified grid point (vector version only)
 EXPBYK : Function to compute p to the power kappa
 FILEFT : Filter a one-dimensional array by wave number (scalar version only)
 GEOHT : Calculate Phillips normalized geopotential heights at sigma edges
 GWSGCM : The MAIN
 INCHMS : Hour-minute-second arithmetic
 INCYMD : Increment the year-month-day by one day or compute number of days in the year (Julian date)
 INITSD : Initialize model global diagnostic arrays
 INPUT : Read model control namelist and model initial conditions and set dependent parameters
 IOQ : Utility subroutine to skip, read, or write model restart records
 LAPSE : Computes mean vertical lapse rate for high latitude filtering (vector version only)
 LINKHO : Calculate longwave radiation (only at the poles in the vector version, everywhere in the scalar version)
 LOGTOB : Convert a logical array to a bit array (vector version only)
 MOIST : Routine for moist adiabatic adjustment (vector version only)
 MSGOP : Send message to console operator (vector version only)

NAMEZ : Read model control namelist INPUTZ (vector version only)
NAMPHY : Read model control namelist INPHYS (vector version only)
ORBIT : Calculate planetary orbital position (vector version only)
OZONE2 : Calculate ozone amounts for solar radiation routine
O3INT : Calculate ozone amounts for longwave radiation routine
PGMAP : Map common blocks to Cyber virtual memory page (vector version only)
PMEAN : Calculate global mean surface pressure
POLINP : Copy pole values from global model array into stereographic pole
or copy stereographic pole to model array
PRDIAG : Print diagnostic quantities and halt execution if the surface
pressure is out of specified bounds
QSAT : Function to compute saturation mixing ratio
RADIO : Driver for longwave and solar radiation routines
RDCLI : Read climatological fields of sea surface temperature, ground
wetness, etc.; in CYGWSLIB
RESTQM : Restore saved base fields onto differential fields for the Matsuno
corrector step
RIOQ : Utility subroutine for reading model band restart records (vector
version only)
SAVEQM : Save base fields temporarily for Matsuno corrector step or leapfrog step
SCALEQ : Scale base fields by volume element
SHAP : Shapiro filter for a two-dimensional array (vector version only)
SHCORN : Correct base specific humidity field for negative values
SM SHAP : Apply two-way Shapiro filter to prevent nonlinear instability of model
global fields: sea level pressure, sea level temperature, potential
temperature and u and v winds
SOLAR1 : Compute solar radiation in atmosphere
STRATM : Introduce climatological temperatures in upper atmosphere
TIMAVG : Time filter differential fields using new base fields and save base
fields for leapfrog step
TWRITE : Write model history and restart records

C-3

VERT : Calculate omega (vertical velocity)

VEXPBYK : Function to compute p to the power kappa (vector version only)

VLINKHO : Calculate longwave radiation away from the poles (vector version only)

VQSAT : Function to compute saturation mixing ratio (vector version only)

VOZON : Calculate solar radiation absorbed due to ozone (vector version only)

VWATER : Calculate solar radiation absorbed due to water vapor (vector version only)

ZEIT : Utility to measure run time efficiency (vector version only);
in CYGWSLIB

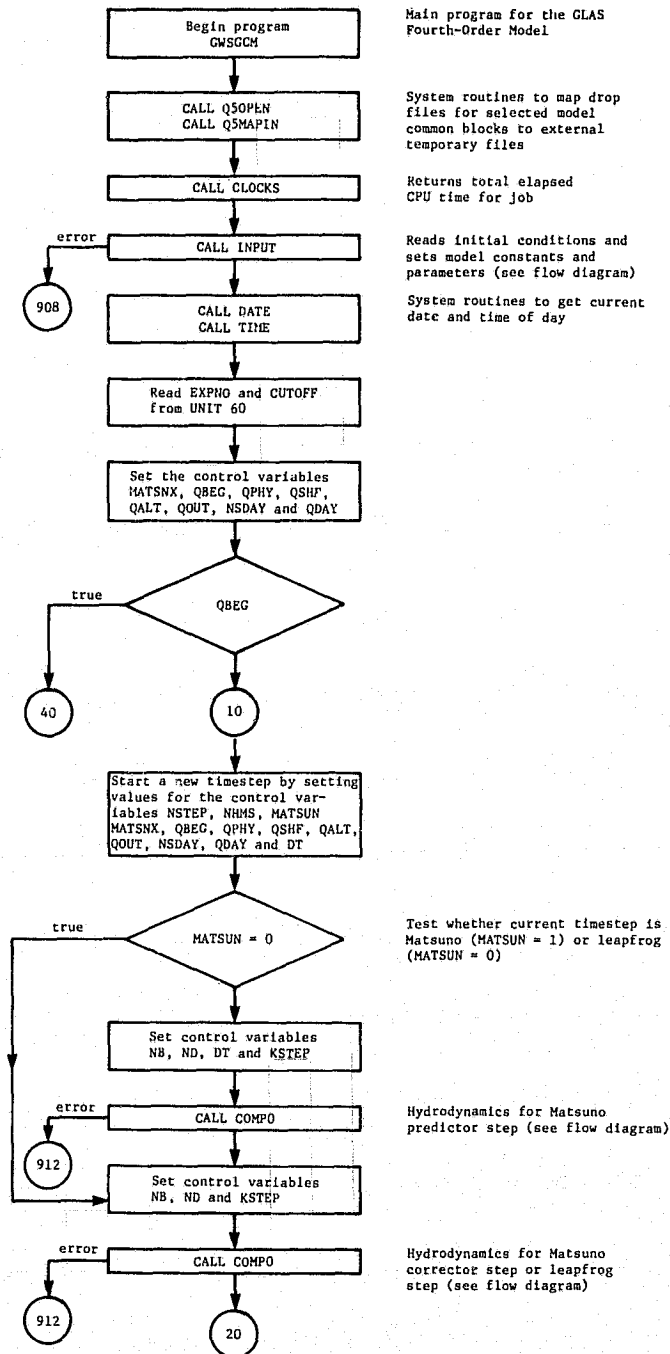
VII.51 Program Control

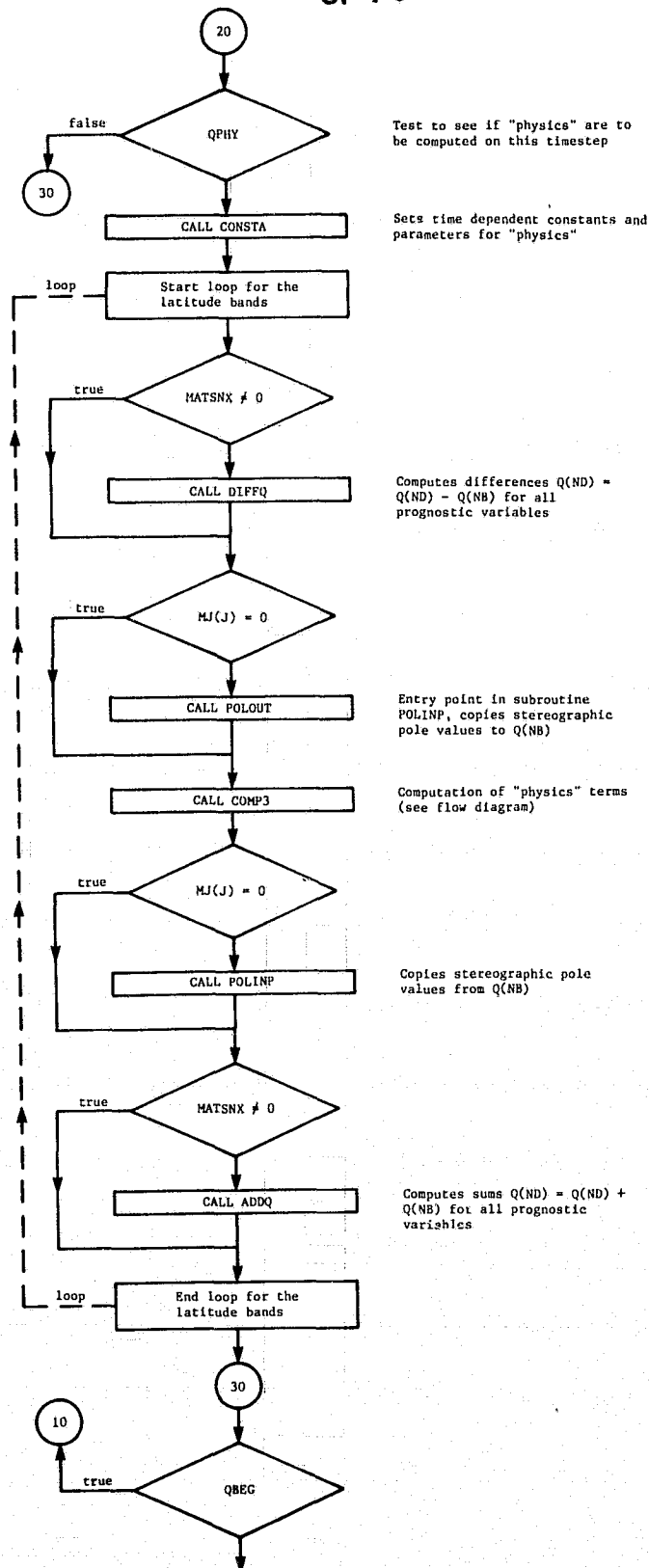
The MAIN or PROGRAM GWSGCM controls the sequence of steps that are required during integration of the model.

That is, "housekeeping", initialization, integration start and end times, fourier and time filtering, time scheme control and error termination, are the principal functions performed in this section of the code.

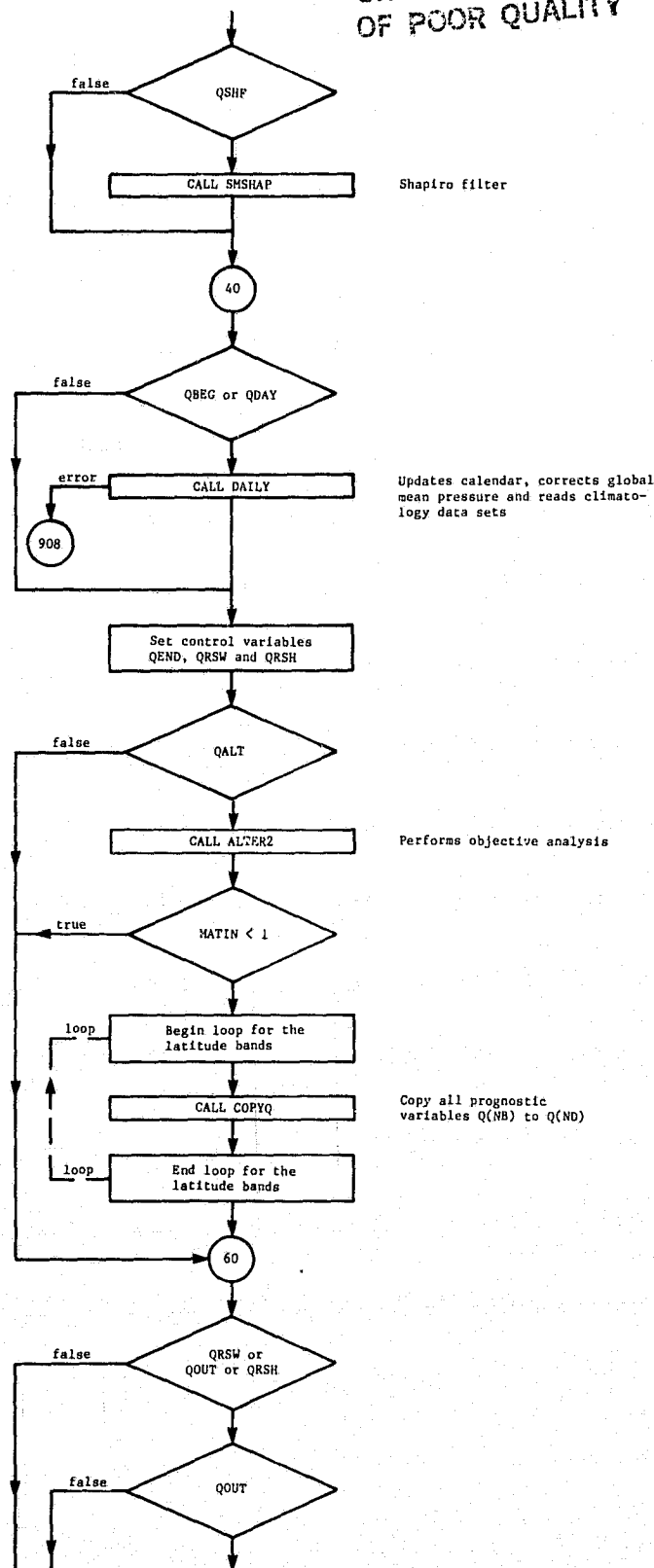
One important function of the model is that of operating in-line with an objective analysis program. In this mode, referred to as the analysis cycle, the program passes control to subroutine ALTER2 which receives the forecast fields in common block /QANDQT/ and proceeds to update this "first guess" atmosphere with global observations.

The analyzed fields replace the "first guess" in /QANDQT/ and control is returned to the model where the cycle is repeated at selected intervals, currently set at 00, 06, 12 and 18 GMT.

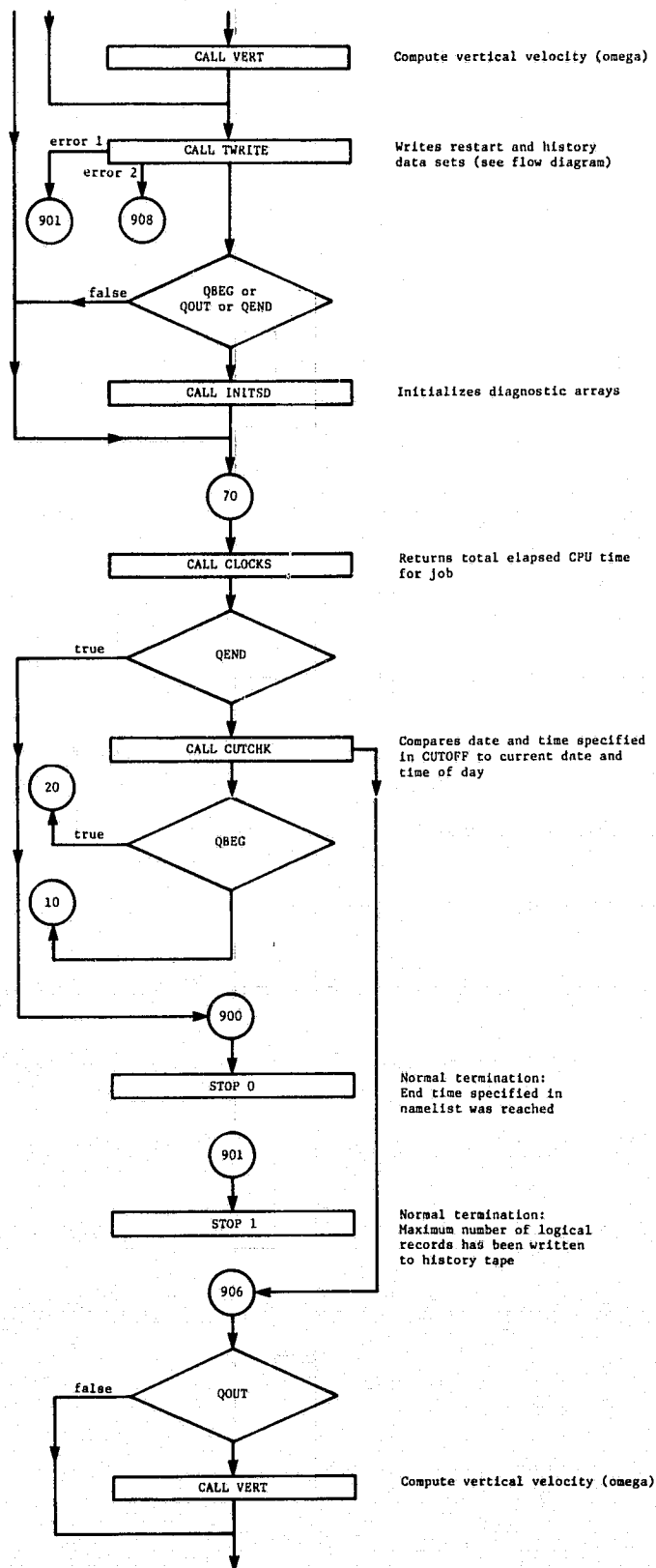




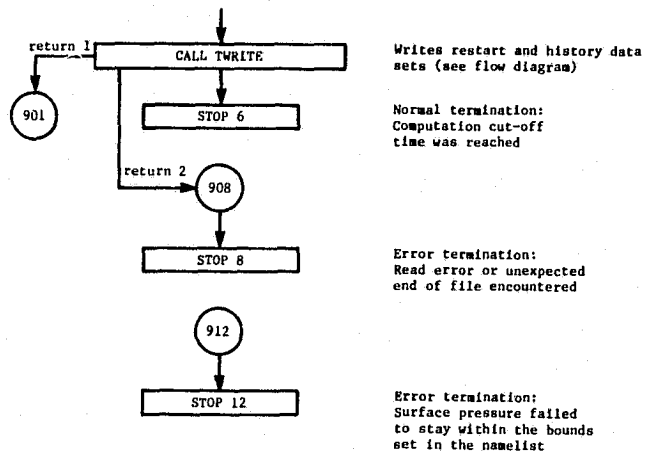
ORIGINAL PAGE IS
OF POOR QUALITY



ORIGINAL PAGE IS
OF POOR QUALITY



ORIGINAL PAGE IS
OF POOR QUALITY



VII.511 Input/Output

The two subroutines described here perform the bulk of the input and output operations required by the model. Subroutine INPUT initializes control variables from namelist INPUTZ and controls the transfer of the initial states of the atmosphere from logical unit 12 to the appropriate common blocks. Subroutine TWRITE controls the output operation to logical unit 8 for both the restart records in V8RSTR format and for the history records in V8SIGM format. In addition it controls the output of V8RSTR format restart records to units 12 and 14.

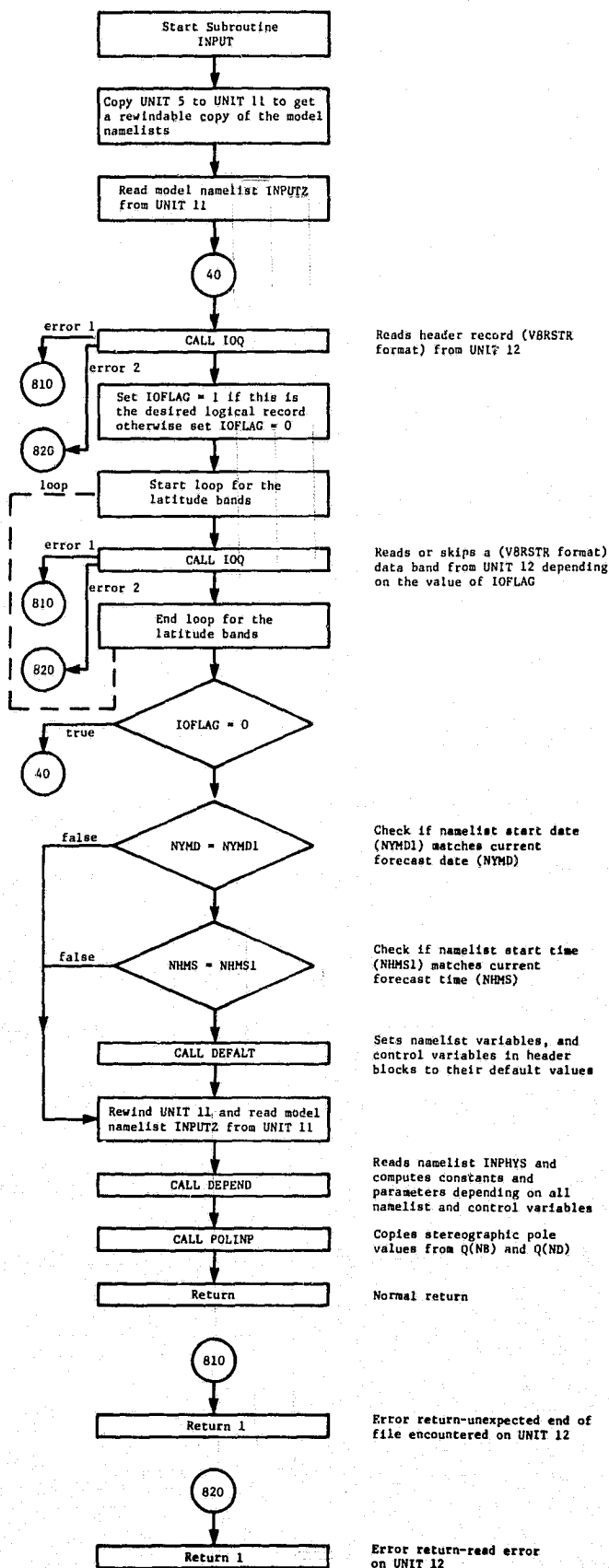
There are, in addition, two input/output utilities used by these subroutines which perform the actual FORTRAN I/O operations. The first is subroutine IOQ which reads and/or writes records in the restart (V8RSTR) format.

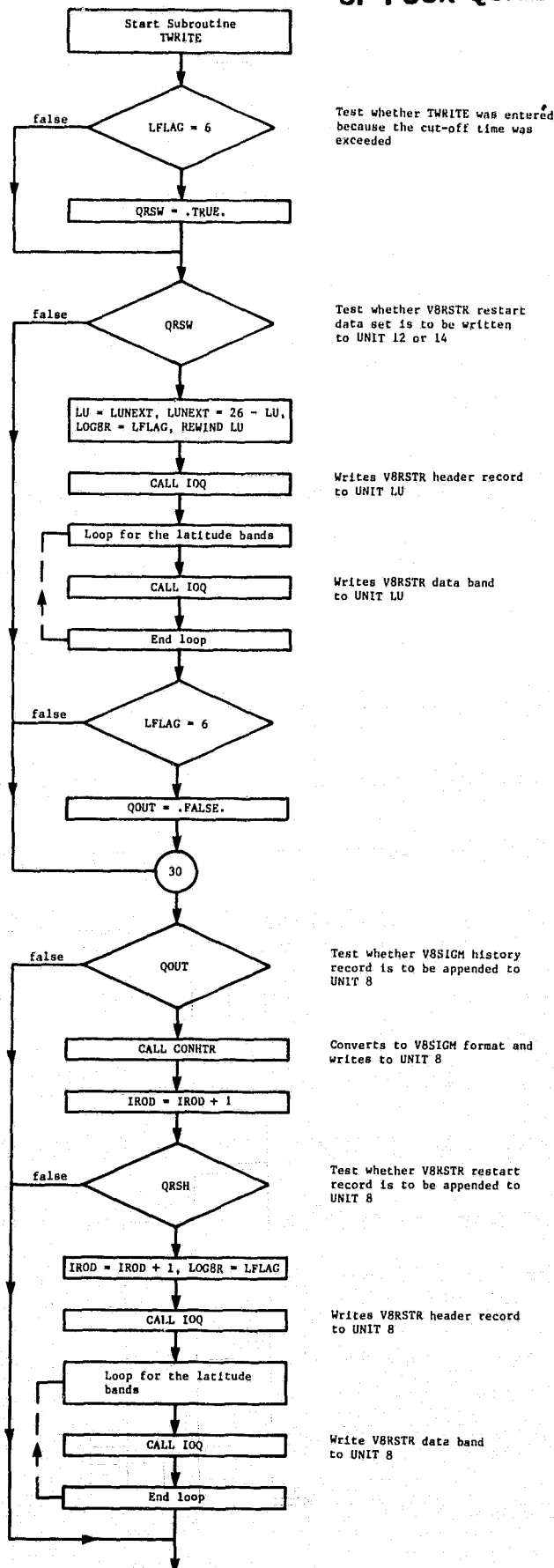
The second, subroutine CONHTR, performs format conversion from V8RSTR to V8SIGM and writes the results to the history data set.

Direct FORTRAN I/O operations are also performed in subroutines DAILY and LINKHO.

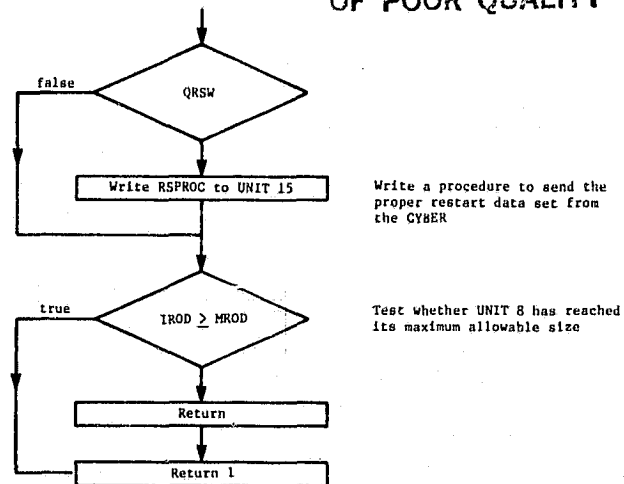
Surface boundary conditions for sea surface temperature, albedo and ground wetness are read by DAILY at the initiation of a forecast segment and again at 00 GMT of each succeeding forecast day.

Subroutine LINKHO, a part of the longwave radiation package, reads the ozone and carbon dioxide coefficients for the atmospheric transmittances.



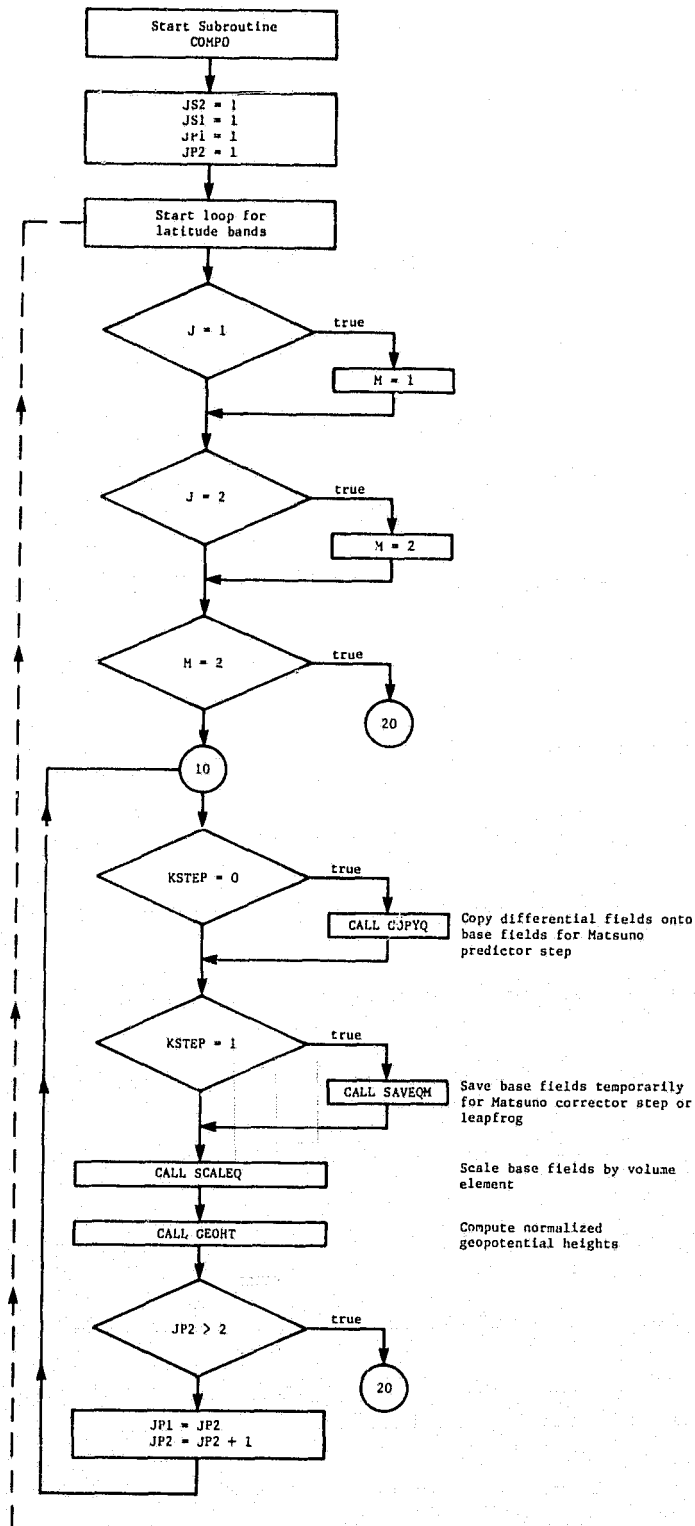


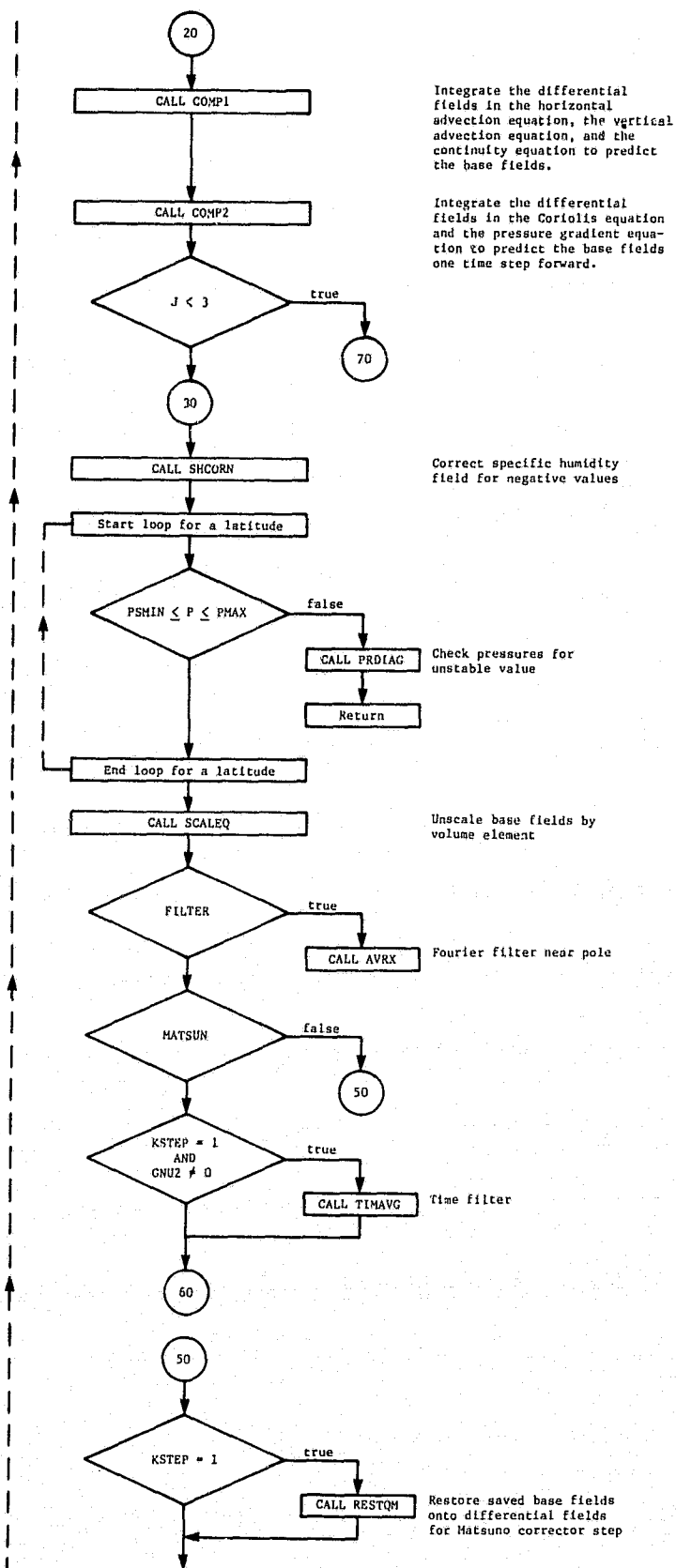
ORIGINAL PAGE IS
OF POOR QUALITY



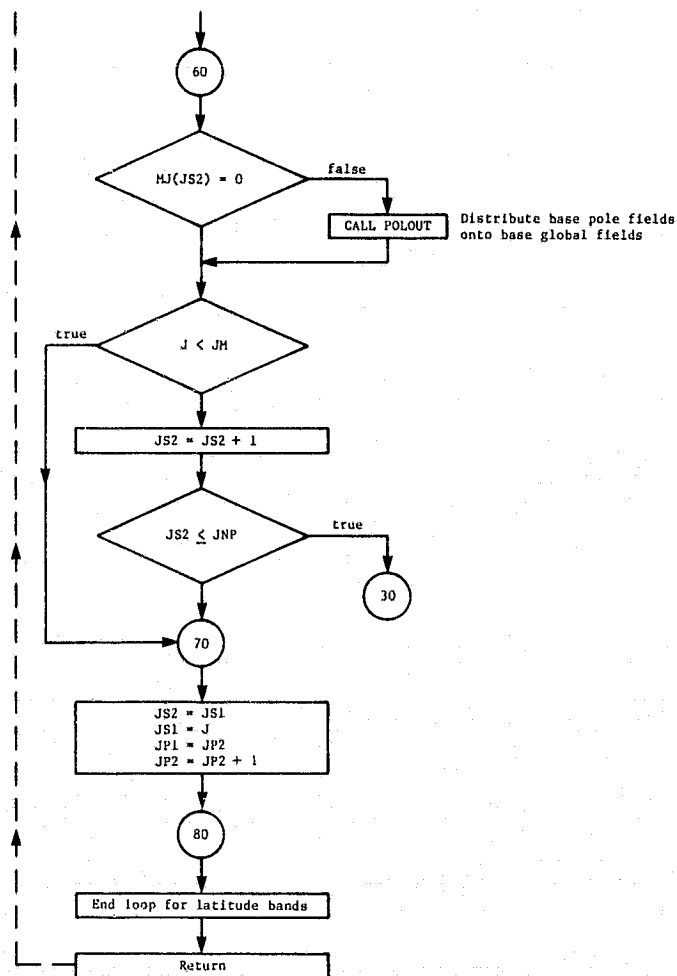
VII.5111 Hydrodynamics

The hydrodynamics computations are performed by subroutines COMPO, COMPl and COMP2. Subroutine COMPO is the main driver for COMPl and COMP2, invoking these subroutines once for each latitude band of the model's horizontal grid.

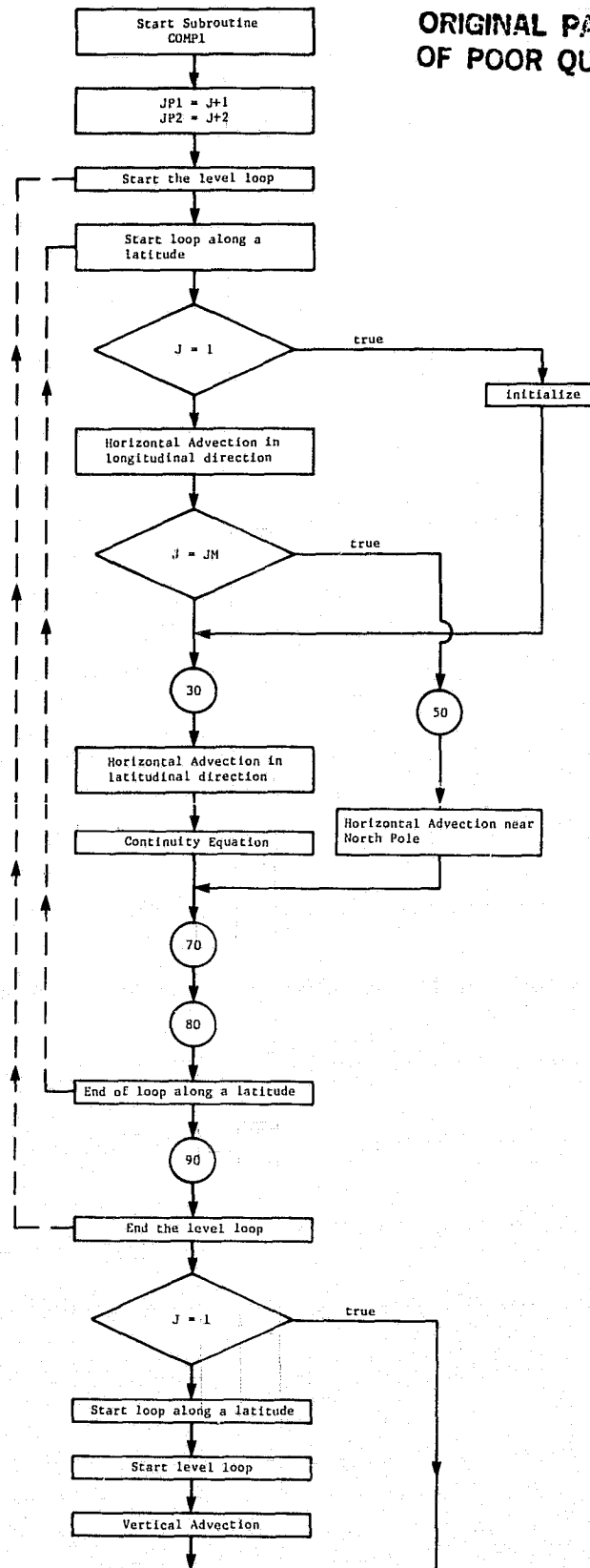




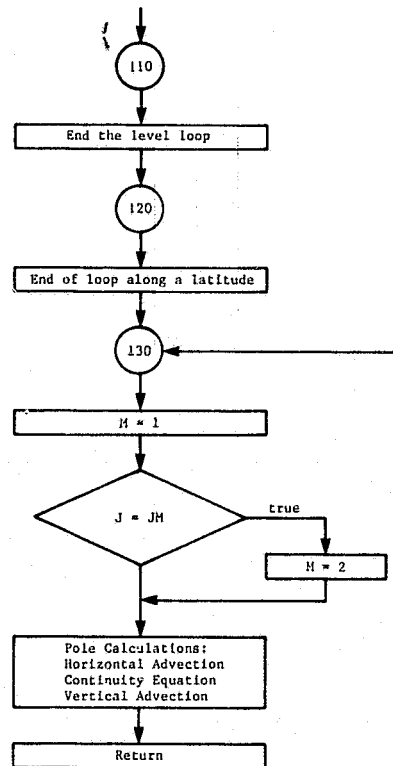
ORIGINAL PAGE IS
OF POOR QUALITY

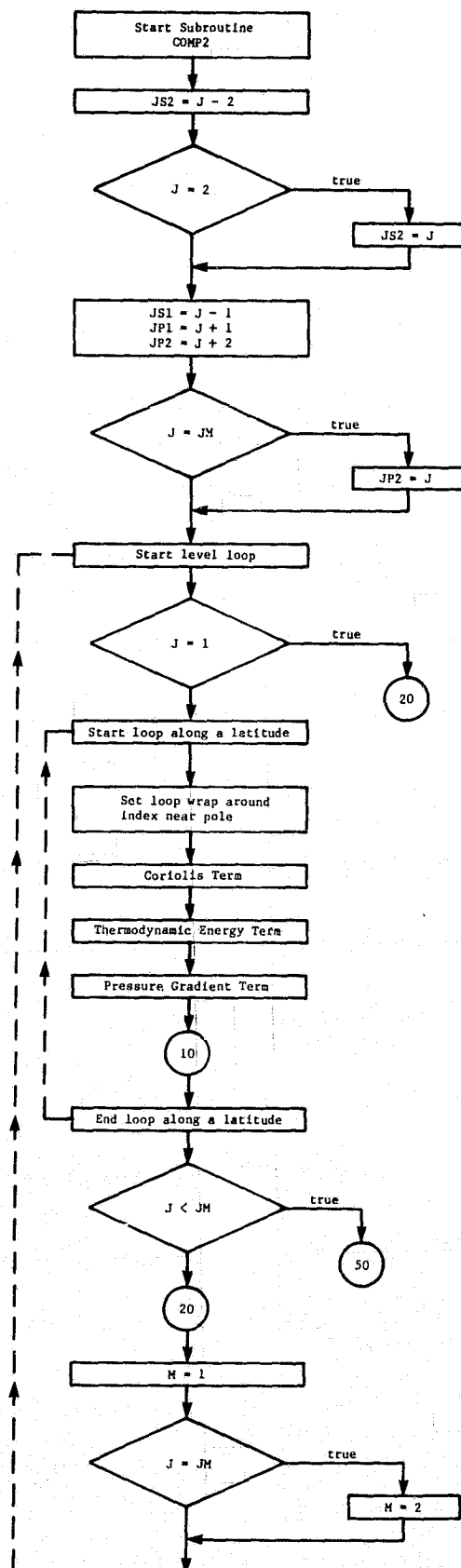


ORIGINAL PAGE 19
OF POOR QUALITY

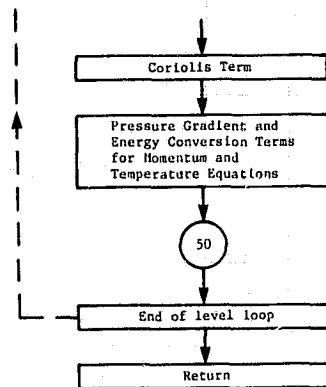


ORIGINAL PAGE IS
OF POOR QUALITY



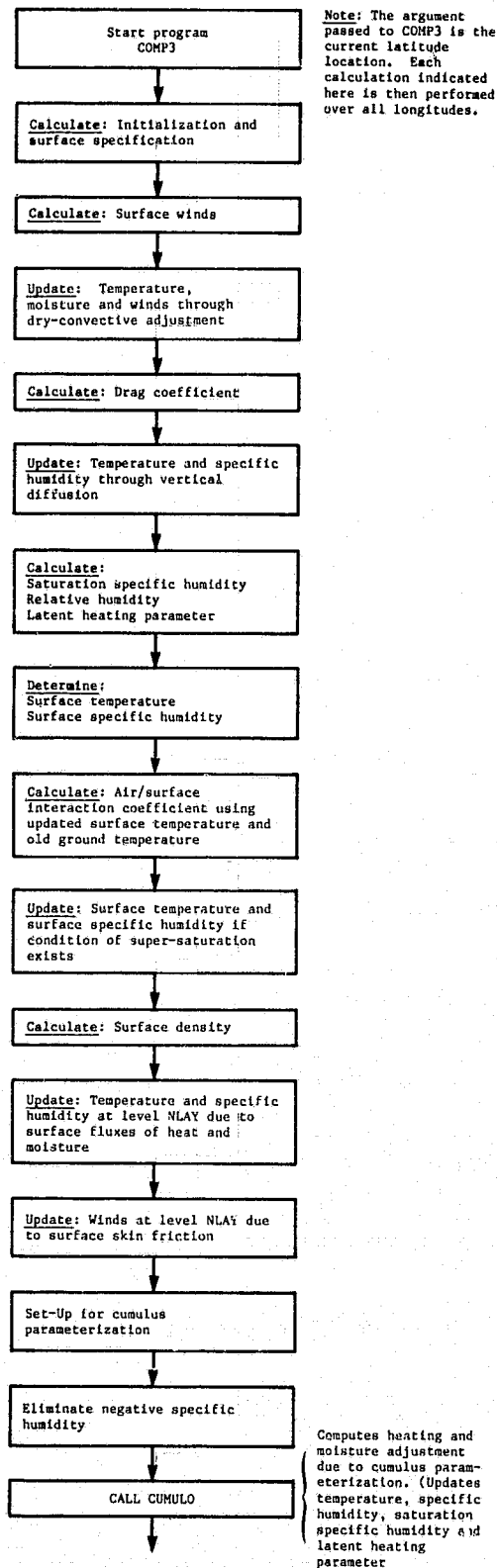


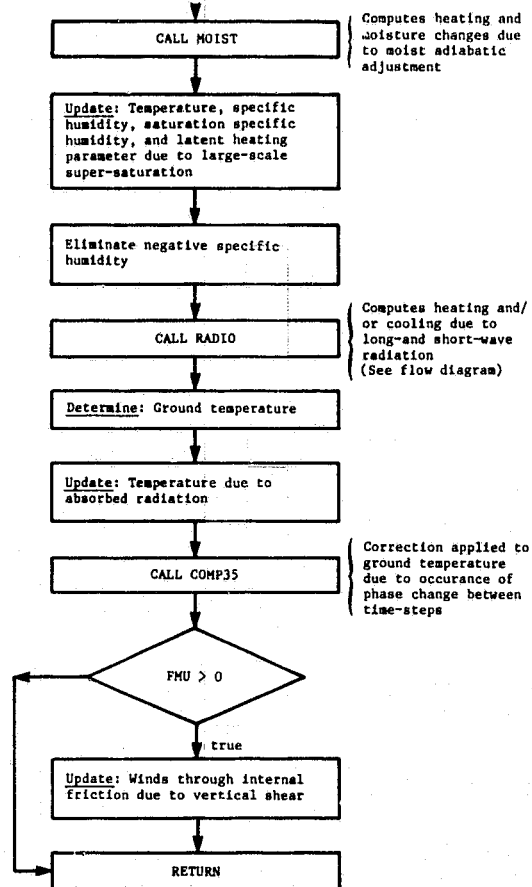
ORIGINAL PAGE IS
OF POOR QUALITY



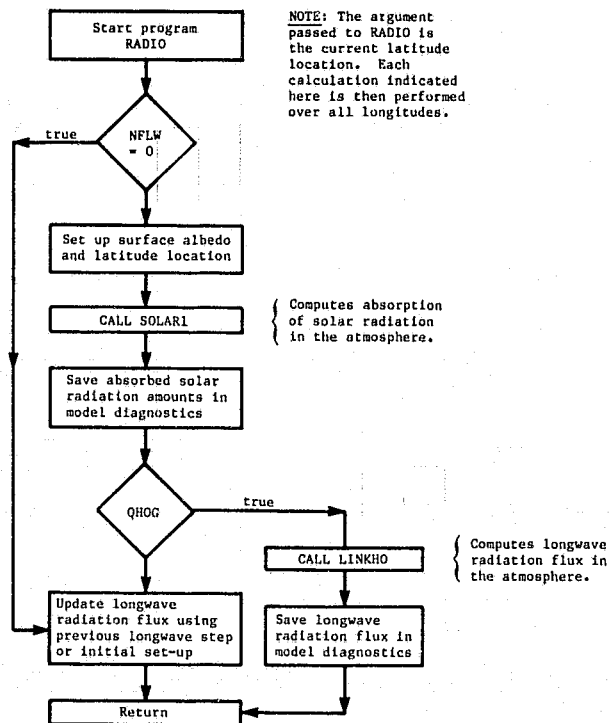
VII.5iv Physics

The "physics" code, subroutine COMP3, embodies a top-down process. That is, for one latitude band at a time, the physical processes are applied in sequence to the vertical slice consisting of all longitudinal grid points at each of the NLAY levels.





ORIGINAL PAGE IS
OF POOR QUALITY



CHAPTER VIII

INPUT/OUTPUT

JAMES W. PFAENDTNER

VIII. INPUT/OUTPUT

VIII.1 Namelists

Many run-time control variables and parameters can be set using the model namelists, INPUTZ and INPHYS. INPUTZ is read in subroutine INPUT from unit 11, which is a rewindable copy of the card images contained on unit 5. The second namelist, INPHYS, is read from unit 11 in subroutine DEPEND.

VIII.11 Control (INPUTZ)

A complete list of the control variables which can be set using namelist INPUTZ is given in Appendix A. The control variables which are used for a particular forecast segment are determined as follows. First, subroutine INPUT gets variables NYMD1 and NHMS1 from namelist INPUTZ. It then reads the V8RSTR format initial/restart conditions from unit 12. This fills the header arrays CC, IC, LC, and RC. A comparison is then made to see if the starting date and time from the namelist (given by NYMD1 and NHMS1) matches the date and time of the fields read from unit 12 (given by NYMD and NHMS contained in array IC). If the dates and times match, subroutine DEFALT is called. Subroutine DEFALT uses only the variables JOB, IM, JM, LOG8R, NB, ND, NHMS, NYMD, NLAY and PTOPT to set default values for all other variables in the control arrays CC, IC, LC and RC and those in namelists INPUTZ and INPHYS. Subroutine DEFALT is not called if the dates and times do not match. Namelist INPUTZ is then read a second time, overriding the values in the control arrays. Subroutine DEPEND is then called. It reads namelist INPHYS and computes all constants and parameters which depend on the control and namelist constants. Refer to Section 5 of Chapter VII for a flow diagram of subroutine INPUT.

VIII.111 Physics (INPHYS)

This namelist contains tuning parameters for the various physical parameterizations used by the model, and logical switches for choosing which diagnostic quantities are to be computed. A complete list with default values is given in Appendix A. Again, only those variables which are to be set to a value other than the default value need to be contained in the namelist. If only default values are to be used, the entire namelist can be omitted.

VIII.2 Boundary Conditions

VIII.2i Topography, Ground Wetness, Albedo, Sea Surface Temperature

The topography used by the model is that which is read as part of the initial condition data set. No provision is made within the model for changing topography at the start of an experiment. Alterations of the terrain height necessitate a redefinition of all model fields because of pressure changes at the sigma levels. See Appendix D for a map of the orography currently being used in the 4 degree latitude by 5 degree longitude versions of the model.

As the model integrates, the possibility exists of periodically updating the surface boundary fields. Presently these fields are obtained from monthly mean climatology data sets (see Appendix D for maps of these fields). The namelist variables KLIALB, KLIGW, and KLISST control the desired time interpolation. If they are set to 0, the boundary conditions which were read as part of the initial condition data set are used throughout the experiment. If they are set to 1, the boundary conditions from the initial condition data set are replaced with the appropriate monthly mean value and are updated with new monthly means whenever the forecast advances into a new month. If they are set to 2, the boundary conditions from the initial condition data set are replaced with time interpolated (between the monthly mean climatologies) values appropriate to the starting date of the experiment. They will be updated with new time interpolated values whenever the forecast advances into a new day. The three control variables KLIALB (for the surface albedo), KLIGW (for the surface ground wetness and ice extent) and KLISST (for the sea surface temperature) can be set independently.

The time interpolations and updating described above are done by subroutine DAILY. It uses the utility routine RDCLI to read the climate data sets it needs. Sea surface temperature fields are read from unit 41, ground wetness/

ice extent fields from unit 42 and albedo fields from unit 43. Each of these three files contains $12 * (1 + JNP)$ physical records. For each month there is a small header record followed by JNP data records (one for each latitude band) of IM words. The climate data sets have the same horizontal resolution as that used by the model. No horizontal interpolation is done.

VIII.2ii Format of the Surface Boundary Conditions (V8SURF)

Data Set Naming Convention

All data sets, except the topography, are cataloged, OS partitioned data sets residing on shared DASD with names of the form

F400.fff.ttt.Riii jjj.VERnnn(ppp)

where:

- fff specifies the field type
 - 'TOP' for topography
 - 'SST' for sea surface temperature
 - 'ALB' for surface albedo
 - 'GWT' for ground wetness
 - 'LWI' for land-water-ice type designator
- ttt specifies the type of average
 - 'CLI' if for more than one period
 - 'Ynn' if for a particular period in one year where nn is the last two digits of the year
- iii specifies the east-west resolution
 - '072' for 5 degree resolution
 - '144' for 2.5 degree resolution
- jjj specifies the north-south resolution
 - '046' for 4 degree resolution
 - '091' for 2 degree resolution
- nnn specifies the version number used to distinguish data from different sources, or data derived in alternate fashions from the same source.
- ppp specifies the averaging period for one or several periods
 - 'M01' for January, 'M02' for February etc.
 - 'S01' for Winter, 'S02' for Spring etc.
 - 'YYY' for annual average

The topography data sets are ordinary sequential data sets (no partitions) but are otherwise organized exactly like the other V8SURF data sets.

Data Set Format

The DCB settings RECFM=VBS, LRECL=19065, BLKSIZE=19069 are used for all data sets. Each data set (partition) consists of one header record followed by jjj data records.

The header record consists of the three arrays CSURF, ISURF and RSURF in that order. CSURF is declared REAL*8 and contains character (EBCDIC) information.

CSURF (1) to CSURF (4)	contains the data set name, left justified
CSURF (5) to CSURF (14)	contains a title for the field, centered in the 80 characters
CSURF (15) to CSURF (20)	contains descriptions of the units used for the data set, left justified
CSURF (21) to CSURF (120)	contains more detailed information on the data set, 10 card images

The array ISURF is declared INTEGER and contains

ISURF (1)	iii which defines the east-west resolution and the size of the following jjj data records
ISURF (2)	jjj which defines the north-south resolution and the number of data records to follow
ISURF (3)	is a grid type indicator (set to 0 for the standard fourth order GCM grid)
ISURF (4) to ISURF (30)	spares (set to -999)

The array RSURF is declared REAL*4 and contains

RSURF (1)	fill value used for missing data
RSURF (2) to RSURF (30)	spares (set to -999.0)

The header record therefore, contains $120*8 + 30*4 + 30*4 = 1200$ bytes.

The jjj data records each contain iii REAL*4 values and are $4*iii$ bytes long. For the standard fourth order GCM grid the first value in each record is on the prime meridian and increases eastward by increments of $(360/iii)$ degrees. The first record for the standard grid is at the south pole (hence

contains iii identical values). The next record is (180/(jjj-1)) degrees north of the south pole etc. Any deviations from the standard fourth order GCM grid is flagged by setting ISURF (3) greater than 0 and are described in CSURF (21) through CSURF (120).

LWI Data Set

This cataloged OS partitioned data set is used to describe non-numeric aspects of the model grid cells. The data set is in the V8SURF format. For each grid point, space for four bytes of information is provided. Bytes 1-3, the leftmost bytes, are reserved for future use. Byte 4 is set to one of the five characters L, W, I, G or M where

L - Land point not permanently covered by ice

W - Water point that never freezes

I - Water point that is frozen but sometimes melts

G - Land or Water point which is permanently frozen

M - Water point that is not frozen but sometimes does.

VIII.2111 Transmission Functions of Carbon Dioxide and Ozone

The Wu-Kaplan radiation routine (longwave radiation) uses precalculated transmission functions of carbon dioxide and ozone. These transmission functions are read from unit 55 in subroutine LINKHO. The records corresponding to carbon dioxide are read first using the code

```
DO 20 N = 1, 2
DO 20 I = 1, 19
READ (55, 10) CTINF (I, N), CTIN (I, N), (CTTRANS (J, I, N), J = 1, I)
10 FORMAT (13F6.4)
20 CONTINUE
```

Here, the index N represents the spectral intervals 500-660 cm^{-1} and 660-800 cm^{-1} . The variables in the READ statement are the transmission functions of carbon dioxide at the radiation level I (I = 1,, 19) for various paths as described below

CTINF(I,N) - Path between 1 mb level and radiation level I
CTIN(I,N) - Path between 5 mb level and radiation level I
CTRANS(I,J,N) - Path between radiation levels J and I

From the READ statement, it can be seen that not all the transmission functions CTRANS are available for all possible paths. But it is obvious that the transmission function has the same value whether the radiation traverses a path starting at level I and arriving at level J or the other way, i.e.,
 $\text{CTRANS}(I,J,N) = \text{CTRANS}(J,I,N)$

where I = 1,, 19, J = 1,, 19, N = 1, 2

Since these transmission functions are calculated with an assumed standard temperature sounding and a uniform mixing ratio of CO_2 , all grid points have the same values of the transmission functions of CO_2 .

The records corresponding to ozone in the data set are read next using the code

```
DO 6 N = 1, 5
READ (55, 9)    (T01(I, N), I = 1, 19)
READ (55, 9)    (T02(I, N), I = 1, 19)
DO 7 I = 1, 19
7 READ (55, 9)   (TR03(I, J, N), J = 1, 19)
9 FORMAT (10F8.5)
6 CONTINUE
```

These transmission functions correspond to absorption by ozone in the 800-1200 cm^{-1} spectral interval, and are evaluated at latitudes 15°, 30°, 45°, 60° and 75°. The ozone transmission functions are assumed to be symmetrical about the equator. The index N in the above code represents the latitude with N = 1 corresponding to 15° and N = 5 to 75°. The transmission functions of ozone at any latitude are obtained by linear interpolation using subroutine 03INT. The paths for which the transmission functions in the READ statements are computed are described below.

T01(I, N) - Path between 1 mb level and radiation level I

T02(I, N) - Path between 5 mb level and radiation level I

TR03(I, J, N) - Path between radiation levels I and J

In the model, the longwave radiation routine is called at each grid point. However, it is sufficient to read the transmission function data of CO₂ and O₃ only once, i.e., when the routine is called for the first time. Tables of the transmission functions as they are used in current model versions can be found in Appendix E.

VIII.3 Model History Data Sets

This section describes the formats of the model history data sets which are currently used to save the output of the GLAS fourth order GCM. In each data set there are a series of logical records each composed of a number of physical records. In this discussion the following definitions are adhered to:

A logical record describes a model state at a particular instant, in either pressure or sigma coordinates. The description of the model state is usually complete in the sense that all prognostic variables are defined over the entire domain. In addition, a number of diagnostic variables may be included. Nominally, a model state is associated with a single time level but for a leapfrog integration the prognostic variables at two levels are needed to precisely define the future evolution of the model. The restart format described below therefore contains values of the prognostic variables at two time levels.

A physical record is the object of a single FORTRAN I/O operation. The first physical record of each logical record contains enough information to determine the total number of physical records making up the logical record.

Normally the logical records within a history data set are time ordered. Note that there may be several logical records at the same time level to accommodate before/after assimilation, before/after initialization and restart records.

Since the history data set (IBM floating point) must be independent of the model restart data set (CYBER floating point), the history data sets are arranged to minimize paging in the post-processing programs. Also, since

many of the post-processing programs produce products relative to pressure coordinates, a pressure coordinate model history data set has been established. The basic archival data set remains the sigma coordinate model history data set.

The model history data sets described in this section are the following:

- V8SIGM - Basic archival history data set at the sigma coordinates of the model.
- V8MAND - History data set at pressure coordinates obtained by interpolating the V8SIGM data set, or obtained directly from the objective analysis.
- V8RSTR - Internal format used for the model restart data sets and initial conditions data sets.

VIII.3i Sigma Coordinate Model History (V8SIGM)

This data set is composed of one data file which totally defines and describes a particular experiment. This is the basic and most important data set of the model. For ease of documentation, the contents of the data set will be addressed in two segments; the first containing the source code and experiment control information, and the second containing the model history.

Data Control Block (DCB)

LABEL: SL1
RECFM: VBS
LRECL: 19065
BLOCK: 19069

Code: BINARY (32-bit IBM floating point) -- History segment
ASCII (CYBER 205) -- Source code segment
EBCDIC (Amdahl V/6, V/7B) -- Source code segment

Contents of the Source Code Segment

This segment of the data set contains the FORTRAN source code of the GCM and the namelist card images, which in combination with the parameters defined in the CC, IC, LC, and RC arrays of the data records, generate the

atmospheric history contained in the history segment of the data set.

This segment occurs only once at the beginning of every volume (tape) of the data set.

The card images are contained in a variable (n) number of records of 2920 characters each, in either ASCII or EBCDIC code, depending on whether the history data set was generated on the CYBER or Amdahl, respectively. However, the first 5 words (40 characters) of each record, are always coded in EBCDIC and contain the following information:

Word Number	Contents
1	'CDCbbbb' or IBMbbbbbb' or HCDCbbbb'
2	'EXPbxxxx' where xxxx identifies the experiment number
3	'MM/DD/YY' date on which the experiment was initiated
4	'HH.MM.SS' time when the experiment was initiated
5	'LASTbbbb' to indicate the last record of the source code segment or 'CONTINUE' to indicate that additional records in the segment follow.

Contents of the History Segment

This segment contains a series of logical history records each composed of several physical records, the number of which may increase as additional upper air prognostic or diagnostic quantities are included, and/or the horizontal and vertical resolution of the model is increased. In general, the first physical record of a logical record will be referred to as the 'header' record, the next set of records as the 'surface' records, and all subsequent ones, as the 'upper air' records.

Header Record

The first physical record consists of the six arrays that contain the constants and parameters that define the model integration as well as other descriptive information. These arrays are described in the following table.

Variable Name	Dimension	Type	Contents
CC	200	REAL*8	Character variables
IC	200	INTEGER	Integer variables
LC	200	LOGICAL	Logical variables
RC ³	200	REAL	Real variables
XORDS	KS	REAL*8	Characters for surface variables ¹
XORDU	KU	REAL*8	Characters for upper air variables ²

Appendix B contains a full description of the contents of the first four arrays.

Surface Records

DIMENSION (IM)

These records include physical record 2 through physical record $JNP * KS + 1$. They contain the quantities that define the state of the model's surface and other two-dimensional quantities. The KS two-dimensional quantities are each organized in JNP consecutive records, increasing from south pole ($J = 1$) to north pole ($J = JNP$), each of IM longitude elements, increasing from the prime meridian ($I = 1$) in the eastward direction. The number of quantities, which is variable, is defined in IC(16) by the variable KS. The grid dimensions are defined in IC(2) and IC(9) by the variables IM and JNP respectively. Each data field is of dimension IM by JNP and is of type REAL with the exception of

¹ Mnemonics for surface variables; also implies their ordering.

² Mnemonics for upper air variables; also implies the record ordering.

³ The RC array is declared half precision in model versions using half precision arithmetic on the CYBER and contains 400 elements.

the ICLOUD field which is of type INTEGER (see Appendix C). An alphanumeric description of each field is given in XORDS.

All prognostic fields represent instantaneous values. The diagnostic fields, on the other hand, are values per unit time defined by taking differences over NDOUT, the time increment at which the model history is written to the data set (found in IC(41)). The ordering and choice of fields given in the table below is that obtained with the default settings for diagnostic quantity selection.

Variable Name	Initialization Rate (h)	Sequence Number	Description: Units
PHIS		1	Surface geopotential height: m^2/s^2
SMTH		2	High latitude Fourier filter coefficients
ALBEDO		3	Albedo x 100: 1
GT		4	Ground temperature: °K
GW		5	Ground wetness: 0 to 0.99 land points : 1 water points : 10^6 ice points
TS		6	Temperature of the air above the surface: °K
SHS		7	Specific humidity at the surface: gm/gm
P		8	Reference pressure: mb; difference between surface pressure and the pressure at the top of the model - P _{TOP} defined in RC (25), currently 10mb
TMIN	24	9	Minimum (TS) daily temperature: °K
TMAX	24	10	Maximum (TS) daily temperature: °K
PREACC	NDOUT	11	Total accumulated precipitation: 0.1 mm/day
PRECON	NDOUT	12	Total convective precipitation: 0.1 mm/day
HFLUX	NDOUT	13	Sensible heat flux: ly/day
EFLUX	NDOUT	14	Evaporative flux: ly/day
FUSION	NDOUT	15	Fusion heat stored at the ground: ly/day

(Cont'd)

RADSWG	NDOUT	16	Shortwave radiation stored at the ground: ly/day
RADLWG	instantaneous values	17	Longwave radiation at the ground: ly/day
ICLOUD	NDOUT	18	Convective and supersaturation clouds: (see Appendix C)

Upper Air Records

DIMENSION (IM)

These records include physical record $JNP * KS + 2$ through physical record $(JNP * KS + 1) + (NLAY * JNP * KU)$ where KU , defined in IC(17), is the number of upper air fields (defaults to 9) and where $NLAY$, defined in IC(48), is the number of sigma levels.

Each of the KU three-dimensional quantities is organized in groups of $NLAY$ consecutive records of IM longitude elements for each of the JNP latitude bands. The ordering of the sigma levels is such that the first occurrence corresponds to the topmost level and the last occurrence to the level nearest to the surface. Thus, the fields are of dimension IM by $NLAY$ by JNP and are of type REAL. An alphanumeric description of each field is given in XORDU. The ordering and choice of fields given in the table below is that obtained with the default settings for diagnostic quantity selection.

Variable Name	Initialization Rate (h)	Sequence Number	Description: Units
U		1	Zonal wind component: m/s
V		2	Meridional wind component: m/s
T		3	Temperature: °K
SH		4	Specific humidity: gm/gm
PHI		5	Geopotential height: m^2/s^2

(Cont'd)

OMEGA	NDOUT	6	Vertical velocity: nanobar/s
DIABAT	NDOUT	7	Diabatic heating (10 times the actual amount): °K/day
RADSW	NDOUT	8	Shortwave radiation: ly/day
RADLW	instantaneous values	9	Longwave radiation: ly/day

NOTE: OMEGA is defined at the lower edges of the layers rather than at the mid-layer.

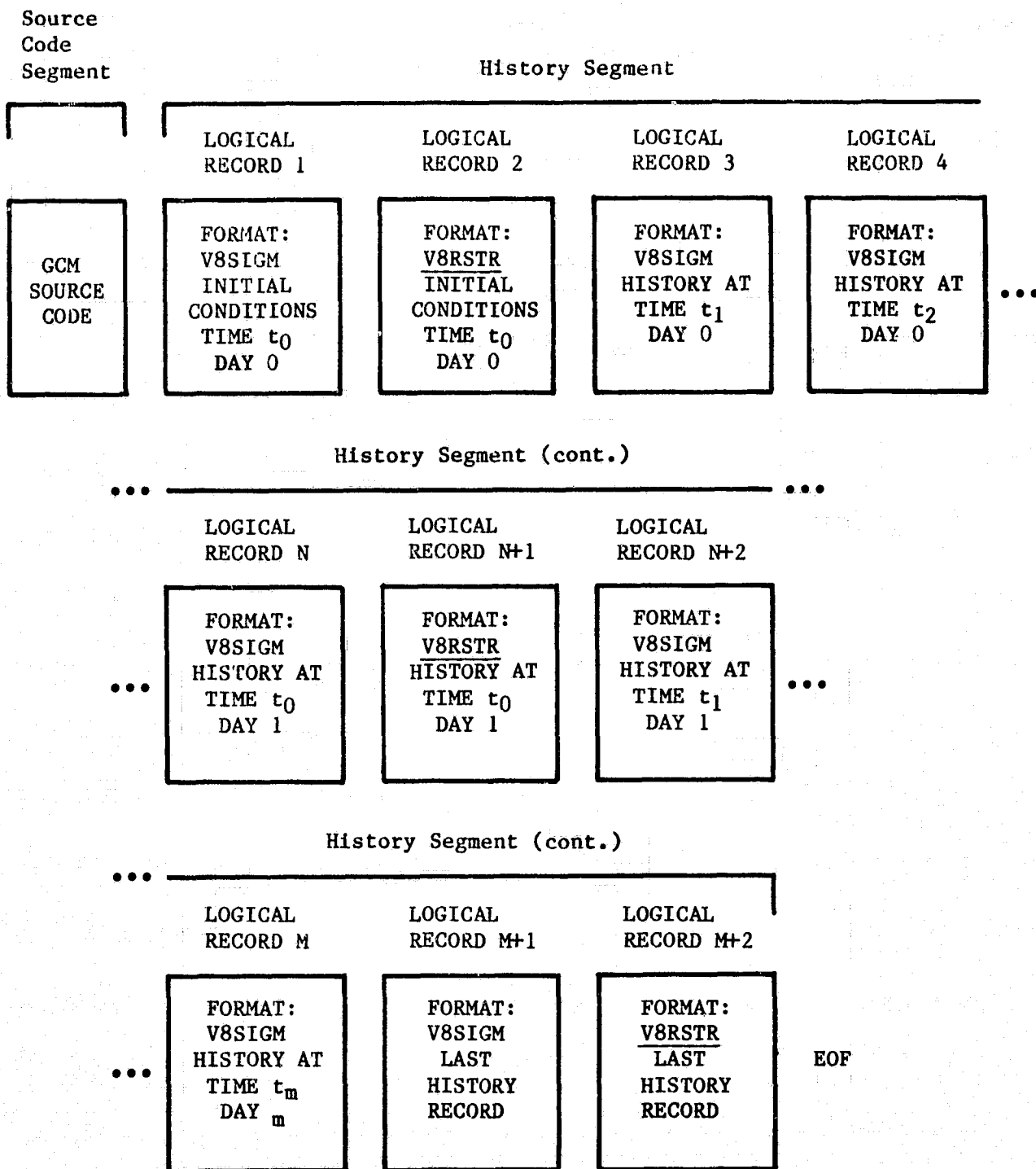
Organization of the Logical Records

Because of the desirability of archiving in a single data set all the necessary information for reproducibility (and transportability), the V8SIGM data set also incorporates logical records in the model restart format V8RSTR (see Figure VIII.3a). These records are coded in CDC floating point representation for model integrations performed on the CYBER.

To allow the front-end user to identify these records, the following conventions have been established:

- o A V8RSTR record will always be preceded by a matching V8SIGM record.
- o The first word of the first physical record of the V8RSTR data - CC(1) - will contain the character string
 - 'IBMbbbb' for 32-bit IMB generated records (EBCDIC), or
 - 'CDCbbbb' for 64-bit CDC generated records (ASCII), or
 - 'HCDCbbbb' for 32-bit CDC generated records (ASCII).
- o The first word of the logical array - LC(1) - will be .TRUE. if the logical record which follows the one currently being processed is a (32-bit or 64-bit) restart record. This will occur in the matching V8SIGM record.

FIGURE VIII.3a: TYPICAL* ORGANIZATION OF THE LOGICAL RECORDS IN THE V8SIGM DATA SET



*The increment at which the V8RSTR records are written to the V8SIGM data set is determined by the variable NKRSH to be found in IC(35).

o The first word of the integer array - IC(1) - will be

- 0 if the next record is not a V8RSTR record
- 1 if the next record is a 32-bit V8RSTR record, IBM Format
- 2 if the next record is a 64-bit V8RSTR record, CDC Format
- 3 if the next record is a 32-bit V8RSTR record, CDC Format

VIII.3ii Pressure Coordinate Model History (V8MAND)

This data set consists of one file which describes the model states interpolated to constant pressure coordinates. This is the basic data set for all diagnostic studies.

DATA CONTROL BLOCK (DCB)

LABEL: SL1
RECFM: VBS
LRECL: 19065
BLOCK: 19065

CODE: Binary (32-bit IBM floating point)

Contents

A series of logical records consisting of $1 + JNP * KS + (JNP * KU * NMLEV)$ physical records. The first record is the 'header' record, the next $KS * JNP$ records contain the surface and sea level fields, and the last $JNP * KU * NMLEV$ records contain the upper air quantities at each of the NMLEV pressure levels. The variables are defined as follows:

KS = IC(16)
KU = IC(17)
NMLEV = IC(60)

Header Record

This is the first physical record. See the documentation of the V8SIGM data set for a description.

Surface Records

DIMENSION (1 + IM)

They include physical record 2 through physical record $JNP * KS + 1$. They contain the quantities that define the model's surface and sea level, as well as other two-dimensional quantities. The KS two-dimensional quantities are each organized in JNP consecutive records, increasing from south pole ($J = 1$) to north pole ($J = JNP$), each of IM longitude elements, increasing from the prime meridian ($I = 1$) in the eastward direction. Each physical record contains a 4 character alphanumeric (EBCDIC) descriptor prefix. The number of quantities, which currently defaults to 18, is defined in the variable KS. Each data field is of dimension IM by JNP and is of type REAL with the exception of the ICLOUD field which is of type INTEGER (see Appendix C). The following table provides the ordering of the quantities and their description.

Variable Name	Initialization Rate (h)	Sequence Number	Description: Units
PHIS		1	Surface geopotential height: m^2/s^2
SMTH		2	High latitude Fourier filter coefficient
ALBEDO		3	Surface albedo x 100: 1
GT		4	Ground temperature: °K
GW		5	Ground wetness: 0 to 0.99 land points : 1 water points : 10^6 ice points
TSL		6	Temperature at sea level: °K
RHS		7	Surface relative humidity: 0 to 1
PSL		8	Pressure at sea level: mb
TMIN	24	9	Minimum surface (air) temperature: °K
TMAX	24	10	Maximum surface (air) temperature: °K
PREACC	NDOUT	11	Total accumulated precipitation: 0.1 mm/day

(Cont'd)

PRECON	NDOUT	12	Total convective precipitation: 0.1 mm/day
HFLUX	NDOUT	13	Sensible heat flux: 1y/day
EFLUX	NDOUT	14	Evaporative flux: 1y/day
FUSION	NDOUT	15	Fusion heat stored at the ground: 1y/day
RADSWG	NDOUT	16	Shortwave radiation stored at the ground: 1y/day
RADLWG	instantaneous values	17	Longwave radiation at the ground: 1y/day
ICLOUD	NDOUT	18	Convective and supersaturation clouds: (see Appendix C)

Upper Air Records

DIMENSION (1 + IM)

These records include physical record $JNP * KS + 2$ through physical record $(JNP * KS + 1) + (JNP * KU * NMLEV)$ where KU , defined in IC(17), is the number of upper air fields, which currently defaults to 9, and where $NMLEV$, defined in IC(60), is the number of constant pressure levels, currently 12. These records contain the model's upper air prognostic and diagnostic quantities.

The KU three-dimensional quantities are organized in JNP consecutive records, each of IM longitude elements. Each physical record contains a 4 character alphanumeric (EBCDIC) prefix descriptor. The group consisting of $JNP * KU$ records is repeated for each of the $NMLEV$ levels. Consequently, the first JNP records will complete the U wind field at the 1000 mb surface, the second set of JNP records will complete the V field at 1000 mb and so on. Fields are of dimension IM by JNP by $NMLEV$ and are of type REAL.

The order of the levels and their corresponding pressure is:

Level Number	Pressure (mb)
1	1000
2	850
3	700
4	500
5	400
6	300
7	250
8	200
9	150
10	100
11	70
12	50

These pressures are stored in the array PLEVS in RC(60) to RC(84). Note, that in contrast to the sigma levels, the first mandatory pressure level is at the bottom of the atmosphere. The following table shows the ordering of the upper air quantities along with their description.

Variable Name	Initialization Rate (h)	Sequence Number	Description: Units
U		1	Zonal wind component: m/s
V		2	Meridional wind component: m/s
PHI		3	Geopotential height: m^2/s^2
T		4	Temperature: °K
RH		5	Relative humidity: 0 to 1
OMEGA	NDOUT	6	Vertical velocity: nanobar/s
DIABAT	NDOUT	7	Diabatic heating (10 times the actual amount): K/day
RADSW	NDOUT	8	Shortwave radiation: ly/day
RADLW	instantaneous values	9	Longwave radiation: ly/day

VIII.3iii Sigma Coordinate Model Restart (V8RSTR)

This data set consists of one file which totally defines and describes a particular experiment. This is the basic restart data set of the model. The format described below for the history file is identical to that used in the checkpoint/restart data sets. These online data sets contain a single logical record as described below.

DATA CONTROL BLOCK (DCB)

LABEL: SL1
RECFM: VBS
LRECL: 19065
BLOCK: 19069

CODE: Binary (64-bit CDC floating point for CYBER 205, full precision arithmetic)
Binary (32-bit IBM floating point for Amdahl V/6, V/7B)
Binary (32-bit CDC floating point for CYBER 205, half precision arithmetic)

Contents

The data set contains a series of logical history records each composed of 1 + JNP physical records. The first record is the 'header' record, which is described in the documentation of the V8SIGM data set. All subsequent records, one for each latitude band of the model grid, contain all surface and upper air quantities.

Header Record

This is the first physical record. See the documentation of the V8SIGM data set for a description.

Surface and Upper Air Records

These records include physical record 2 through physical record JNP + 1.

The total number of data records is defined in IC(9) by the variable JNP. The length (number of 32-bit or 64-bit words) of the records is determined from the longitudinal resolution (IM), number of surface and upper air quantities (KS and KU respectively), number of vertical sigma levels (NLAY), and for CDC records, whether a half or full precision model was run. The data are of type REAL with the exception of the ICLOUD field which is of type INTEGER (see Appendix C).

Consequently, Record Length = Surface (IM * KS) + Upper Air (IM * NLAY * KU)

where IM = IC(2)
 KS = IC(16)
 KU = IC(17)
 NLAY = IC(48)

Note that because two time levels of some of the variables (P, U, V, T, SH, PHI) are stored, KS is one greater and KU is 5 greater than in the V8SIGM records.

The following table provides the order of the quantities and their description.

Variable Name	Initialization Rate (h)	Sequence Number	Length	Description: Units
PHIS		1	IM	Surface geopotential height: m^2/s^2
SMTH		2	IM	High latitude Fourier filter coefficient
ALBEDO		3	IM	Surface albedo x 100: 1
GT		4	IM	Ground temperature: °K
GW		5	IM	Ground wetness: 0 to 0.99 land points : 1 water points : 10^6 ice points
TS		6	IM	Temperature of the air above the surface: °K
SHS		7	IM	Surface specific humidity: gm/gm
(*)P 1		8	IM	Reference pressure: mb
(*)P 2		9	IM	Reference pressure: mb
TMIN	24	10	IM	Minimum (TS) temperature: °K

(Cont'd)

TMAX	24	11	IM	Maximum (TS) temperature: °K
PREACC	NDOUT	12	IM	Total accumulated precipitation: 0.1 mm/day
PRECON	NDOUT	13	IM	Total convective precipitation: 0.1 mm/day
HFLUX	NDOUT	14	IM	Sensible heat flux: ly/day
EFLUX	NDOUT	15	IM	Evaporative flux: ly/day
FUSION	NDOUT	16	IM	Fusion heat stored at the ground: ly/day
RADSWG	NDOUT	17	IM	Shortwave radiation stored at the ground: ly/day
RADLWG	instantaneous values	18	IM	Longwave radiation at the ground: ly/day
ICLOUD	NDOUT	19	IM	Convective and supersaturation clouds: (see Appendix C)
(*)U	1	20	IM*NLAY	Zonal wind component: m/s
(*)U	2	21	IM*NLAY	Zonal wind component: m/s
(*)V	1	22	IM*NLAY	Meridional wind component: m/s
(*)V	2	23	IM*NLAY	Meridional wind component: m/s
(*)T	1	24	IM*NLAY	Temperature: °K
(*)T	2	25	IM*NLAY	Temperature: °K
(*)SH	1	26	IM*NLAY	Specific humidity: gm/gm
(*)SH	2	27	IM*NLAY	Specific humidity: gm/gm
(*)PHI	1	28	IM*NLAY	Geopotential height: m ² /s ²
(*)PHI	2	29	IM*NLAY	Geopotential height: m ² /s ²
OMEGA	NDOUT	30	IM*NLAY	Vertical velocity: nanobar/s
DIABAT	NDOUT	31	IM*NLAY	Diabatic heating (10 times the actual amount): K/day
RADSW	NDOUT	32	IM*NLAY	Shortwave radiation: ly/day
RADLW	instantaneous values	33	IM*NLAY	Longwave radiation: ly/day

Note (*): These quantities are saved for the current and previous time steps for the purpose of restarting integrations performed with the leapfrog time scheme. To identify which field contains the current (or previous) time step, reference must be made to the variables NB and ND in IC(37) and IC(38) respectively.

The combination NB = 1, ND = 2 indicates that the first occurrence of the field contains the current time step, NB = 2, ND = 1 indicates that the first occurrence of the field contains the previous time step. Combinations 1,1 and 2,2 are not possible.

Note: Omega is defined at the lower edges of the layers rather than at the mid-layer.

CHAPTER IX

USER'S GUIDE

JAMES W. PFAENDTNER

IX. USER'S GUIDE

IX.1 Introduction

The Global Modeling and Simulation Branch's (GMSB) general circulation model can be thought of as an experimental instrument for conducting atmospheric research. Every effort has been made to design the model and its associated run procedures so that meaningful forecast experiments can be made without extensive knowledge of computer operating systems, model structure, data set formats, etc. All these elements are of only secondary interest to most atmospheric scientists. Consequently, this user's guide is of a less technical nature. It describes how, using existing software, the user can set up and carry out numerical experiments with the model.

IX.2 Running a Forecast Experiment

In general, the work to be done can be divided into the following six steps.

(Step 1) Decide which model code to use.

There are three choices.

(a) Standard FORTRAN for running on the Amdahl V/6 or V/7

(b) Standard FORTRAN for running on the CYBER 205

(c) FORTRAN with vector extensions for running on the CYBER 205

The production code for the model is maintained in these three forms. Choices

(a) and (b) are almost identical, while (c) is machine dependent code designed to use the CYBER 205 to best advantage. To do an experiment with minimal or no changes to the production source code, choice (c) is recommended. On the other hand, if extensive model changes are going to be made, and the user is not very familiar with the CYBER vector FORTRAN, choice (b) is probably best.

The total amount of computation time that is to be used should also enter into the decision. The vector code (c) is more than an order of magnitude faster than (a) or (b).

(Step 2) Create modification(s) to the model code. This work is done on a CMS virtual machine on the Amdahl V/6. The user is allowed to access the production source code selected and can modify it to meet requirements.

(Step 3) Alter the production run procedure to use the modified model version. This will usually consist of creating files in the CMS virtual machine and/or CYBER account having predefined names and purposes. For example, if the model will be running on the CYBER and it is desired to replace selected subroutines in the production source code with modified versions, the user only needs to place the modified subroutines in a file called USERFTN in the user's own CYBER account. The production run procedure will do the rest; i.e. it will

compile the contents of USERFTN, and see that the modified subroutines are used when the model is run. More extensive modifications to the model source code, such as the addition of input or output data sets, will require more extensive alterations to the run procedures.

(Step 4) Create a namelist file containing run time parameters for the experiment and an initial model restart file containing the initial conditions for the experimental forecast. There are two CMS execs to aid the user in this task; GCMNLSET to create the namelist file, and GCMICSET to create the initial model restart file.

(Step 5) Carry out the experimental forecast. To do this the user is provided with the CMS exec GCMSET. This exec allows the execution of a long forecast as a series of short forecast segments. It will use the production run procedures (in the user's altered form) to do all the needed data manipulation, such as creating restart files and merging history tapes, at the end of each forecast segment.

(Step 6) Examine the results. There are a number of existing programs to print and/or plot selected meteorological fields from the history tapes produced during the model forecast. Of course, the user can produce personalized diagnostics either at forecast run time by suitably modifying the model code or by writing post-processing programs to extract the desired information from the model history tapes.

IX.3 Model Production Code

The general circulation model is maintained in a scalar and a vector version. Both of these incorporate exactly the same physical processes and produce identical results. The difference between them lies in the computer programs used to define the model. Whereas the scalar version uses only standard FORTRAN code, the vector version makes free use of an extended FORTRAN provided by CDC to make optimal use of the CYBER 205. In general, for those not familiar with the CDC FORTRAN vector extensions, model development will be much easier using the scalar version as a starting point. The scalar version can also be implemented on any sufficiently large digital computer, while the vector version is specifically designed to run on a CDC vector machine. Model portability is one of the main reasons why the scalar code is maintained.

The master copies and updates defining the scalar and vector production codes are kept in the virtual machine F400M. The vector code is kept in mini-disks 206 and 207. The scalar code is kept in mini-disks 204 and 205. Typing the following sequence at the terminal will allow access to the production code

```
REL D
REL E
REL F
REL G
LINKTO F400M
LINKTO SYSLIB 192 222 G
GMSFSET GWSGCMS (use GWSGCMV for the vector code)
```

The user can now obtain a list of the subroutines used to define the selected production model by typing

```
LISTFILE * FORTRAN F
```

To create a copy of one of these subroutines in the user's own virtual machine, type

```
GMSFMSTR subroutine-name version-lev (RSLV resolution
```

where

subroutine-name is the name of the subroutine to be copied

version-lev is an integer which specifies the version level to use when creating the copy

resolution is a key word which specifies which model grid resolution to use

Although the user could create modified subroutines to define the model by obtaining copies in this manner and changing them, we recommend that the updating procedures described in the next section be used to define the model changes.

IX.4 How to Produce Modified Code

If the experiment will require more than superficial changes to a version of the model production code, it is recommended that modified source code be developed by using the updating procedures outlined in this section. There are a number of advantages to using the update facility for model development:

- (a) The user's only concern is with the subprograms to which modifications are being made.
- (b) There is a large saving in space because the local update files that are created and saved are much smaller than the modified subprogram. There is no need to keep the modified subprograms, only the changes (in the form of local updates) needed to produce them.
- (c) The modification process is structured and self-documenting to a large extent.

The update facility is designed to allow a number of users to independently modify an existing program base. In our case, the program base to be modified is the set of production source code subprograms which are put together by the update facility by applying a set of "permanent" updates to the master source of the model. The update facility allows the user to carry this process one step further by aiding in the creation of "local" updates, which reside in the user's virtual machine and transform the model production code into the user's personalized code. The following figure may help in visualizing the update process.

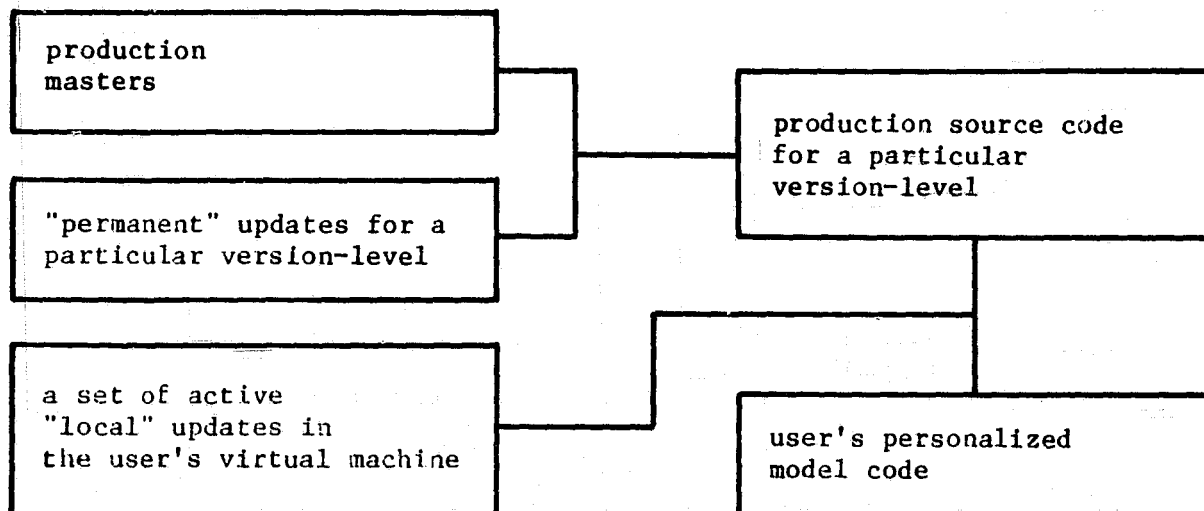


Fig. IX.4a Schematic View of the Update Process

To set up the update capability for the user's virtual machine the following CMS command sequence should be entered:

```

REL D
REL E
REL F
REL G
LINKTO F400M
LINKTO SYSLIB 192 222 G
GMSFSET GWSGCM (use GWSGCMV for the vector code)

```

This sequence will link the virtual machine to the update facility command disk (SYSLIB 192), the disk for model production code masters (F400M 205 or 207), and the disk containing the permanent updates for the various production code version-levels (F400M 204 or 206). These commands could be put in the PROFILE exec so that the update capability is available whenever the user has access to the computer.

The following is a brief description of some of the more often used update facility commands. There are others, and they are all documented via HELP commands in CMS. The commands described here will suffice in most cases.

GMSFUE sub-name ver-level (NEW

This command is used to update a subprogram of the model. The command requires a subprogram name and version-level as arguments. Using permanent and any preexisting active local update files the command will update the specified subprogram up to the specified version-level and leave the user in edit mode. If the user makes changes and files them, these changes are kept in a local update file. If the option NEW was specified, a new local update file will be created to hold the changes that were just made. In this case the user will also be given an opportunity to document the new changes. If the NEW option is not chosen, any changes made will be appended to the last active local update file which the user created for the specified subprogram. Changes can be structured and documented by judiciously creating new local update files to correspond to meaningful stages in the model development effort.

GMSFAUX sub-name ver-level PAUSE update-no

For each subprogram which is changed via GMSFUE, the update facility creates a single index file (called the AUX file) which contains pointers to the local update files for that subprogram. The local update files as well as the AUX file have the same CMS file name as the subprogram to which they apply. The CMS file type of the local update files contains two numbers, the version-level and an update number. The GMSFAUX command is used to remove (PAUSE), or to restore (RESTORE) the changes in previously created local update files to the set of changes which are considered active. The active changes are those contained in local update files which are pointed to by entries in the AUX file.

GMSFMSTR sub-name ver-level (RSLV resolve-name

This command is used to create a copy of a specified subprogram using all the active local updates in the user's virtual machine. If the option RSLV resolve-name is specified, all common decks scheduled for inclusion in the subprogram will be included and their variable dimensions will be resolved according to the parameter values given in the specified RESOLVE file. Common decks consist of source card sequences which should be inserted in more than one subprogram (such as FORTRAN common block definitions). The user specifies that a particular common deck is to be included in the subprogram by inserting a card image which begins in column 1 with the characters .INCL, followed by the common deck name. Common decks in turn, can contain symbolic parameters for which numerical values are only inserted when the common deck is included in a subprogram. This process of replacing the parameters by their numerical values is called "resolving" the common deck. The numerical values to use when resolving common decks are contained in a file (the RESOLVE file). The option RSLV resolve-name specifies that common decks should be resolved with the specified RESOLVE (resolve-name) file and included in the source code being created. If the RSLV resolve-name option is not specified, no common deck resolution will be done, i.e. the source code produced will have the common decks included but they will not have numerical values substituted for the symbolic parameters.

In addition to the update facility commands, there is a CMS exec called GCMCONC on the F400M 191 disk which can be useful. It serves essentially the same function as GMSFMSTR (which it uses) but instead of specifying only one subprogram name, the user provides it with a list of subprograms which are to be updated to a given version-level. The combined source code of all the subprograms on the list is placed in a single output file. The list, which the user

must create before executing this command, should be placed in a CMS file in the user's virtual machine having file name GCMskk or GCMVkk, where kk is the version-level number (expanded to two digits if needed), and file type EXEC. A typical entry (line) in the list looks like:

&1 &2 VCOMPl FORTRAN F

The command structure is:

GCMCONC machine-id ver-level resolve-name fn ft fm

where

machine-id is GWSGCMS or GWSGCMV

ver-level is the version-level to be used for updating

resolve-name is the name of the RESOLVE file to be used in resolving common decks

fn ft fm is the output file specification

IX.5 Files and Tapes Used by the Model

Every data file or tape produced by a forecast experiment is cataloged using a fixed naming convention. Every forecast experiment is identified by a unique four character experiment ID, which becomes a part of the catalog name of the data sets for the experiment. Four digit numbers are reserved for production forecast experiments and should not be used by the general user without prior permission. In the following the experiment ID will be denoted by nnnn.

F400.EnnnnHkk

This is the naming convention for the history tapes (V8SIGM format). The sequence numbers kk start at 01 for the first tape produced and are incremented by one for each additional tape. A complete documentation of the format for these tapes is to be found in Section 3 of Chapter VIII.

F400.EnnnnHTR

This is the name of a history tape (V8SIGM format) which is only of interest while the forecast experiment is being run. It contains the same information as the most advanced history tape in the normal history tape sequence. It is used to provide a level of security during history tape generation and to facilitate the merging of newly produced history segments with the results on existing history tapes in the normal sequence.

F400.EnnnnNL.DATA

This is an OS data set (RECFM = FB, LRECL = 80, BLKSIZE = 3120) containing the card images of the namelist parameters for the experimental forecast. Each experiment must have a namelist data set. There is a CMS exec to aid the user in its creation which is explained in Section 8 of this user's guide.

F400.EnnnnRS.DATA

This is the basic restart data set required by the model (V8RSTR format). The user must create one of these data sets containing the initial conditions for the experiment before the experiment can be started. There is also a CMS exec to aid the user in creating this initial condition data set (see Section 8). The model automatically creates the restart data sets that it will need to complete the experiment as the forecast advances. A complete description of the format for these data sets can also be found in VIII.3.

F400.EnnnnRSC.DATA

The model will rename the initial condition data set which the user created under this name when it is no longer needed by the model.

F400.EnnnnHT.DATA

F400.EnnnnHTS.DATA

F400.EnnnnRSR.DATA

These are temporary data sets which are produced, and later deleted or renamed, by the model. The HT data set is used to initialize the source code segment of the first model history tape. The HTS data set contains the history data produced by one forecast run. It is deleted as soon as the data has been successfully merged into the history tape sequence. The RSR data set is produced at the end of a forecast run to define the restart data set for the next forecast run. It is renamed as an RS data set (for the next forecast segment) after the successful completion of a forecast run. The possibility exists of having the HTS and RSR data sets placed on the MASSTOR device. This can be particularly useful when running forecast experiments which generate large amounts of history output.

F400.GCMCATLG.DATA

This is a catalog of GCM history tapes from all forecast experiments. It is updated by the production procedures every time a new history tape is created or an existing history tape is extended for any experiment.

F400.EnnnnCAT.DATA

This is a temporary data set which is created every time experiment nnnn is revising the GCM catalog.

F400.EnnnnRS1.DATA

F400.EnnnnRS2.DATA

F400.EnnnnRSX.DATA

F400.EnnnnRSY.DATA

F400.EnnnnHTX.DATA

F400.EnnnnHTQ.DATA

These data sets are created by the model only when some unrecoverable error has occurred during model execution. If these data sets appear during execution of the experiment, the user should contact someone familiar with the production procedures and seek help to recover/restart the experiment.

There are a number of CMS execs located on the F400M 191 disk which may be of help in manipulating the model's OS data sets and history tapes.

GCMLISTC nnnn

This exec will search the OS catalog and type at the terminal all entries which begin with the characters F400.Ennnn. If the user creates data sets other than those listed above for the forecast experiment, they should be cataloged using names which begin with these characters. In additon GCMLISTC will search the GCM catalog and type all entries which pertain to experiment nnnn.

V7DELETE node1 node2 node3 node4 etc.

This exec will delete (scratch and uncatalog) the given data set by sending a short job to MVS. If the given data set is not in the OS catalog, the user will still be permitted to send an MVS job to scratch it.

V7RENAME / nodes for old file name / nodes for new file name /

This exec will send an MVS job to rename an OS data set if it finds the specified old file name in the OS catalog.

V7COPBIN / nodes for input file name / nodes for output file name /

This exec will send an MVS job to copy an OS data set. All file characteristics of the output data set will be the same as those of the input data set.

GCMNLSET CATL

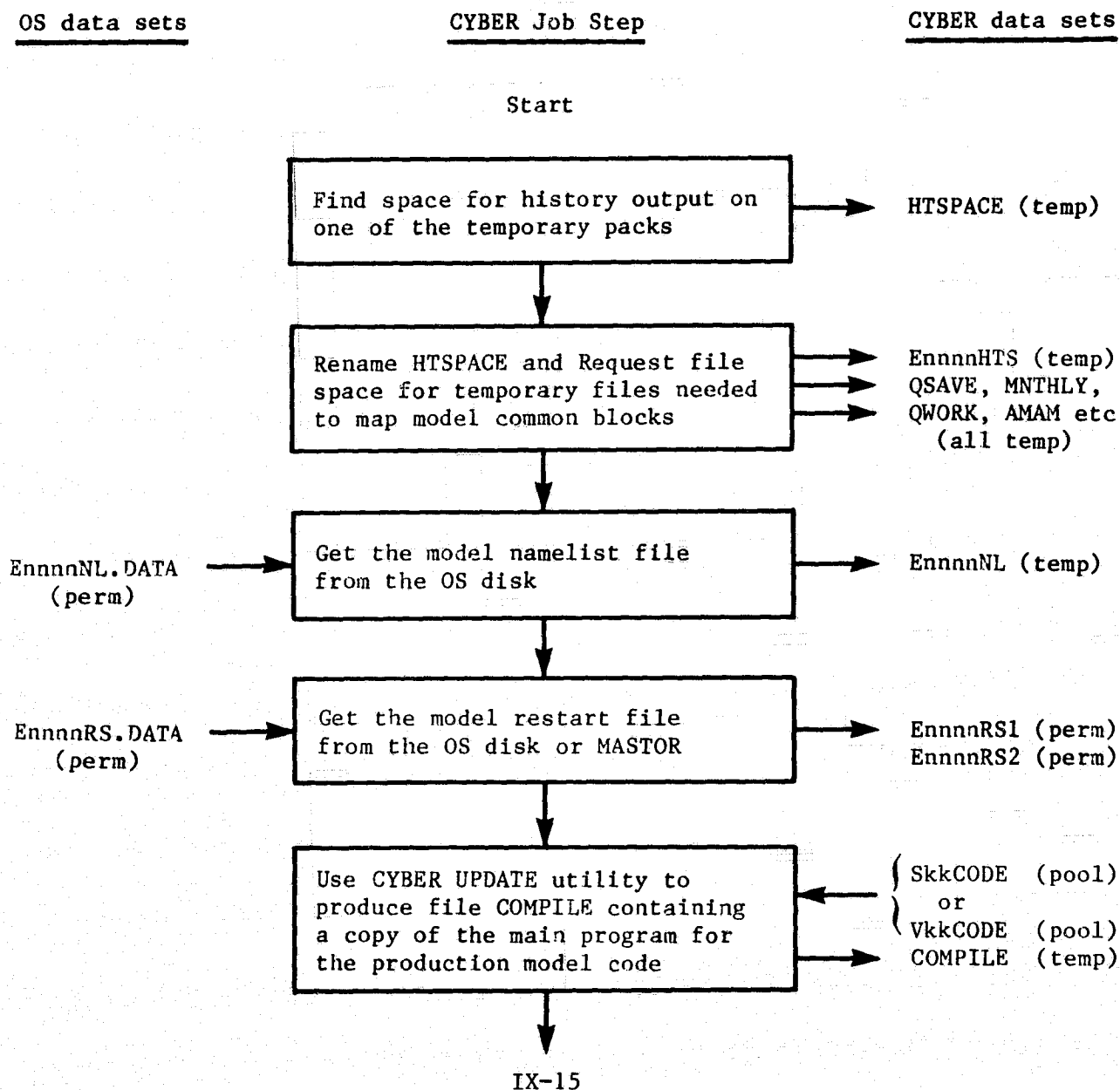
This exec allows the user to edit the GCMCATLG data set. Normally there should be no need to do this, but situations do arise when entries must be deleted from the GCM catalog. The most common case being when it is desired to restart experiment nnnn from the beginning after history tapes have already been produced for the same experiment number nnnn.

OSUNCAT node1 node2 node3 etc.

This exec is part of the system library and can be used to remove entries in the OS catalog for history tapes which are no longer needed.

IX.6 Production Run Procedures

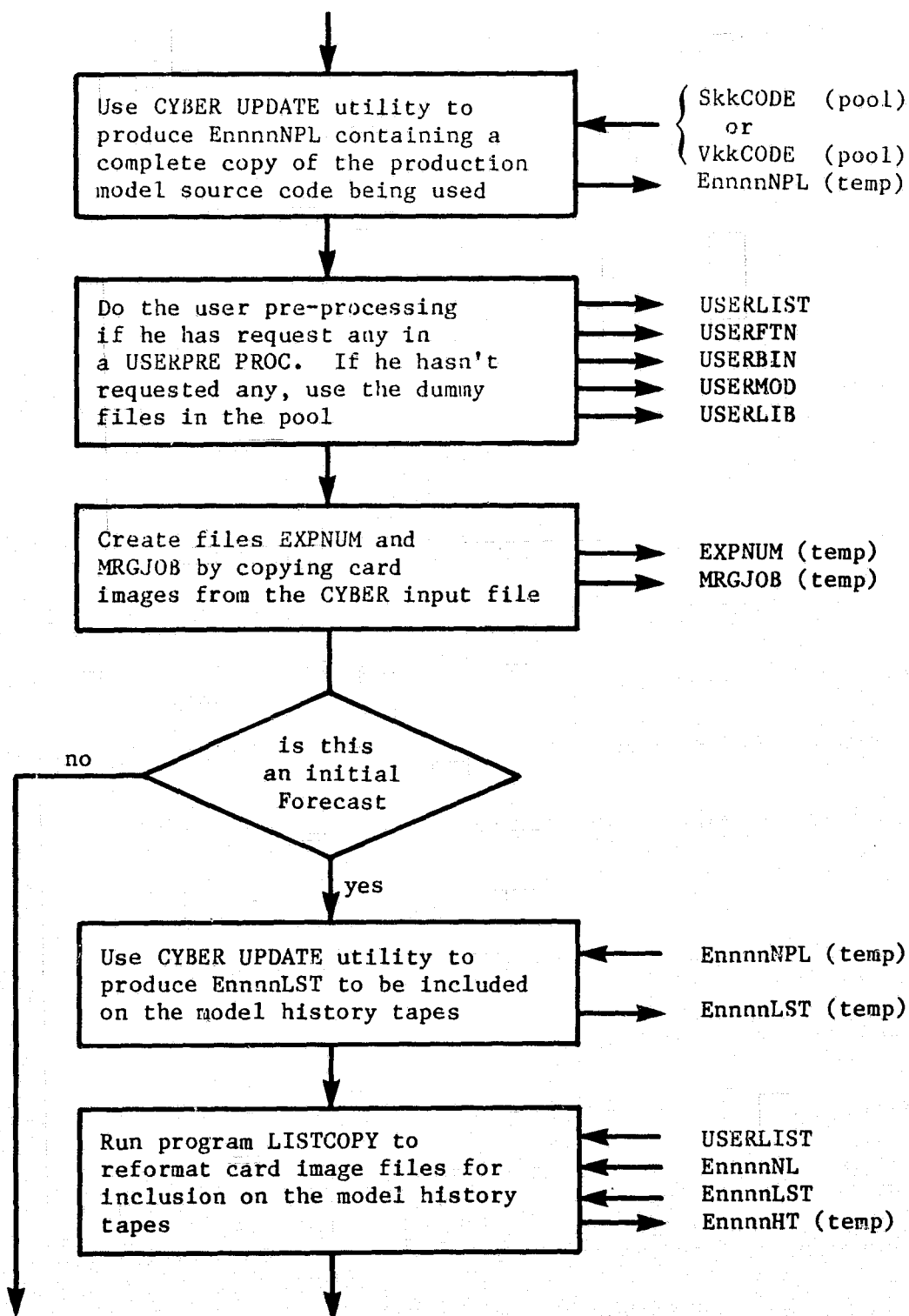
The production run procedures are of course dependent on the machine used to run the model. It is recommended that all forecast experiments be carried out on the CYBER 205 using either the scalar or vector version of the model code. It is the run procedures for the CYBER which are described here. The run procedure for the Amdahl V/6 (under CMS and Amdahl V/7 under MVS) follow the same general outlines but there are significant differences in detail. The run procedures are kept on the CYBER in pool CYGWSGCM. The skeleton procedure is in the file named DRIVER in that pool.



OS data sets

CYBER Job Step

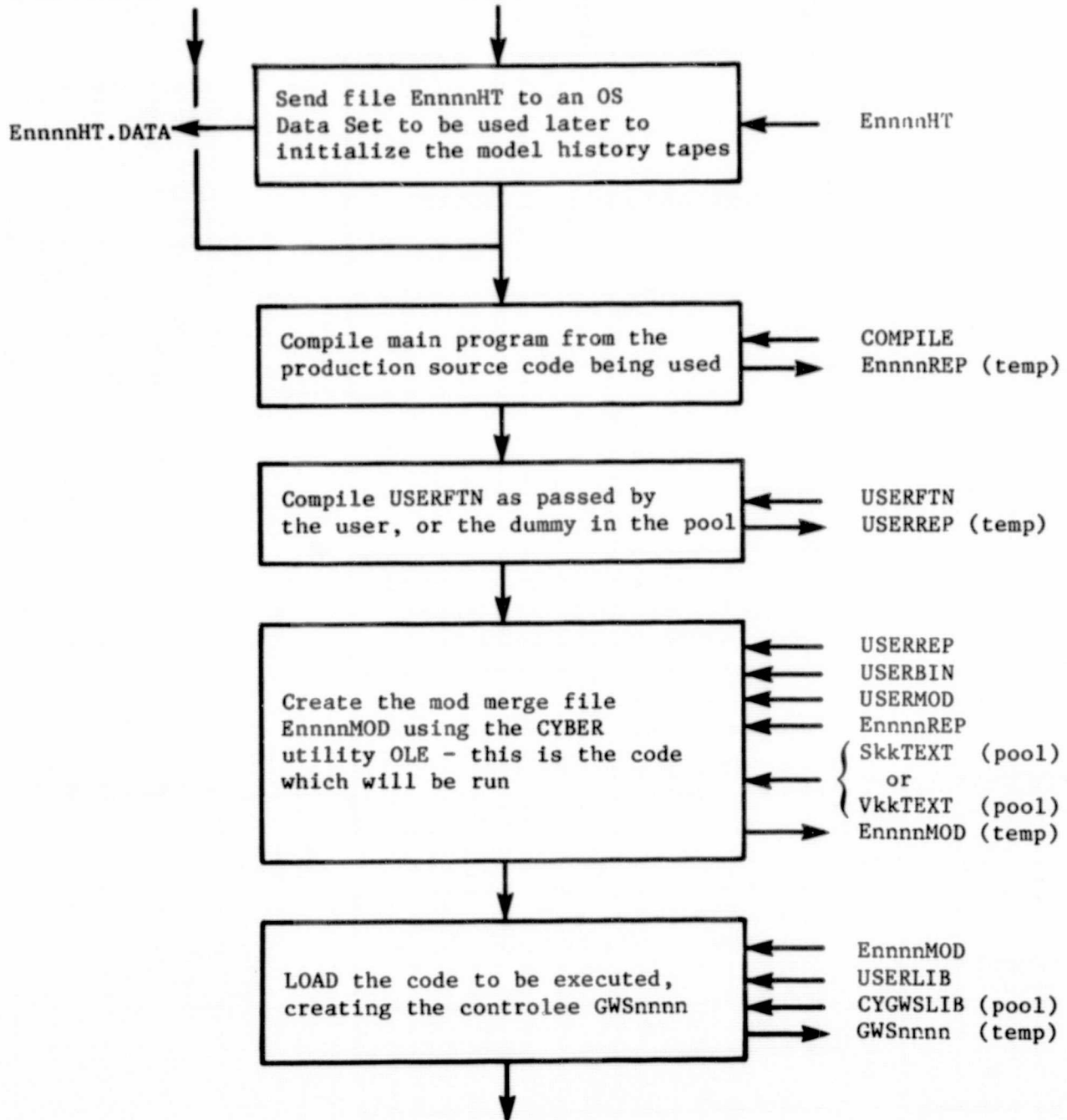
CYBER data sets



OS data sets

CYBER Job Step

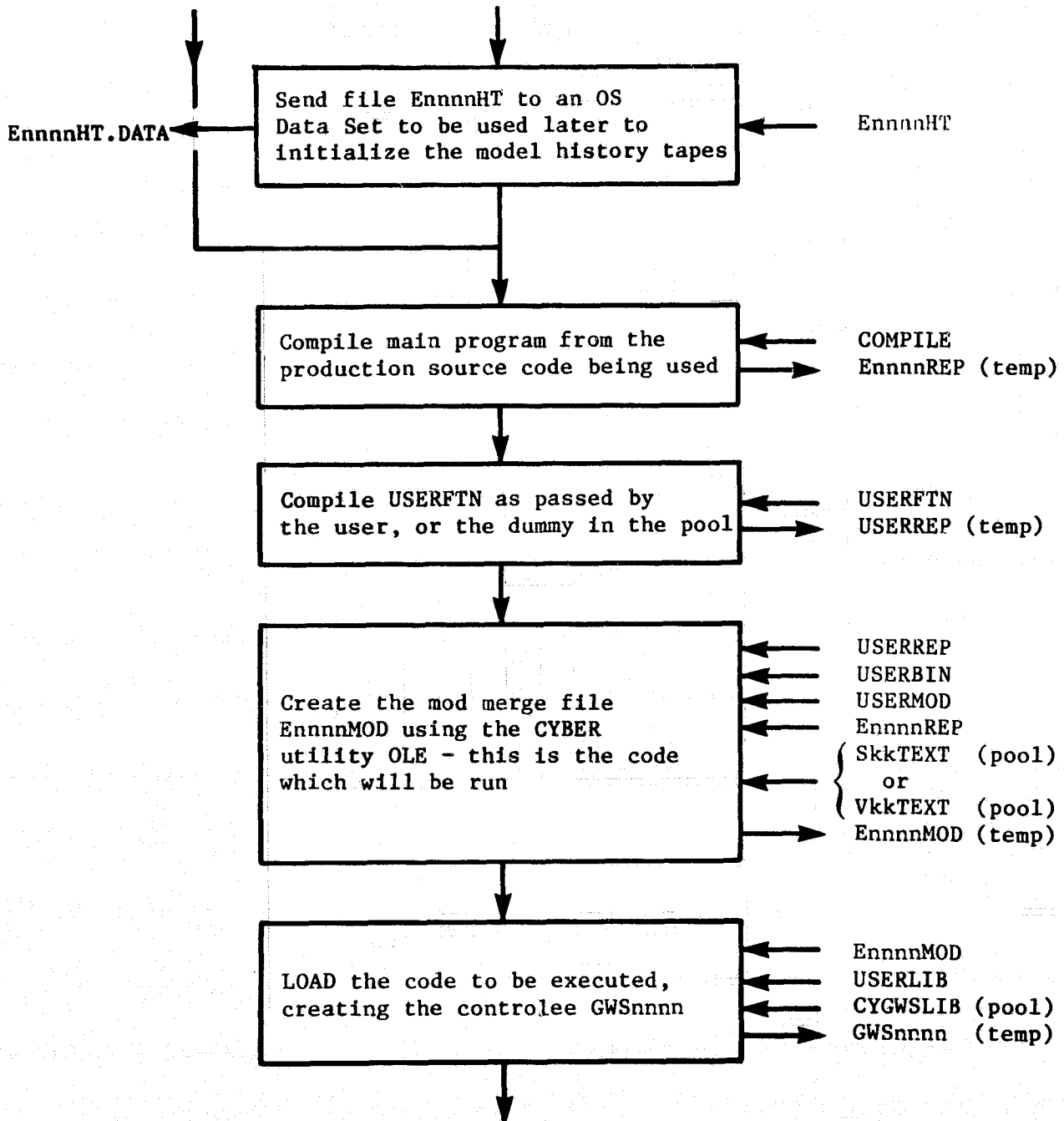
CYBER data sets



OS data sets

CYBER Job Step

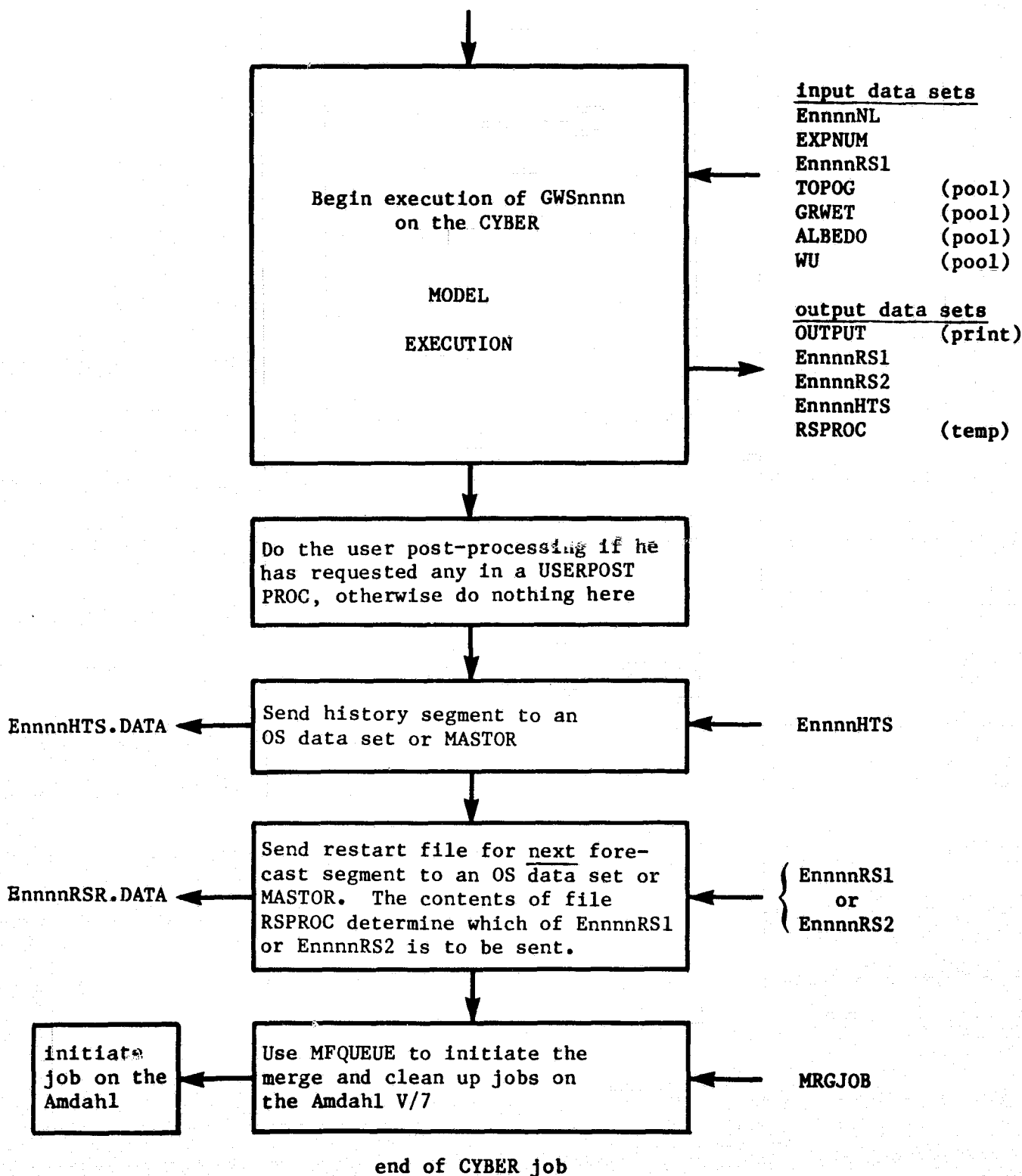
CYBER data sets



OS data sets

CYBER Job Step

CYBER data sets



Control is now passed to the Amdahl V/7 which runs the so-called "merge job". The main function of this job is to merge the history tape segment which was just created on the CYBER and placed in the OS data set F400.EnnnnHTS.DATA with the history data on the last (not fully written) history tape in the history tape sequence. The merge job also updates the GCM catalog to reflect the true contents of any history tape which is written and cleans up the OS data set environment in preparation for running the next forecast segment. The merging of the history data and updating of the GCM catalog are done by a FORTRAN program. The source code for this program resides in the OS data set F400.MRGJOB.SOURCE (on MVS006). This program is used to either initialize a new history tape sequence or to extend an existing sequence.

When a new history sequence is to be initialized the following data set assignments are made:

Unit 8	F400.EnnnnHT.DATA	(source code just sent from CYBER)
Unit 9	F400.EnnnnHTS.DATA	(history segment just sent from CYBER)
Unit 10	F400.EnnnnH01	(first history tape - new)
Unit 11	dummy	
Unit 12	F400.EnnnnHTR	(partial history tape backup - new)
Unit 20	F400.GCMCATLG.DATA	(existing GCM catalog - disp = old)
Unit 21	F400.EnnnnCAT.DATA	(updated catalog - new)
Unit 61	Print output	

If an existing history tape sequence is to be extended, the following changes are made to the above assignments:

Unit 8	F400.EnnnnHTR	(partial history tape backup)
Unit 10	F400.EnnnnHjj	(most advanced history tape in the sequence which contains data for experiment nnnn)
Unit 11	F400.EnnnnHkk	(next history tape in the sequence - it will be mounted and used only if the tape on unit 10 fills; $kk = jj + 1$)
Unit 12	dummy	

The user must keep the variable meanings of the unit numbers in mind when trying to understand the operation of the history merge program.

A word of caution: The tape assignments for units 10 and 11 are placed in the job control language for the merge job when the forecast segment is submitted for execution. Hence, the user should not submit a new forecast segment for an experiment until the merge job from the current forecast segment for the same experiment has successfully ran.

There is a second job step in the merge job which is only executed if the tape merge has been completed without error. Its purpose is to clean up the OS data sets from the forecast segment just completed in preparation for the next forecast segment. The following is done in this step:

- (a) If the forecast segment was the initial one

F400.EnnnnHT.DATA is deleted

F400.EnnnnRS.DATA is renamed F400.EnnnnRS0.DATA

- (b) If the forecast segment was not the initial one

F400.EnnnnRS.DATA is deleted

- (c) In all cases

F400.EnnnnHTS.DATA is deleted

F400.GCMCATLG.DATA is deleted

F400.EnnnnCAT.DATA is renamed F400.GCMCATLG.DATA

F400.EnnnnRSR.DATA is renamed F400.EnnnnRS.DATA

IX.7 Altering the Production Procedures

The CYBER production run procedure outlined in the previous section contains features which allow for user modification of the model to be run and for alterations of the run procedure itself. In order to use these features, the user must define certain permanent files in the user's own CYBER account prior to running the model. The production run procedure recognizes the following file names as possibly coming from the user's CYBER account. For those files that the user does not want to define, there are dummy files of the same name in the CYBER pool CYGWSGCM which will be used by default.

USERLIST If the user places card images in a file with the name USERLIST, these card images will be placed at the beginning of the source code segment of every history tape produced during the forecast experiment.

USERFTN If the user places FORTRAN subprogram source modules in a file called USERFTN, these subprograms will be compiled (with optimization and listing) and the resulting binaries will be used at execution time.

USERBIN If the user has a file called USERBIN, which contains compiled versions of subprograms, then any modules which appear in USERBIN, but not in USERFTN will be used at execution time.

USERMOD If the user has a file called USERMOD, which was created by the CYBER utility OLE, then any subprogram modules which appear in USERMOD but do not appear in USERFTN or USERBIN will be used at execution time.

USERLIB If the user has a file called USERLIB, which was created by the CYBER utility OLE, then any subprogram module(s) in USERLIB having the same name as subprogram(s) in the production library (CYGWSLIB) will be used at execution time. That is, USERLIB appears before CYGWSLIB in the library search order.

USERPRE and USERPOST User defined files having these names can cause alterations to be made to the run procedures themselves. The production run procedure executes a CYBER PROC called USERPRE immediately after it transfers the restart data set to the CYBER, and a CYBER PROC called USERPOST immediately after the model execution step. See the CDC VSOS Version 2 reference manual for a description of CYBER PROC statements. The user is allowed to place any CYBER job control language in these files to be executed at the specified place in the production run procedure. If a USERPRE file is defined by the user, its first line must contain PROC(USERPRE,NNNN,BEGRES). Likewise, if a USERPOST file is defined by the user, its first line must be PROC(USERPOST,NNNN,BEGRES). NNNN will be passed to the user's PROC set to the four character experiment identifier and the argument BEGRES will be passed as either 'BEG' or 'RES'.

Once the user understands the use of CYBER PROCs, practically any part of the production run procedure can easily be changed. All that is needed is to redefine (in the CYBER account) that part of the production run procedure which is to be changed by placing the user's altered control language in a PROC having the same name as the one used in the production procedure.

IX.8 Namelist and Initial Condition Data Sets

Before model execution can be started, two OS data sets must be created: F400.EnnnnNL.DATA containing input values for the two model namelists (INPUTZ and INPHYS) and F400.EnnnnRS.DATA containing a set of initial conditions for the forecast experiment (in V8RSTR format). By linking the user's virtual machine to F400M 191, access is gained to two CMS execs which can be used to create the needed files.

GCMNLSET This exec is used to create the namelist file for the experiment. The user is given three choices (prompted by the exec). The user can either (a) type in the complete namelist at a terminal or (b) obtain a skeleton namelist to edit, where all of the parameters in the skeleton are set to the production model default values or (c) specify the four character identifier from some previous experiment and obtain the namelist from that experiment as a skeleton. After editing is completed and the namelist is fully defined, the user files it and GCMNLSET will include it in an MVS job which can then be submitted (by prompting) to create and catalog F400.EnnnnNL.DATA for the experiment. GCMNLSET can also be used to edit existing namelist files. Appendix A contains a list of the namelist parameters in INPUTZ and INPHYS, gives their default values and a brief description of each variable's function.

GCMICSET This exec is used to prepare the initial restart data set (F400.EnnnnRS.DATA) for the experiment. These data sets are V8RSTR format data sets and come in three types.

IBM -- Suitable for running experiments on the Amdahl V/6 or Amdahl V/7
CDC -- Suitable for running on the CYBER using full precision arithmetic
HCDC -- Suitable for running on the CYBER using half precision arithmetic.

The exec has two modes of operation, copy/extract and conversion. In those cases where the input data set resides on tape and a conversion of data set types is required, the user will have to create the initial conditions in two steps. First, extract the input data set from tape and second, do the type conversion. Input data can come from (a) an OS data set in V8RSTR format, (b) a tape data set in V8RSTR format or (c) a tape data set in V8SIGM format. In case (c) the V8RSTR data set to use for input is extracted from those saved on history tape. Table IX.8a contains a complete list of all the possible actions of the CMS exec GCMICSET. The user will be prompted to specify the output data set type and the input data set type and storage medium. The exec will determine the best course of action to accomplish the required task.

Table IX.8a Possible Actions of the CMS Exec GCMICSET

Case (a) Input from V8RSTR format OS data set

IBM to IBM	by renaming the input data set	(MVS job)
IBM to IBM	by copying the input data set	(MVS job)
IBM to CDC	by conversion	(CYBER job)
IBM to HCDC	by conversion	(CYBER job)
CDC to IBM	by conversion	(CYBER job)
CDC to CDC	by renaming the input data set	(MVS job)
CDC to CDC	by copying the input data set	(MVS job)
CDC to HCDC	by conversion	(CYBER job)
HCDC to IBM	by conversion	(CYBER job)
HCDC to CDC	by conversion	(CYBER job)
HCDC to HCDC	by renaming the input data set	(MVS job)
HCDC to HCDC	by copying the input data set	(MVS job)

Case (b) Input from a V8RSTR format tape

IBM to IBM	by copying the input data set	(MVS job)
CDC to CDC	by copying the input data set	(MVS job)
HCDC to HCDC	by copying the input data set	(MVS job)

Case (c) Input from history tape V8SIGM format

IBM to IBM	by extraction of the desired data set	(MVS job)
CDC to CDC	by extraction of the desired data set	(MVS job)
HCDC to HCDC	by extraction of the desired data set	(MVS job)

Note: Cases (b) and (c) require that the data be first staged to disk. For this, GCMICSET will move the data from tape to a file called F400.EnnnnRS.TTT.DATA where TTT is the type (IBM, CDC or HCDC).

IX.9 Running the Experiment

After the user has modified the model production code to meet specific needs, set up the alterations to the production run procedures and created the namelist and initial condition files, the experiment is ready to start running. The CMS exec GCMSET is used to submit forecast segments for experiments. The user must link to F400M 191 to gain access to this exec. GCMSET will prompt the user to specify information it needs to build the appropriate job deck for submission. The items which the user will be asked to enter are:

- (a) The four character identifier, nnnn, of the experiment.
- (b) A specification of the production model code (machine, vector/scalar, version-level) which is to be used to define the model being run.
- (c) A computation start time in the form DDHHMM, if it is desired that computations for the forecast segment be delayed until a later time. This feature can be used to schedule longer runs to be done in off-peak hours.
- (d) A computation cutoff time in the form DDHHMM, if execution is to be interrupted at the specified time.
- (e) An indication of whether this is the initial segment of the forecast experiment or whether an existing experiment is being continued.

GCMSET not only initiates a forecast segment but it also causes the merge job for that segment to be executed after the forecast has been completed.

If the forecast experiment is running on the CYBER, GCMSET operates as follows:

1. It creates a file on the A-disk of the user's virtual machine with the file name nnnnCY and with file type DDHHMM where this is the desired computation start time. Enter DDHHMM = 000000 for immediate job submission. This file consists of three parts. The first part is an MVS job to submit the rest to the CYBER. The second part is the job control language for the CYBER job and the third

part, which is in the input stream for the CYBER job, is the MVS job control language for the merge job. The merge job will be submitted to MVS from the CYBER when the forecast segment has been completed.

2. If the user specified delayed job submission, a second file is created in the A-disk (nnnnCY EXEC A). This is a short CMS exec which submits (nnnnCY DDHHMM A) to MVS, erases (nnnnCY DDHHMM A) and logs the virtual machine off. The delayed job submission feature works by automatically logging on the virtual machine at the specified time and executing (nnnnCY EXEC A).

3. If immediate job submission was specified, the file (nnnnCY 000000 A) will be given to the F400 production machine and then erased. The job will be submitted to MVS (and hence to the CYBER) by GWS production personnel at the end of the day to run in the GWS block time.

GCMSET does a good amount of checking to ensure that the OS data set environment is correct when it is building the job deck for submission. If it displays warning messages, they are to be taken seriously and not ignored. They usually indicate that the merge job for the previous forecast segment either has not finished or has terminated abnormally. Some of the more commonly occurring "merge job" problems with suggested fix ups are listed below. The next section contains a more general list of error messages.

Problem 1 The merge job from the previous forecast segment terminated abnormally before writing to unit 8 or unit 12. This can be determined from the merge job output listing. The RSR, HTS and (if the previous forecast segment was the initial one) HT files should still exist on the OS disks. Use GCMLISTC nnnn to see which files exist for the forecast experiment.

Fix up Rerun the merge job for the previous forecast segment. This is done by executing GCMSET and specifying MRGJOB when the user is prompted to enter the computation start-up time. The responses given to GCMSET questions should be the same as those that were given when the forecast segment was submitted.

Problem 2 The merge job from the previous forecast segment terminated abnormally after it had begun writing to unit 8 or unit 12.

Fix up The merge job is essentially done. The user must clean things up manually.

- (a) Use the CMS exec V7COPTAP to copy the history tape that the merge job was reading when it failed to the HTR tape for the experiment.
- (b) Use the CMS exec GCMNLSET CATL to update the GCM catalog to reflect the true contents of the history tape sequence.
- (c) Use V7DELETE to get rid of the HTS and RS files from the previous forecast segment.
- (d) Use V7RENAME to rename the RSR file as an RS file.

Problem 3 The user discovers an error in the model and would like to start the experiment over again using the same experiment identifier.

Fix up

- (a) Delete all OS files except the NL and RSO files.
- (b) Use V7RENAME to rename the RSO file as an RS file.
- (c) Use GCMNLSET CATL to remove all references to experiment nnnn from the GCM catalog.
- (d) Use OSUNCAT to remove OS catalog entries for any history tapes which were written.

Problem 4 The user has files RS1, RS2 and HTQ for the experiment, or files RSX, RSY and HTX.

Fix up These files are only created if the model terminated abnormally on the CYBER. The appearance of the RSX, RSY and HTX files usually indicates that there are still errors in the model. The appearance of the RS1, RS2 and HTQ files indicates that the production run procedure has had difficulty transferring output files to the AMDAHL V/7.

But, if the user is certain that they contain useful results that are to be saved, the following actions are required:

(a) Rename (RS1 or RSX) or (RS2 or RSY) whichever is the least furthest advanced, as RSR.

Delete the remaining file.

(b) Rename (HTQ or HTX) as HTS.

(c) Run the merge job for the forecast segment which failed. (See Problem 1)

Problem 5 The GCM catalog has disappeared. A first indication of this is that the CMS exec GCMLISTC does not work properly.

Fix up Try GCMLISTC again in 10 minutes or so. It may be that there is a merge job just finishing up from someone else's experiment. Each merge job deletes the GCM catalog and creates a new one. The user may have tried to access it just at the moment when it was not there.

IX.10 Error Messages

Certain error conditions seem to occur with a frequency that indicates that a list, such as the one contained in this section, could prove useful. The errors come from two main sources. First, some parts of the hardware and system software are rather new and lack the stability and robustness that one usually expects. Second, the LOAD program in the CYBER is rather complicated and not completely documented. Its use requires a deeper understanding of the load process than might be required on other computers.

Refer to the previous section for a list of some commonly occurring problems with the "merge job".

MFLINK Problems

MFLINK is a CYBER utility used to transfer files to or from the CYBER. Some of the error messages which frequently occur, what they mean and how to avoid them are included here.

- a) BAD NAD RESPONSE - This rather cryptic message usually means that a file which has started to move to a 3350 disk pack requires extents for which there is no room on the volume. It indicates that the primary/secondary space allotment for the file should be revised or that the volume is full or fragmented. Delete some files from the volume or place the file on another volume or MASSTOR.
- b) PATH STATE BAD - TRANSFER ABORTED - The connection to the IBM side is not working. Try again.
- c) SPACE NOT AVAILABLE, TRANSFER ABORTED - There was not enough room on the specified 3350 volume for the primary space allotment for the file. Delete some files from the volume or put the file on MASSTOR.

d) ATC WAS ENTERED, TRANSFER ABORTED - This seems to be similar to the BAD NAD RESPONSE error, but at times the CYBER continues on as if nothing has happened i.e. no error return code gets passed to the CYBER job. See a) above for possible fix ups.

e) FAILED TO CONNECT IN TIME, TRANSFER ABORTED - This means that the IBM side is not responding. It will happen repeatedly until the operations staff notice the problem and reestablish the connection. Try again.

Problems with LOAD

a) DROP FILE MAP OVERFLOW - As a program is loaded for execution, the loader places pointers to pages in the controlee drop file in a list (the drop file map) which is located in the minus page of the controlee. This drop file map has a fixed upper bound on its length which is often exceeded. The problem can be circumvented by mapping code and/or data onto large pages. This requires the use of the grouping parameters on the call to LOAD and/or the use of explicit mapping via the Q5MAPIN system subroutine. Changing the order in which subprograms are loaded can also help in some situations.

b) VIRTUAL ADDRESS OVERLAP IN COMMON BLOCK XXXX - This occurs when the user has used Q5MAPIN to map common blocks to large pages, but has not correctly computed the group length or has specified the wrong variable name on the 'VBA =' parameter of Q5MAPIN. The length of the external file used for Q5MAPIN must be the smallest multiple of 128 small pages which will contain the group of common blocks. This length must agree with that specified in the Q5MAPIN call, and the 'VBA =' parameter must be set to the first variable of the first common block within the group which appears in the main program.

Other Problems on the CYBER

a) NO SPACE AVAILABLE - When requesting files, either explicitly using REQUEST or DEFINE or implicitly by executing control statements which create temporary files, it can happen that the volume chosen by the system has insufficient room. In most cases this problem can be avoided by placing the file on one of the temporary disk packs TPAK24 or TPAK25. However, the user is not permitted the use of these packs for permanent file storage. Large permanent data sets should be kept on the front end and brought up to the CYBER using MFLINK at execution time.

b) ILLEGAL INSTRUCTION - INDEFINITES - Although these problems usually indicate program errors on the user's part, there are times when hardware problems on the CYBER have caused operational code to abort with illegal instructions or indefinites. If no errors can be found in the user code, it may be wise to ask other users if they have been having similar problems. Try running again at a later time.

IX.11 Looking at the Results

A large collection of programs exists for use in evaluating and comparing the standard model output products (V8SIGM and V8MAND history tapes). The complete set of post-processing programs is described in a separate document. Among other things, programs exist for:

Format conversions	V8SIGM ---> V8MAND
	V8SIGM ---> V8RSTR
	V8RSTR ---> V8MAND
Plotting from V8MAND	All model prognostic and diagnostic quantities
Output statistics	Allow comparisons to be made between model forecasts and analysis from various sources.

Note that the main input format for these post-processing programs is the V8MAND format described in Section 3 of Chapter VIII. Users wishing to use the existing diagnostic software should create V8MAND tapes.

The model development group has a diagnostic program (called DIFFY) which is used to examine and compare V8RSTR format data sets on the CYBER. Access to this program is through the CMS exec, GCMRSDIF, which resides on F400M 191. By linking to F400M and typing GCMRSDIF the user will be prompted to enter all the information needed to build the namelist for program DIFFY. GCMRSDIF then submits the work to the CYBER. The DIFFY program operates in one of two modes. It either examines a particular V8RSTR data set, or compares (takes differences) two such data sets. The user can specify the fields and the model sigma levels which are to be examined. Three forms of printed output can be chosen.

Entire fields printed at every grid point.

Differences of fields printed at every grid point.

Printer plots of fields or field differences.

This tool has proven invaluable to the model development group. Before modifications are made to the model, a set of initial conditions and the forecast results from a short forecast (from a few timesteps and up to 3 simulated hours) are saved in V8RSTR data sets. The changes to the model are then made and the resulting forecast differences compared in detail with the help of DIFFY.

CHAPTER X

CODE MANAGEMENT PROCEDURES

JAMES W. PFAENDTNER

X.1 CODE MANAGEMENT PROCEDURES

X.1 Introduction

This chapter describes the procedures that have been implemented to maintain and develop the production source code and run procedures for the scalar and vector versions of the GCM. In addition, a number of CMS execs, utility programs and libraries are described.

Any revisions to the model masters, model permanent updates, utility programs, library subroutines, CYBER production procedures or CMS production execs must be completely documented. The possibility always exists that any given GMSB forecast experiment will have to be repeated or extended at a later date. Every change in model forecast results should be attributable to some cause. If major changes to an existing subprogram or procedure are to be made, a pre-revision copy should always be saved in a secure place and its location documented.

X.2 The Model Group Library Machine F400M

The group machine is a CMS virtual machine designed to hold all codes necessary to run and develop the fourth order model. It consists of a number of separate mini-disks. The organization of the machine can be viewed by executing the CMS exec F400MORG located in F400M 191. The 191 disk contains all model production execs. By linking to F400M 191 the general user obtains all that is needed to run fourth order model experiments. The 192 disk contains the model group's library of CMS utility execs. The 193 disk contains compiled versions of programs and TEXTLIB files for execution under CMS on the Amdahl V/6. The 204 disk contains the permanent updates for the scalar versions of the model as well as the compiled versions of the model for execution under CMS on the Amdahl V/6. The 205 disk has the masters for the scalar model. The 206 and 207 disks have the permanent updates and masters for the vectorized model version.

The 191, 192, and 193 disks contain index files (file name \$\$\$INDEX) which should be maintained to accurately describe the disk's contents. In general, all changes to a program, procedure or EXEC should be documented internally in the program or EXEC. All codes having a direct influence on the production procedures should be saved in their current condition before any changes are made. There is a CMS exec called VECSAVE located on F400M 191 which can be used to archive obsolete versions of programs and EXECs in the OS partitioned data set F400M.VECSAVE. The index partition in this data set should be updated to indicate the date on which each particular program or EXEC was taken out of service. VECSAVE is also used to archive changes to the vector version of the model. There is a SCASAVE exec for use in the archiving changes to the scalar version of the model.

The major steps involved in defining a new production version of the scalar or vector model are the same and are outlined in the next section.

X.3 Management of the Production Code

The steps involved in implementing a new or revised version-level of the model are described in this section. Adherence to these procedures will tend to minimize (but not eliminate) the disruption to other users of the fourth order model caused by the changes.

(Step 1) The local updates defining the revised model version should be gathered together on one particular CMS virtual machine.

(Step 2) The source code and compiled version of the model version being revised should be copied from the pool CYGWSGCM to the private CYBER account of the user making the revision.

(Step 3) Using the CMS exec GCMCONC, the user should revise the source and compiled versions in his private CYBER account to incorporate the changes.

(Step 4) All other persons doing model development work should be consulted to ensure that the future inclusion of the user's changes as permanent updates or new masters in the F400M library machine will not invalidate local updates made by the other users. These conflicts cannot be entirely avoided and must be resolved to everyone's satisfaction before changes are made to the library machine.

(Step 5) The revised model must be tested in a professional manner. That means that model output products from forecasts done with the revised model must be examined in detail to see that (a) there are no unintended negative consequences of the changes and (b) that the forecast changes that are actually observed are those which were intended.

(Step 6) Place the revised model in production. This is done by moving the source and compiled versions from the user's CYBER account into the pool CYGWSGCM, and adding the new model version to the list of possible model production versions recognized by the CMS exec GCMSET.

(Step 7) Inform the analysis and post-processing/diagnostics groups of the changes so that they can make any needed revisions to accommodate the new version.

(Step 8) Move the local updates to the library machine F400M. This is done by logging on to the library machine, linking to the machine containing the local updates and using the CMS exec GMSFAVER to copy the local updates to the mini-disk of F400M containing the permanent updates. GMSFAVER also revises the AUX file for the permanent updates to include the specified local update. If a subroutine will be deleted from the model as a result of the changes, it should be archived (via VECSAVE or SCASAVE) before being erased from the library machine. If a new master is to be created for any subroutine or common deck, the old master as well as the updates needed to create the new master should be archived before deleting the old master and updates. The new master should be serialized using SERIAL ALL 10 10.

(Step 9) Help other users of the model resolve conflicts caused by the new masters or permanent updates created in Step 8. The production staff should be informed of the phase-in plan for the new model version. Experiments which have been started with a particular model version should normally be carried to completion with that version. New model versions should be used to start new experiments.

(Step 10) Delete the local updates from the user's virtual machine. They will no longer produce valid code.

X.4 Utility Programs for the Production Run Procedures.

There are a number of stand-alone programs which are used by the production procedures to do data processing. A short description and the location of the code will be given here.

LISTCOPY

This program is in CYBINLIB. It is used to read formatted character information (source code) and write it unformatted and blocked to another file. This is the program which runs on the CYBER to prepare the model source code for inclusion in the source code segment of the model V8SIGM history tapes.

GCMCOPY

This FORTRAN program resides on F400M 191 and runs on the Amdahl machines. It can be used to do one of three things: (a) it can copy a specified V8RSTR data set with specific designations for date and time and for pre or post-analysis records (LOG8R) from one data set to another, (b) it can extract a specified V8RSTR data set from a V8SIGM data set or, (c) it can be used to extract the source code segment from a V8SIGM data set. The output will be formatted. It reads and unblocks the source code segment written by program LISTCOPY. This program is used by the CMS exec GCMICSET.

HISTMRG

This program runs on the Amdahl machines and does two things. It (a) merges history segments generated on the CYBER into the history tape sequence and (b) updates the catalog F400.GCMCATLG. The source code resides on the OS data set F400.MRGJOB.SOURCE.

RSITOC, RSCTOI, RSCTOH, RSHTOC, RSITOH, RSHTOI

These are stand-alone programs which run on the CYBER. They are contained

in CYBINLIB and are loaded and executed by CYBER procedures in CYPROCLB. They are used by GCMICSET to convert from one type V8RSTR data set to another.

MSGSEND

This program, which is in CYBINLIB and its associated CYBER procedure SENDMSG, is used to send messages from CYBER JCL to the operator's console (K-display).

RDCLI

This is a subroutine contained in CYGWSLIB which can be used to transfer V8SURF data sets (described in VIII.2) to the CYBER to be read from inside a FORTRAN program.

X.5 The Libraries CYPROCLB, CYGWSLIB and CYBINLIB

The Global Weather Studies (GWS) group maintains a set of libraries for use on the CYBER 205. Since additions to the libraries are made frequently, no attempt will be made here to catalog their contents. A separate index for each library is maintained.

CYPROCLB

This is a library of CYBER procedures. Refer to the CDC VSOS - Version 2 reference manual for a description of the use of the CYBER PROC and BEGIN control statements. The procedures in this library are contained in the CYBER pool CYGWSGCM. Each procedure is contained in a separate pool file having the same name as the procedure. Thus, to execute the procedure in FILEA for example, the user must PATTACH (CYGWSGCM) and include the control statement BEGIN(,FILEA,arg1,arg2,etc.) in the CYBER job control language.

A list of the procedures in the library, together with a brief description of each, can be viewed by executing the CMS exec CYPROCLB located on the F400M 191 disk. The CMS exec (CYPROCLB EXEC) allows the general user to place a copy of any desired procedure in the user's own virtual machine. This exec also permits the pool boss for CYGWSGCM to edit the library contents. For security reasons, and to have the library contents accessible from CMS, the library is also maintained in a parallel fashion on the OS partitioned data set F400.CYPROCLB. Using the CMS exec CYPROCLB mentioned above, the pool boss can add or delete members from the library and can also edit existing procedures in the library replacing the old copies with new ones.

CYGWSLIB

This is a library of FORTRAN subprograms for use on the CYBER 205. On the CYBER, the library is maintained in a source code version and a compiled version. The compiled version is in the file CYGWSLIB in the pool CYGWSGCM. To use subprograms from the library, the user must PATTACH (CYGWSGCM) and include the LIB = CYGWSLIB key words on the CYBER LOAD control statement. Refer to the VSOS - Version 2 reference manual for details concerning the use of program libraries with the LOAD control statement. The source code version of the library is in the file CYGWSLBS in the CYGWSGCM pool. This is a so-called UPDATE program library file, which is organized much like an OS partitioned data set. Details of the CYBER utility UPDATE can also be found in the VSOS - Version 2 reference manual. The UPDATE utility must be used to obtain source code suitable for compilation on the CYBER from CYGWSLBS.

A list of the subprograms in the library, together with a brief description of each can be obtained by executing the CMS exec CYGWSLIB located on the F400M 191 disk. The CMS exec (CYGWSLIB EXEC) also allows the general user to place a copy of any desired subprogram from the library in the user's own virtual machine. This exec also permits the CYGWSLIB librarian to edit the library contents. For security reasons, and to have the library contents accessible from CMS, the source code version of the library is also maintained in a parallel fashion on the OS partitioned data set F400.CYGWSLIB. Using the CMS exec CYGWSLIB mentioned above, the librarian can add or delete members from the library (both in the OS data set and in the source and compiled versions on the CYBER). The librarian can also edit existing subprograms in the library replacing old copies with new ones.

CYBINLIB

This is a library of FORTRAN main programs for use on the CYBER 205. On the CYBER, each program in the library is kept in a separate file in the CYGWSGCM pool. Only the compiled versions are kept on the CYBER. On the Amdahl, the programs in the library are kept in the OS partitioned data set F400.CYBINLIB. To use the programs on the CYBER the user must PATTACH(CYGWSGCM) and then load them to create a CYBER controlee for execution. Refer to the VSOS - Version 2 reference manual for an explanation of the LOAD control statement on the CYBER. Several of these programs can be loaded and executed with the aid of predefined CYBER procedures in the library CYPROCLB.

A list of the programs in the library, together with a brief description of each, can be obtained by executing the CMS exec CYBINLIB located on the F400M 191 disk. The CMS exec (CYBINLIB EXEC) also allows the general user to place a copy of any program in the library in the user's own virtual machine. This exec also permits the pool boss to edit the library contents. Programs can be added or deleted from the library. Existing programs can be edited and the old copies replaced with new ones.

X.6 Benchmark Procedures and Documentation of Changes

In order to accurately assess the effects of changes to the model and as an aid to producing error free code, a collection of V8RSTR benchmark data sets is maintained. For each production version of the model, the initial conditions and the 3 hour forecast results for a test case are kept.

New model versions to be tested are integrated for 3 simulated hours starting from a benchmark initial condition. The three hour forecast is then compared to the benchmark forecast using the DIFFY program described in Section 11 of Chapter IX. The difference fields produced are examined and kept for later reference. In this way, at any later time, it can be determined which model changes produced which changes in the model forecasts.

Model revisions that produce significant changes to the forecasts should be integrated over a longer period (~ 5 simulated days) and a set of difference plots produced which can be used for later reference.

APPENDICES

JAMES W. PFAENDTNER

Appendix A: Namelist variables

NAMelist INPUTZ

<u>Name</u>	<u>Location</u>	<u>Default</u>	<u>Description</u>
NYDM1	/IDPARM/	000000	YYMMDD at start of experiment
NHMS1	/IDPARM/	000000	HHMMSS at start of experiment
NYMDE	/ICNTRL/	000000	YYMMDD for end of forecast segment
NHMS2	/ICNTRL/	000000	HHMMSS for end of forecast segment
JOB	/CCNTRL/	'EXP NNNN'	8 character experiment identifier
XLABEL	/CCNTRL/	blank	80 character experiment description
NDOUT	/ICNTRL/	030000	HHMMSS increment for writing model history records
NDRSW	/ICNTRL/	060000	HHMMSS increment for writing restart records to EnnnnRS1 or EnnnnRS2.
NKRSH	/ICNTRL/	-1	key for write of restart records to history. (-1 for beginning and end of experiment, 0 for never n for every n'th day)
MROD	/ICNTRL/	25	maximum allowable number of logical history records to write in one forecast segment.
NDALT	/ICNTRL/	000000	HHMMSS increment between calls to the analysis
NDPHY	/ICNTRL/	003000	HHMMSS increment between calls to the physics
NDSHF	/ICNTRL/	023000	HHMMSS increment between calls to the Shapiro filter
KLITOP	/ICNTRL/	0	topography replacement flag 0 - use values from initial conditions 1 - replace topography at beginning of experiment 2 - replace topography at beginning of experiment and adjust upper air and surface fields

NAMelist INPUTZ (Cont.)

<u>Name</u>	<u>Location</u>	<u>Default</u>	<u>Description</u>
KLILWI	/ICNTRL/	0	land-water-ice replacement flag 0 - use values from initial conditions 1 - replace at begining of experiment 2 - replace on a monthly basis
KLIALB	/ICNTRL/	1	albedo flag 0 - use values from initial conditions 1 - use monthly climatological value 2 - use linear interpolation in time to get new values on a daily basis
KLIGW	/ICNTRL/	1	ground wetness flag (0, 1 or 2 as for KLIALB)
KLISST	/ICNTRL/	1	sea surface temperature flag (0, 1 or 2 as for KLIALB)
MATIN	/ICNTRL/	1	number of Matsuno time steps to do at the beginning of the experiment before entry into the normal cycle
MFL	/INCTRL/	1,11*0	normal cycle descriptor (0 for leapfrog step, 1 for Matsuno step)
NDT	/ICNTRL/	43200/IM	timestep length in seconds (IM is the number of grid points per latitude circle in the model)
NSEQ	/ICNTRL/	1	number of timesteps in the regular cycle (see variable MFL)
NS2FLG	/LCNTRL/	.FALSE.	PBL sigma profile flag
PIMEAN	/RCNTRL/		global mean pressure (the default is to compute it from initial conditions)
PSMAX	/RCNTRL/	1200.	maximum allowable surface pressure
PSMIN	/RCNTRL/	350	minimum allowable surface pressure
PSTD	/RCNTRL/	1000.	reference pressure for normalization
TSTD	/RCNTRL/	280.	reference temperature for normalization
SIGE	/RCNTRL/	(uniform)	sigma values at edges of vertical layers

NAMELIST INPUTZ (Cont.)

<u>Name</u>	<u>Location</u>	<u>Default</u>	<u>Description</u>
GNU2	/RCNTRL/	0.	constant for use in time averaging
SMTHNL	/QANDQT/	analytic	damping factors for gravity wave filter (the default values are set in subroutine DEFALT)

NAMelist INPHYS

<u>Name</u>	<u>Location</u>	<u>Default</u>	<u>Description</u>
CDXL	/CNTRLP/	0.5	constant for surface drag computation over land points
CDXO	/CNTRLP/	0.5	constant for surface drag computation over ocean points
ED	/CNTRLP/	0.5	constant used for vertical diffusion of heat and momentum
FMU	/CNTRLP/	.00067	constant used for horizontal momentum diffusion (friction)
FWET	/CNTRLP/	0.5	constant used in PBL computation
NDHOG	/CNTRLP/	06000	HHMMSS increment for longwave radiation computation
NFLW	/CNTRLP/	10	number of frequencies used in longwave radiation computation; setting NFLW to 0 turns off both the short and longwave radiation
LTMIN	/LCNTRL/	.true.	minimum surface temperature diagnostic
LTMAX	/LCNTRL/	.true.	maximum surface temperature diagnostic
LPREACC	/LCNTRL/	.true.	accumulated precipitation diagnostic
LPRECON	/LCNTRL/	.true.	convective precipitation diagnostic
LHFLUX	/LCNTRL/	.true.	surface sensible heat flux diagnostic
LEFLUX	/LCNTRL/	.true.	surface evaporative flux diagnostic
LFUSION	/LCNTRL/	.true.	heat stored in freezing at ground diagnostic
LRADSWG	/LCNTRL/	.true.	solar radiation at ground diagnostic
LUDRAG	/LCNTRL/	.false.	u-momentum drag diagnostic
LVDRAG	/LCNTRL/	.false.	v-momentum drag diagnostic
LICLOUD	/ICNTRL/	.true.	cloud flags diagnostic
LOMEGA	/LCNTRL/	.true.	upper air vertical velocity diagnostic
LDIABAT	/LCNTRL/	.true.	upper air diabatic heating diagnostic
LRADSW	/LCNTRL/	.true.	upper air solar heating diagnostic

NAMelist INPHYS (Cont.)

<u>Name</u>	<u>Location</u>	<u>Default</u>	<u>Description</u>
DSNTOP	/MNTHLY/	See DEPEND	Data set for new TOP field when KLITOP > 0
DSNLWI	/MNTHLY/	See DEPEND	Data set for new LWI field when KLILWI > 0
DSNSST	/MNTHLY/	See DEPEND	Data set for new SST field when KLISST > 0
DSNALB	/MNTHLY/	See DEPEND	Data set for new ALB field when KLIALB > 0
DSNGWT	/MNTHLY/	See DEPEND	Data set for new GWT field when KLIGWT > 0

Appendix B: CONTENTS OF THE HEADER RECORD (STANDARD FOR V8SIGM, V8RSTR & V8MAND)

Location	Variable	Dimension	Description: Default
	CC	200	Array containing all character variables on the history record
CC(1)	CC0		'IBMbbbb' or 'CDCbbbb' or 'HCDCbbbb'
CC(2)	ADATE		Date at the start of current forecast segment
CC(3)	ATIME		Time at the start of current forecast segment
CC(4)	JIC		Jobname of initial conditions
CC(5)	JOB		Jobname of current forecast: blank
	CC(6)		Spare
	CC(7)		Spare
	CC(8)		Spare
CC(9)	VER		Version number of current model
CC(10)	XLABEL	10	80-character forecast description label: blank
CC(20)	CQS	30	Labels for surface diagnostics
CC(50)	CQU	10	Labels for upper air diagnostics
	CC(60) - CC(200)		Spares
	IC	200	Array containing all integer variables on history record
IC(1)	IC0		0, 1, 2 or 3 indicates type of next record in sequence
IC(2)	IM		Number of meridians in grid: 72
IC(3)	IMD2		Half the number of meridians: IM/2
IC(4)	IMD2P1		Number of wave amplitudes in a band: IM/2+1
IC(5)	NDSRW		HHMMSS increment for model V8RSTR writes (not to V8SIGM)
IC(6)	JM		Number of band segments in grid: 45

Appendix B (cont.)

Location	Variable	Dimension	Description: Default
IC(7)	JMD2		Half the number of bands: $(JM + 1)/2$
IC(8)	JMT2		Number of grid segments in a complete meridian: $JM \times 2$
IC(9)	JNP		North pole band number: $JM + 1$
IC(10)	JO4		Band number up to which to apply 4th order Shapiro filter: 0
IC(11)	JO8		Band number up to which to apply 8th order Shapiro filter: 0
IC(12)	JSP		South pole band number: 1
IC(13)	KLIALB		Albedo climatology flag (0 for initial conditions, 1 for monthly update, 2 for time interpolation): 1
IC(14)	KLIGW		Ground wetness climatology flag (0 for initial conditions, 1 for monthly update, 2 for time interpolation): 1
IC(15)	KLISST		Sea surface temperature climatology flag (0 for initial conditions, 1 for monthly update, 2 for time interpolation): 1
IC(16)	KS		Number of surface fields: 19
IC(17)	KU		Number of upper-air fields: 14
IC(18)	LOG8R		Record type indicator: -1 V8RSTR pre-analysis 0 V8RSTR post-analysis 1 V8SIGM pre-analysis 2 V8SIGM post-analysis 3 V8MAND pre-analysis 4 V8MAND post-analysis
IC(19)	MATIN		Number of Matsuno steps to integrate initially before entering regular cycle: 1
IC(20)	MATSNX		Next time step scheme (0 for leapfrog, 1 for Matsuno)
IC(21)	MATSUN		Current time step scheme (0 for leapfrog, 1 for Matsuno)

Appendix B (cont.)

Location	Variable	Dimension	Description: Default
IC(22)	MLF	12	NSEQ time step scheme identifiers in a complete sequence (0 for leapfrog, 1 for Matsuno): 1
IC(34)	MROD		Maximum allowable number of writes to history file
IC(35)	NKRSH		Frequency of V8RSTR records in history: -1 at initial and end times only, 0 none, m>0 every m days at time zero
IC(36)	MSM		Number of bands to keep in storage at one time: 5
IC(37)	NB		Index of current time step fields
IC(38)	ND		Index of previous time step fields
IC(39)	NDALT		Time increment to invoke analysis in HHMMSS format: 0
IC(40)	NDAY		Current Julian day
IC(41)	NDOUT		Time increment to write history record in HHMMSS format: 30000
IC(42)	NDPHY		Time increment to invoke physics in HHMMSS format: 30000
IC(43)	NDSHF		Time increment to invoke Shapiro filter in HHMMSS format
IC(44)	NDT		Time step in seconds: 43200/IM
IC(45)	NHMS		Current time in HHMMSS format
IC(46)	NHMSE		Ending time in HHMMSS format
IC(47)	NHMSO		Beginning time in HHMMSS format
IC(48)	NLAY		Number of vertical layers in grid: 9
IC(49)	NLAYM1		One less than the number of vertical layers in grid: NLAY-1
IC(50)	NLAYP1		One more than the number of vertical layers in grid: NLAY+1
IC(51)	NSDAY		Current time of day in seconds

Appendix B (cont.)

Location	Variable	Dimension	Description: Default
IC(52)	NSEQ		Number of steps in a complete time step sequence: 1
	IC(53)		Spare
IC(54)	NSTEP		Number of time steps since initial start
IC(55)	IBLSZ		Record size for data set (IM, 4096 or IM*JNP)
IC(56)	NYMD		Current date in YYMMDD format
IC(57)	NYMDE		Ending date in YYMMDD format
IC(58)	NYMDO		Beginning date in YYMMDD format
IC(59)	NZINIT		Gravity wave initialization flag
IC(60)	NMLEV		Number of mandatory pressure levels (0 if not a V8MAND data set): 12
IC(61)	NDHOG		Increment between calls to long wave radiation in HHMMSS: 30000
IC(62)	IQS	30	Pointers to surface diagnostics
IC(92)	IQU	10	Pointers to upper air diagnostics
	IC(102) - IC(200)		Spares
	LC	200	Array containing all logical variables on the history record
LC(1)	LC0		T if next record is V8RSTR
LC(2)	QALT		T if current time step is an analysis step
LC(3)	QBEG		T if current time step is the initial step
LC(4)	QDAY		T if current time step is the first step of the day
LC(5)	QEND		T if current time step is the last step
LC(6)	QOUT		T if current time step is written to the history file
LC(7)	QPHY		T if current time step is a physics step

Appendix B (cont.)

Location	Variable	Dimension	Description: Default
LC(8)	QSHF		T if current time step is a Shapiro filter step
LC(9)	SN2FLG		T for the sine-squared PBL sigma profile: F
LC(10)	QRSW		T if current step is to be written to restart
LC(11)	QRSH		T if current step restart is to be written to history
LC(12)	LQS	30	Logical switches for surface diagnostics
LC(42)	LQU	10	Logical switches for upper air diagnostics
	LC(52) - LC(200)		Spares
	RC	200	Array containing all real variables on the history header (dimensioned 400 for half precision model)
RC(1)	RCO		Equivalence of RC(1) - spare
RC(2)	APHEL		Day of the year of the apogee of the earth's orbit: 183
RC(3)	BETA		Moist adiabatic lapse rate: .0065 °K/m
RC(4)	COSD		Cosine of solar declination
RC(5)	CP		Specific heat of air: 1003.5 J/(kg °K)
RC(6)	DAYSPLY		Number of days in a year: 365
RC(7)	DEC		Current declination of the earth: 23.5*PI/180
RC(8)	DECMAX		Maximum declination of the earth
RC(9)	DIST		Current position of the earth with respect to the apogee
RC(10)	DLAT		Grid distance between bands in radians: PI/JM
RC(11)	DLON		Grid distance between meridians in radians: 2 x PI/IM

Appendix B (cont.)

Location	Variable	Dimension	Description: Default
RC(12)	DT		Model time step in seconds
RC(13)	ECCN		Eccentricity of earth's orbit: .0178
RC(14)	GNU1		Center term coefficient in time averaging for leapfrog scheme: 1.-2. x GNU2
RC(15)	GNU2		Outer term coefficient in time averaging for leapfrog scheme: 0
RC(16)	GRAV		Gravitational acceleration in m/s^2 : 9.81
RC(17)	OMEGA2		Twice the angular velocity of the earth
RC(18)	PI		Mathematical constant: ACOS(-1)
RC(19)	PI180		Mathematical constant to convert degrees to radians: PI/180
RC(20)	PI2		Mathematical constant: PI x 2
RC(21)	PSTD		Standard reference pressure for normalization: 1000
RC(22)	PIMEAN		Global mean reference pressure: initial conditions
RC(23)	PSMAX		Maximum allowable reference pressure: 1200
RC(24)	PSMIN		Minimum allowable reference pressure: 300
RC(25)	PTOP		Pressure at top of first layer: 10 mb
RC(26)	RADE		Radius of the earth in m: 6375000
RC(27)	RGAS		Gas constant for dry air: $287.m^2/(^{\circ}Ks^2)$
RC(28)	ROCP		Gas constant divided by specific heat of air (dimensionless): RGAS/CP
RC(29)	RSDIST		Ratio of actual to mean earth-sun distance
RC(30)	SDAY		Number of seconds per day: 86400
RC(31)	SEASON		Current position of the earth with respect to the summer solstice

Appendix B (cont.)

Location	Variable	Dimension	Description: Default
RC(32)	SIGE	25	Layer interface sigma values: 0, 1/NLAY,, NLAYM1/NLAY,1
RC(57)	SIND		Sine of solar declination
RC(58)	SOLS		Day of the year of maximum declination (summer solstice): 173
RC(59)	TSTD		Standard temperature for normalization: 280
RC(60)	PLEVS	25	Array of NMLEV mandatory pressure levels: 12 standard mandatory levels; zero if not a V8MAND data set
RC(85)	HEATW		Heat capacity over land and water: 597.2 cal/gm
RC(86)	HEATI		Heat capacity over ice, snow and frost 680.0 cal/gm
RC(87)	EPS		Ratio of molecular weights of water vapor to dry air: 0.6220
RC(88)	EPSFAC		EPS*HEATW/RGAS * CALTOJ
RC(89)	PZERO		Reference pressure for scaling water vapor absorption: 1013.25 mb
	RC(90) - RC(200)		Spares

Appendix C: Bit Configuration for Cloud Data

Bit Number (*)	Cloud Type	Model Level (**)	Value (***)
0-1	Mid-level convective	5	1
		6	2
2-3	Penetrative convective	4	1
		5	2
		6	3
4-5	Low-level convective	7	1
		8	2
6-14	Super saturation	1-9	1

NOTE (*): Bit 0 (zero) is the least significant bit.

NOTE (**): This configuration is valid only for the 9 level model.

NOTE (***): A value of zero for the 2-bit convective clouds and a zero bit for super saturation clouds, indicates the absence of clouds.

Appendix D: Global Maps of the Boundary Fields

D.i - Continental Outline.

D.ii - Orography.

Source: Area weighted averages computed from the Gates and Nelson (1975) one degree global terrain heights. Global filtering of shortwaves was done using a sixteenth order Shapiro (1979) filter and poleward of 60° latitude, use was made of the fourier filter. Negative terrain heights resulting from the smoothing process, particularly in regions of steep orography, were set to zero.

D.iii - Sea Surface Temperature.

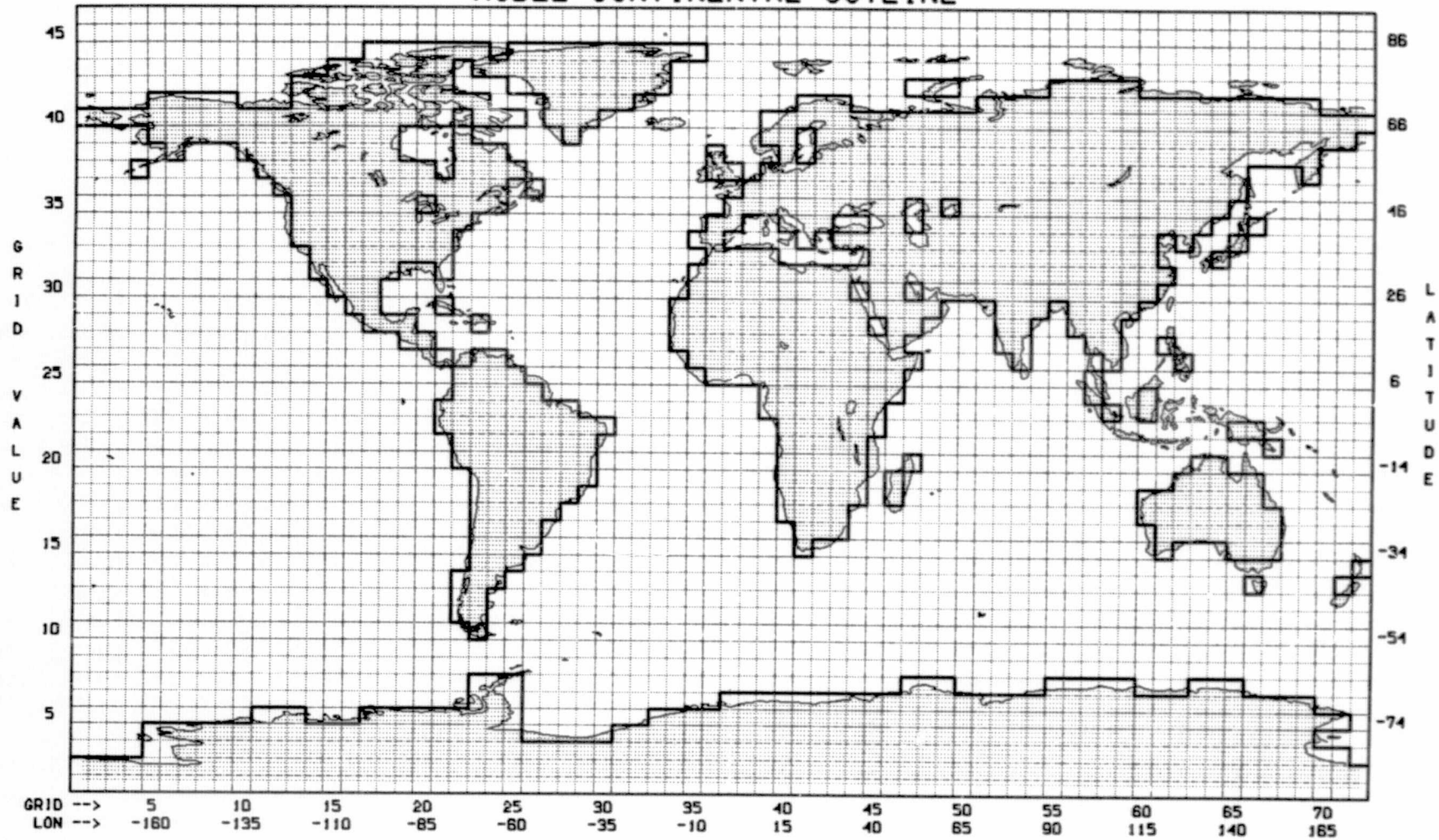
D.iv - Ground Wetness.

Source: Mintz and Serafini, 1981.

D.v - Surface Albedo.

Source: Sud and Fennessy, 1981, page 107, paragraph (d).

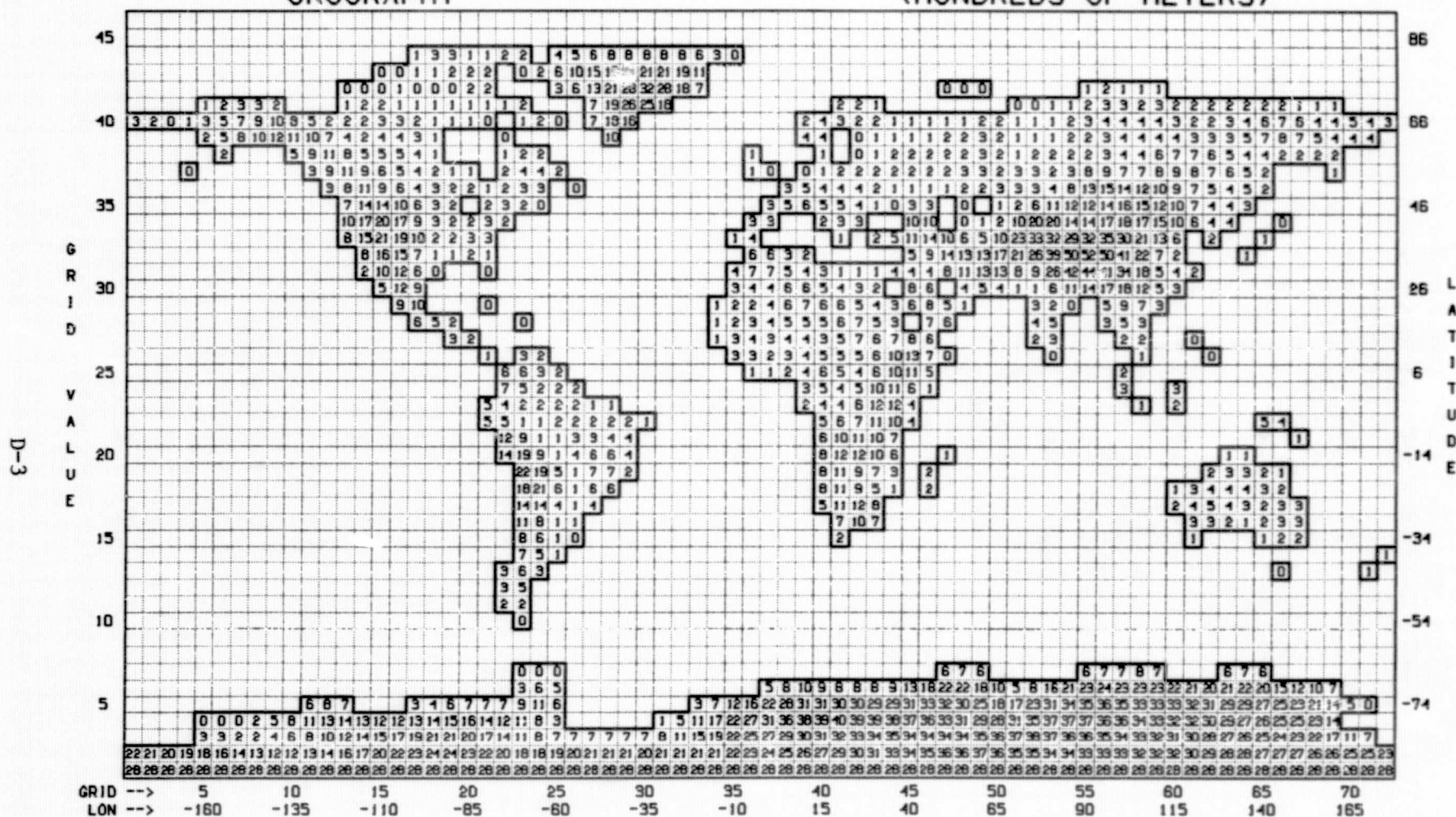
MODEL CONTINENTAL OUTLINE



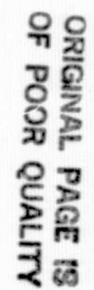
ORIGINAL PAGE IS
OF POOR QUALITY

OROGRAPHY

(HUNDREDS OF METERS)



JANUARY

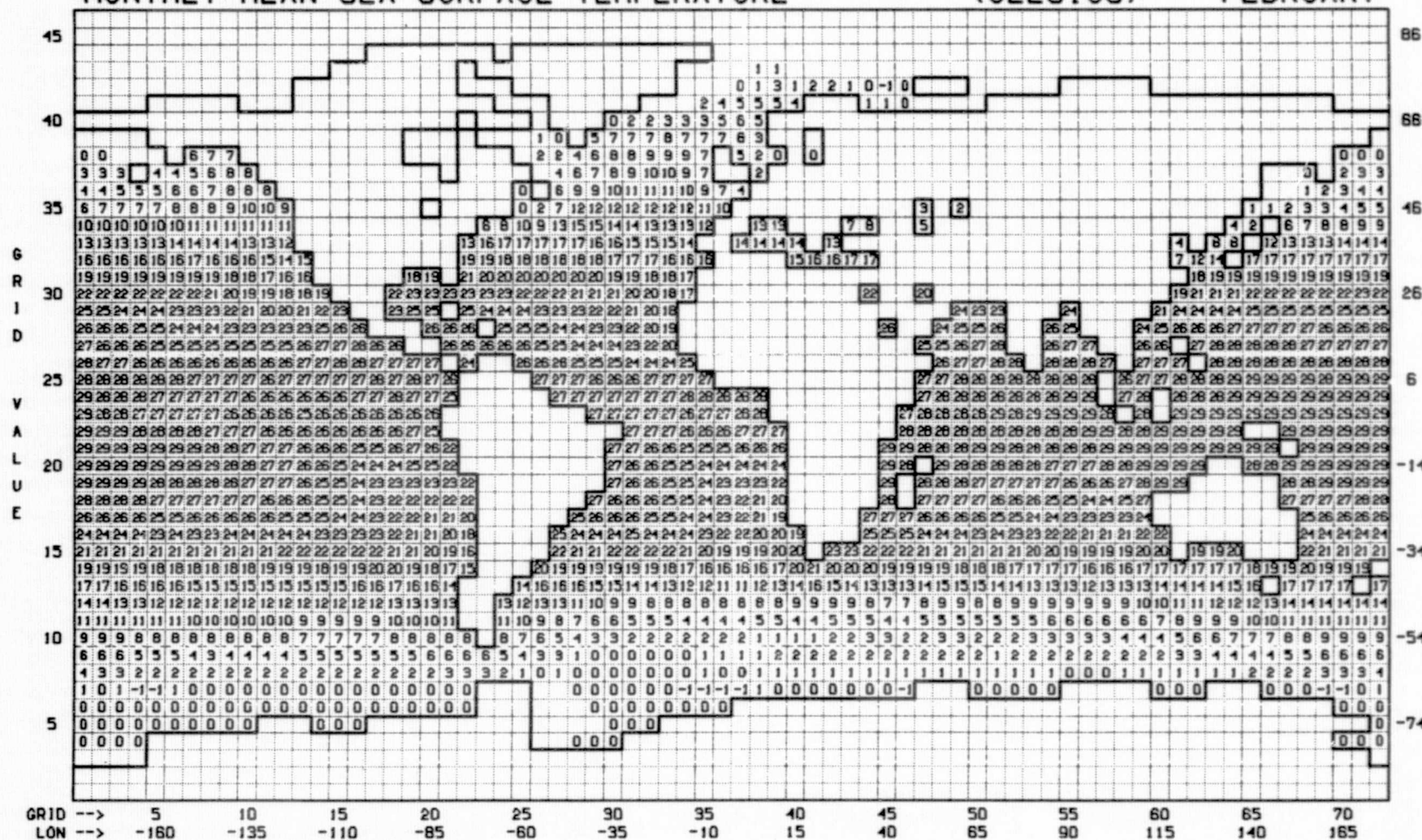


D-4

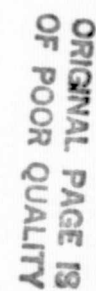
MONTHLY MEAN SEA SURFACE TEMPERATURE

(CELSIUS)

FEBRUARY

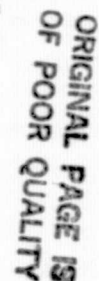


MARCH

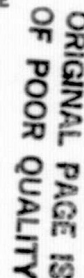


D-6

APRIL

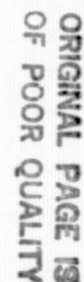


MAY



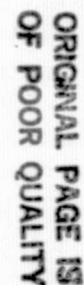
D-8

JUNE



D-9

JULY

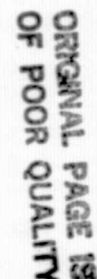


AUGUST



D-111

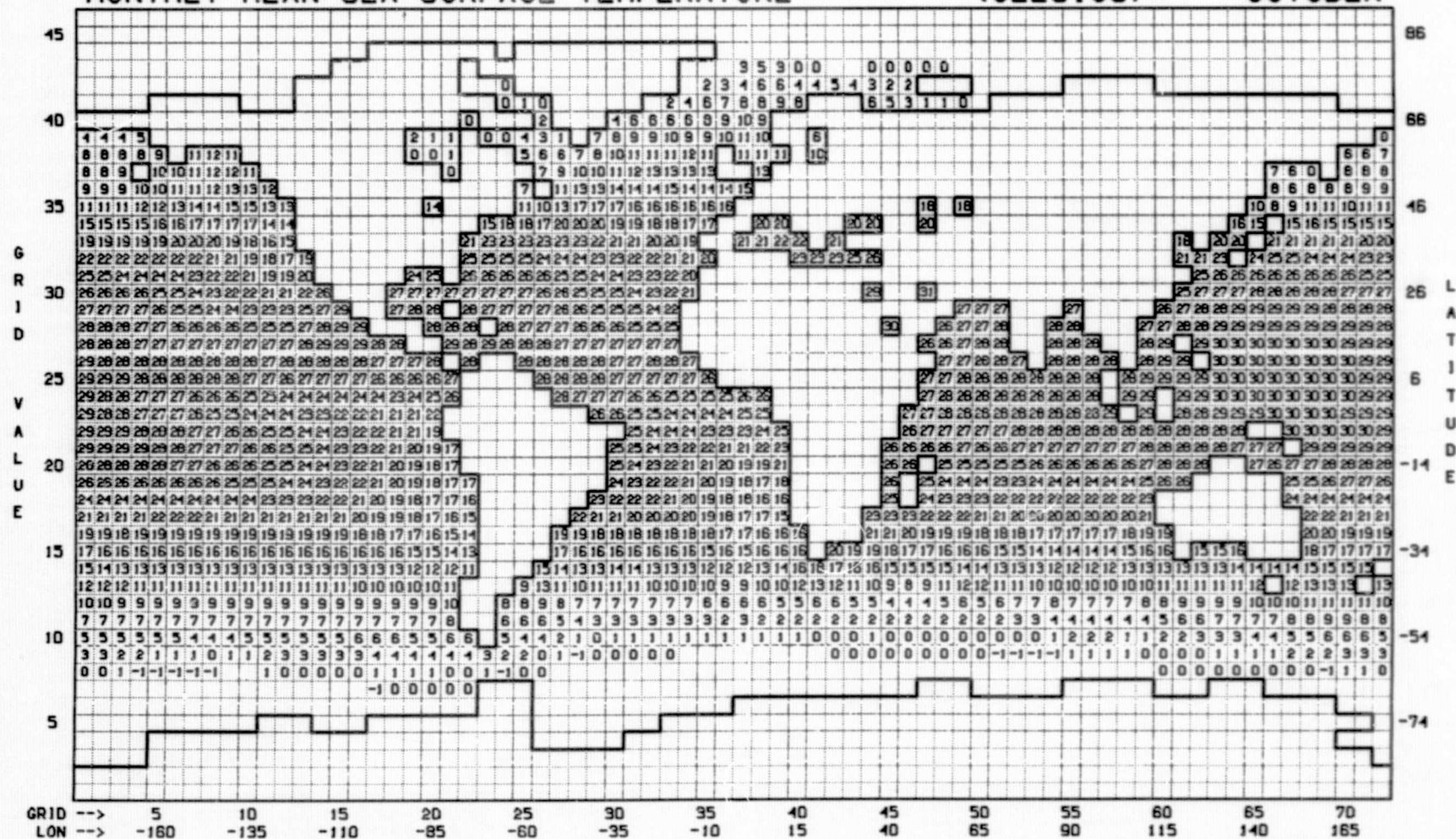
SEPTEMBER



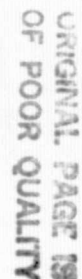
MONTHLY MEAN SEA SURFACE TEMPERATURE

(CELSIUS)

OCTOBER



NOVEMBER



D-14

DECEMBER

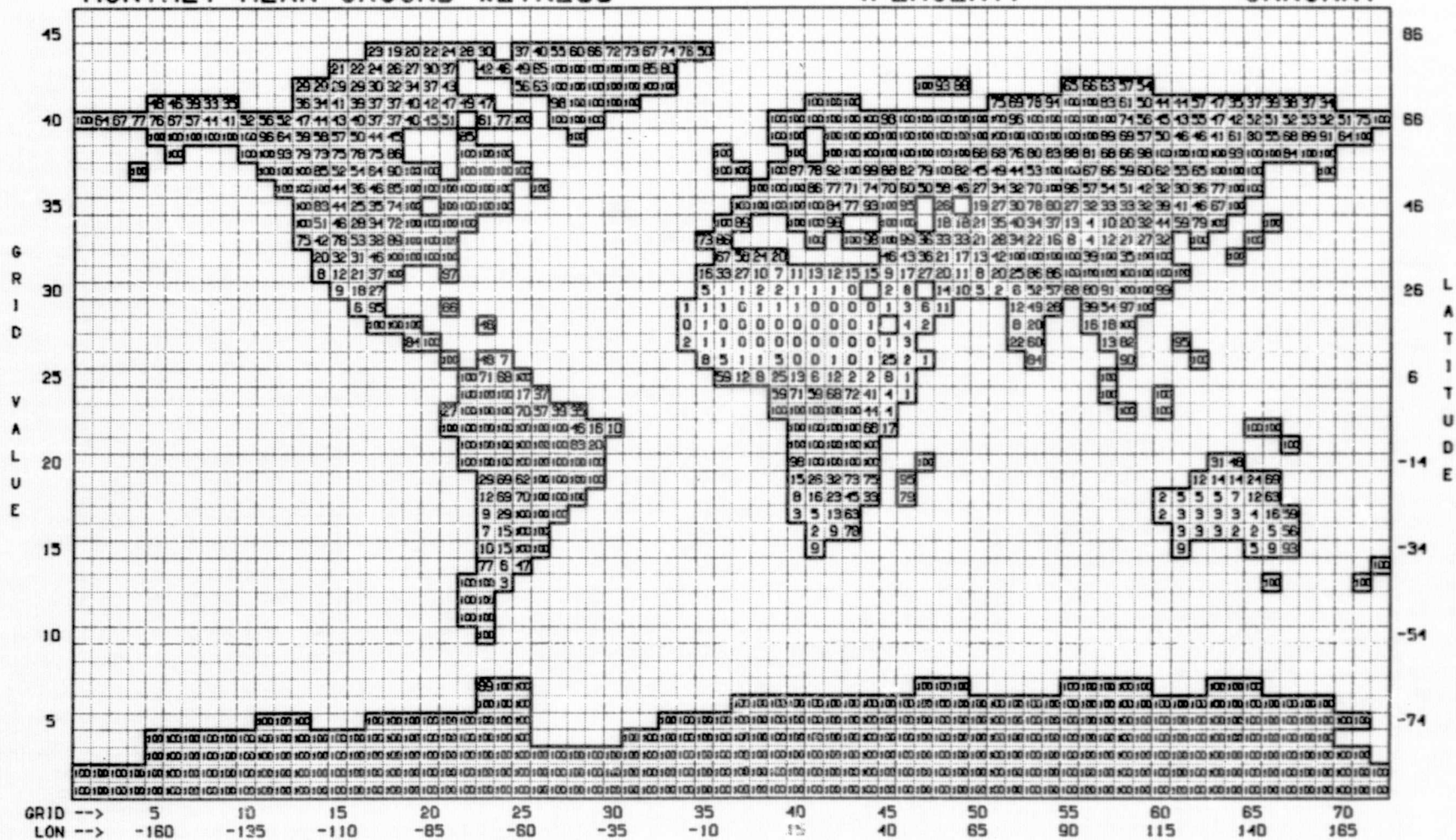


D-15

MONTHLY MEAN GROUND WETNESS

(PERCENT)

JANUARY

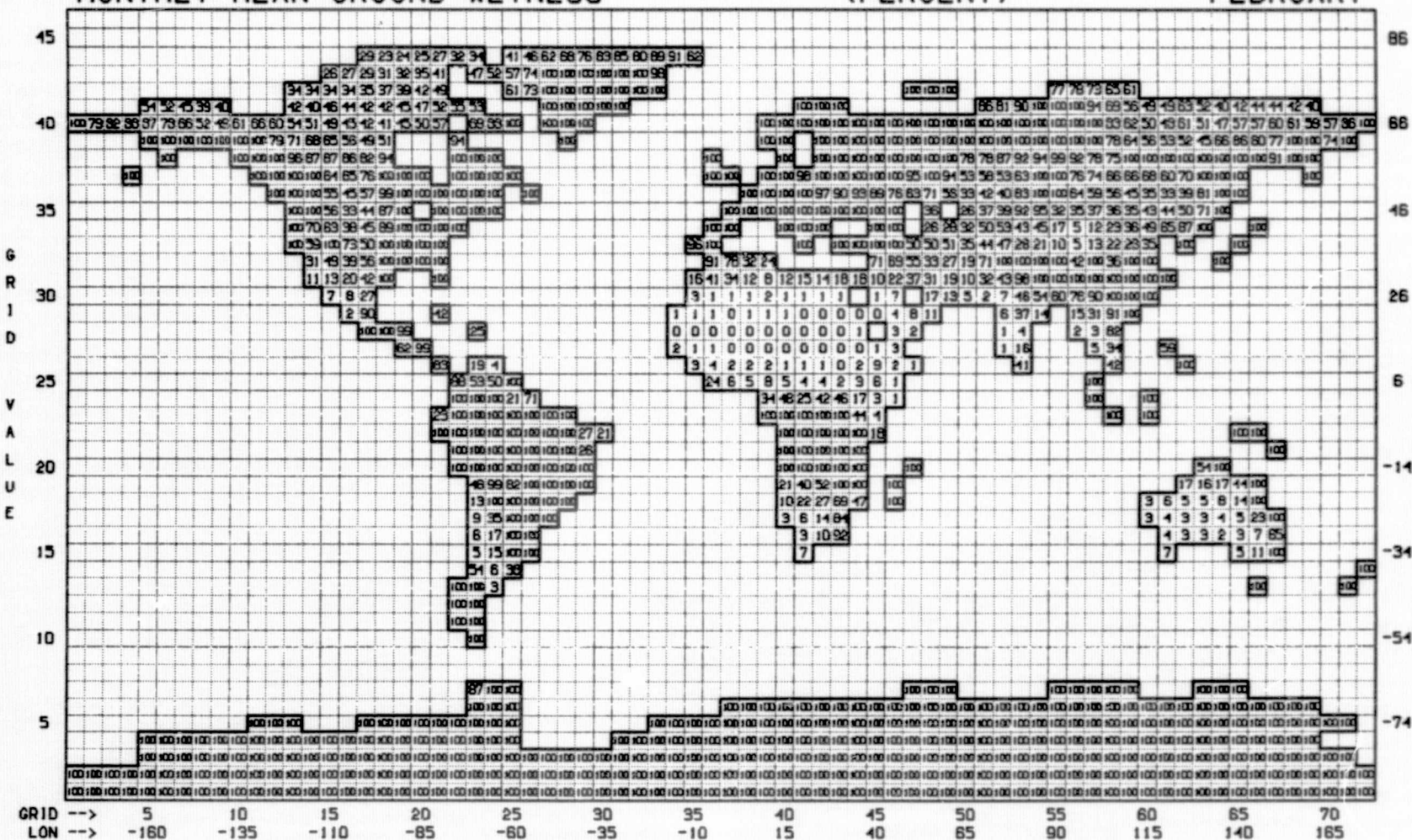


MONTHLY MEAN GROUND WETNESS

(PERCENT)

FEBRUARY

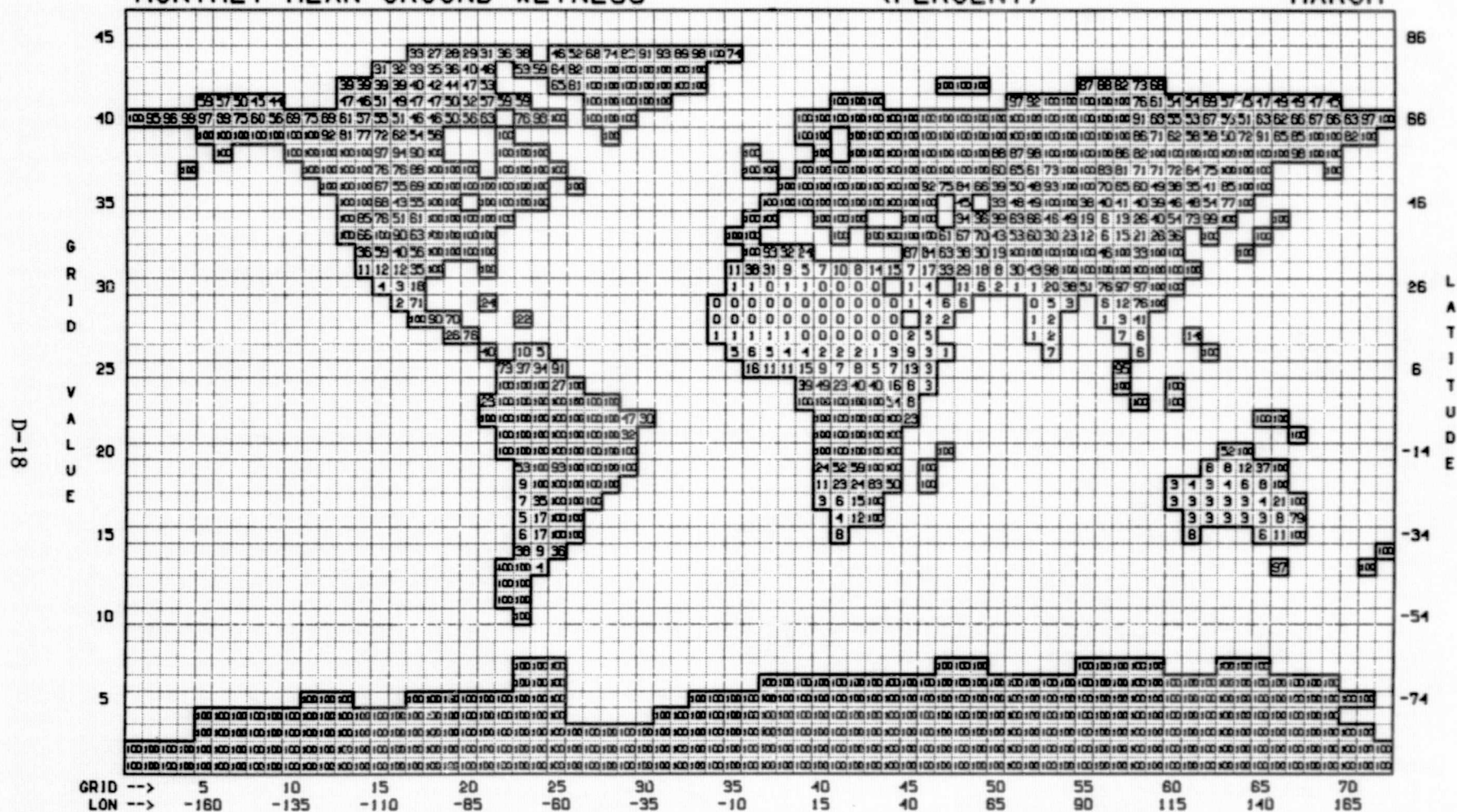
D-17

ORIGINAL PAGE IS
OF POOR QUALITY

MONTHLY MEAN GROUND WETNESS

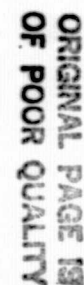
(PERCENT)

MARCH



ORIGINAL PAGE IS
OF POOR QUALITY

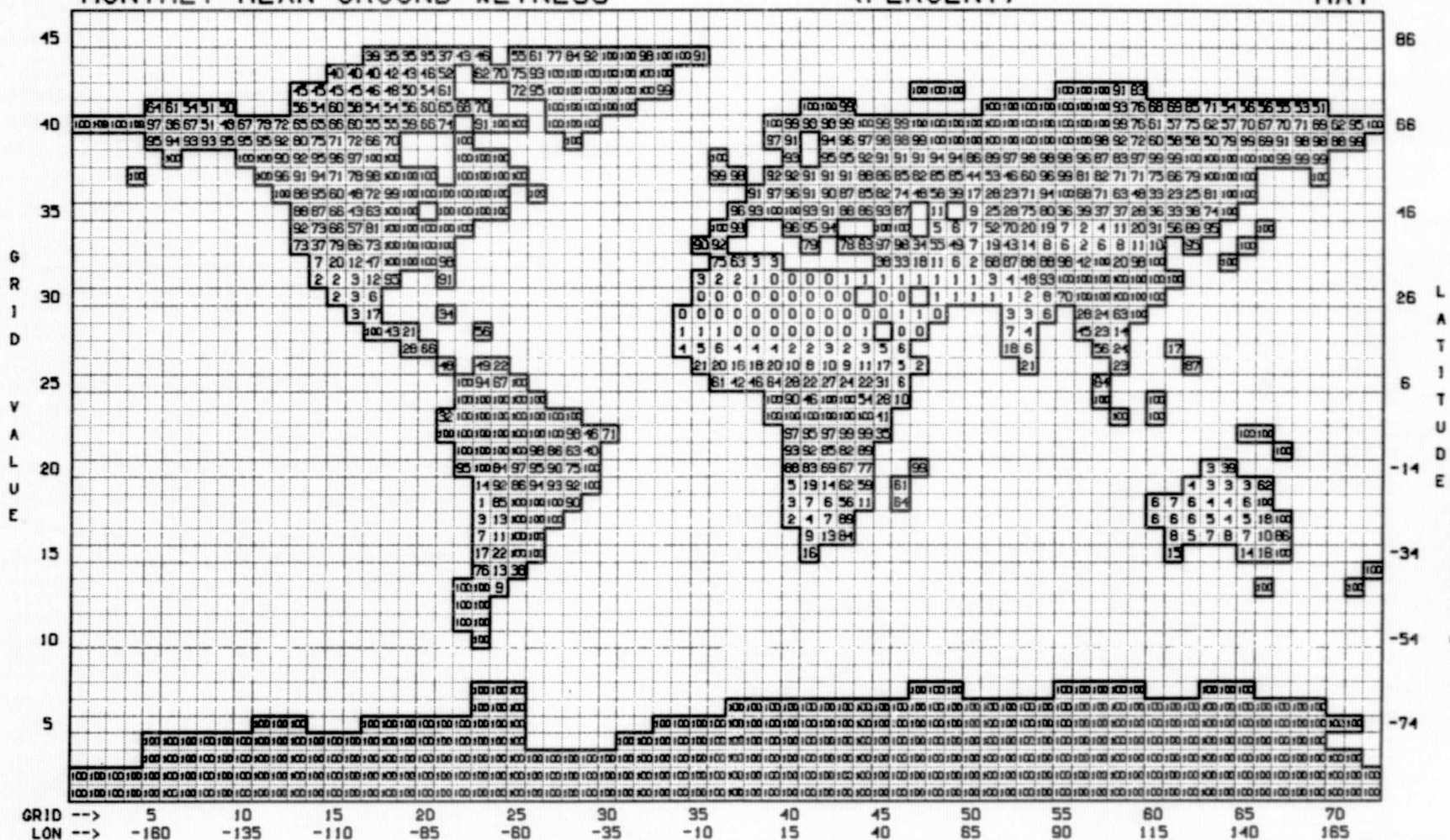
APRIL



MONTHLY MEAN GROUND WETNESS

(PERCENT)

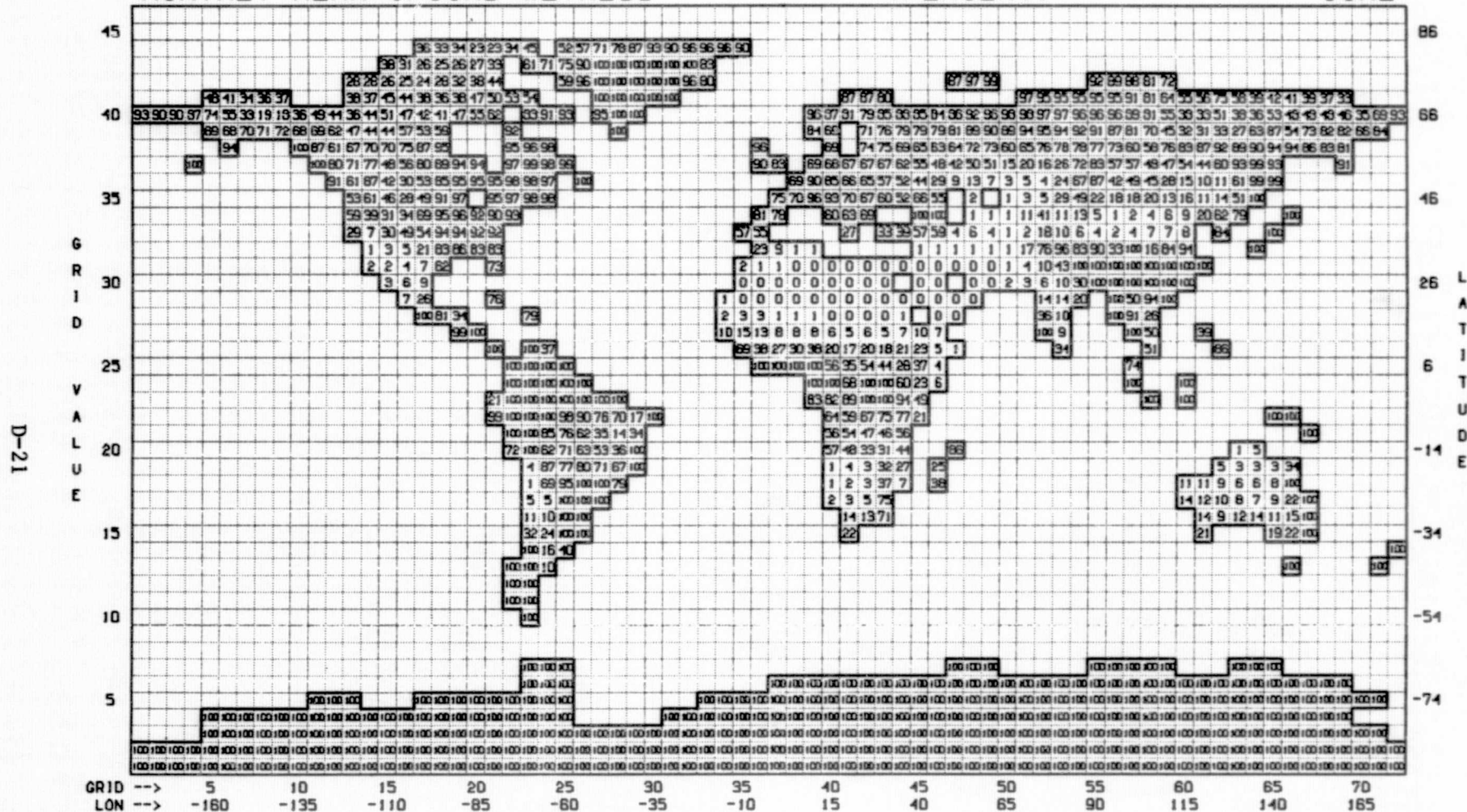
MAY



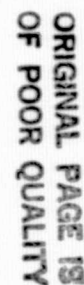
MONTHLY MEAN GROUND WETNESS

(PERCENT)

JUNE



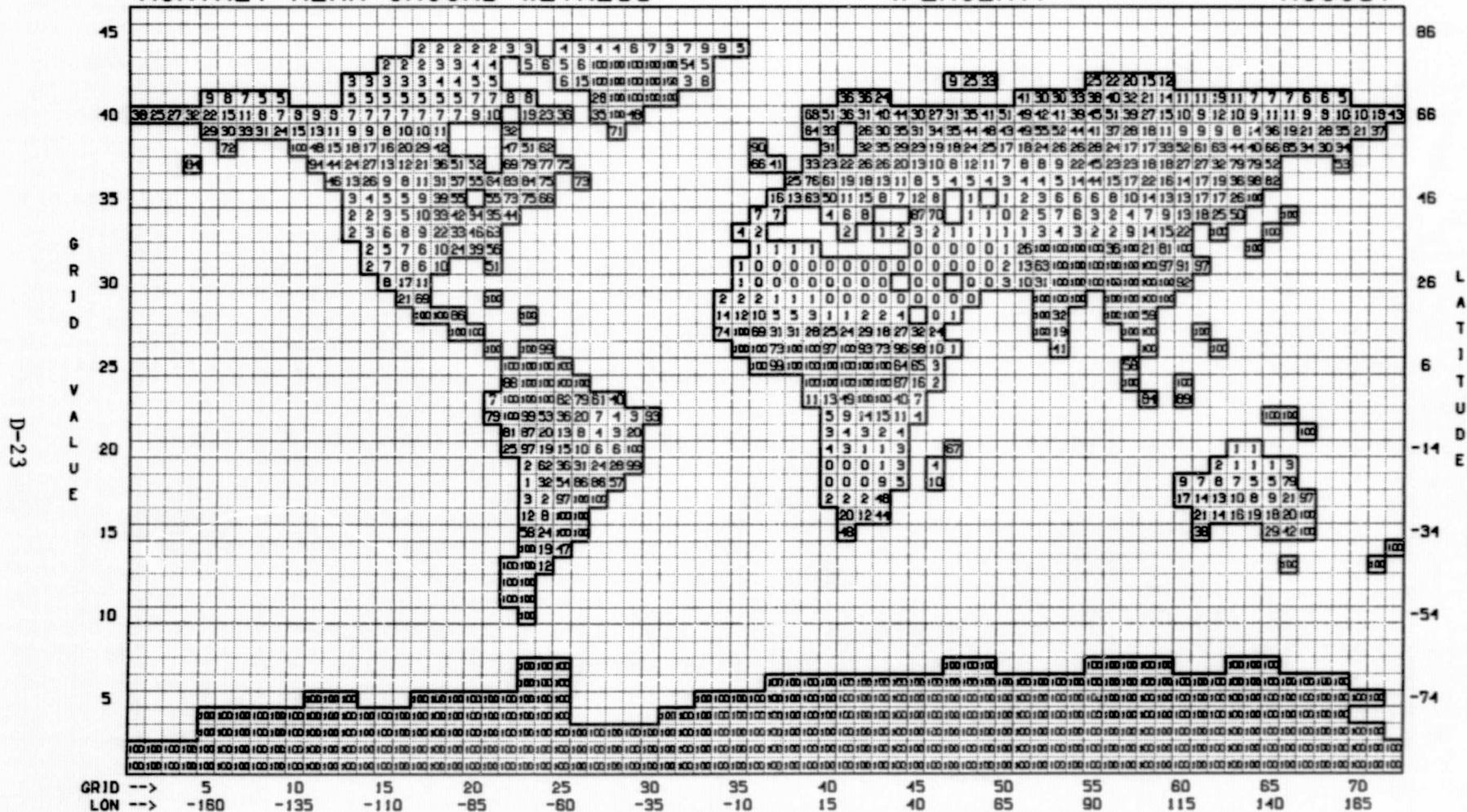
JULY



MONTHLY MEAN GROUND WETNESS

(PERCENT)

AUGUST



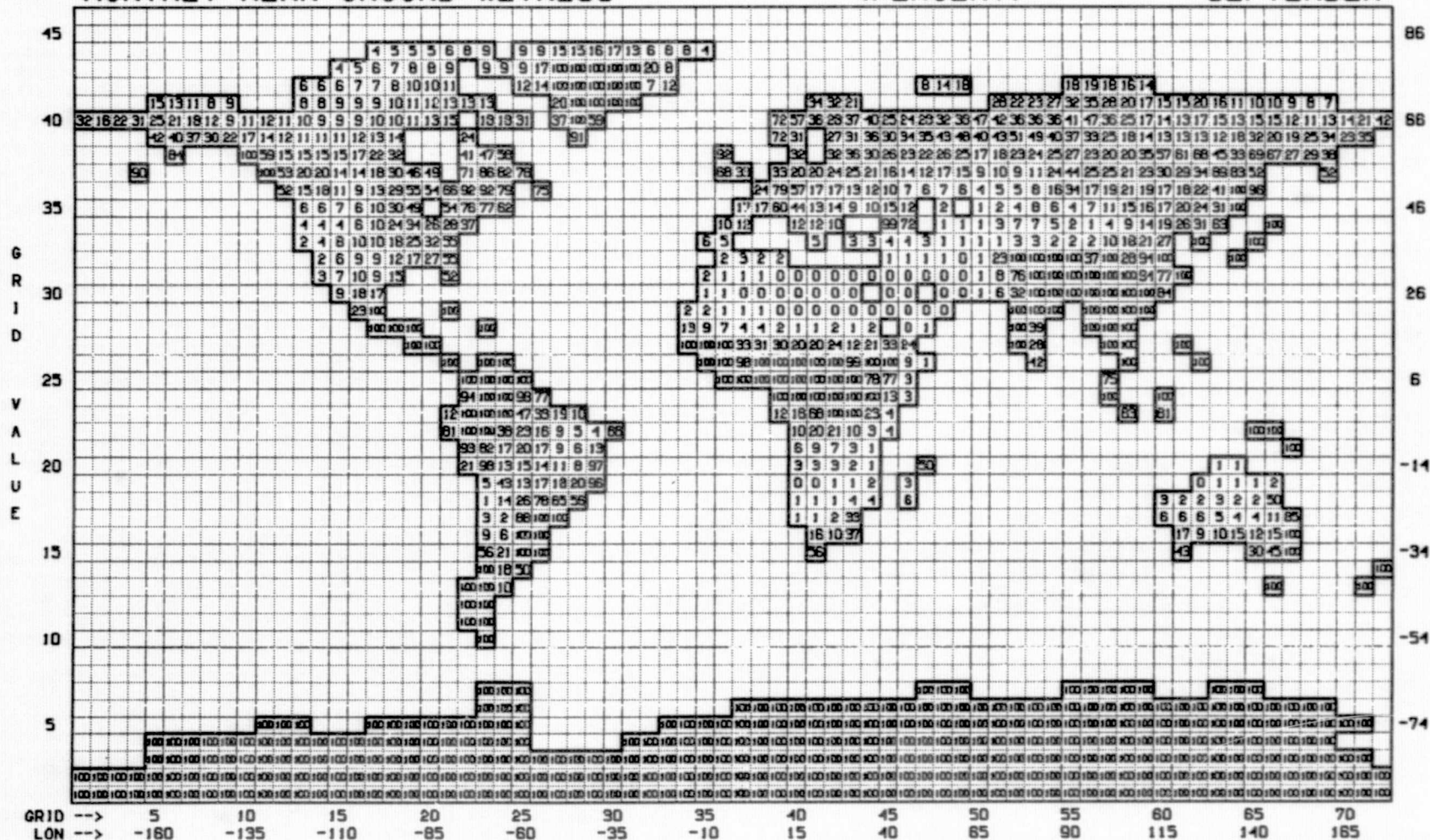
D-23

ORIGINAL PAGE 13
OF POOR QUALITY

MONTHLY MEAN GROUND WETNESS

(PERCENT)

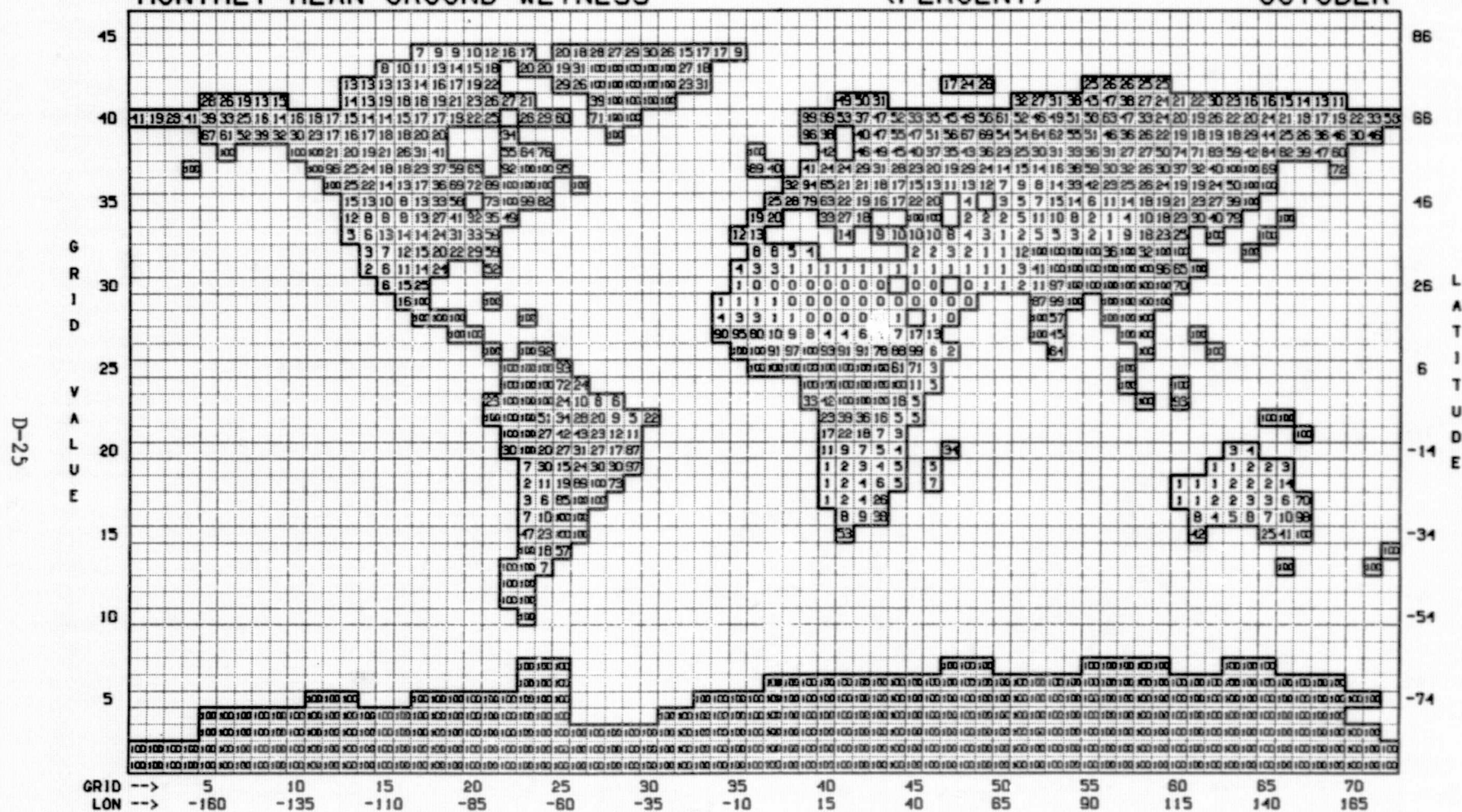
SEPTEMBER



MONTHLY MEAN GROUND WETNESS

(PERCENT)

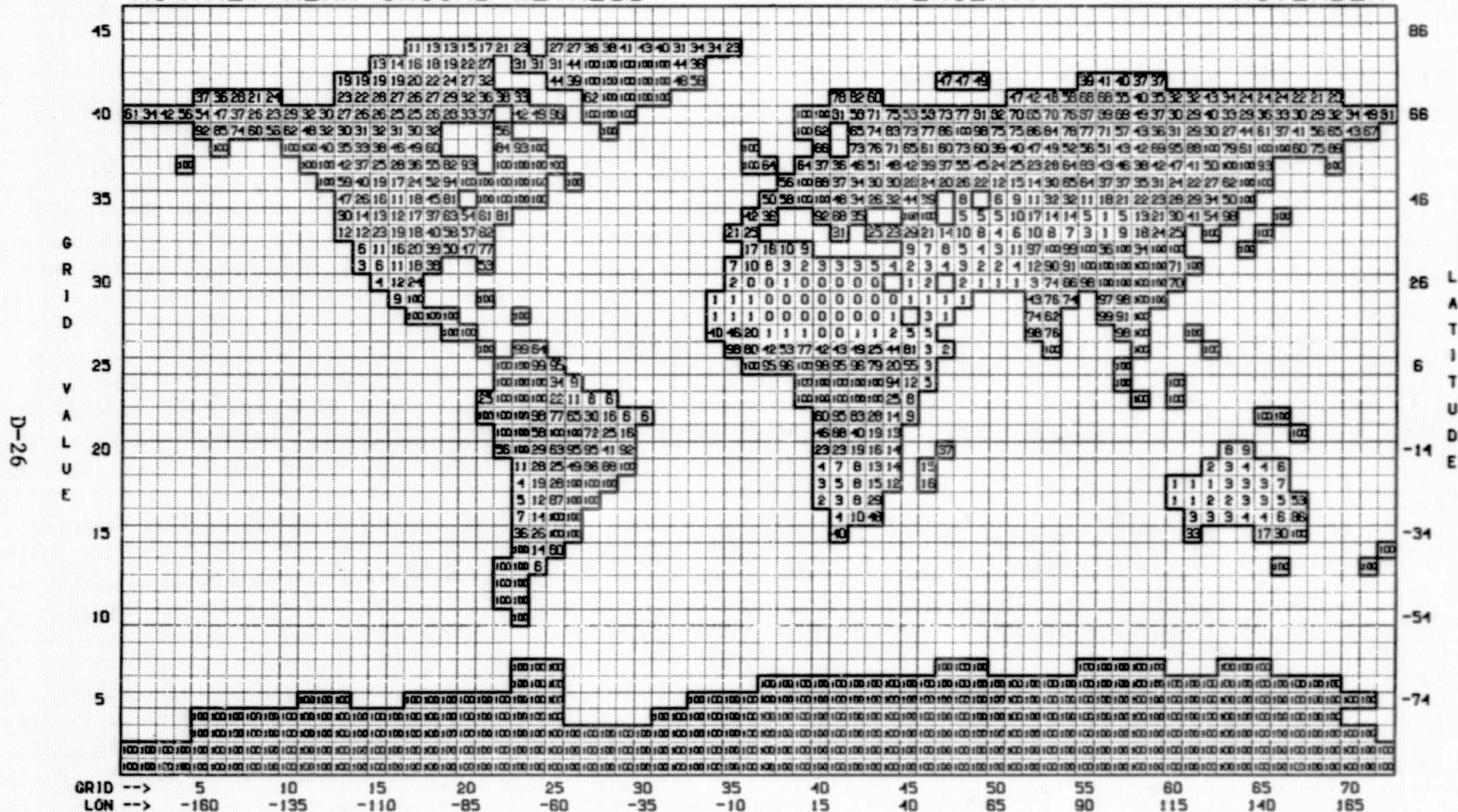
OCTOBER



MONTHLY MEAN GROUND WETNESS

(PERCENT)

NOVEMBER



ORIGINAL PAGE IS
OF POOR QUALITY

DECEMBER



JANUARY

ORIGINAL PAGE IS
OF POOR QUALITY

FEBRUARY

ORIGINAL PAGE IS
OF POOR QUALITY

MARCH

ORIGINAL PAGE IS
OF POOR QUALITY

APRIL

ORIGINAL PAGE IS
OF POOR QUALITY

MAY

ORIGINAL PAGE IS
OF POOR QUALITY

JUNE

[illegible]

ORIGINAL PAGE IS
OF POOR QUALITY

JULY

ORIGINAL PAGE IS
OF POOR QUALITY

AUGUST

ORIGINAL PAGE IS
OF POOR QUALITY

SEPTMBER

ORIGINAL PAGE IS
OF POOR QUALITY

OCTOBER

ORIGINAL PAGE IS
OF POOR QUALITY

NOVEMBER

ORIGINAL PAGE IS
OF POOR QUALITY

DECEMBER

[illegible]

ORIGINAL PAGE IS
OF POOR QUALITY

Appendix E: Tables of the Longwave Radiation Data Sets

- E.i.1 - Carbon Dioxide Transmission Function for Spectral Interval 500-660 cm^{-1} .
- E.i.2 - Carbon Dioxide Transmission Function for Spectral Interval 660-800 cm^{-1} .
- E.ii.1 - Ozone Transmission Functions for Spectral Interval 800-1200 cm^{-1} for Paths between 1 mb and Level I and between 5 mb and Level I as a Function of Latitude.
- E.ii.2 - Ozone Transmission Function for Spectral Interval 800-1200 cm^{-1} for Paths between Levels I and J at Latitudes ± 15 Degrees.
- E.ii.3 - Ozone Transmission Function for Spectral Interval 800-1200 cm^{-1} for Paths between Levels I and J at Latitudes ± 30 Degrees.
- E.ii.4 - Ozone Transmission Function for Spectral Interval 800-1200 cm^{-1} for Paths between Levels I and J at Latitudes ± 45 Degrees.
- E.ii.5 - Ozone Transmission Function for Spectral Interval 800-1200 cm^{-1} for Paths between Levels I and J at Latitudes ± 60 Degrees.
- E.ii.6 - Ozone Transmission Function for Spectral Interval 800-1200 cm^{-1} for Paths between Levels I and J at Latitudes ± 75 Degrees.

E-2

		1	2	3	4	5	6	7	8	9	10	11	12	13	14	15	16	17	18	19
1	.9674 .9731	1.0000	.8645	.8115	.7747	.7429	.7138	.6879	.6648	.6440	.6250	.6077	.5919	.5773	.5639	.5516	.5402	.5298	.5201	.5112
2	.8617 .8628	.8645	1.0000	.8344	.7858	.7493	.7179	.6907	.6669	.6456	.6263	.6087	.5927	.5780	.5645	.5521	.5406	.5301	.5204	.5115
3	.8098 .8106	.8115	.8344	1.0000	.8094	.7599	.7238	.6944	.6695	.6474	.6276	.6098	.5935	.5787	.5650	.5525	.5410	.5304	.5207	.5117
4	.7737 .7742	.7747	.7858	.8094	1.0000	.7861	.7361	.7016	.6742	.6508	.6301	.6117	.5950	.5798	.5659	.5533	.5416	.5309	.5211	.5120
5	.7420 .7424	.7429	.7493	.7599	.7861	1.0000	.7659	.7164	.6834	.6571	.6348	.6151	.5977	.5820	.5677	.5547	.5428	.5319	.5219	.5127
6	.7131 .7135	.7138	.7179	.7238	.7361	.7659	1.0000	.7500	.7008	.6683	.6426	.6211	.6023	.5856	.5706	.5570	.5447	.5335	.5233	.5138
7	.6873 .6876	.6879	.6907	.6944	.7016	.7164	.7500	1.0000	.7369	.6876	.6553	.6302	.6092	.5910	.5749	.5605	.5476	.5359	.5253	.5155
8	.6644 .6646	.6648	.6669	.6695	.6742	.6834	.7008	.7369	1.0000	.7256	.6760	.6440	.6193	.5987	.5810	.5654	.5515	.5391	.5280	.5178
9	.6437 .6439	.6440	.6456	.6474	.6508	.6571	.6683	.6876	.7256	1.0000	.7155	.6658	.6340	.6095	.5893	.5720	.5569	.5436	.5316	.5209
10	.6247 .6249	.6250	.6263	.6276	.6301	.6348	.6426	.6553	.6760	.7155	1.0000	.7069	.6570	.6253	.6009	.5810	.5640	.5493	.5364	.5248
11	.6075 .6076	.6077	.6087	.6098	.6117	.6151	.6211	.6302	.6440	.6658	.7069	1.0000	.6993	.6491	.6173	.5931	.5734	.5568	.5425	.5299
12	.5917 .5918	.5919	.5927	.5935	.5950	.5977	.6023	.6092	.6193	.6340	.6570	.6993	1.0000	.6924	.6418	.6161	.5861	.5666	.5503	.5362
13	.5771 .5772	.5773	.5780	.5787	.5798	.5820	.5856	.5910	.5987	.6095	.6253	.6491	.6924	1.0000	.6860	.6353	.6034	.5796	.5604	.5443
14	.5638 .5639	.5639	.5645	.5650	.5659	.5677	.5706	.5749	.5810	.5893	.6009	.6173	.6418	.6860	1.0000	.6803	.6293	.5975	.5738	.5547
15	.5514 .5515	.5516	.5521	.5525	.5533	.5547	.5570	.5605	.5654	.5720	.5810	.5931	.6101	.6353	.6803	1.0000	.6751	.6239	.5920	.5683
16	.5401 .5402	.5402	.5406	.5410	.5416	.5428	.5447	.5476	.5515	.5569	.5640	.5734	.5861	.6034	.6293	.6751	1.0000	.6704	.6188	.5869
17	.5297 .5297	.5298	.5301	.5304	.5309	.5319	.5335	.5359	.5391	.5436	.5493	.5568	.5666	.5796	.5975	.6239	.6704	1.0000	.6660	.6141
18	.5200 .5201	.5201	.5204	.5207	.5211	.5219	.5233	.5253	.5280	.5316	.5364	.5425	.5503	.5604	.5738	.5920	.6188	.6660	1.0000	.6619
19	.5111 .5111	.5112	.5115	.5117	.5120	.5127	.5138	.5155	.5178	.5209	.5248	.5299	.5362	.5443	.5547	.5683	.5869	.6141	.6619	1.0000

TABLE E.1.1
CARBON DIOXIDE TRANSMISSION FUNCTION FOR
SPECTRAL INTERVAL 500 - 660 CM^{-1}

ORIGINAL PAGE IS
OF POOR QUALITY

		1	2	3	4	5	6	7	8	9	10	11	12	13	14	15	16	17	18	19
1	.9321 .9423	1.0000	.7552	.6779	.6307	.5889	.5497	.5146	.4834	.4556	.4306	.4083	.3884	.3704	.3542	.3397	.3273	.3151	.3041	.2940
2	.7511 .7527	.7552	1.0000	.7083	.6442	.5967	.5546	.5178	.4857	.4574	.4319	.4093	.3892	.3710	.3547	.3401	.3276	.3154	.3043	.2942
3	.6758 .6768	.6779	.7083	1.0000	.6730	.6089	.5613	.5220	.4885	.4593	.4334	.4104	.3900	.3717	.3553	.3405	.3279	.3156	.3045	.2944
4	.6292 .6299	.6307	.6442	.6730	1.0000	.6404	.5758	.5305	.4941	.4632	.4362	.4125	.3916	.3729	.3562	.3413	.3285	.3161	.3049	.2947
5	.5879 .5884	.5889	.5967	.6089	.6404	1.0000	.6120	.5485	.5052	.4707	.4416	.4165	.3946	.3753	.3581	.3427	.3297	.3171	.3056	.2953
6	.5489 .5493	.5497	.5546	.5613	.5758	.6120	1.0000	.5898	.5268	.4845	.4512	.4235	.3999	.3793	.3612	.3452	.3317	.3187	.3070	.2964
7	.5139 .5143	.5146	.5178	.5220	.5305	.5485	.5898	1.0000	.5717	.5086	.4668	.4346	.4081	.3856	.3660	.3490	.3349	.3212	.3090	.2981
8	.4829 .4832	.4834	.4857	.4885	.4941	.5052	.5268	.5717	1.0000	.5560	.4927	.4516	.4202	.3946	.3730	.3544	.3393	.3247	.3119	.3004
9	.4552 .4554	.4556	.4574	.4593	.4632	.4707	.4845	.5086	.5560	1.0000	.5422	.4789	.4383	.4076	.3827	.3619	.3453	.3296	.3158	.3036
10	.4304 .4305	.4306	.4319	.4334	.4362	.4416	.4512	.4668	.4927	.5422	1.0000	.5303	.4670	.4268	.3965	.3723	.3536	.3360	.3210	.3078
11	.4081 .4082	.4083	.4093	.4104	.4125	.4165	.4235	.4346	.4516	.4789	.5303	1.0000	.5199	.4564	.4163	.3866	.3648	.3446	.3277	.3133
12	.3882 .3883	.3884	.3892	.3900	.3916	.3946	.3999	.4081	.4202	.4383	.4670	.5199	1.0000	.5104	.4467	.4070	.3802	.3561	.3366	.3203
13	.3703 .3704	.3704	.3710	.3717	.3729	.3753	.3793	.3856	.3946	.4076	.4268	.4564	.5104	1.0000	.5017	.4380	.4023	.3718	.3484	.3294
14	.3541 .3542	.3542	.3547	.3553	.3562	.3581	.3612	.3660	.3730	.3827	.3965	.4163	.4467	.5017	1.0000	.4940	.4369	.3942	.3643	.3413
15	.3396 .3396	.3397	.3401	.3405	.3413	.3427	.3452	.3490	.3544	.3619	.3723	.3866	.4070	.4380	.4940	1.0000	.5057	.4290	.3869	.3575
16	.3272 .3272	.3273	.3276	.3279	.3285	.3297	.3317	.3349	.3393	.3453	.3536	.3648	.3802	.4023	.4369	.5057	1.0000	.4805	.4165	.3777
17	.3150 .3151	.3151	.3154	.3156	.3161	.3171	.3187	.3212	.3247	.3296	.3360	.3446	.3561	.3718	.3942	.4290	.4805	1.0000	.4746	.4105
18	.3040 .3040	.3041	.3043	.3045	.3049	.3056	.3070	.3090	.3119	.3158	.3210	.3277	.3366	.3484	.3643	.3869	.4165	.4746	1.0000	.4691
19	.2940 .2940	.2940	.2942	.2944	.2947	.2953	.2964	.2981	.3004	.3036	.3078	.3133	.3203	.3294	.3413	.3575	.3777	.4105	.4691	1.0000

TABLE E.1.2
CARBON DIOXIDE TRANSMISSION FUNCTION FOR
SPECTRAL INTERVAL 660 - 800 cm^{-1}

	LAT = ± 15 DEG.		LAT = ± 30 DEG.		LAT = ± 45 DEG.		LAT = ± 60 DEG.		LAT = ± 75 DEG.	
1	.97740	.98079	.97816	.98172	.97917	.98296	.97926	.98314	.97938	.98343
2	.92896	.93011	.92431	.92541	.91971	.92073	.92044	.92146	.91959	.92060
3	.92401	.92510	.91432	.91530	.89829	.89912	.89369	.89444	.89152	.89224
4	.92256	.92364	.91019	.91114	.88822	.88897	.88064	.88130	.87749	.87811
5	.92159	.92266	.90783	.90876	.88380	.88451	.87540	.87602	.87203	.87261
6	.92071	.92177	.90611	.90703	.88154	.88225	.87313	.87373	.86956	.87013
7	.92001	.92107	.90481	.90572	.88033	.88102	.87184	.87244	.86824	.86880
8	.91946	.92052	.90373	.90463	.87961	.88030	.87102	.87161	.86757	.86812
9	.91892	.91997	.90274	.90364	.87899	.87967	.87043	.87102	.86707	.86761
10	.91837	.91941	.90183	.90272	.87845	.87913	.86990	.87048	.86661	.86715
11	.91782	.91886	.90099	.90187	.87799	.87867	.86943	.87001	.86620	.86673
12	.91727	.91831	.90016	.90103	.87757	.87825	.86901	.86959	.86584	.86638
13	.91681	.91785	.89934	.90021	.87720	.87787	.86867	.86924	.86554	.86608
14	.91645	.91748	.89870	.89956	.87687	.87753	.86838	.86895	.86530	.86583
15	.91608	.91711	.89812	.89898	.87654	.87720	.86813	.86870	.86508	.86561
16	.91573	.91675	.89758	.89843	.87620	.87686	.86787	.86844	.86486	.86539
17	.91536	.91638	.89703	.89788	.87587	.87652	.86763	.86819	.86464	.86517
18	.91500	.91602	.89650	.89734	.87554	.87620	.86737	.86794	.86443	.86495
19	.91464	.91565	.89597	.89681	.87521	.87586	.86713	.86769	.86421	.86473

TABLE E.11.1
 OZONE TRANSMISSION FUNCTIONS FOR SPECTRAL
 INTERVAL $800 - 1200 \text{ CM}^{-1}$ FOR PATHS BETWEEN
 1 MB AND LEVEL I AND BETWEEN 5 MB AND
 LEVEL I AS A FUNCTION OF LATITUDE

	1	2	3	4	5	6	7	8	9	10
1	1.00000	.93307	.92787	.92638	.92537	.92446	.92375	.92318	.92262	.92205
2	.93307	1.00000	.98507	.98243	.98067	.97909	.97786	.97688	.97592	.97495
3	.92787	.98507	1.00000	.99698	.99498	.99319	.99179	.99069	.98960	.98851
4	.92638	.98243	.99698	1.00000	.99794	.99611	.99467	.99354	.99243	.99131
5	.92537	.98067	.99498	.99794	1.00000	.99813	.99668	.99553	.99440	.99326
6	.92446	.97909	.99319	.99611	.99813	1.00000	.99852	.99736	.99621	.99506
7	.92375	.97786	.99179	.99467	.99668	.99852	1.00000	.99882	.99766	.99650
8	.92318	.97688	.99069	.99354	.99553	.99736	.99882	1.00000	.99883	.99765
9	.92262	.97592	.98960	.99243	.99440	.99621	.99766	.99883	1.00000	.99881
10	.92205	.97495	.98851	.99131	.99326	.99506	.99650	.99765	.99881	1.00000
11	.92148	.97399	.98743	.99021	.99214	.99392	.99534	.99649	.99764	.99882
12	.92091	.97304	.98636	.98911	.99102	.99279	.99420	.99534	.99648	.99765
13	.92044	.97225	.98547	.98820	.99010	.99185	.99326	.99439	.99552	.99668
14	.92007	.97163	.98477	.98749	.98938	.99112	.99251	.99363	.99476	.99591
15	.91969	.97100	.98406	.98676	.98864	.99037	.99176	.99287	.99399	.99513
16	.91932	.97038	.98337	.98606	.98792	.98964	.99102	.99213	.99324	.99438
17	.91895	.96975	.98267	.98534	.98720	.98891	.99028	.99138	.99249	.99362
18	.91857	.96914	.98198	.98464	.98648	.98818	.98955	.99064	.99174	.99287
19	.91820	.96852	.98129	.98393	.98576	.98745	.98881	.98990	.99099	.99211

TABLE E.11.2

OZONE TRANSMISSION FUNCTION FOR SPECTRAL
 INTERVAL 800 - 1200 cm^{-1} FOR PATHS BETWEEN
 LEVELS I AND J AT LATITUDES ± 15 DEG.

	10	11	12	13	14	15	16	17	18	19
1	.92205	.92148	.92091	.92044	.92007	.91969	.91932	.91895	.91857	.91820
2	.97495	.97399	.97304	.97225	.97163	.97100	.97038	.96975	.96914	.96852
3	.98851	.98743	.98636	.98547	.98477	.98406	.98337	.98267	.98198	.98129
4	.99131	.99021	.98911	.98820	.98749	.98676	.98606	.98534	.98464	.98393
5	.99326	.99214	.99102	.99010	.98938	.98864	.98792	.98720	.98648	.98576
6	.99506	.99392	.99279	.99185	.99112	.99037	.98964	.98891	.98818	.98745
7	.99650	.99534	.99420	.99326	.99251	.99176	.99102	.99028	.98955	.98881
8	.99765	.99649	.99534	.99439	.99363	.99287	.99213	.99138	.99064	.98990
9	.99881	.99764	.99648	.99552	.99476	.99399	.99324	.99249	.99174	.99099
10	1.00000	.99882	.99765	.99668	.99591	.99513	.99438	.99362	.99287	.99211
11	.99882	1.00000	.99882	.99784	.99707	.99629	.99553	.99476	.99400	.99324
12	.99765	.99882	1.00000	.99901	.99824	.99745	.99668	.99591	.99514	.99437
13	.99668	.99784	.99901	1.00000	.99922	.99842	.99765	.99687	.99610	.99533
14	.99591	.99707	.99824	.99922	1.00000	.99920	.99843	.99764	.99687	.99609
15	.99513	.99629	.99745	.99842	.99920	1.00000	.99922	.99843	.99765	.99687
16	.99438	.99553	.99668	.99765	.99843	.99922	1.00000	.99921	.99842	.99764
17	.99362	.99476	.99591	.99687	.99764	.99843	.99921	1.00000	.99921	.99842
18	.99287	.99400	.99514	.99610	.99687	.99765	.99842	.99921	1.00000	.99921
19	.99211	.99324	.99437	.99533	.99609	.99687	.99764	.99842	.99921	1.00000

TABLE E.11.2 (CONT.)

OZONE TRANSMISSION FUNCTION FOR SPECTRAL

INTERVAL 800 - 1200 CM^{-1} FOR PATHS BETWEENLEVELS I AND J AT LATITUDES ± 15 DEG.ORIGINAL PAGE IS
OF POOR QUALITY

	1	2	3	4	5	6	7	8	9	10
1	1.00000	.92783	.91741	.91317	.91074	.90897	.90763	.90653	.90551	.90458
2	.92783	1.00000	.97106	.96338	.95903	.95590	.95355	.95163	.94987	.94826
3	.91741	.97106	1.00000	.99001	.98437	.98035	.97734	.97488	.97265	.97061
4	.91317	.96338	.99001	1.00000	.99386	.98949	.98622	.98356	.98114	.97893
5	.91074	.95903	.98437	.99386	1.00000	.99539	.99196	.98916	.98662	.98430
6	.90897	.95590	.98035	.98949	.99539	1.00000	.99644	.99353	.99090	.98850
7	.90763	.95355	.97734	.98622	.99196	.99644	1.00000	.99701	.99430	.99183
8	.90653	.95163	.97488	.98356	.98916	.99353	.99701	1.00000	.99723	.99470
9	.90551	.94987	.97265	.98114	.98662	.99090	.99430	.99723	1.00000	.99742
10	.90458	.94826	.97061	.97893	.98430	.98850	.99183	.99470	.99742	1.00000
11	.90371	.94678	.96874	.97691	.98218	.98630	.98958	.99239	.99506	.99759
12	.90286	.94533	.96691	.97493	.98011	.98415	.98737	.99013	.99275	.99524
13	.90202	.94391	.96513	.97301	.97810	.98207	.98524	.98795	.99052	.99297
14	.90136	.94280	.96373	.97150	.97652	.98044	.98355	.98623	.98877	.99118
15	.90077	.94181	.96250	.97018	.97513	.97900	.98208	.98472	.98723	.98961
16	.90021	.94087	.96132	.96891	.97381	.97763	.98067	.98328	.98576	.98811
17	.89965	.93994	.96017	.96767	.97251	.97629	.97930	.98188	.98433	.98666
18	.89910	.93903	.95904	.96645	.97124	.97497	.97794	.98049	.98291	.98522
19	.89856	.93813	.95791	.96524	.96997	.97366	.97659	.97912	.98151	.98379

TABLE E.11.3

OZONE TRANSMISSION FUNCTION FOR SPECTRAL
INTERVAL 800 - 1200 CM⁻¹ FOR PATHS BETWEEN
LEVELS I AND J AT LATITUDES ±30 DEG.

ORIGINAL PAGE IS
 OF POOR QUALITY

	10	11	12	13	14	15	16	17	18	19
1	.90458	.90371	.90286	.90202	.90136	.90077	.90021	.89965	.89910	.89856
2	.94826	.94678	.94533	.94391	.94280	.94181	.94087	.93994	.93903	.93813
3	.97061	.96874	.96691	.96513	.96373	.96250	.96132	.96017	.95904	.95791
4	.97893	.97691	.97493	.97301	.97150	.97018	.96891	.96767	.96645	.96524
5	.98430	.98218	.98011	.97810	.97652	.97513	.97381	.97251	.97124	.96997
6	.98850	.98630	.98415	.98207	.98044	.97900	.97763	.97629	.97497	.97366
7	.99183	.98958	.98737	.98524	.98355	.98208	.98067	.97930	.97794	.97659
8	.99470	.99239	.99013	.98795	.98623	.98472	.98328	.98188	.98049	.97912
9	.99742	.99506	.99275	.99052	.98877	.98723	.98576	.98433	.98291	.98151
10	1.00000	.99759	.99524	.99297	.99118	.98961	.98811	.98666	.98522	.98379
11	.99759	1.00000	.99760	.99529	.99347	.99187	.99035	.98886	.98740	.98595
12	.99524	.99760	1.00000	.99765	.99579	.99417	.99261	.99110	.98961	.98813
13	.99297	.99529	.99765	1.00000	.99811	.99646	.99488	.99334	.99183	.99032
14	.99118	.99347	.99579	.99811	1.00000	.99832	.99672	.99516	.99363	.99210
15	.98961	.99187	.99417	.99646	.99832	1.00000	.99838	.99680	.99525	.99370
16	.98811	.99035	.99261	.99488	.99672	.99838	1.00000	.99840	.99683	.99527
17	.98666	.98886	.99110	.99334	.99516	.99680	.99840	1.00000	.99841	.99683
18	.98522	.98740	.98961	.99183	.99363	.99525	.99683	.99841	1.00000	.99840
19	.98379	.98595	.98813	.99032	.99210	.99370	.99527	.99683	.99840	1.00000

TABLE E.11.3 (CONT.)

OZONE TRANSMISSION FUNCTION FOR SPECTRAL

INTERVAL 800 - 1200 CM^{-1} FOR PATHS BETWEENLEVELS I AND J AT LATITUDES ± 30 DEG.

	1	2	3	4	5	6	7	8	9	10
1	1.00000	.92254	.90050	.89019	.88567	.88337	.88213	.88139	.88076	.88021
2	.92254	1.00000	.94956	.93005	.92169	.91748	.91524	.91394	.91282	.91185
3	.90050	.94956	1.00000	.96883	.95570	.94918	.94574	.94375	.94205	.94060
4	.89019	.93005	.96883	1.00000	.98261	.97402	.96953	.96694	.96474	.96286
5	.88567	.92169	.95570	.98261	1.00000	.99002	.98482	.98182	.97929	.97712
6	.88337	.91748	.94918	.97402	.99002	1.00000	.99434	.99109	.98834	.98600
7	.88213	.91524	.94574	.96953	.98482	.99434	1.00000	.99660	.99372	.99127
8	.88139	.91394	.94375	.96694	.98182	.99109	.99660	1.00000	.99705	.99452
9	.88076	.91282	.94205	.96474	.97929	.98834	.99372	.99705	1.00000	.99742
10	.88021	.91185	.94060	.96286	.97712	.98600	.99127	.99452	.99742	1.00000
11	.87974	.91104	.93937	.96128	.97531	.98403	.98921	.99241	.99526	.99780
12	.87931	.91030	.93827	.95987	.97369	.98228	.98738	.99053	.99334	.99584
13	.87893	.90965	.93731	.95863	.97227	.98074	.98578	.98889	.99165	.99412
14	.87859	.90906	.93644	.95752	.97100	.97937	.98435	.98742	.99015	.99259
15	.87825	.90849	.93560	.95644	.96977	.97804	.98296	.98599	.98869	.99110
16	.87790	.90790	.93473	.95534	.96850	.97668	.98153	.98453	.98720	.98958
17	.87757	.90733	.93389	.95427	.96728	.97536	.98016	.98312	.98576	.98811
18	.87723	.90676	.93306	.95322	.96609	.97407	.97881	.98174	.98434	.98667
19	.87690	.90620	.93224	.95217	.96489	.97278	.97747	.98036	.98293	.98523

TABLE E.11.4

OZONE TRANSMISSION FUNCTION FOR SPECTRAL
INTERVAL 800 - 1200 CM^{-1} FOR PATHS BETWEEN
LEVELS I AND J AT LATITUDES ± 45 DEG.

	10	11	12	13	14	15	16	17	18	19
1	.88021	.87974	.87931	.87893	.87859	.87825	.87790	.87757	.87723	.87690
2	.91185	.91104	.91030	.90965	.90906	.90849	.90790	.90733	.90676	.90620
3	.94060	.93937	.93827	.93731	.93644	.93560	.93473	.93389	.93306	.93224
4	.96286	.96128	.95987	.95863	.95752	.95644	.95534	.95427	.95322	.95217
5	.97712	.97531	.97369	.97227	.97100	.96977	.96850	.96728	.96609	.96489
6	.98600	.98403	.98228	.98074	.97937	.97804	.97668	.97536	.97407	.97278
7	.99127	.98921	.98738	.98578	.98435	.98296	.98153	.98016	.97881	.97747
8	.99452	.99241	.99053	.98889	.98742	.98599	.98453	.98312	.98174	.98036
9	.99742	.99526	.99334	.99165	.99015	.98869	.98720	.98576	.98434	.98293
10	1.00000	.99780	.99584	.99412	.99259	.99110	.98958	.98811	.98667	.98523
11	.99780	1.00000	.99801	.99626	.99470	.99319	.99164	.99015	.98868	.98722
12	.99584	.99801	1.00000	.99823	.99665	.99511	.99354	.99202	.99054	.98906
13	.99412	.99626	.99823	1.00000	.99839	.99684	.99525	.99371	.99220	.99070
14	.99259	.99470	.99665	.99839	1.00000	.99843	.99682	.99526	.99374	.99222
15	.99110	.99319	.99511	.99684	.99843	1.00000	.99837	.99680	.99526	.99372
16	.98958	.99164	.99354	.99525	.99682	.99837	1.00000	.99841	.99685	.99529
17	.98811	.99015	.99202	.99371	.99526	.99680	.99841	1.00000	.99842	.99685
18	.98667	.98868	.99054	.99220	.99374	.99526	.99685	.99842	1.00000	.99841
19	.98523	.98722	.98906	.99070	.99222	.99372	.99529	.99685	.99841	1.00000

TABLE E.11.4 (CONT.)

OZONE TRANSMISSION FUNCTION FOR SPECTRAL
INTERVAL 800 - 1200 CM⁻¹ FOR PATHS BETWEEN
LEVELS I AND J AT LATITUDES ± 45 DEG.

	1	2	3	4	5	6	7	8	9	10
1	1.00000	.92327	.89565	.88233	.87697	.87465	.87334	.87251	.87190	.87136
2	.92327	1.00000	.93799	.91376	.90434	.90032	.89807	.89667	.89565	.89475
3	.89565	.93799	1.00000	.95617	.93968	.93276	.92894	.92657	.92489	.92340
4	.88233	.91376	.95617	1.00000	.97508	.96477	.95911	.95563	.95318	.95103
5	.87697	.90434	.93968	.97508	1.00000	.98713	.98010	.97579	.97277	.97012
6	.87465	.90032	.93276	.96477	.98713	1.00000	.99215	.98735	.98400	.98106
7	.87334	.89807	.92894	.95911	.98010	.99215	1.00000	.99488	.99130	.98817
8	.87251	.89667	.92657	.95563	.97579	.98735	.99488	1.00000	.99627	.99300
9	.87190	.89565	.92489	.95318	.97277	.98400	.99130	.99627	1.00000	.99664
10	.87136	.89475	.92340	.95103	.97012	.98106	.98817	.99300	.99664	1.00000
11	.87088	.89397	.92212	.94919	.96786	.97855	.98549	.99022	.99377	.99706
12	.87045	.89327	.92099	.94757	.96588	.97635	.98316	.98779	.99127	.99449
13	.87010	.89271	.92007	.94626	.96428	.97459	.98128	.98583	.98925	.99242
14	.86981	.89223	.91931	.94518	.96297	.97313	.97973	.98422	.98760	.99072
15	.86955	.89182	.91864	.94423	.96181	.97185	.97837	.98281	.98614	.98923
16	.86930	.89140	.91799	.94330	.96068	.97061	.97705	.98143	.98473	.98778
17	.86904	.89100	.91734	.94238	.95956	.96937	.97574	.98007	.98332	.98634
18	.86878	.89058	.91668	.94145	.95843	.96813	.97442	.97869	.98191	.98488
19	.86853	.89019	.91605	.94057	.95737	.96695	.97316	.97739	.98057	.98351

TABLE E.11.5

OZONE TRANSMISSION FUNCTION FOR SPECTRAL
 INTERVAL 800 - 1200 CM^{-1} FOR PATHS BETWEEN
 LEVELS I AND J AT LATITUDES ± 60 DEG.

	10	11	12	13	14	15	16	17	18	19
1	.87136	.87088	.87045	.87010	.86981	.86955	.86930	.86904	.86878	.86853
2	.89475	.89397	.89327	.89271	.89223	.89182	.89140	.89100	.89058	.89019
3	.92340	.92212	.92099	.92007	.91931	.91864	.91799	.91734	.91668	.91605
4	.95103	.94919	.94757	.94626	.94518	.94423	.94330	.94238	.94145	.94057
5	.97012	.96786	.96588	.96428	.96297	.96181	.96068	.95956	.95843	.95737
6	.98106	.97855	.97635	.97459	.97313	.97185	.97061	.96937	.96813	.96695
7	.98817	.98549	.98316	.98128	.97973	.97837	.97705	.97574	.97442	.97316
8	.99300	.99022	.98779	.98583	.98422	.98281	.98143	.98007	.97869	.97739
9	.99664	.99377	.99127	.98925	.98760	.98614	.98473	.98332	.98191	.98057
10	1.00000	.99706	.99449	.99242	.99072	.98923	.98778	.98634	.98488	.98351
11	.99706	1.00000	.99737	.99526	.99352	.99199	.99051	.98903	.98755	.98614
12	.99449	.99737	1.00000	.99784	.99607	.99451	.99299	.99149	.98998	.98854
13	.99242	.99526	.99784	1.00000	.99820	.99661	.99507	.99354	.99200	.99055
14	.99072	.99352	.99607	.99820	1.00000	.99839	.99683	.99528	.99372	.99225
15	.98923	.99199	.99451	.99661	.99839	1.00000	.99842	.99685	.99527	.99378
16	.98778	.99051	.99299	.99507	.99683	.99842	1.00000	.99841	.99682	.99531
17	.98634	.98903	.99149	.99354	.99528	.99685	.99841	1.00000	.99838	.99685
18	.98488	.98755	.98998	.99200	.99372	.99527	.99682	.99838	1.00000	.99845
19	.98351	.98614	.98854	.99055	.99225	.99378	.99531	.99685	.99845	1.00000

TABLE E.11.5 (CONT.)

OZONE TRANSMISSION FUNCTION FOR SPECTRAL
INTERVAL 800 - 1200 CM⁻¹ FOR PATHS BETWEEN
LEVELS I AND J AT LATITUDES ±60 DEG.

	1	2	3	4	5	6	7	8	9	10
1	1.00000	.92227	.89332	.87900	.87344	.87092	.86957	.86889	.86837	.86790
2	.92227	1.00000	.93429	.90801	.89821	.89388	.89159	.89044	.88959	.88881
3	.89332	.93429	1.00000	.95006	.93225	.92456	.92056	.91857	.91712	.91581
4	.87900	.90801	.95006	1.00000	.97108	.95882	.95253	.94943	.94718	.94517
5	.87344	.89821	.93225	.97108	1.00000	.98406	.97594	.97196	.96907	.96651
6	.87092	.89388	.92456	.95882	.98406	1.00000	.99067	.98612	.98282	.97989
7	.86957	.89159	.92056	.95253	.97594	.99067	1.00000	.99507	.99150	.98835
8	.86889	.89044	.91857	.94943	.97196	.98612	.99507	1.00000	.99628	.99300
9	.86837	.88959	.91712	.94718	.96907	.98282	.99150	.99628	1.00000	.99661
10	.86790	.88881	.91581	.94517	.96651	.97989	.98835	.99300	.99661	1.00000
11	.86746	.88813	.91467	.94342	.96429	.97736	.98562	.99016	.99369	.99699
12	.86712	.88755	.91369	.94195	.96241	.97523	.98332	.98777	.99123	.99447
13	.86682	.88706	.91288	.94072	.96086	.97346	.98142	.98579	.98919	.99238
14	.86657	.88666	.91223	.93974	.95963	.97206	.97991	.98423	.98758	.99072
15	.86635	.88631	.91165	.93887	.95853	.97082	.97857	.98284	.98615	.98925
16	.86612	.88595	.91107	.93799	.95742	.96957	.97722	.98143	.98471	.98777
17	.86590	.88560	.91049	.93713	.95634	.96834	.97590	.98006	.98330	.98632
18	.86568	.88525	.90993	.93629	.95528	.96714	.97461	.97872	.98192	.98491
19	.86546	.88490	.90935	.93544	.95421	.96592	.97331	.97737	.98053	.98348

TABLE E-11.6
 OZONE TRANSMISSION FUNCTION FOR SPECTRAL
 INTERVAL 800 - 1200 CM⁻¹ FOR PATHS BETWEEN
 LEVELS I AND J AT LATITUDES ± 75 DEG.

	10	11	12	13	14	15	16	17	18	19
1	.86790	.86748	.86712	.86682	.86657	.86635	.86612	.86590	.86568	.86546
2	.88881	.88813	.88755	.88706	.88666	.88631	.88595	.88560	.88525	.88490
3	.91581	.91467	.91369	.91288	.91223	.91165	.91107	.91049	.90993	.90935
4	.94517	.94342	.94195	.94072	.93974	.93887	.93799	.93713	.93629	.93544
5	.96651	.96429	.96241	.96086	.95963	.95853	.95742	.95634	.95528	.95421
6	.97989	.97736	.97523	.97346	.97206	.97082	.96957	.96834	.96714	.96592
7	.98835	.98562	.98332	.98142	.97991	.97857	.97722	.97590	.97461	.97331
8	.99300	.99016	.98777	.98579	.98423	.98284	.98143	.98006	.97872	.97737
9	.99661	.99369	.99123	.98919	.98758	.98615	.98471	.98330	.98192	.98053
10	1.00000	.99699	.99447	.99238	.99072	.98925	.98777	.98632	.98491	.98348
11	.99699	1.00000	.99741	.99527	.99358	.99207	.99056	.98907	.98763	.98617
12	.99447	.99741	1.00000	.99782	.99609	.99455	.99301	.99150	.99002	.98853
13	.99238	.99527	.99782	1.00000	.99824	.99668	.99511	.99357	.99207	.99055
14	.99072	.99358	.99609	.99824	1.00000	.99841	.99682	.99526	.99374	.99221
15	.98925	.99207	.99455	.99668	.99841	1.00000	.99839	.99681	.99527	.99372
16	.98777	.99056	.99301	.99511	.99682	.99839	1.00000	.99840	.99684	.99527
17	.98632	.98907	.99150	.99357	.99526	.99681	.99840	1.00000	.99842	.99683
18	.98491	.98763	.99002	.99207	.99374	.99527	.99684	.99842	1.00000	.99839
19	.98348	.98617	.98853	.99055	.99221	.99372	.99527	.99683	.99839	1.00000

TABLE E.11.6 (CONT.)

OZONE TRANSMISSION FUNCTION FOR SPECTRAL
INTERVAL 800 - 1200 CM^{-1} FOR PATHS BETWEEN
LEVELS I AND J AT LATITUDES ± 75 DEG.

ORIGINAL PAGE IS
OF POOR QUALITY

Appendix F: Test Initial Conditions for the Model's Dynamics

Chao and Geller (1982) and Chao (1983) suggested some test initial conditions to detect errors in the dynamics part of primitive equation models. To test the linear terms in the model dynamics, Chao and Geller used normal mode initial conditions. Normal modes are the eigen solutions of the linearized primitive equations. They move around the earth's axis without change in shape and with known phase speed. Model output, after one time step starting from such initial conditions, can be compared with the expected analytic results. If any one of the prognostic variables deviates from the theoretical results, it is obvious that there is an error(s) in the formulation or in the coding of the equation governing that variable.

To test the nonlinear term Chao (1983) relied on hand calculation. He suggested simple initial conditions to make the hand calculation very easy.

Because the model is frequently revised, there is a constant need for testing. Thus, it is advisable to include these initial conditions as a part of the model to facilitate the error detection process. These initial conditions also serve as good tools for comparing the performance of different models.

Appendix G: Comparison of Simulated and Observed January and July Climatologies

In this appendix we present global sea level pressure, upper level and precipitation fields obtained by averaging the last 30 days of 45 days winter and summer climate integrations with the GLAS Fourth Order Model. These simulation experiments (number 3041 and 3040) were started from initial conditions corresponding to 15 December 1978 and 15 June 1979 respectively.

For comparison, we present climatological sea level pressure and 500 mb geopotential heights derived from 15 years of Northern Hemisphere NMC analysis (1963 to 1977) and 9 years of Southern Hemisphere Australian analysis (1972 to 1981), with no data between 20°N to 10°S. The observed sea level pressure and upper level fields corresponding to January and July 1979 derived from the ECMWF analysis are also shown for further comparison.

For the precipitation fields we present the monthly averaged computed precipitation rate (mm/day) and the climatological fields derived by Jaeger (1976). In these plots the scale is logarithmic (1, 2, 4, 8, 16 mm/day) and regions with more than 4 mm/day are shaded.

Legends

Figure G1.1 Simulated Sea Level Pressure (mb) - January

Figure G1.2 Observed Sea Level Pressure (mb) - January 1979

Figure G1.3 Climatological Sea Level Pressure (mb) - January

Figure G2.1 Simulated 500 mb Geopotential Height (m) - January

Figure G2.2 Observed 500 mb Geopotential Height (m) - January 1979

Figure G2.3 Climatological 500 mb Geopotential Height (m) - January

Figure G3.1 Simulated 200 mb Geopotential Height (m) - January

Figure G3.2 Observed 200 mb Geopotential Height (m) - January 1979

Appendix G: (cont.)

Figure G4.1 Simulated Precipitation Rate (mm/day) - January

Figure G4.2 Climatological Precipitation Rate (mm/day) - January

Figure G5.1 Simulated Sea Level Pressure (mb) - July

Figure G5.2 Observed Sea Level Pressure (mb) - July 1979

Figure G5.3 Climatological Sea Level Pressure (mb) - July

Figure G6.1 Simulated 500 mb Geopotential Height (m) - July

Figure G6.2 Observed 500 mb Geopotential Height (m) - July 1979

Figure G6.3 Climatological 500 mb Geopotential Height (m) - July

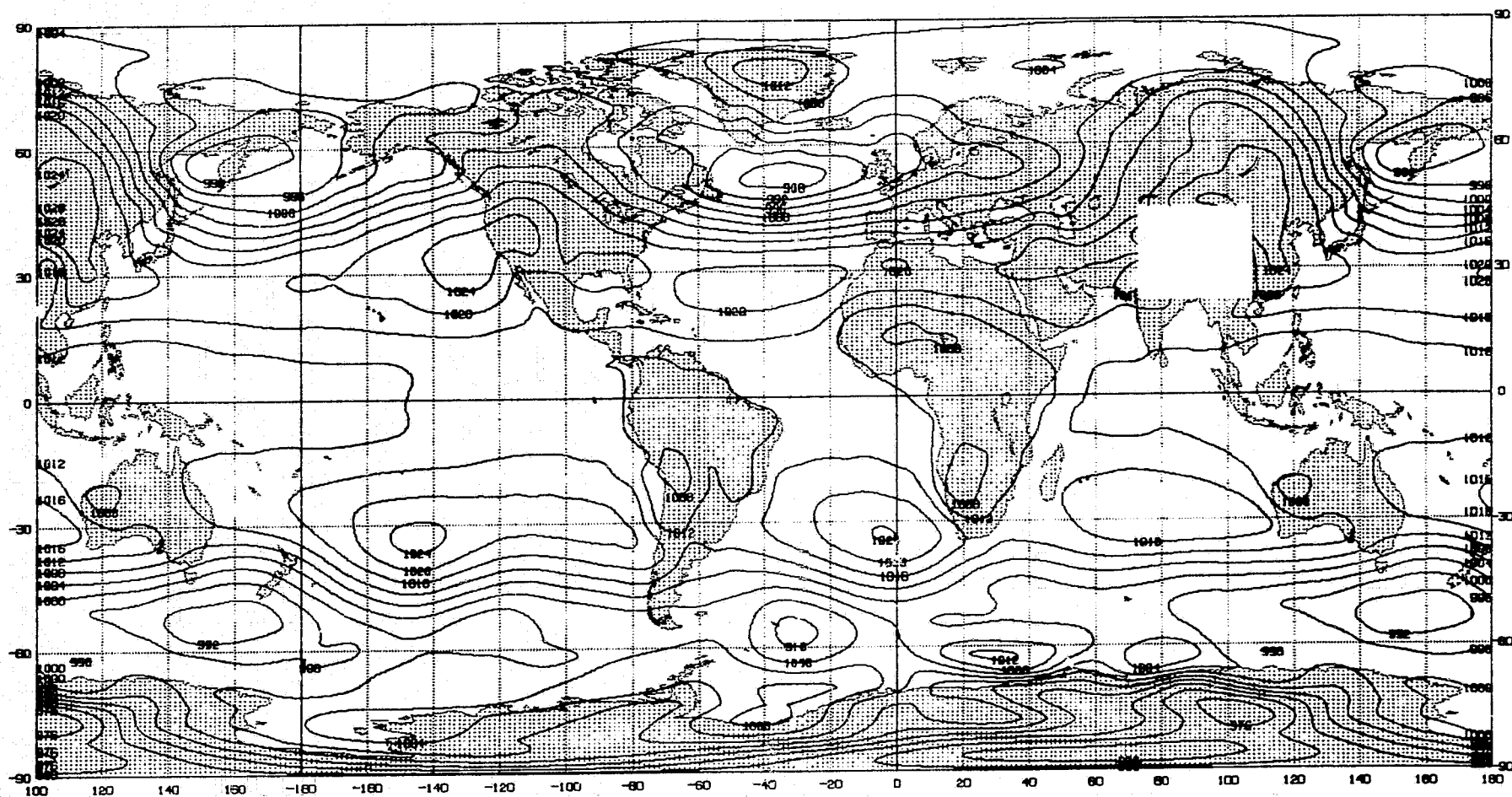
Figure G7.1 Simulated 200 mb Geopotential Height (m) - July

Figure G7.2 Observed 200 mb Geopotential Height (m) - July 1979

Figure G8.1 Simulated Precipitation Rate (mm/day) - July

Figure G8.2 Climatological Precipitation Rate (mm/day) - July

G-3



G-4

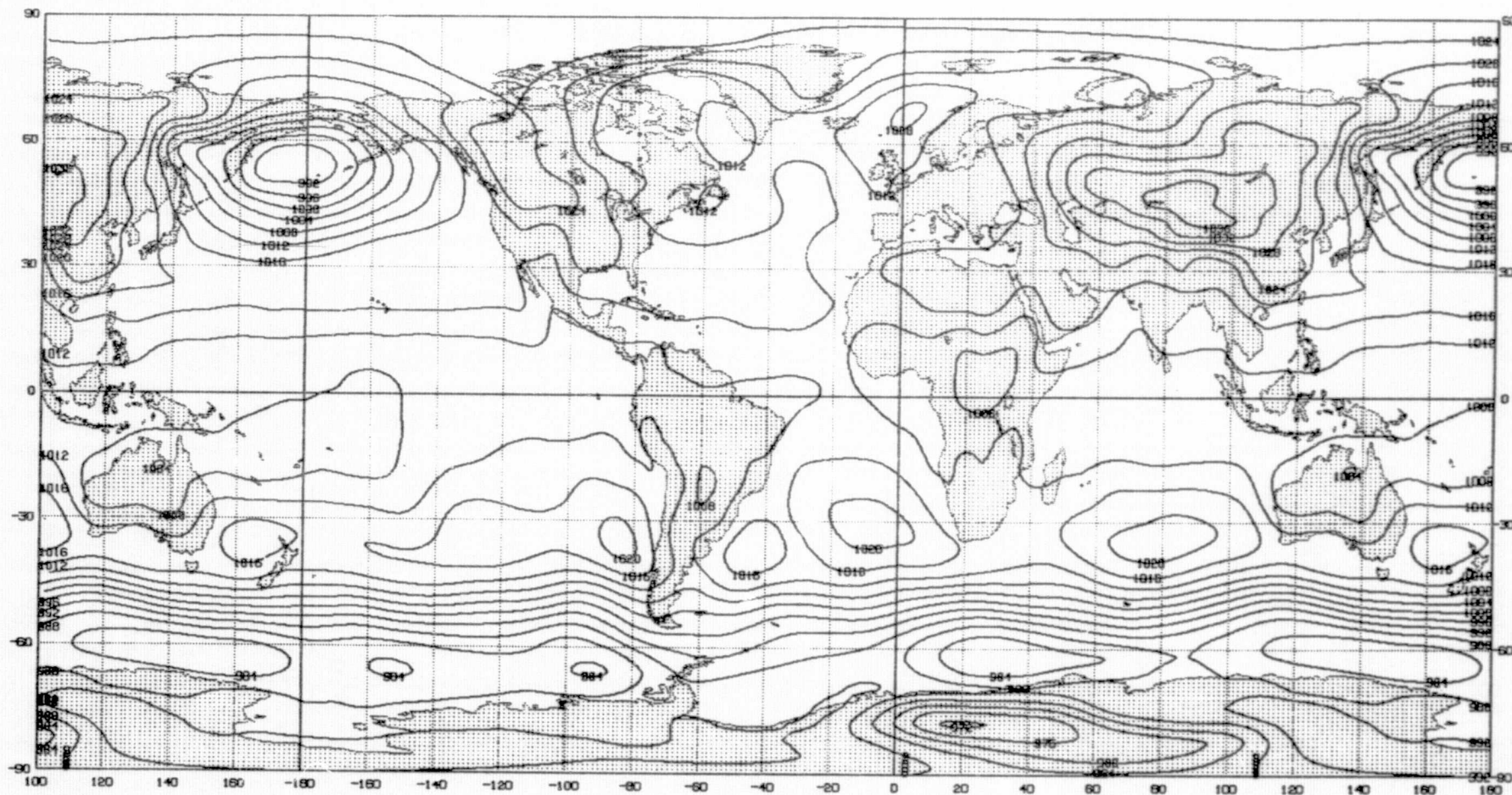


Figure G1.2 Observed Sea Level Pressure (mb) - January 1979

ORIGINAL PAGE IS
OF POOR QUALITY

G-5

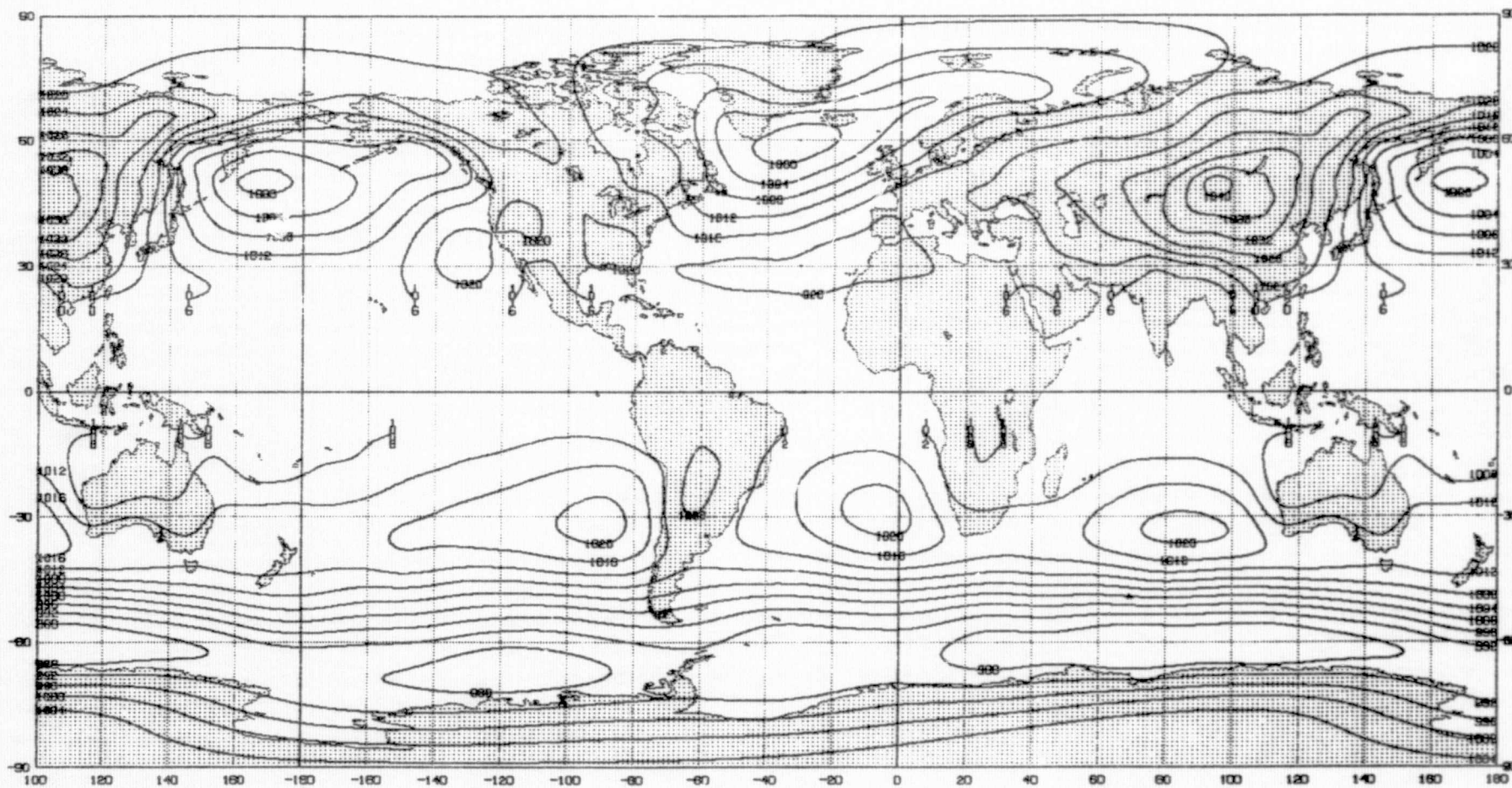


Figure G1.3 Climatological Sea Level Pressure (mb) - January

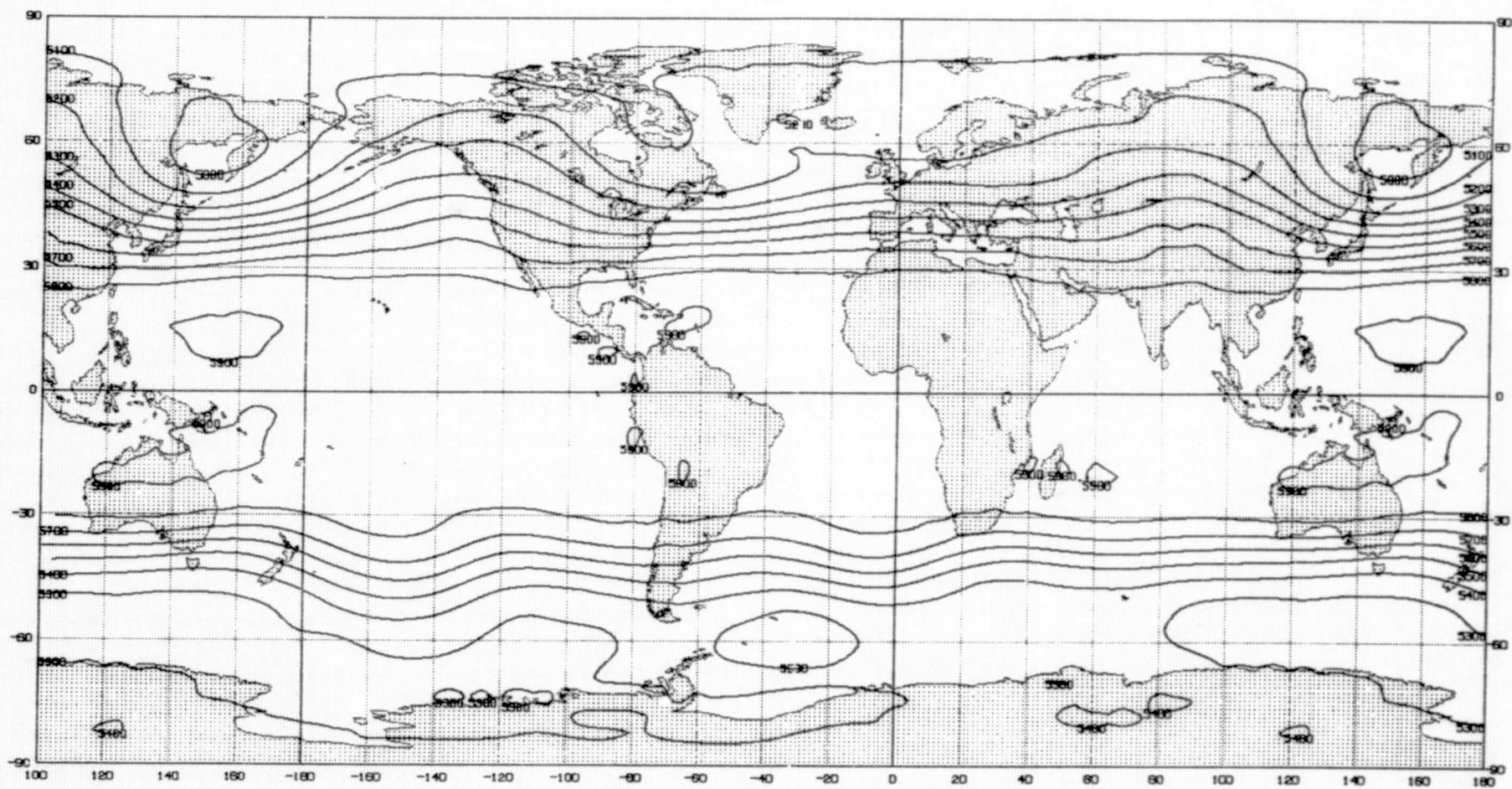


Figure G2.1 Simulated 500 mb Geopotential Height (m) - January

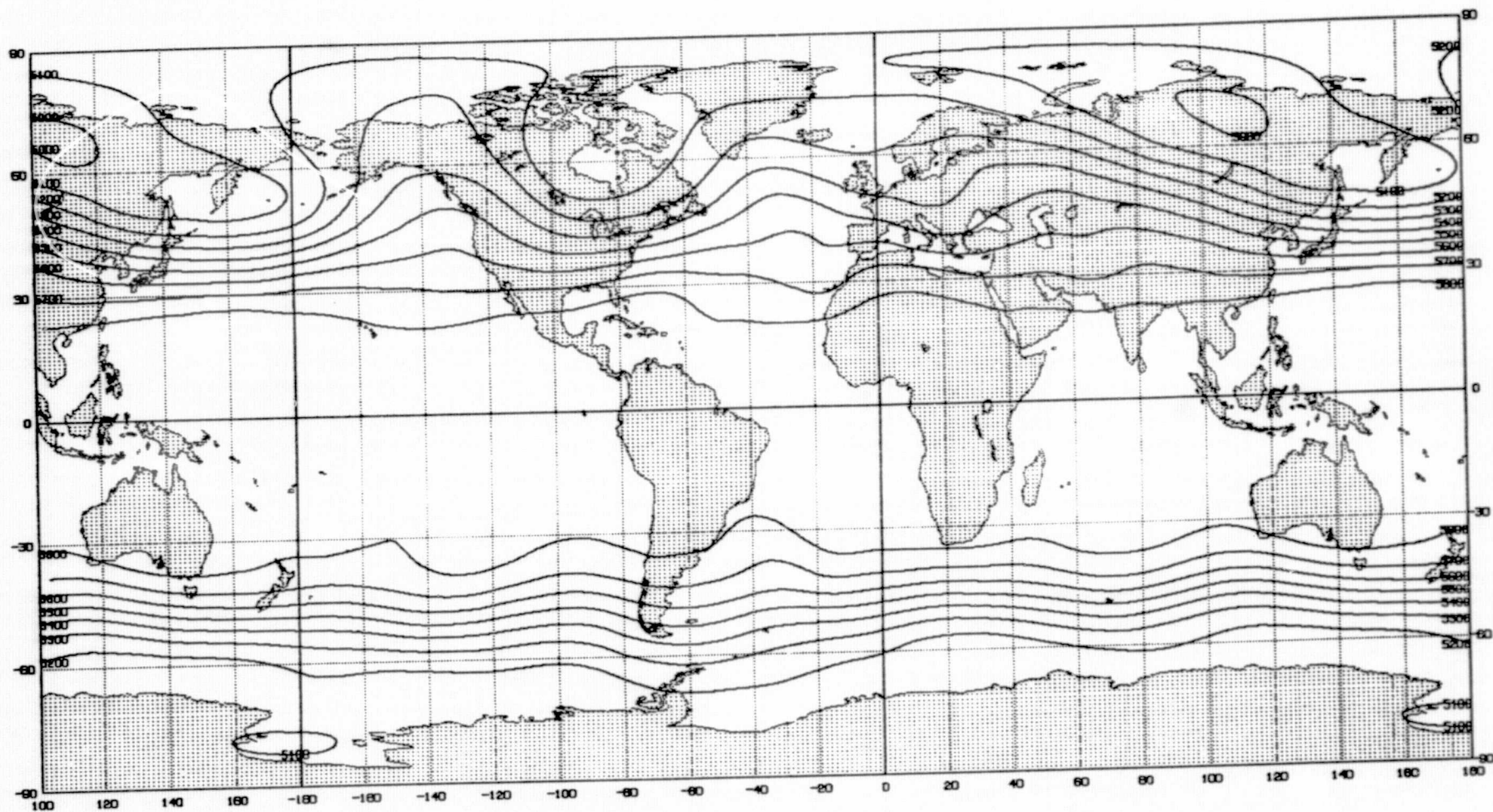


Figure G2.2 Observed 500 mb Geopotential Height (m) - January 1979

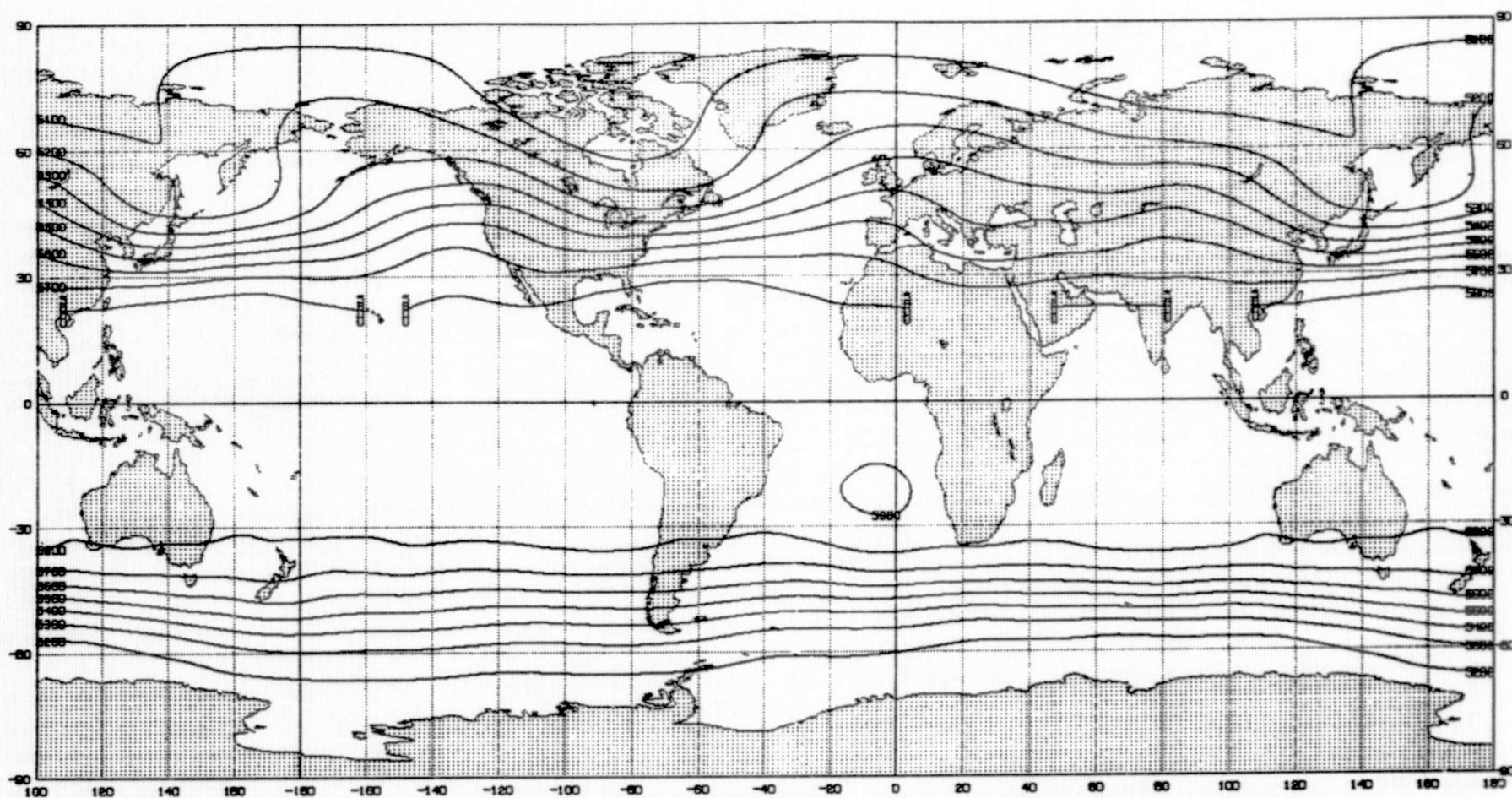


Figure G2.3 Climatological 500 mb Geopotential Height (m) - January

G-9

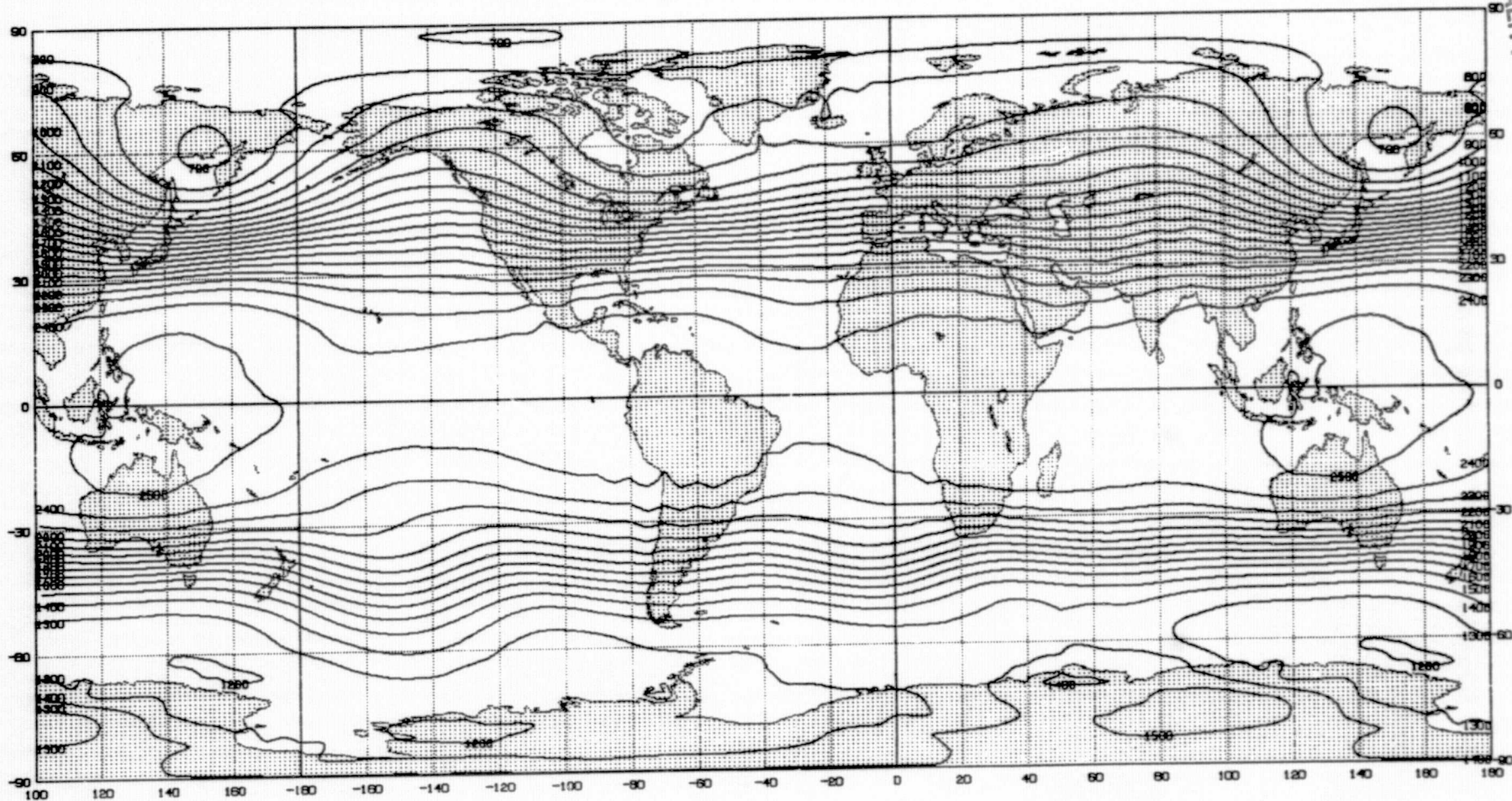


Figure G3.1 Simulated 200 mb Geopotential Height (m) - January

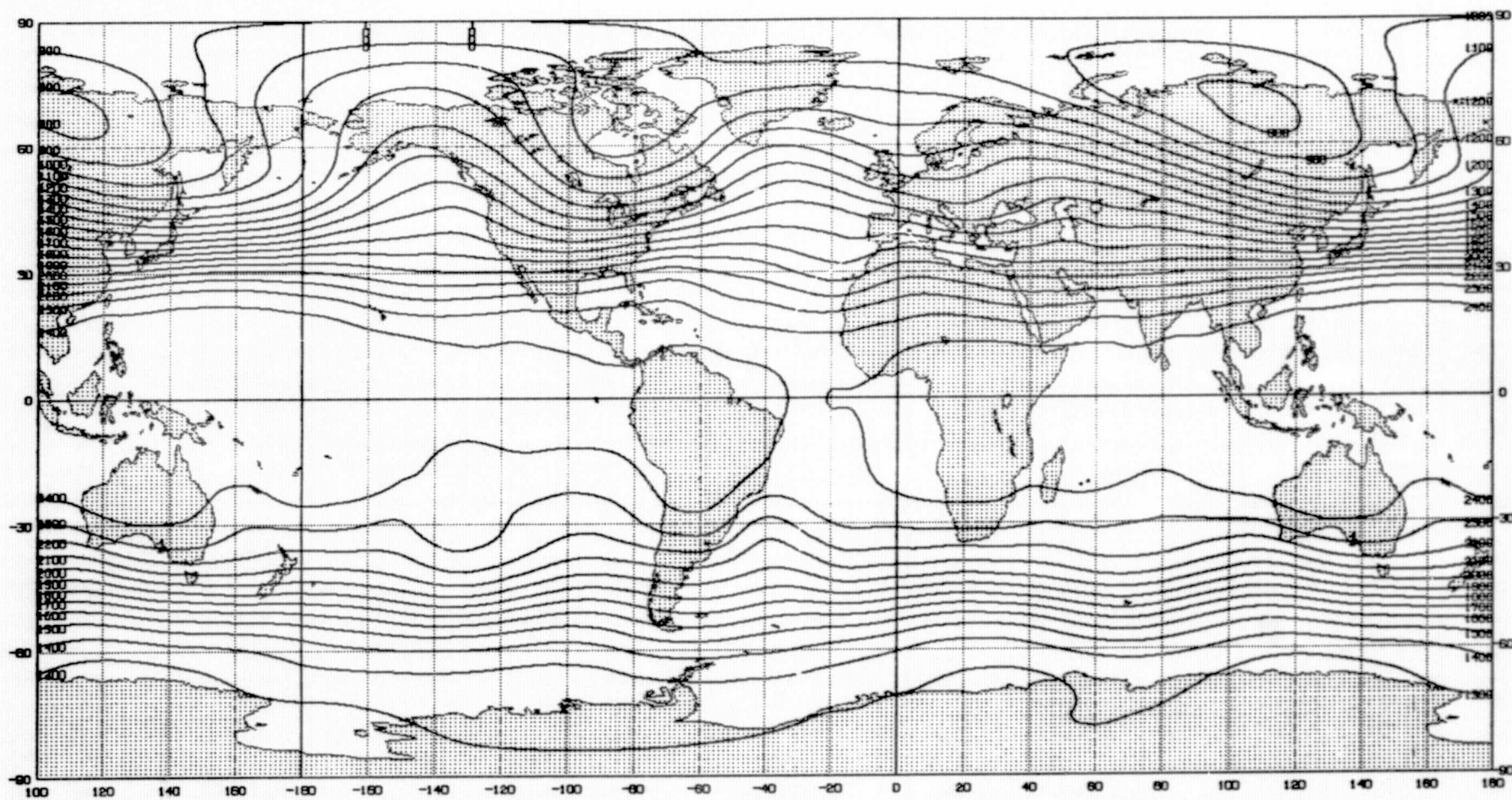


Figure G3.2 Observed 200 mb Geopotential Height (m) - January 1979

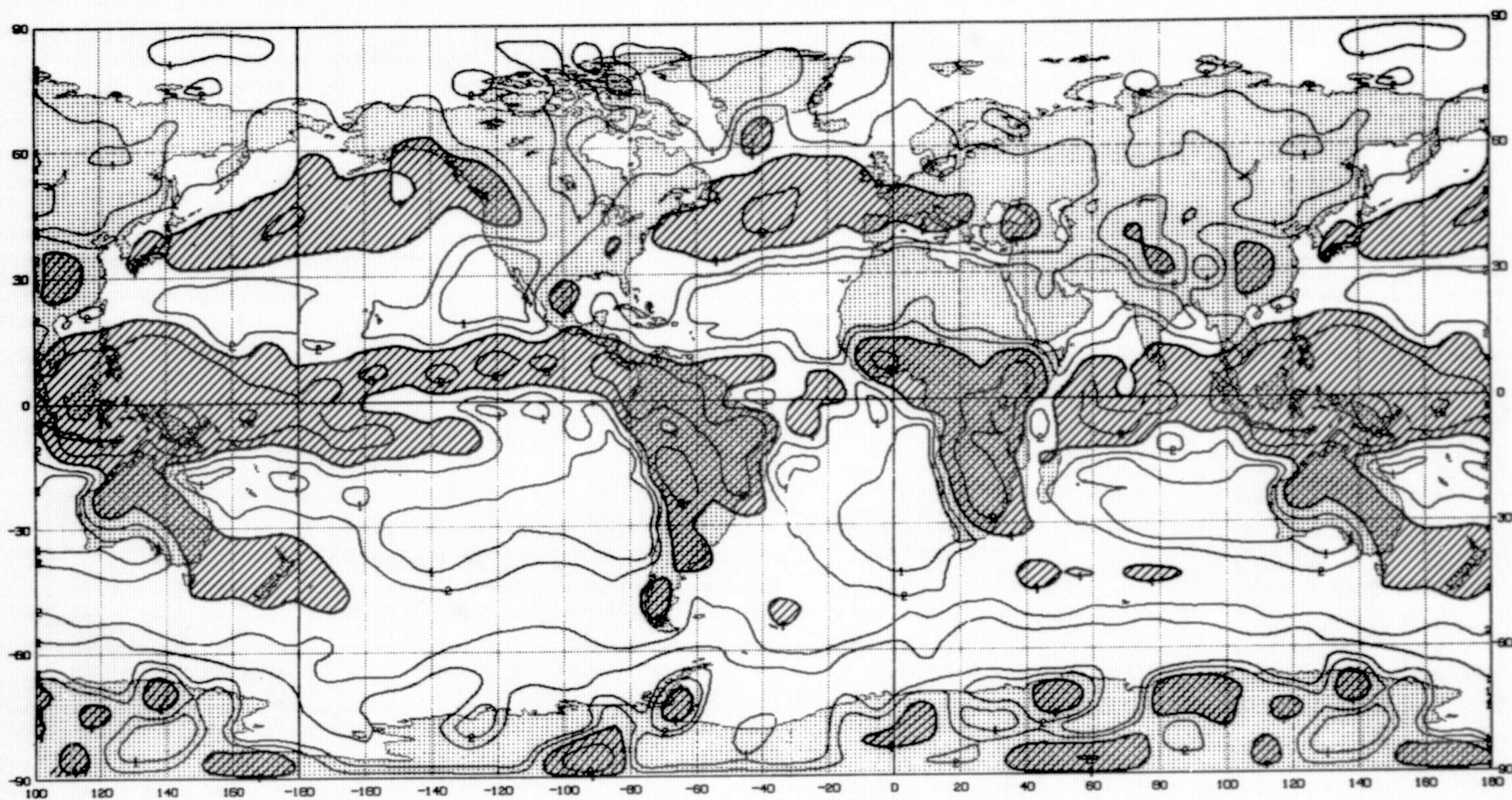


Figure G4.1 Simulated Precipitation Rate (mm/day) - January

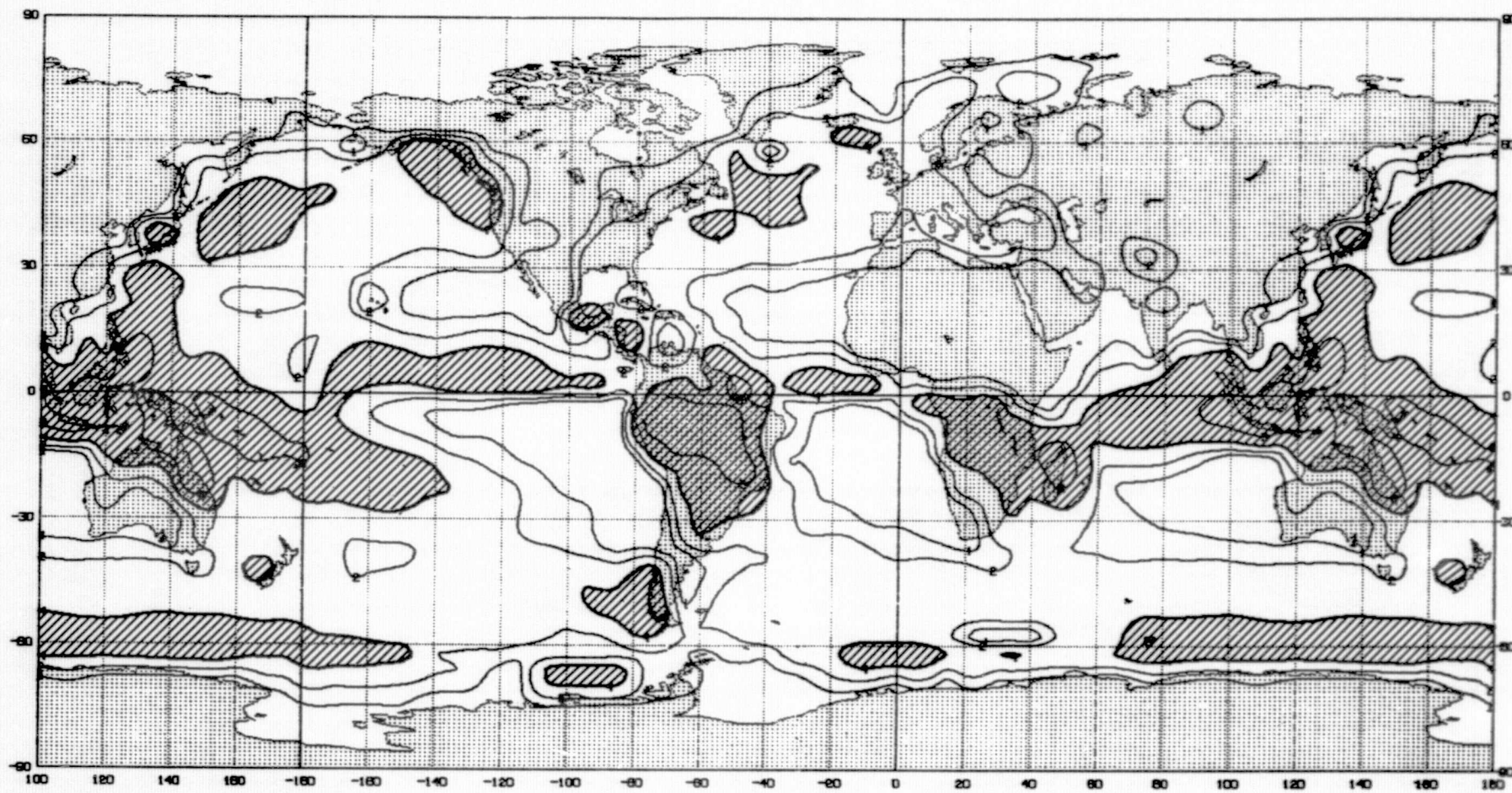
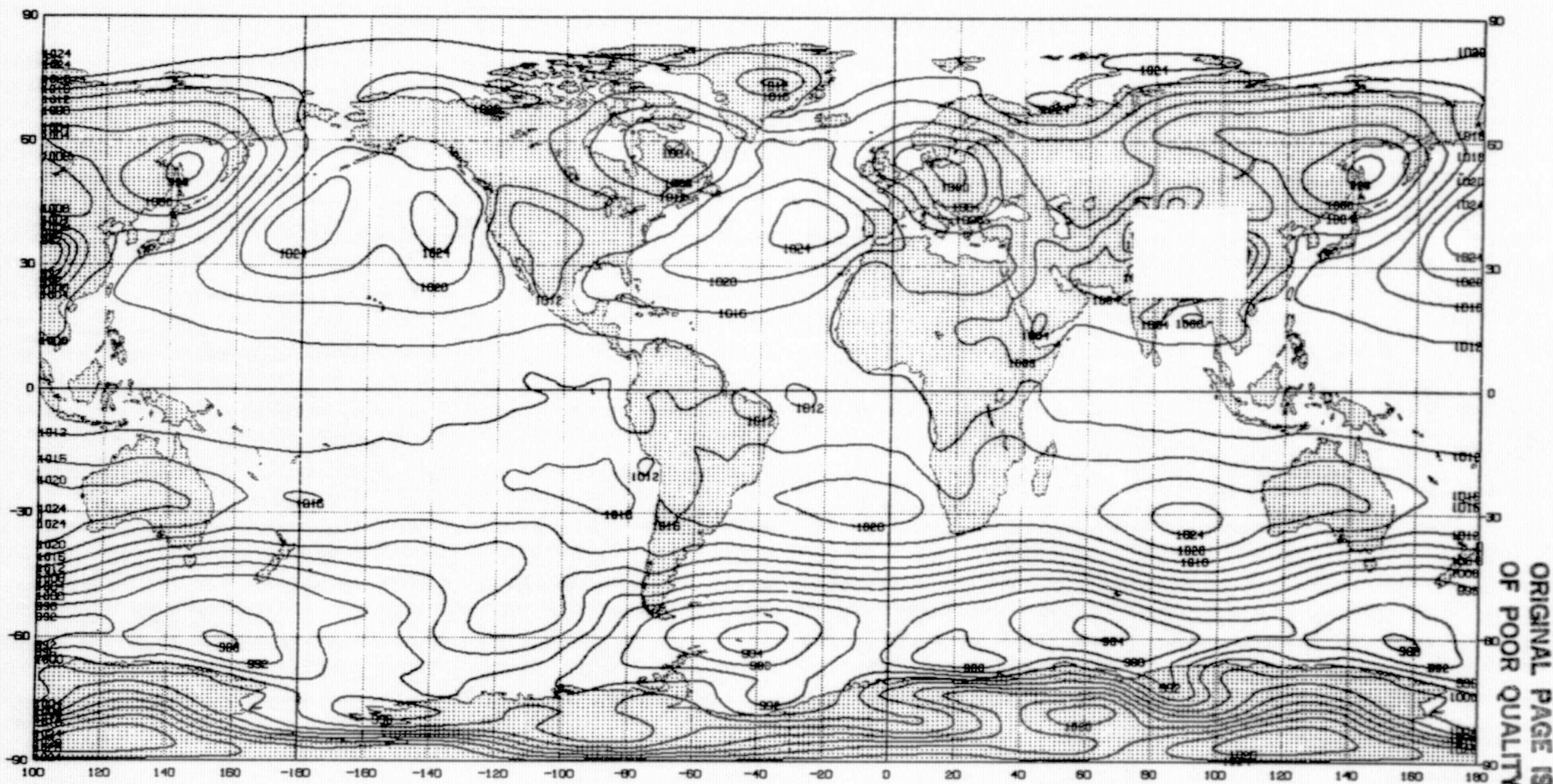


Figure G4.2 Climatological Precipitation Rate (mm/day) - January



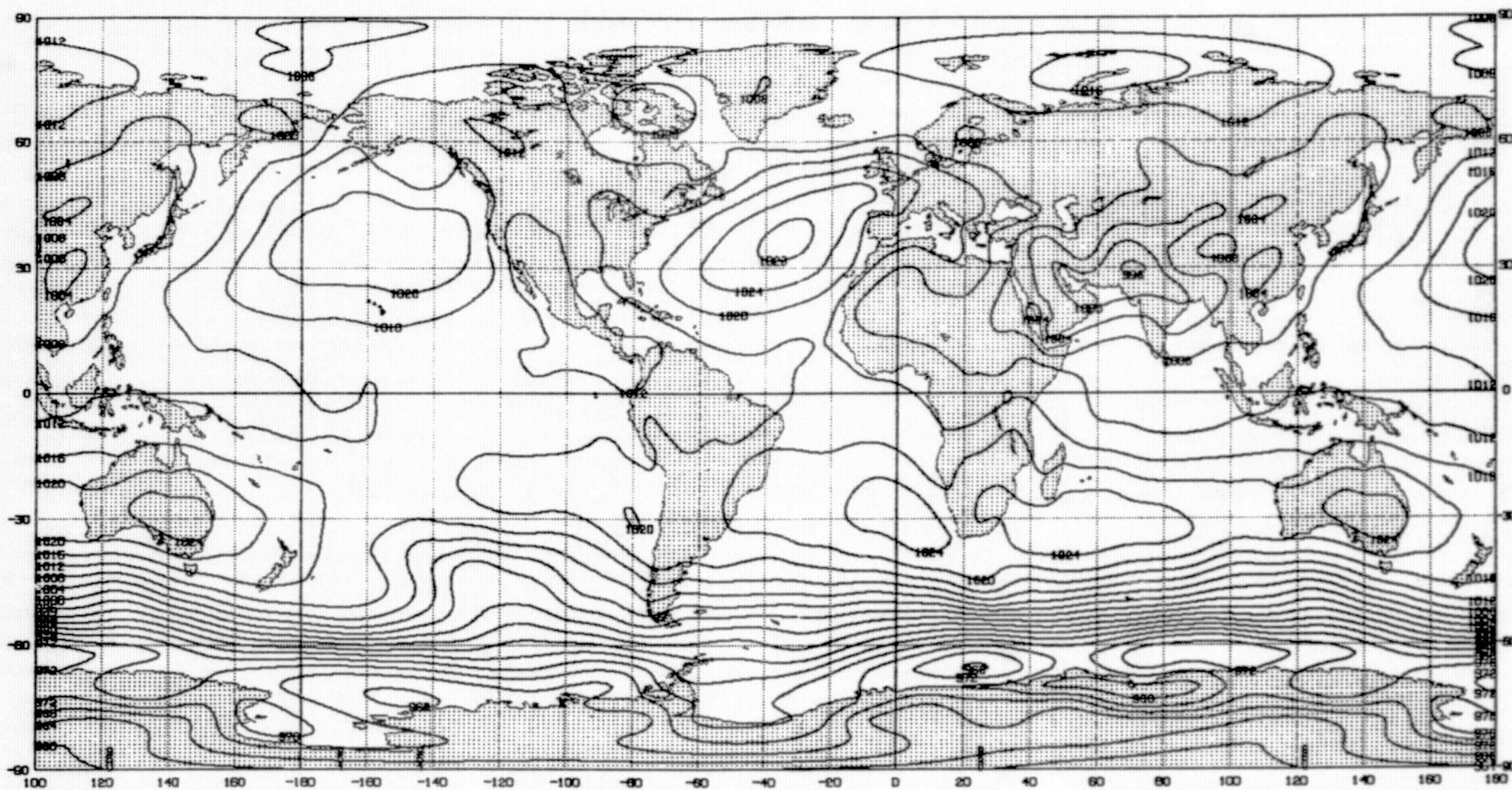


Figure G5.2 Observed Sea Level Pressure (mb) - July 1979

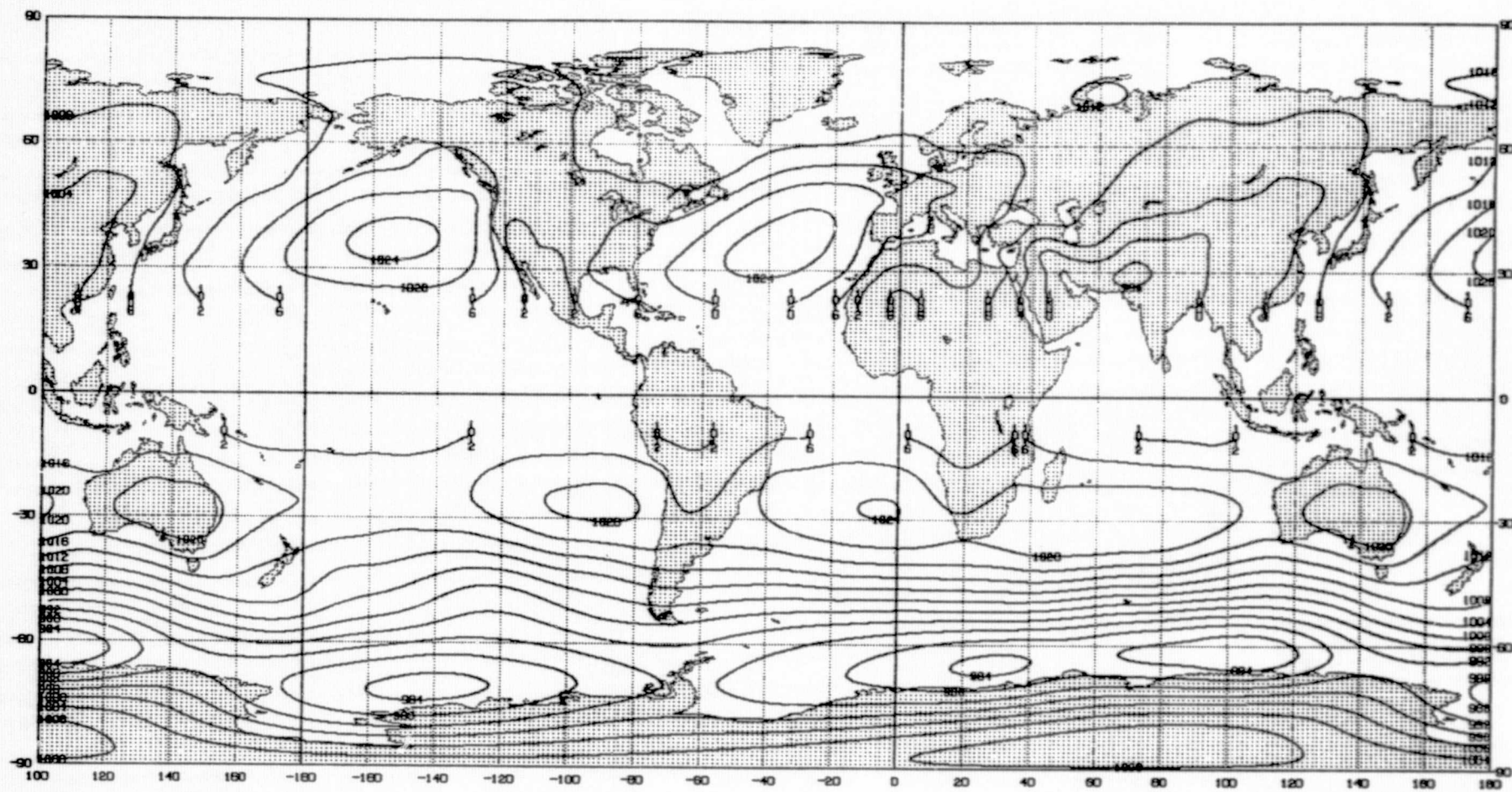


Figure G5.3 Climatological Sea Level Pressure (mb) - July

G-16

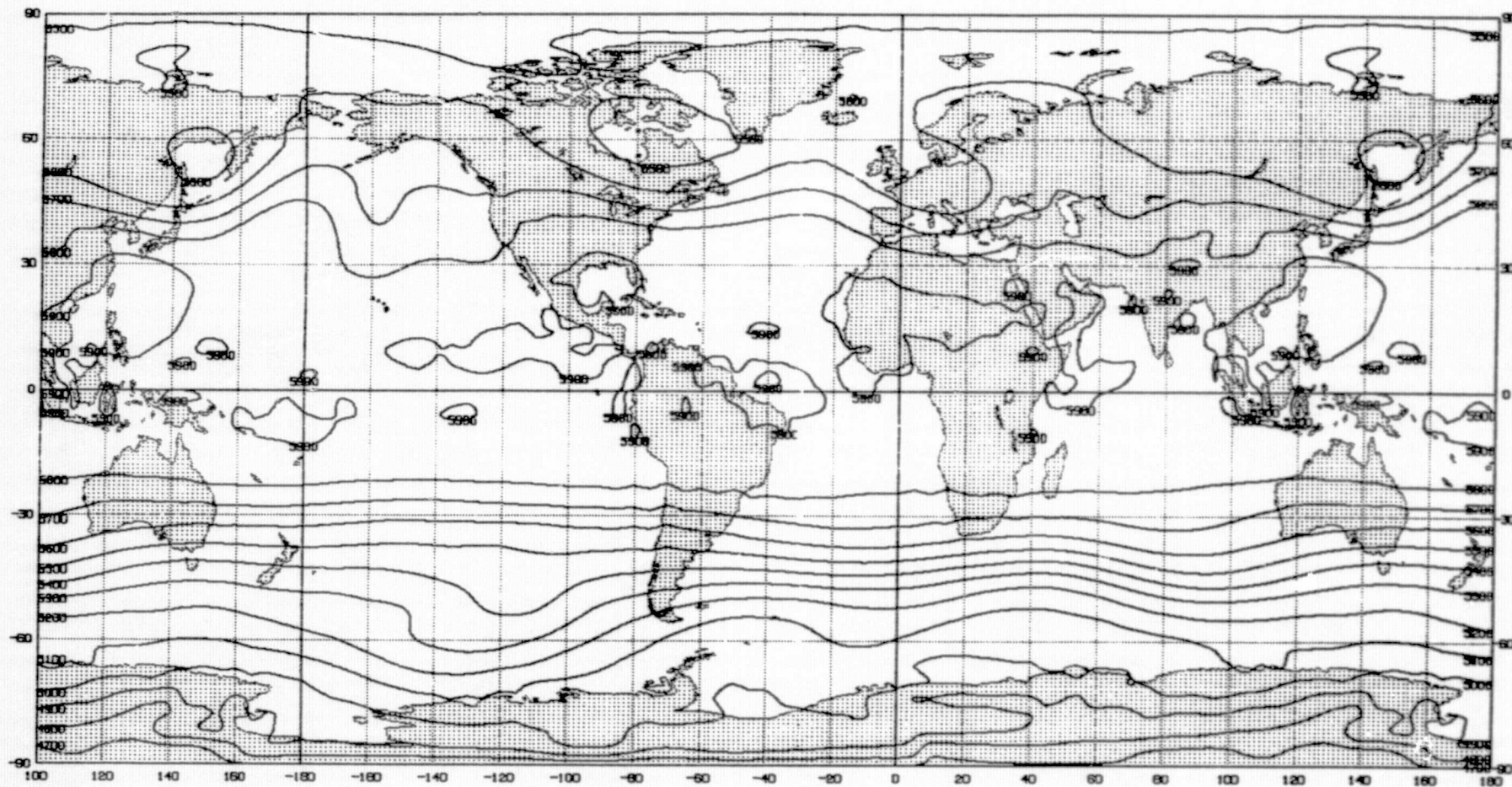


Figure G6.1 Simulated 500 mb Geopotential Height (m) - July

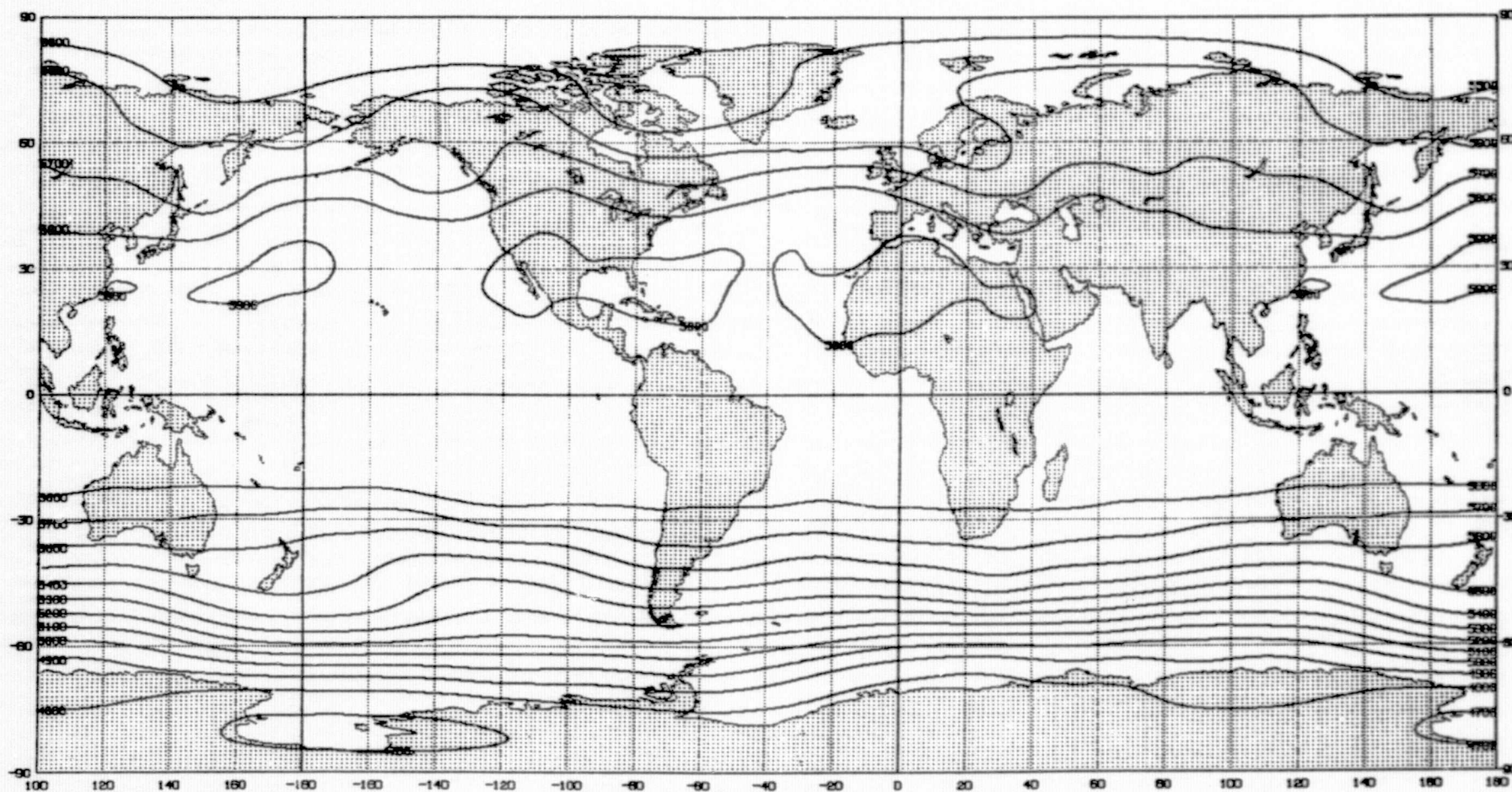


Figure G6.2 Observed 500 mb Geopotential Height (m) - July 1979

ORIGINAL PAGE IS
OF POOR QUALITY

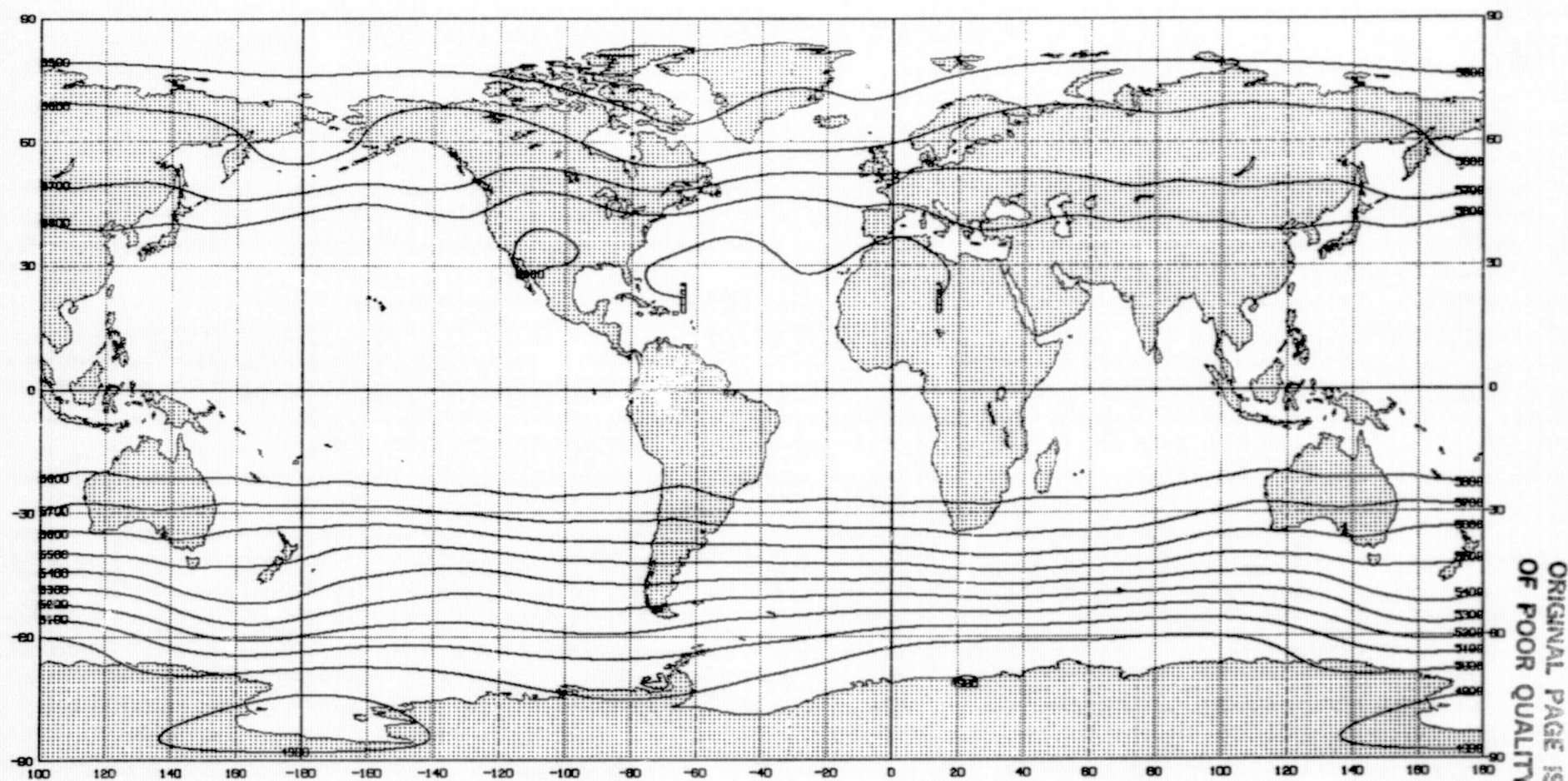


Figure G6.3 Climatological 500 mb Geopotential Height (m) - July

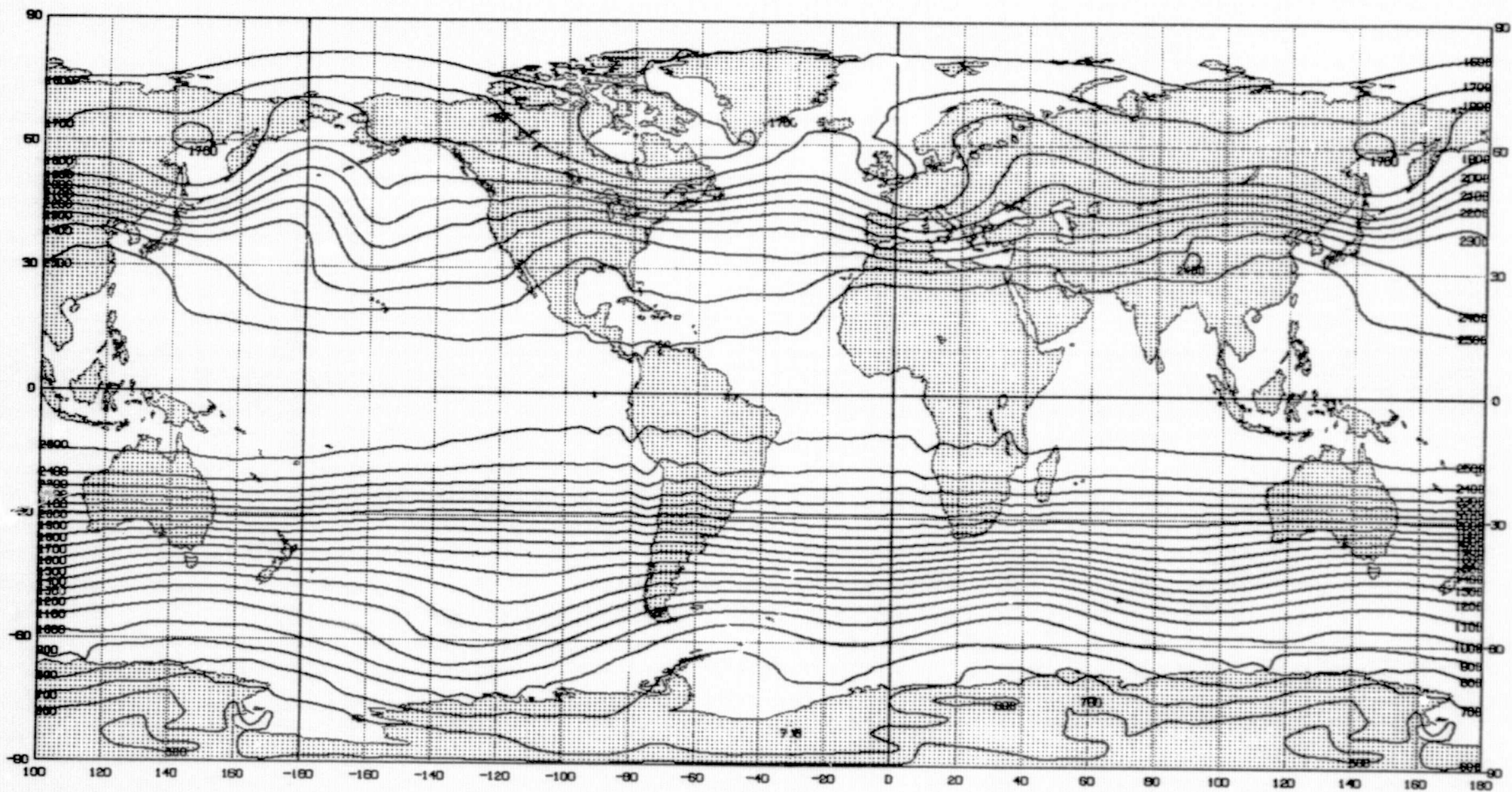


Figure G7.1 Simulated 200 mb Geopotential Height (m) - July

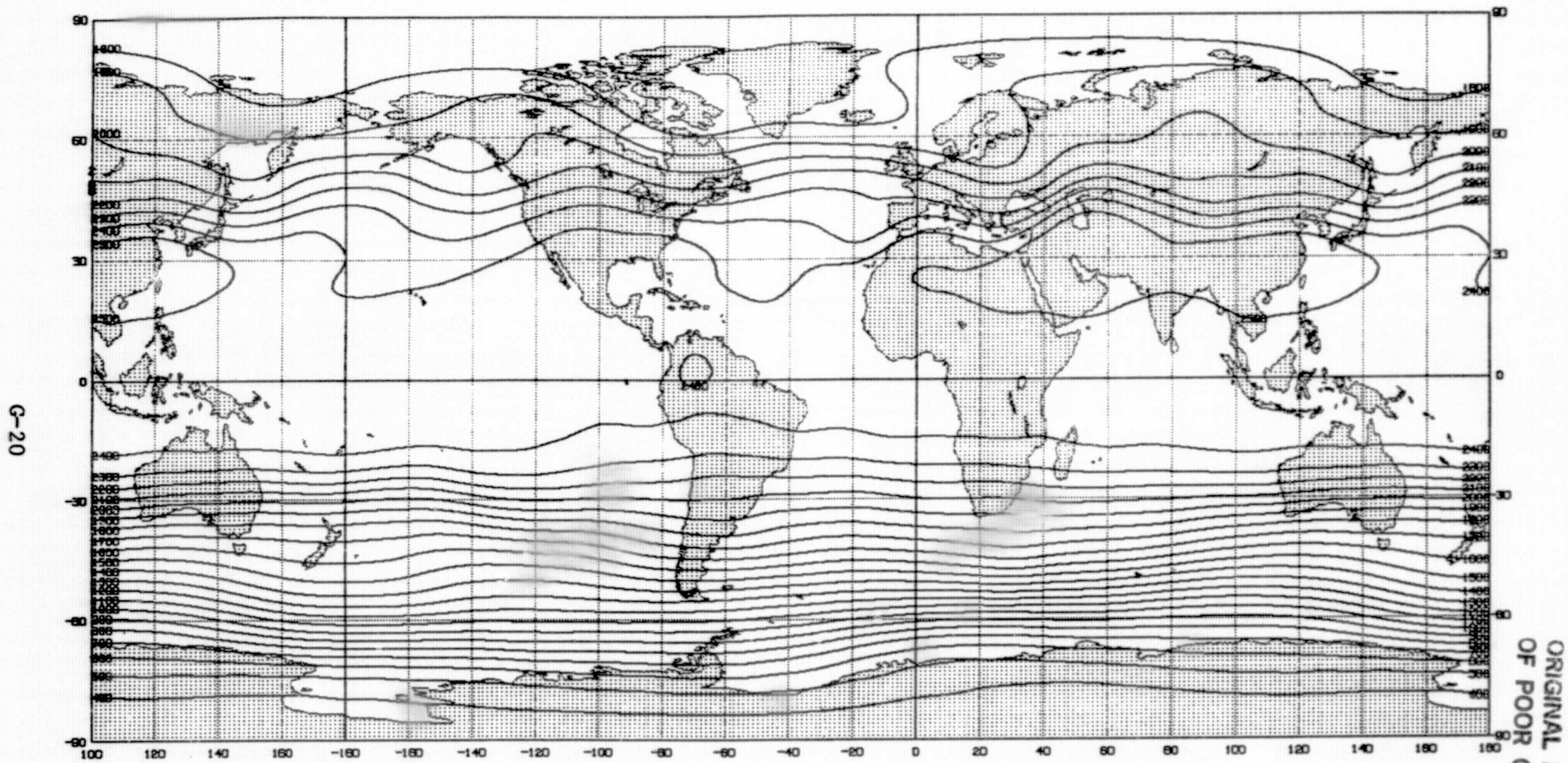


Figure G7.2 Observed 200 mb Geopotential Height (m) - July 1979

G-21

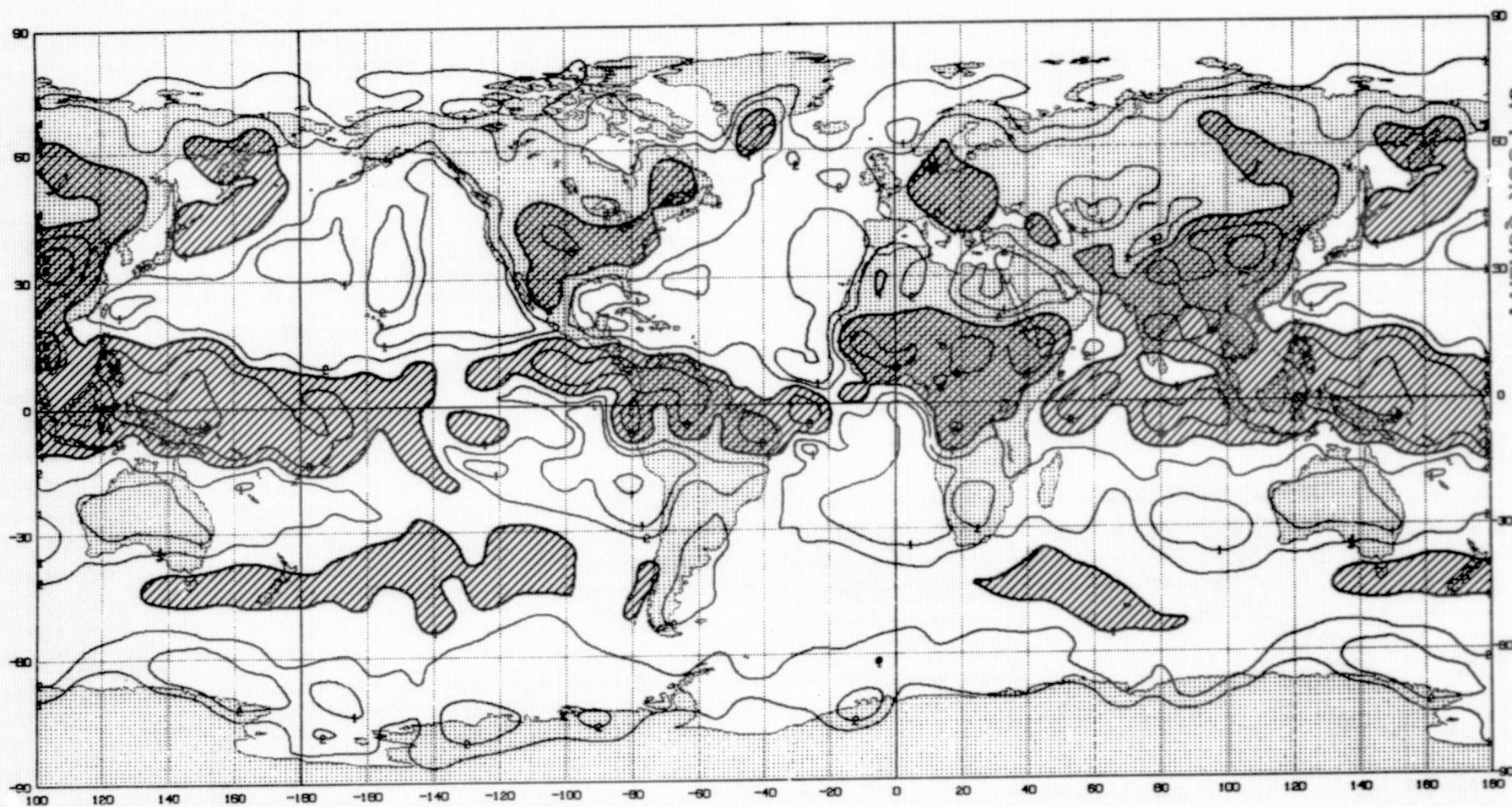


Figure G8.1 Simulated Precipitation Rate (mm/day) - July

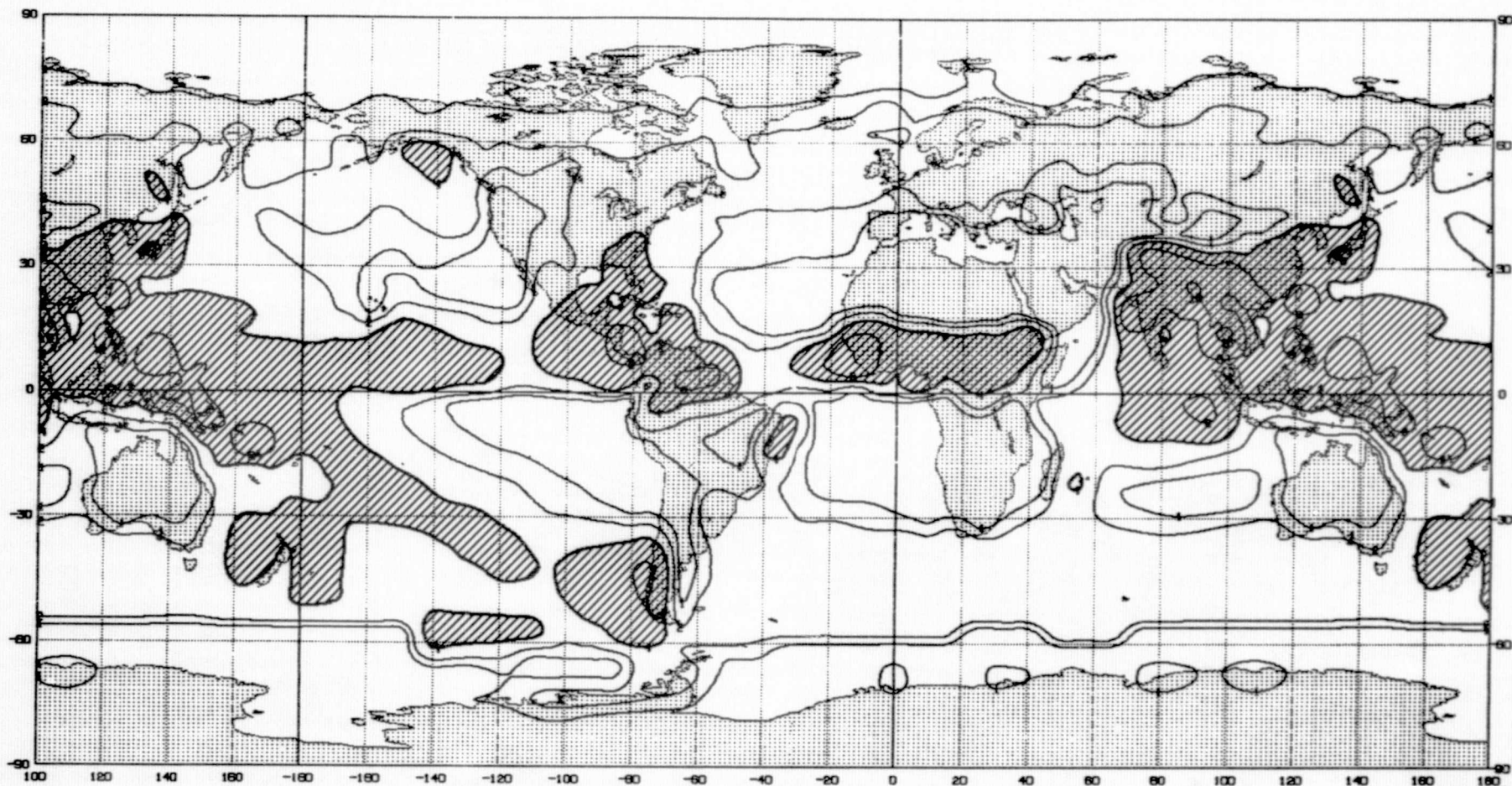


Figure G8.2 Climatological Precipitation Rate (mm/day) - July

BIBLIOGRAPHY

- APRUZESE, J. P., M. R. SCHOEBERL, and D. F. STROBEL, 1982: Parameterization of IR cooling in a middle atmosphere dynamics model. 1. Effects on the zonally averaged circulation. J. Geophys. Res., 87, 8951-8966.
- ARAKAWA, A. 1972: Design of the UCLA general circulation model. Tech. Rept. No. 7, Dept. of Meteorology, UCLA, 116 pp. Numerical Simulation of Weather and Climate.
- _____, and V. R. LAMB, 1977: Computational design of the basic dynamical processes of the UCLA general circulation model. Methods in Computational Physics, 17, Academic Press, 173-265.
- _____, and M. J. SUAREZ, 1983: Vertical differencing of the primitive equations in sigma coordinates. Mon. Wea. Rev., 111, 34-45.
- BAKER, W. E., R. ATLAS, M. HALEM, and J. SUSSKIND, 1983: A case study of the sensitivity of forecast skill to data and data analysis techniques. Sixth Conference on Numerical Weather Prediction, June 6-9, Omaha, Nebr., pp. 200-205.
- Chao, W. C., and M. A. GELLER, 1982: Utilization of normal mode initial conditions for detecting errors in the dynamics part of primitive equation global models. Mon. Wea. Rev., 110, 304-306; corrigendum, 110, 1324.
- _____, 1983: On error detection in the dynamics part of primitive equation models. Preprints, June 6-9, 1983, Omaha, Nebr., Sixth Conference on Numerical Weather Prediction, Amer. Meteor. Soc., 401-403.
- FELS, S. B., and M. D. SCHWARZKOPF, 1981: An efficient, accurate algorithm for calculating CO₂ 15 μ m band cooling rates. J. Geophys. Res., 86, 1205-1232.
- GATES, W. L., and A. B. NELSON, 1975: A new (revised) tabulation of the Scripps topography on a 1° global grid. Part I: Terrain heights. Defense Advanced Research Projects Agency, R-1276-1-ARPA, 132 pp.
- GODBOLE, R. V. and J. SHUKLA, 1981: Global Analysis of January and July Sea Level Pressure. NASA Technical Memorandum 82097.
- HALEM, M., E. KALNAY, W. E. BAKER, and R. ATLAS, 1982: An assessment of the FGGE satellite observing system during SOP-1. Bull. Amer. Meteor. Soc., 63, 407-426.
- JAEGER, L., 1976: Monatskarten des Niederschlags für die ganze Erde. Berichte des Deutschen Wetterdienstes, 18, No. 139. Im Selbstverlag des Deutschen Wetterdienstes, Offenbach, W. Germany.
- KALNAY-RIVAS, E., 1976: High-latitude truncation errors of box-type primitive equation models. Mon. Wea. Rev., 104, 1066-1069.
- _____, A. BAYLISS and J. STORCH, 1977: The 4th order GISS model of the global atmosphere. Beitr. Phys. Atmos., 50, 299-311.

- _____, and D. HOITSMA, 1979a: Documentation of the fourth order band model. NASA Tech. Memo. 80608, NASA/Goddard Space Flight Center, Greenbelt, MD.
- _____, and D. HOITSMA, 1979b: The effect of accuracy, conservation and filtering on numerical weather forecasting. Preprints, Fourth Conference on Numerical Weather Prediction, Oct. 29-Nov. 1, 1979, Silver Spring, MD, Amer. Meteor. Soc., 302-312.
- _____, R. ATLAS, W. BAKER, and M. HALEM, 1983: FGGE forecast impact studies in the Southern Hemisphere. Proceedings of the First International Conference on Southern Hemisphere Meteorology, Brazil, American Meteorology Society, pp. 180-183.
- KRISHNAMURTHY, V., 1982: The documentation of the Wu-Kaplan radiation parameterization. NASA Tech. Memo. 83926, NASA/Goddard Space Flight Center, Greenbelt, MD, 93 pp.
- LACIS, A. A., and J. E. HANSEN, 1974: A parameterization for the absorption of solar radiation in the earth's atmosphere. J. Atmos. Sci., 31, 118-133.
- MINTZ, Y., and Y. SERAFINI, 1981: Monthly normal global fields of soil moisture and land surface evaporation. Paper presented at the Int. Symp. on Variation in Global Water Budget, August 10-15, 1981, Oxford, England.
- PAEGLE, J. AND W. E. BAKER, 1983: The influence of the tropics on the prediction of ultralong waves.. Part II: Latent heating. Mon. Wea. Rev., 111, 1356-1371.
- PHILLIPS, N. A., 1974: Application of Arakawa's energy-conserving layer model to operational numerical weather prediction. NMC Office Note 104.
- RAMANATHAN, V., 1976: Radiative transfer within the earth's troposphere and stratosphere: A simplified radiative-convective model. J. Atmos. Sci., 33, 1330-1346.
- _____, and R. D. CESS, 1974: Radiative transfer within the mesospheres of Venus and Mars. Astrophys. J., 188, 407-416.
- SHAPIRO, R., 1970: Smoothing, filtering and boundary effects. Rev. Geophys. and Space Phys., 8, 359-387.
- SOMERVILLE, R. C. J., P. H. STONE, M. HALEM, J. E. HANSEN, J. S. HOGAN, L. M. DRUYAN, G. RUSSELL, A. A. LACIS, W. J. QUIRK, and J. TENENBAUM, 1974: The GISS model of the global atmosphere. J. Atmos. Sci., 31, 84-117.
- STROBEL, D. F., 1978: Parameterization of the atmospheric heating rate from 15 to 120 km due to O₂ and O₃ absorption of solar radiation. J. Geophys. Res., 83, 6225-6230.
- SUD, Y. C., and J. A. ABELES, 1981: Calculation of surface temperature and surface fluxes in the GLAS GCM. NASA Tech. Memo. 82167, NASA/Goddard Space Flight Center, Greenbelt, MD, 24 pp.
- _____, and M. FENNESSY, 1981: A study of the influence of surface albedo on July circulation in semi-arid regions using the GLAS GCM. J. Climatology, 2, 105-125.

TAKACS, L. L. and R. BALGOVIND, 1983: High latitude filtering in global grid point models. Mon. Wea. Rev., 111, 2005-2015.

TOKIOKA, T., 1978: Some considerations on vertical differencing. J. Meteor. Soc. Japan, 56, 98-111.

WILLIAMSON, D. L., and G. L. BROWNING, 1973: Comparison of grids and difference approximations for numerical weather prediction over a sphere. J. Appl. Meteor., 12, 264-274.

WU, M.-L. C., 1976: Longwave radiation and its effect on the atmosphere.
Ph.D. Thesis, Department of Geophysical Sciences, University of Chicago.